P-07-80

Forsmark site investigation

Method evaluation of single-hole hydraulic injection tests at site investigations in Forsmark

Jan-Erik Ludvigson, Kent Hansson, Calle Hjerne
Geosigma AB

April 2007

Svensk Kärnbränslehantering AB
Swedish Nuclear Fuel
and Waste Management Co
Box 5864
SE-102 40 Stockholm Sweden
Tel 08-459 84 00
+46 8 459 84 00
Fax 08-661 57 19
+46 8 661 57 19

ISSN 1651-4416
SKB P-07-80

Forsmark site investigation

Method evaluation of single-hole hydraulic injection tests at site investigations in Forsmark

Jan-Erik Ludvigson, Kent Hansson, Calle Hjerne
Geosigma AB

April 2007

Keywords: Forsmark, Hydrogeology, Hydraulic tests, Injection tests, Single-hole tests, Hydraulic parameters, Transmissivity, Hydraulic conductivity.

Abstract

In the frame of the site characterization programs for the Forsmark and Oskarshamn sites, SKB has conducted a large number of injection tests with the aim of deriving the hydraulic properties of the rock formations at the two sites. In some of the boreholes, complementary pressure pulse tests were performed in very low-transmissive borehole sections. The present report describes the methodology used for the measurement and analysis of the injection tests and pressure pulse tests conducted in boreholes KFM01A–KFM07A at the Forsmark site during the period May, 2003–April, 2005. In addition, statistics of the outcome of the tests regarding special items associated with the analysis, e.g. effects of packer compliance, non-unambiguous interpretation and inconsistent responses during the injection- and recovery period, is presented.

Packer compliance, which may affect the evaluation of hydraulic tests in low-transmissive sections, includes i) linear-elastic deformation and ii) time-dependent deformation of packers. The latter deformation involves two processes, i.e. material creeping and flow generated by the packers, respectively. Packer compliance was measured in the laboratory and compared with results of field tests. In addition, numerical simulations of packer compliance effects are presented.

The tests at Forsmark indicated that the injection period, in general, was the most appropriate for analysis due to longer analysable part of the flow rate curve after a constant pressure was achieved and more representative of the rock conditions close to the borehole. No disturbing effects of wellbore storage are present during the injection period. In most tests, a certain time interval of pseudo-radial flow could be identified during the injection period on which the transient evaluation was based.

The recovery period of the tests was frequently disturbed by wellbore storage effects, thus decreasing the part of the pressure data curve representative of the rock conditions. In low-transmissive sections, it was difficult to obtain an unambiguous transient evaluation during the recovery period due to dominating wellbore storage effects. During the recovery period, a lower number of tests for which a well-defined pseudo-radial flow regime could be identified were observed. In some boreholes, an increased number of tests showing an unexpectedly fast pressure recovery were observed.

In certain boreholes, an increased number of tests showing effects of apparent no-flow boundaries, probably reflecting flow features of limited extent or decreasing aperture further away from the borehole, were observed during the injection period. In several such tests, a slow and incomplete pressure recovery was observed during the recovery period. On the other hand, in some boreholes, an increased number of tests approaching a pseudo-stationary flow both during the injection and recovery period were observed. In many cases, such tests could be correlated to extensive deformation zones as interpreted from the geological borehole investigations.

The selected, representative transmissivity T_R from the injection tests was in most boreholes consistent with the estimated stationary transmissivity T_M from the injection period. However, in test sections with a dominating fracture with a strong, negative skin factor, the stationary transmissivity may be significantly overestimated in comparison to the transmissivity from transient evaluation. On the other hand, in sections with an estimated high, positive skin factor the stationary transmissivity may be significantly underestimated. This may also be the case if apparent no-flow boundaries are present.

The estimated skin factors from the injection tests are, in general, close to zero or negative which may be expected in fractured, crystalline rock. However, high, positive skin factors were estimated in some tests, possibly associated with turbulent flow in fractures, or alternatively, if pseudo-spherical (leaky) flow is dominating in e.g. thick deformation zones.

The effective wellbore storage coefficient estimated from the transient evaluation of the recovery period of the injection tests was generally in good agreement with the one estimated from previous laboratory tests of the actual test equipment for different test section lengths. The latter values on the effective wellbore storage coefficient were used by the evaluation of the pressure pulse tests. The elastic properties of the PSS test system were documented in conjunction with these tests.

The PSS test system is designed for a lower measurement limit of flow rate of 1 mL/min ($1.7 \cdot 10^{-8}$ m^3/s). The flow generated by the packers at the end of the injection period is c. 0.10–0.15 mL/min. The latter flow is considered to be included in the accuracy of the lower limit of flow rate. If it is desired to decrease the measurement limit for flow rate in the injection tests, either the allowed uncertainty of the measured flow rate must be extended, or alternatively, the flow generated by the packers must be taken into account in the analysis of very low-transmissive test sections. The compensation for the flow generated by the packers may sometimes be problematic.

A simple steady-state method for estimating the transmissivity of very low-transmissive test sections from pressure pulse tests, taking packer compliance effects into account, is presented. The method assumes that the packers and other test equipment perform identically during each test. However, based on current experience, there are indications that the equipment does not perform quite identically during all tests. For a packer sealing time of 60 min it may be possible to estimate transmissivities in the interval c. $5 \cdot 10^{-11}$ to $5 \cdot 10^{-10}$ m^2/s with this method. However, the uncertainty of such estimates is high.

The ”environmental” impact on short-time hydro-tests is generally so small that such factors may be neglected by the evaluation of the tests. The actual data acquisition system of PSS has a standard pressure resolution of ± 0.7 kPa. Some of the tests showing fast recovery may thus exhibit a virtually constant pressure during the major part of the recovery period when the pressure has nearly recovered completely. Improved resolution of pressure may possibly increase the possibilities to extract information from the later part of the recovery curve by the evaluation. However, external effects on the data curve may reduce such possibilities. Such phenomena include tidal effects, precipitation, changes of the atmospheric pressure and of the sea level, earth quakes, drilling and other activities in surrounding boreholes together with re-establishment of the section pressure to formation pressure after packer sealing.

The test statistics shows that non-unambiguous interpretation and inconsistent responses in the tests at Forsmark in many cases correspond to tests with fast recovery and tests influenced by wellbore storage during recovery. Fast recovery may be caused by geological factors, e.g. deformation zones, or possibly, by turbulent flow in fractures intersecting the section.

The estimated transmissivity from the injection tests is generally consistent with the transmissivity calculated from difference flow logging in the same sections. However, discrepancies may occur if fracture(s) with limited extension, which might appear as apparent no-flow boundaries during hydraulic tests, intersect(s) the test section. Such fractures may not be identified as flow anomalies during difference flow logging since the borehole is pumped for several days before these measurements which may make the fractures hydraulically inactive.

Sammanfattning

Inom ramen för platsundersökningsprogrammen för platserna Forsmark och Oskarshamn har SKB utfört ett stort antal injektionstester med syfte att bestämma de hydrauliska egenskaperna för berget på de två platserna. I några av borrhålen utfördes kompletterande pulstester i mycket lågtransmissiva borrhålssektioner. Denna rapport beskriver metodologin som använts för mätningen och analysen av injektionstesterna och pulstesterna som utförts i A-borrhålen i Forsmark under perioden Maj 2003–April 2005. Dessutom presenteras statistik över utfallet av testerna beträffande speciella frågor som är knutna till analysen, t ex effekter av manschett-deformation, ej entydig utvärdering och inkonsistenta responser under injektions- och återhämtningsperioden.

Manschettdeformation, vilken kan påverka utvärderingen av hydrauliska tester i lågtransmissiva sektioner, omfattar i) linjär-elastisk deformation och ii) tidsberoende deformation. Den senare deformationen omfattar två processer, nämligen materialkrypning och flöde genererat av manschetterna. Manschettdeformationen har mätts i laboratorium och jämförts med resultaten av fälttester. Dessutom presenteras numeriska simuleringar av effekter av manschettdeformation.

Testerna i Forsmark indikerade att injektionsperioden vanligen är mest lämpad för analys på grund av längre analyserbar del av flödeskurvan efter att ett konstant tryck erhållits och mer representativ för bergets egenskaper nära borrhålet. Inga störande effekter av brunnsmagasin förekommer under injektionsperioden. För de flesta tester kunde ett visst intervall med pseudo-radiellt flöde identifieras under injektionsperioden på vilket den transienta tolkningen baserades.

Återhämtningsperioden var ofta störd av brunnsmagasinseffekter som sålunda förkortade den del av tryckdatakurvan som är representativ för bergets egenskaper. I lågtransmissiva sektioner var det svårt att erhålla en entydig transient tolkning för återhämtningsperioden på grund av dominerande brunnsmagasinseffekter. Under återhämtningsperioden kunde ett lägre antal tester med en väldefinierad pseudo-radiell flödesregim identifieras. I några borrhål observerade ett ökat antal tester som visade en oväntat snabb tryckåterhämtning.

I vissa borrhål observerades ett ökat antal tester som visade effekter av skenbara negativa hydrauliska gränser under injektionsperioden, sannolikt avspeglande flödesanomalier med begränsad utbredning eller med minskande apertur längre bort från borrhålet. I flera sådana tester observerades en långsam och ofullständig tryckåterhämtning under återhämtningsperioden. Å andra sidan observerades ett ökat antal tester som närmade sig ett pseudostationärt flöde både under injektions- och återhämtningsperioden. I många fall kunde sådana tester korreleras med mäktiga deformationszoner som tolkats från de geologiska borrhålsundersökningarna.

Den valda representativa transmissiviteten T_R från injektionstesterna var i de flesta borrhål konsistent med den skattade stationära transmissiviteten T_M från injektionsperioden. I testsektioner med en dominerande spricka med en hög, negativ skinfaktor kan emellertid den stationära transmissiviteten vara väsentligt överskattad jämfört med transmissiviteten från transient tolkning. Å andra sidan, kan den stationära transmissiviteten vara väsentligt underskattad i sektioner med en skattad hög positiv skinfaktor. Detta kan också vara fallet om skenbara negativa hydrauliska gränser förekommer.

De skattade skinfaktorena från injektionstesterna är vanligen nära noll eller negativa vilket kan förväntas i sprickigt kristallint berg. Höga positiva skinfaktorer beräknades emellertid för några tester, möjligen associerade med turbulent flöde i sprickor, eller alternativt, om pseudosfäriskt (läckande) flöde dominerar inom t ex mäktiga deformationszoner.

Den effektiva brunnsmagasinskoefficienten beräknad från den transienta tolkningen av återhämtningsperioden av injektionstesterna var vanligen i god överensstämmelse med den som bestämts från tidigare laboratorietester med den aktuella utrustningen för olika testsektionslängder. De senare värdena på den effektiva brunnsmagasinskoefficienten användes vid tolkningen av tryckpulstesterna. De elastiska egenskaperna för PSS testsystemet dokumenterades i samband med dessa tester.

PSS-systemet är konstruerat för en nedre flödesmätgräns av 1 mL/min ($1.7 \cdot 10^{-8}$ m^3/s). Flödet som genereras av manschetterna vid slutet av injektionsperioden är ca 0.10–0.15 mL/min. Detta betraktas som inkluderat i mätnoggrannheten för den nedre mätgränsen för flöde. Om det är önskvärt att sänka nedre flödesmätgränsen måste antingen den accepterade osäkerheten av det mätta flödet utökas, eller alternativt, måste hänsyn tas till det manschettgenererade flödet vid analysen av mycket lågtransmissiva testsektioner. Kompensationen för flödet genererat av manschetterna kan dock ibland vara problematisk.

En enkel stationär metod för skattning av transmissiviteten för mycket lågtransmissiva testsektioner, som tar hänsyn till manschettdeformation, presenteras. Metoden förutsätter att manschetter och övrig testutrustning uppträder identiskt vid varje test. Men, baserat på tidigare erfarenheter, finns indikationer på att utrustningen ej uppträder identiskt vid alla tester. För en manschettätningstid av 60 min kan det vara möjligt att skatta transmissiviteter i intervallet ca $5 \cdot 10^{-11}$ to $5 \cdot 10^{-10}$ m^2/s med denna metod. Osäkerheten i sådana skattningar är dock stor.

Omgivningspåverkan på hydrotester är vanligen så liten att sådana faktorer kan negligeras vid utvärderingen av testerna. Det aktuella insamlingssystemet i PSS har för tryck en upplösning av ± 0.7 kPa. Några av testerna som uppvisar snabb återhämtning kan därför uppvisa ett praktiskt taget konstant tryck under större delen av återhämtningsperioden. Förbättrad upplösning av tryck kan eventuellt förbättra möjligheterna att få ut mer information från denna period vid utvärderingen. Externa effekter kan dock reducera sådana möjligheter. Sådana fenomen inkluderar tidaleffekter, nederbörd, variationer av lufttryck och havsnivå, jordbävningar, borrning och andra aktiviteter i omgivande borrhål samt återgång av sektionstrycket till formationstryck efter manschettätning.

Teststatistiken visar att icke entydig utvärdering och inkonsistenta responser vid testerna i Forsmark i många fall är förknippade med tester med snabb återhämtning och tester påverkade av borrhålsmagasin. Snabb återhämtning kan orsakas av geologiska faktorer, t ex deformationszoner, eller möjligen av turbulent flöde i sprickor som skär sektionen.

Den skattade transmissiviteten från injektionstesterna är vanligen konsistent med transmissiviteten beräknad från differensflödesloggning i samma sektioner. Avvikelser kan emellertid förekomma om spricka(or) med begränsad utbredning, som kan uppvisa effekter av skenbara negativa hydrauliska gränser under hydrauliska tester, skär testsektionen. Sådana sprickor kanske inte identifieras som flödesanomalier under differensflödesloggningen eftersom borrhålet pumpas under flera dagar innan dessa mätningar utförs vilket kan göra sprickorna hydrauliskt inaktiva.

1 Introduction

In the frame of the site characterization programs for the Forsmark and Oskarshamn sites, SKB has conducted a large number of injection tests with the aim of deriving the hydraulic properties of the rock formations at the two sites. In some of the boreholes, complementary pressure pulse tests were performed in low-transmissive borehole sections. The present report describes the methodology used for the measurement and analysis of the injection tests and pressure pulse tests conducted in the A-boreholes at the Forsmark site during the period May, 2003–April, 2005. The boreholes tested during this period and the number of injection tests performed using the PSS3 equipment are listed in Table 1-1. The location of the boreholes is presented in the map in Figure 1-1. A corresponding report was prepared for the Oskarshamn site by Golder Associates.

1.1 Structure of the document

The present document was structured as follows:

- The Introduction (Chapter 1) describes the context of the report, the work done during the period May, 2003–April, 2005 at the Forsmark site and lists the related documents relevant to the report.
- Chapter 2 describes the objectives of the report.
- Chapter 3 presents the test design and decision procedures used during the work as well as the equipment used.
- Chapter 4 describes the analysis methodology applied for the tests. Individual sections describe the analysis of constant pressure injection tests (CHi phase), of pressure recovery tests (CHir phase) and of pressure pulse injection tests (PI phase). A final section describes the derivation of recommended values and confidence ranges for the hydraulic parameters.
- Chapter 5 discusses uncertainties which occur during testing, such as packer compliance and background pressure gradients.
- Chapter 6 presents the statistics of the results of the tests conducted during the actual period.
- Chapter 7 highlights differences in the analysis methodology between the two SKB contractors who conducted the work (Geosigma and Golder Associates).
- Chapter 8 summarizes conclusions and recommendations, based on the experience gained from past work.
- Chapters 9 and 10 present the literature references, the nomenclature, and a glossary of abbreviations.

Table 1-1. Hydraulic injection testing work conducted at Forsmark until April, 2005.

Borehole	Testing period	Number of tests
KFM01A	May–June, 2003	75
KFM02A	March, 2004	104
KFM03A	May–June, 2004	157
KFM04A	August–September, 2004	63
KFM05A	December 2004–January, 2005	55
KFM06A	March–April, 2005	115
KFM07A	February–March, 2005	47

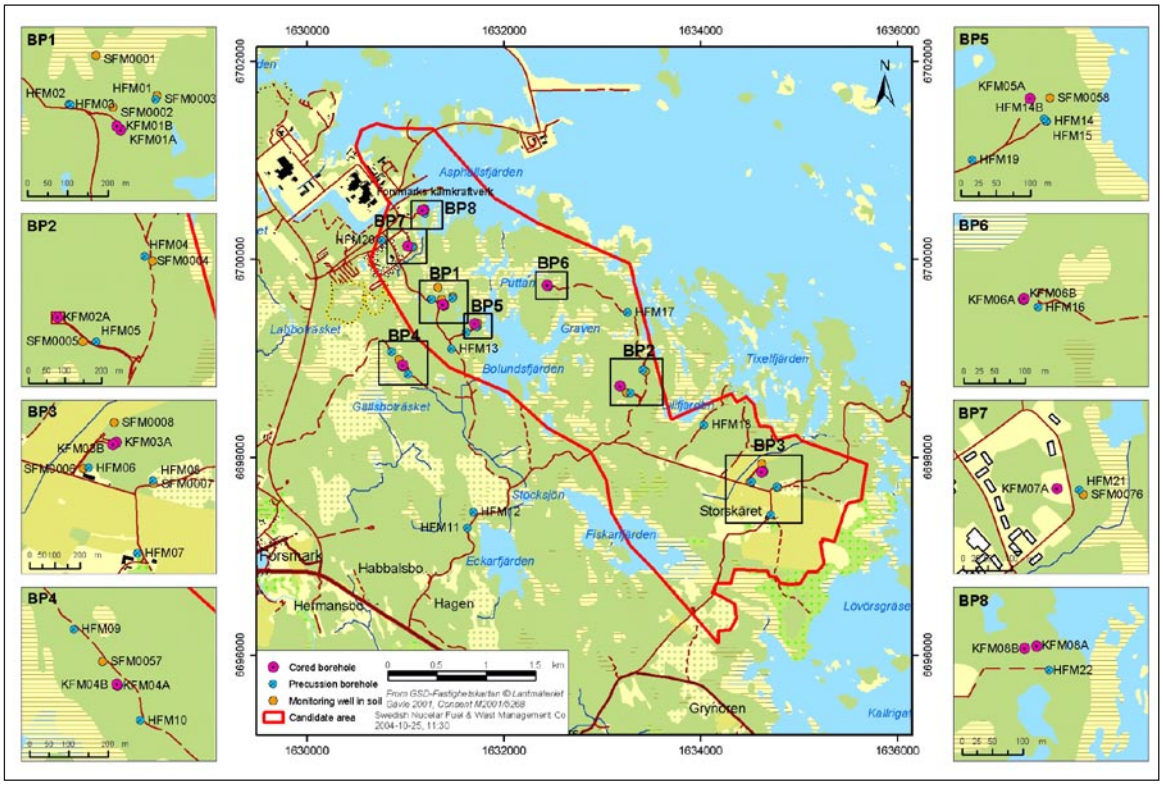

Figure 1-1. *The investigation area at Forsmark including the candidate area selected for more detailed investigations and drill sites BP1–BP8.*

1.2 Related documents

The methods and procedures which govern the testing work conducted at the Forsmark site were defined by SKB and presented in the following documents:

The documents listed above were edited before the start of the SKB site investigations (PLU). In the course of the testing work some of the procedures and analysis techniques were changed with the aim of optimizing and improving the workflow and/or the interpretation of results. Therefore, the current document should be seen as an updated description of these procedures.

The description and analysis of the injection tests conducted at the Forsmark site are presented in the following documents:

- SKB P-04-95: Forsmark site investigation. Single-hole injection tests in borehole KFM01A, April 2004.
- SKB P-04-100: Forsmark site investigation. Single-hole injection tests in borehole KFM02A, May 2004.
- SKB P-04-194: Forsmark site investigation. Single-hole injection tests in borehole KFM03A, July 2004.
- SKB P-04-293: Forsmark site investigation. Single-hole injection tests in borehole KFM04A, January 2005.
- SKB P-05-56: Forsmark site investigation. Single-hole injection tests in borehole KFM05A, March 2005.
- SKB P-05-165: Forsmark site investigation. Single-hole injection tests in boreholes KFM06A and KFM06B, June 2005.
- SKB P-05-133: Forsmark site investigation. Single-hole injection tests in borehole KFM07A, May 2005.

Additional documents cited in this report are presented in the reference list.

2 Objective and scope

The objective of the present report is to describe the methodology used during the past 2–3 years for the measurement and analysis of the injection tests conducted at the Forsmark site.

The report presents both technical and practical details of the work with reference to actual field cases in order to exemplify the individual aspects. References to test analysis theory are made to the extent necessary, in order to clarify the interpretation procedures applied.

Apart from the conclusions and recommendations presented in Chapter 8, the document strictly describes the procedures that were actually applied as opposed to making recommendations about alternative or improved techniques.

3 SKB test design and equipment

3.1 Test design

The main aim of injection tests in PLU is to characterize the hydraulic properties of the rock adjacent to the borehole tested on different measurement scales (100 m, 20 m and 5 m). The primary parameter to be determined is the transmissivity of the tested sections from which the hydraulic conductivity can be derived. Other information of interest from injection tests is the identification of flow regimes and outer hydraulic boundaries as deduced from the transient responses of the tests.

The results of the injection tests provide a database for statistical analyses of the hydraulic conductivity distribution along the borehole on different measurement scales. In addition, the results of the injection tests may be compared with the results of the difference flow logging in the boreholes. Combined analysis of injection tests and difference flow logging provides a more comprehensive understanding of the hydraulic borehole conditions.

Methods and equipment for hydraulic single-hole tests in PLU are described in Morosini et al. (2001) /1/. The principle and procedure of single-hole injection tests used in PLU are described in SKB MD 323.001 (Methodology description for injection tests and single-hole pumping tests). The detailed performance in each borehole is described in the corresponding Activity plans.

In very low-transmissivity sections, pressure pulse tests are sometimes performed as a complement to injection tests. However, no separate methodology description has been prepared for such tests. At Forsmark, pressure pulse tests were performed in selected boreholes according to a special scheme.

3.1.1 Test principle

Injection tests in PLU are carried out by applying a constant head of generally c. 200 kPa (20 m water column) in the test section and monitoring the transient decline of flow rate. Before start of the injection period, approximate steady-state pressure conditions should prevail in the test section. After the injection period, the pressure recovery is measured in the tested section.

Pressure pulse tests are generally performed by introducing a short pressure pulse of c. 200 kPa in the test section and monitoring the subsequent pressure decay in the section.

3.1.2 Test procedure

A complete cycle of an injection test with constant head includes the following phases (Figure 3-1):

1) Registration of initial parameters in open borehole.

2) Packer inflation.

3) Shut-in and pressure stabilisation in the test section. De-aeration of the test system.

4) Injection of water and registration of decline of flow rate in test section.

5) Registration of pressure recovery in test section.

6) Stop of recovery period.

7) Packer deflation and transfer of the down-hole equipment to the next test section.

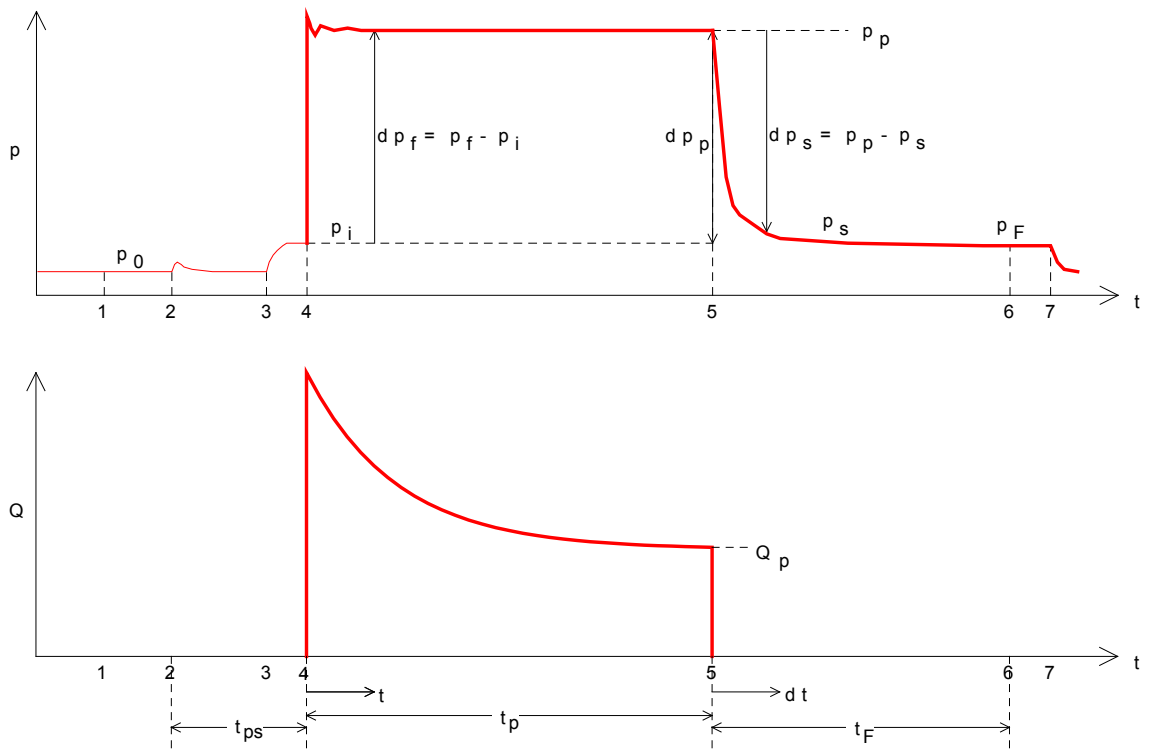

Figure 3-1. *Schematic drawing of pressure (p) and flow rate (Q) behaviour in the test section together with test phases (1–7) and parameter designations during a constant head injection test.*

Standard durations of the different phases of the constant head injection tests in PLU are presented in Table 3-1a. Slightly different packer inflation times and injection- and recovery times are used for the tests in 100 m sections compared to the tests in 20 m and 5 m sections.

In the injection tests with 20 m and 5 m section length, the injection period is interrupted if the flow rate clearly falls below the measurement limit. The subsequent pressure recovery is in such cases measured for at least 5 minutes to verify the low transmissivity of the section.

For pressure pulse tests, the test cycle may be basically the same as for injection tests. However, the duration of the different phases is slightly different. An example of a standard scheme for pressure pulse tests is shown in Table 3-1b. It should be noted that the times are the same regardless of the section length. The pressure pulse is generally created by applying a pressure of c. 200 kPa to the pipe string above the test section and then opening the test valve for a short time, e.g. 2 minutes when the valve is closed and the pressure recovery in the test section is measured. At Forsmark, a special scheme for pressure pulse tests, including a diagnostic test, was prepared and used in later boreholes, see Section 4.3.

Table 3-1a. Standard duration of the different phases of injection tests in PLU.

Section length (m)	Packer inflation (min)	Pressure stabilisation (min)	Injection period (min)	Recovery period (min)	Total time/test (min)[1)]
100	30	15	30	30	105
20	25	5	20	20	70
5	25	5	20	20	70

[1)] Exclusive of trip times in the borehole.

Table 3-1b. Duration of the different phases of pressure pulse tests in PLU applied at Forsmark.

Section length (m)	Packer inflation (min)	Pressure stabilisation (min)	Pulse injection (min)	Recovery (min)	Total time/test (min)[1)]
5, 20 and 100	40	20	2	40	102

[1)] Exclusive of trip times in the borehole.

3.1.3 Test strategy

The standard hydraulic test strategy in PLU is described below. In some of the tested boreholes at Forsmark, deviations from this strategy were made as decided by the Activity Leader. In addition, in some boreholes pressure pulse tests were performed in very low-transmissivity sections as complement to the injection tests.

Firstly, successive injection tests are performed in 100 m long sections in the entire, cored borehole interval from c. 100 m to c. 1,000 m. Secondly, injection tests in 20 m sections are carried out within the 100 m sections with a recorded flow above the measurement limit.

Finally, injection tests with 5 m section length are conducted in the 20 m sections with a definable final flow rate, i.e. above a test-specific lower measurement limit. Four successive tests with 5 m section length are generally performed within the actual 20 m intervals. In some boreholes the number of 20 m and 5 m tests was reduced. The total number of injection tests is thus dependent on the results of the previous tests.

Since the results of the injection tests in 100 m and 20 m sections will have a strong effect on the continued test program in the boreholes, it is particularly important to ensure precise results of these tests. Furthermore, since packer compliance constitute a minor part of the total compressibility (water, rock and packers) in the 100 m tests the results of these tests are considered as more representative for low-transmissive test sections close to the lower measurement limit.

3.2 PSS equipment

3.2.1 Overview

All of the equipment needed to perform the injection tests is located in a steel container (Figure 3-2). The container is divided into two compartments; a computer-room and a workshop. The container is placed on pallets in order to obtain a suitable working level in relation to the borehole casing. The hoisting rig is of a hydraulic chain-feed type. The jaws, holding the pipe string, are opened hydraulically and closed mechanically by springs. The rig is equipped with a load transmitter and the load limit may be adjusted. The maximum load is 22 kN.

The packers and the test valve are operated hydraulically by water filled pressure vessels. Expansion and release of packers, as well as opening and closing of the test valve, is done using magnetic valves controlled by the software in the data acquisition system.

The injection system consists of a tank, a pump and a flow meter. The injection flow rate may be manually or automatically controlled. At small flow rates, a water filled pressure vessel connected to a nitrogen gas regulator is used instead of the pump.

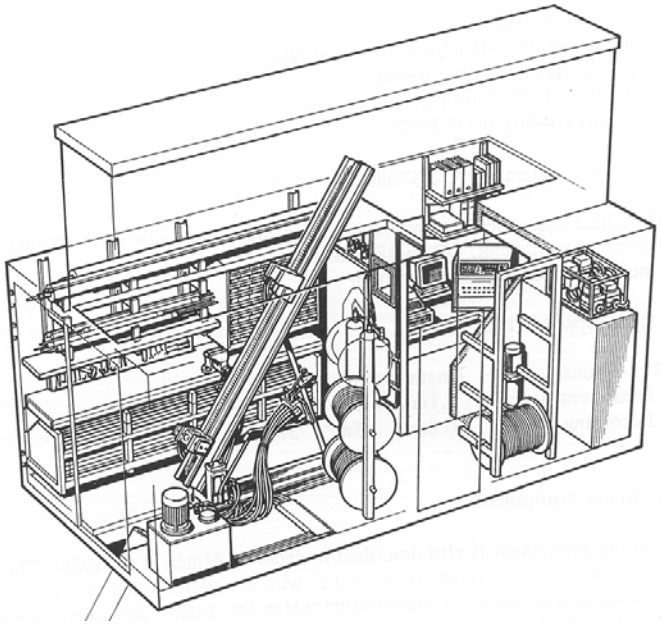

Figure 3-2. *Outline of the PSS3 container showing the test equipment.*

3.2.2 Down-hole equipment

A schematic drawing of the down-hole equipment is shown in Figure 3-3. The pipe string consists of aluminium pipes of 3 m length, connected by stainless steel taps sealed with double o-rings. Pressure is measured above (P_a), within (P) and below (P_b) the test section, which is isolated by two packers. The length of the test section may be varied (5, 20 or 100 metres).

The groundwater temperature in the test section (Te_w) is also currently measured. The hydraulic connection between the pipe string and the test section can be closed or opened by a test valve operated by the measurement system at the surface.

At the lower end of the down-hole equipment in the borehole, a position indicator (caliper type) gives a signal as the actual reference depth marks along the borehole are passed.

Selected technical specifications

Packers	
Type:	RG PU 72
Sealing length:	1,000 mm
Outer diameter:	72 mm (deflated)
Recommended sealing pressure:	2,000 kPa above the hydrostatic pressure at the depth of the test section
Pipes	
Outer/inner diameter	33/21 mm
Building length:	3,000 mm
Sealing:	Two o-rings

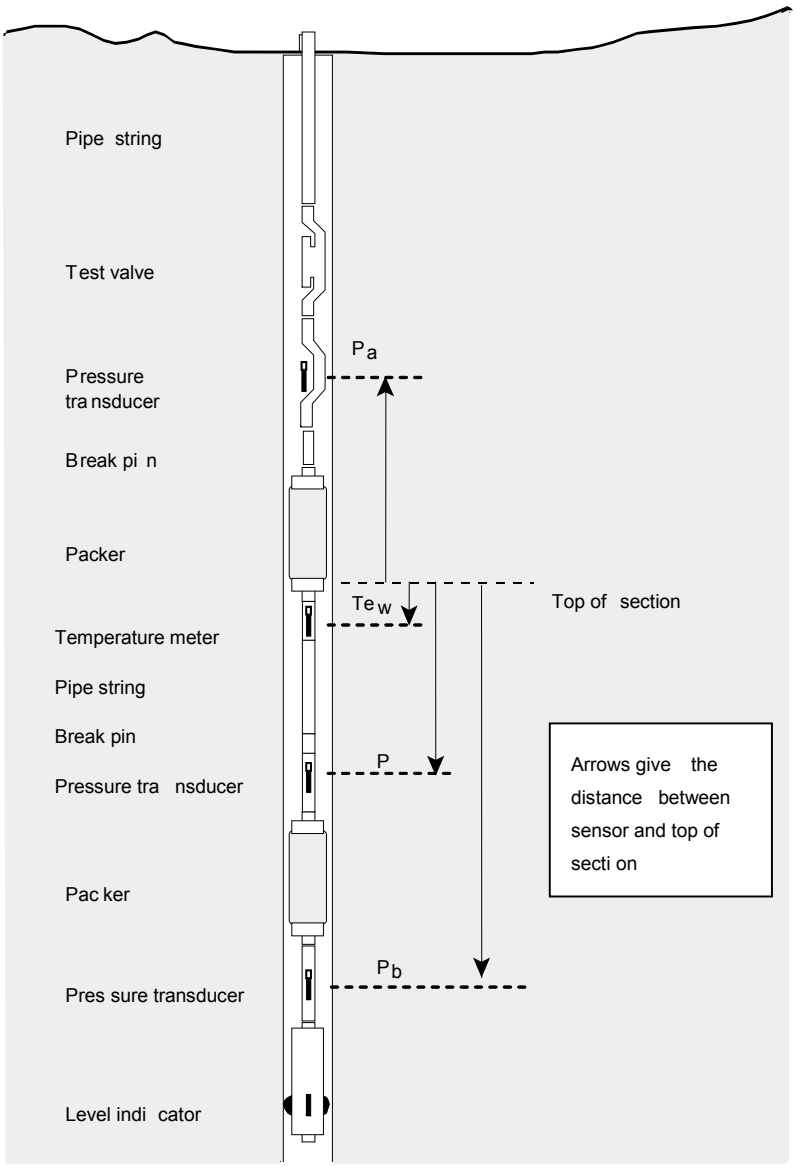

Figure 3-3. *Schematic drawing of the down-hole equipment in the PSS3 system including the positions of sensors. The positions are given in relation to the top of the test section.*

3.2.3 Measurement sensors

Technical data of the measurement sensors in the PSS system together with the estimated data of the entire system are shown in Table 3-2. The sensors are components of the PSS system. The accuracy of the PSS system may also be affected by the I/O-unit, cf Figure 3-4, and the calibration of the system.

By the estimation of the total error of the flow rate into the rock, the volume changes of the packers (packer compliance) must also be considered, cf Section 5.1. The sensor positions are fixed relative to the top of the test section. In Table 3-3, the position of the sensors is given in relation to the top of the test section, cf Figure 3-3. Sensor P measures the absolute pressure in the test section; sensor P_a measures the absolute pressure in the borehole interval above the upper packer to the groundwater level in the borehole while sensor P_b measures the absolute pressure in the borehole interval below the lower packer to the bottom of the borehole.

Table 3-2. Technical data of different sensors together with estimated data for the standard PSS system (based on current experience).

Technical specification Parameter		Unit	Sensor	PSS	Comments
Absolute pressure	Output signal	mA	4–20		
	Meas. range	MPa	0–13.5		
	Resolution	kPa	< 1.0		
	Accuracy[1)]	% F.S	0.1		
Differential pressure, 200 kPa	Accuracy	kPa		< ± 5	Estimated value
Temperature	Output signal	mA	4–20		
	Meas. range	°C	0–32		
	Resolution	°C	< 0.01		
	Accuracy	°C	± 0.1		
Flow Qbig	Output signal	mA	4–20		
	Meas. range	m^3/s	$1.67 \cdot 10^{-5}$–$1.67 \cdot 10^{-3}$		
	Resolution	m^3/s	$6.7 \cdot 10^{-8}$		
	Accuracy[2)]	% o.r	0.15–0.3	0.2–1	The specific accuracy is depending on the actual flow rate
Flow Qsmall	Output signal	mA	4–20		
	Meas. range	m^3/s	$1.67 \cdot 10^{-8}$–$1.67 \cdot 10^{-5}$		
	Resolution	m^3/s	$6.7 \cdot 10^{-10}$		
	Accuracy[2)]	% o.r	0.1–4	0.4–20	The specific accuracy is depending on the actual flow rate

[1)] 0.1% of Full Scale (F.S.). Includes hysteresis, linearity and repeatability.

[2)] Maximum error in % of actual reading (% o.r.). The higher numbers correspond to the lower flow. The error involves residuals between calibration points and calculated calibration curve together with the drift between two calibrations.

Table 3-3. Position of sensors in the borehole in relation to the top of the test section.

Parameter	Length of test section (m)		
	5	20	100
Position of sensor P_a, pressure above the test section, (m above secup)[1)]	1.87	1.87	1.86
Position of sensor P, pressure in the test section, (m above secup)[1)]	–4.13	–19.13	–99.12
Position of sensor Te_w, temperature in the test section, (m above secup)[1)]	–0.98	–0.99	–0.99
Position of sensor P_b, pressure below the test section, (m above secup)[1)]	–7.00	–22.00	–102.00

[1)] Position of sensor relative top of test section. A negative value indicates a position below the top of test section, (secup).

3.2.4 Data acquisition system

The standard data acquisition system in the PSS equipment contains a standard office PC connected to an I/O-unit (Datascan 7320). Using the Orchestrator software, pumping and injection tests are monitored and borehole sensor data are collected. In addition to the borehole parameters, packer and atmospheric pressure, container air temperature and water temperature are logged. Test evaluation may be performed on-site after a conducted test. An external display enables monitoring of test parameters.

The data acquisition system may be used to start and stop the automatic control system (computer and servo motors). These are connected as shown in Figure 3-4. The control system monitors the flow regulator and uses differential pressure across the regulating valve together with pressure in the test section as input signals.

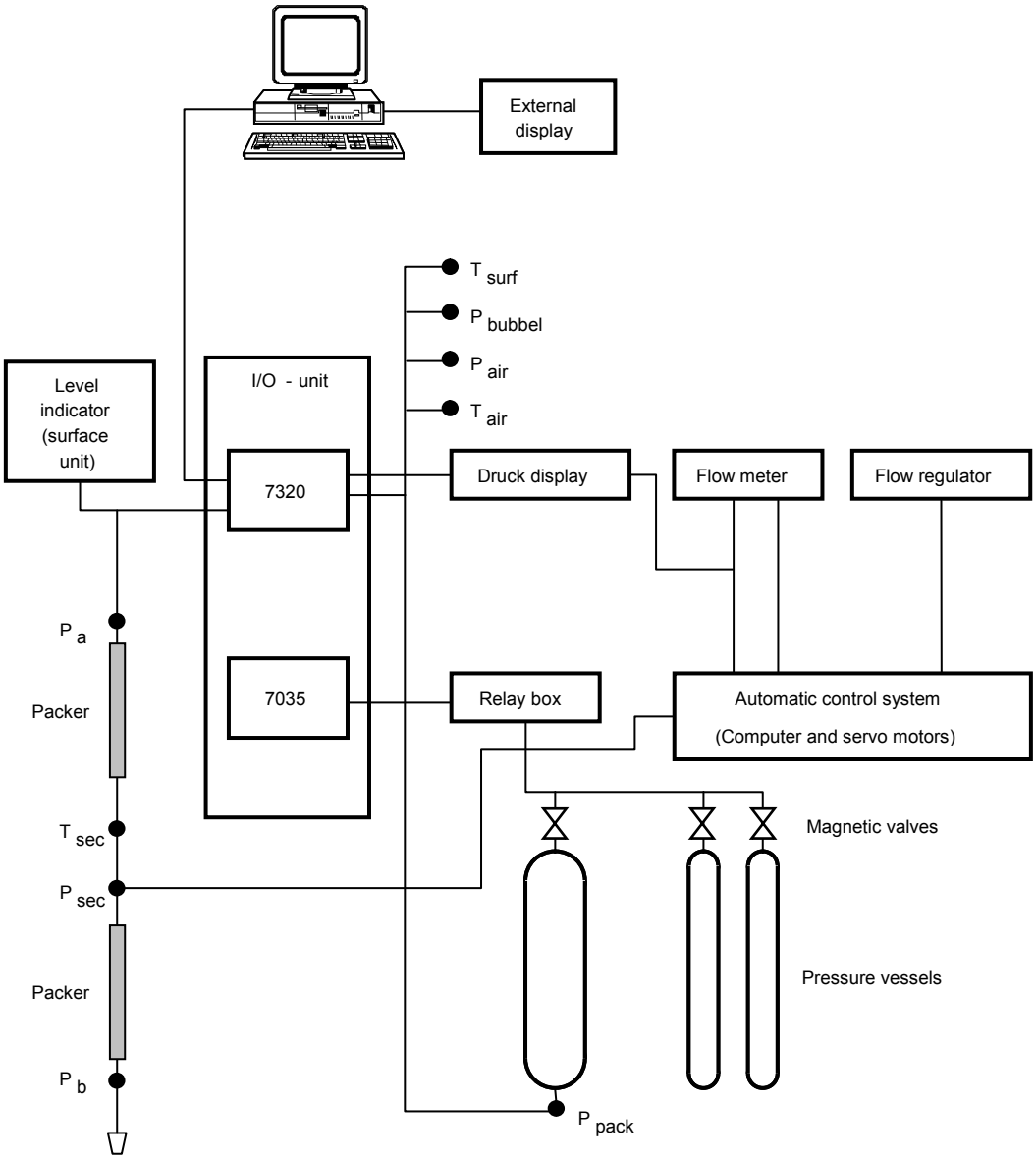

Figure 3-4. *Schematic drawing of the data acquisition system and the automatic control system in PSS.*

3.2.5 Data handling

With the PSS system, primary data are handled using the Orchestrator software (Version 2.3.8). During a test, data are continuously logged in *.odl-files. After the test is finished, a report file (*.ht2) with space separated data is generated. The *.ht2-file (mio-format) contains logged parameters as well as test-specific information, such as calibration constants and background data. Parameter values are presented as percentage of sensor measurement range and not in engineering units. The report file in ASCII-format is the raw data file delivered to the data base Sicada.

The *.ht2-files are automatically named with borehole id, top of test section and date and time of test start (as for example __KFM07A_0154.00_200502231910.ht2). The name differs slightly from the convention stated in Instructions for analysis of injection and single-borehole pump test, SKB MD 320.004.

Using the IPPLOT software (Version 3.0), the *.ht2-files are converted to parameter files suitable for plotting using the code SKB-plot and subsequent test analysis. In IPPLOT, the measured absolute pressures (P, P_a and P_b) are transformed to pressures at the respective top of sections as reference levels from the given borehole inclination and distances from the pressure sensor to the top of each section. For the pressure above the test section (P_a), top of section corresponds to the level of the bottom of the casing while for the pressure below the test section (P_b) top of section corresponds to the lower end of the lower packer.

A backup of data files was created on a regular basis by CD-storage and by sending the files to the Geosigma office in Uppsala by a file transfer protocol.

4 Analysis of hydraulic tests – methodology and experiences

In this chapter the analysis methods of the constant head- and recovery periods of the injection tests and of the pressure pulse tests are described. An example of an overview plot of a constant head injection test performed in PLU is shown in Figure 4-1. The injection- and recovery period are analysed separately.

4.1 Analysis of the constant head injection period

4.1.1 Brief theoretical background

4.1.1.1 Type curve analysis

For the injection period, a modification of the standard theoretical model for constant head tests in porous media by Jacob and Lohman (1952) /2/ is applied for estimating the transmissivity and skin factor when a certain period with apparent pseudo-radial flow could be identified from the data curve. The latter model is modified to include skin effects based on the effective wellbore radius concept to account for non-zero (negative) skin factors according to Hurst, Clark and Brauer (1969) /3/. The transmissivity and skin factor are calculated from the type curve matching according to Almén et al. (1986) /4/.

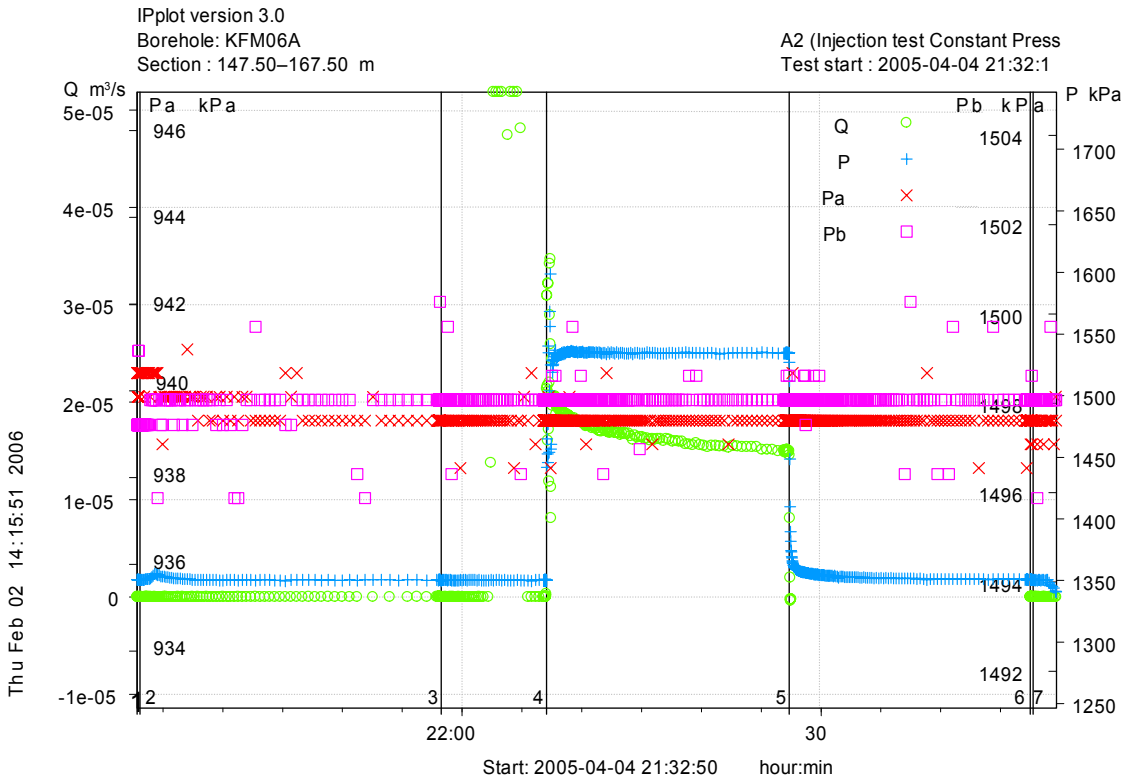

Figure 4-1. *Example of an overview plot of a constant head test showing the test phases (bottom scale), pressure in the test section (blue), flow rate (green), pressure above (red) and below (lilac) the test section. Test phase 4 and 5 correspond to the injection- and recovery period, respectively.*

The relationship between the skin factor and the effective borehole radius is according to Eqn. (4-1). In this concept, the skin factor and storativity are strongly correlated, cf Section 4.1.3.

$$\zeta = ln(r_w/r_{wf}). \quad (4\text{-}1)$$

ζ = skin factor.
r_w = borehole radius (m).
r_{wf} = effective borehole radius.

For tests showing apparent pseudo-spherical (leaky) flow, eventually transitioning to pseudo-stationary flow during the injection period, a model by Hantush (1959) /5/ for constant head tests is used for the evaluation. The effective wellbore radius concept is also implemented in the latter model to account for skin effects. However, the skin factor is not determined explicitly but can be calculated from the simulated (effective) borehole radius according to Eqn. (4-1). In addition, the apparent leakage coefficient K'/b' can be calculated from the simulated value on the leakage factor r/B.

For tests exhibiting fracture responses (a straight line of slope 0.5 or less in a log-log plot), models for single fractures are used for the transient analysis as a complement to the standard models described above. Models by Ozkan-Raghavan (1991a) /6a/ and (1991b) /6b/ for a single vertical fracture as well as the model by Gringarten-Ramey (1974) /7/ for a horizontal fracture were employed. In the fracture models, the hydraulic conductivity of the rock in directions perpendicular to the fracture plane together with the specific storativity of the rock are estimated together with the extension of the equivalent single fracture.

The parameter files of the test data (as described in Section 3.2.5) are imported to the AQTESOLV software and the evaluation of the tests is made according to the models described above. By the evaluation, the semi-log derivative of the inversed flow rate data was calculated using different algorithms and filter factors to achieve appropriate smoothing of the data. The routine data processing of the measured data was done according to the Instruction for analysis of injection and single-hole pumping tests (SKB MD 320.004).

For evaluation of the test data, no corrections of the measured flow rate and absolute pressure data (e.g. due to barometric pressure variations or tidal fluctuations) have been made. For short-time single-hole tests, such corrections are generally not needed, unless very small pressure changes are applied. No subtraction of the barometric pressure from the measured absolute pressure has been made, since the length of the test periods are short relative to the time scale for barometric pressure changes. In addition, pressure differences rather than the pressure magnitudes are used by the evaluation.

The transient analysis of the tests was performed using a special version of the analysis software AQTESOLV, which enables both manual and automatic type curve matching. The analysis may be performed forward (a simulated response curve is generated for a given set of parameters and matched to the data curve) or backward (the best fitting parameters to a given response curve are determined). The transient evaluation is generally carried out as an iterative process of manual type curve matching and automatic matching. The sensitivity on the response curve of each parameter can be tested individually.

4.1.1.2 Steady-state analysis

In conjunction with the transient analysis, a preliminary steady-state analysis of transmissivity according to Moye's formula (denoted T_M) is made from the injection period of all tests according to the following equation (Almén et al. 1986) /4/:

$$T_M = \frac{Q_p \cdot \rho_w \cdot g}{dp_p} \cdot C \qquad (4\text{-}2)$$

$$C_M = \frac{1 + \ln\left(\frac{L_w}{2r_w}\right)}{2\pi}$$

Q_p = flow rate by the end of the flow period (m^3/s).
ρ_w = density of water (kg/m^3).
g = acceleration of gravity (m/s^2).
C_M = geometrical shape factor (–).
dp_p = p_p–p_i (Pa).
r_w = borehole radius (m).
L_w = section length (m).

The designations of the flow rate and pressure parameters are shown in Figure 3-1.

4.1.2 Determination of the flow model

Firstly, a qualitative evaluation of actual flow regimes, e.g. wellbore storage (WBS), pseudo-radial flow regime (PRF), pseudo-spherical flow regime (PSF) and pseudo-stationary flow regime (PSS), respectively, is performed. In addition, indications of outer boundary conditions, i.e. apparent no-flow boundaries (NFB) or constant head boundaries (CHB) during the tests are identified. The qualitative evaluation of the injection period is mainly interpreted from the log-log plots of flow rate together with the corresponding derivative.

Flow regimes may be described in terms of a generalized radius of influence from the borehole:

- **Inner zone (iz).** Representing very early response which reflects the hydraulic interaction between the borehole and rock close to the borehole. It may be affected by turbulent losses or other head losses or improved by fractures intersecting the borehole. The hydraulic properties of the inner zone are generally captured as the skin factor.
- **Middle zone (mz**). Representing the first response from which it is considered possible to evaluate representative hydraulic properties of the rock or hydraulic feature near the borehole, in the time span from t_1 to t_2.
- **Outer zone (oz).** Representing the response of hydraulic feature(s)/boundary conditions connected to the actual hydraulic feature interpreted from the middle zone, at times later than t_2. Some times it is possible to deduce the possible character of the hydraulic feature or boundary and sometimes possible to evaluate the hydraulic properties or boundary conditions.

In particular, time intervals with pseudo-radial flow, reflected by a constant (horizontal) derivative in the test diagrams, are identified. Pseudo-linear flow, indicating flow in a single fracture, is reflected by a straight line of slope 0.5 or less in log-log diagrams at the beginning of the test, both for the measured variable (flow rate) and its derivative. A true spherical flow regime (3D) is reflected by a straight line with a slope of –0.5 for the derivative. However, steeper slopes of the derivative may indicate transitions to pseudo-spherical (leaky) or ultimately, pseudo-stationary flow if apparent constant head boundaries are present. The latter flow regime corresponds to almost steady-state conditions with a rapidly decreasing derivative towards zero.

Pseudo-spherical flow may be conceptually interpreted in several ways, for example:

- increasing flow dimension with distance from the borehole, e.g. flow in a thick well-connected fracture zone or,
- increasing transmissivity with distance from the borehole, e.g. due to interconnecting fractures with higher transmissivity at some distance.

Examples of different flow regimes are presented in Figure 4-2a-e.

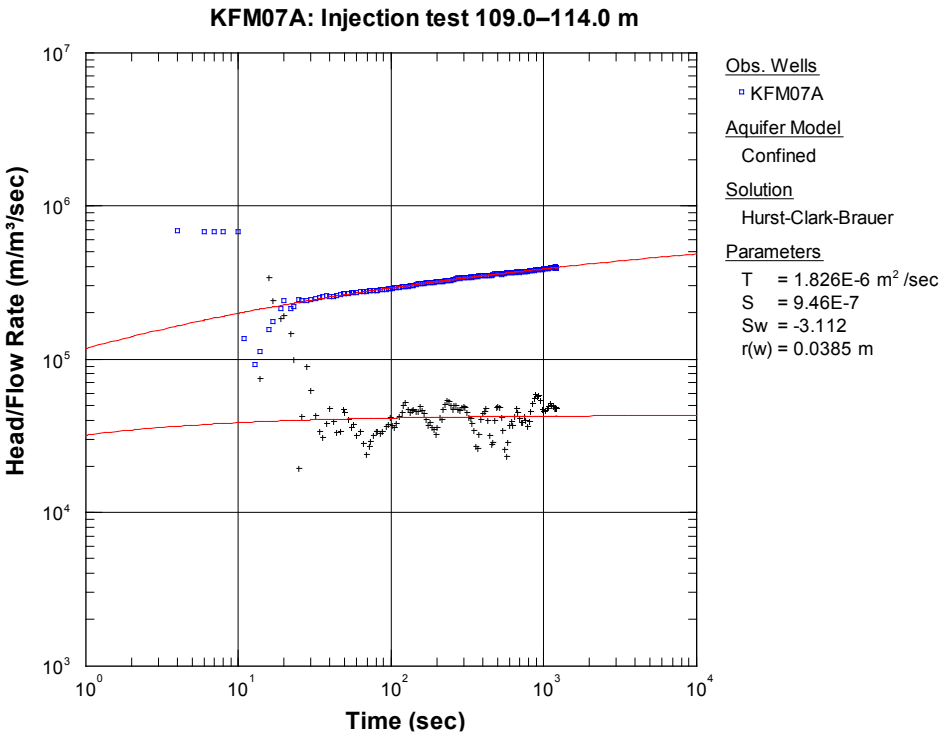

Figure 4-2a. *Example of a dominating pseudo-radial flow regime (PRF) during the injection period of test section KFM07A:109.0–114.0 m (blue = head/flow rate and black = derivative).*

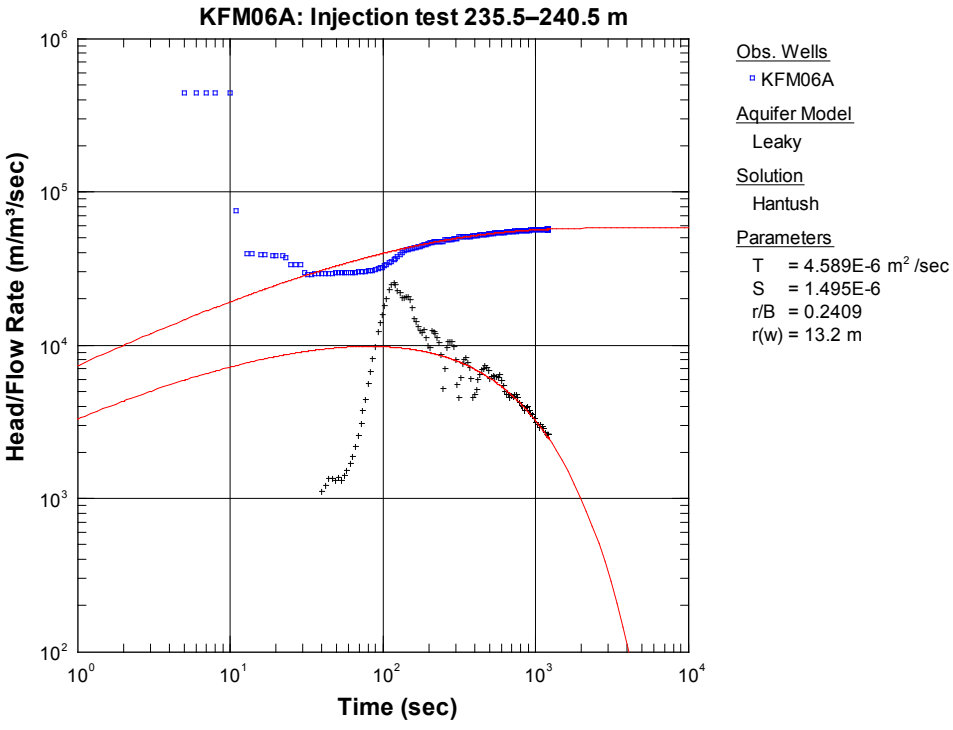

Figure 4-2b. *Example of a dominating pseudo-spherical flow regime (PSF) during the injection period of test section KFM06A:235.5–240.5 m (blue = head/flow rate and black = derivative).*

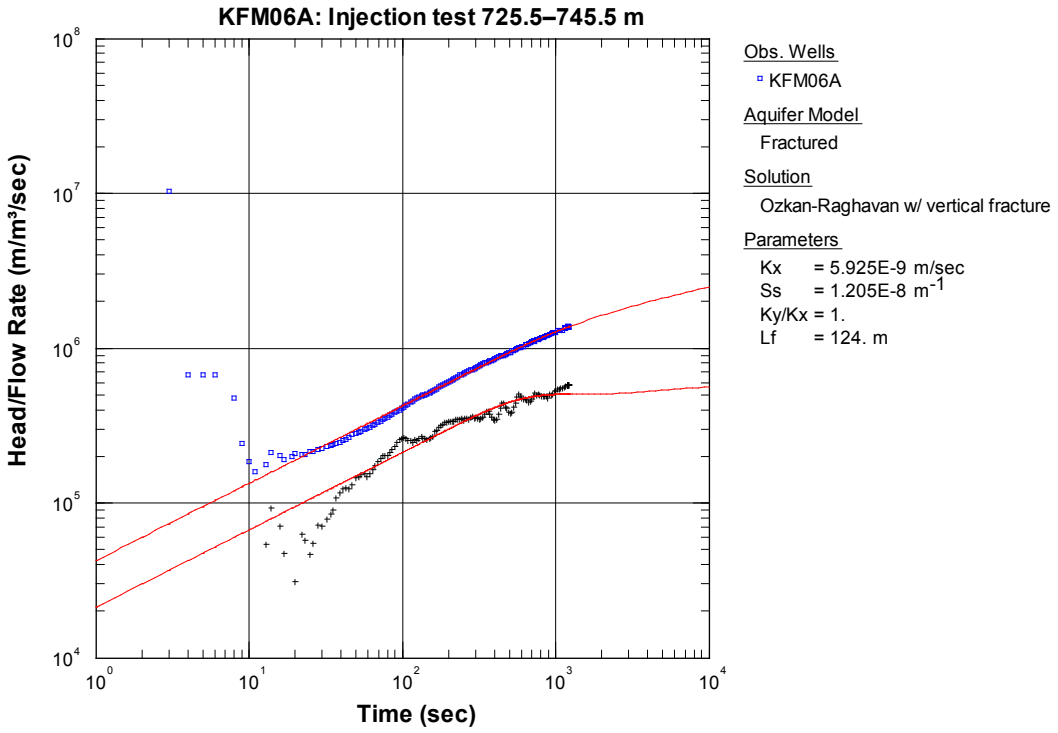

Figure 4-2c. *Example of a dominating pseudo-linear flow regime (PLF) during the injection period of test section KFM06A:725.5–745.5 m (blue = head/flow rate and black = derivative).*

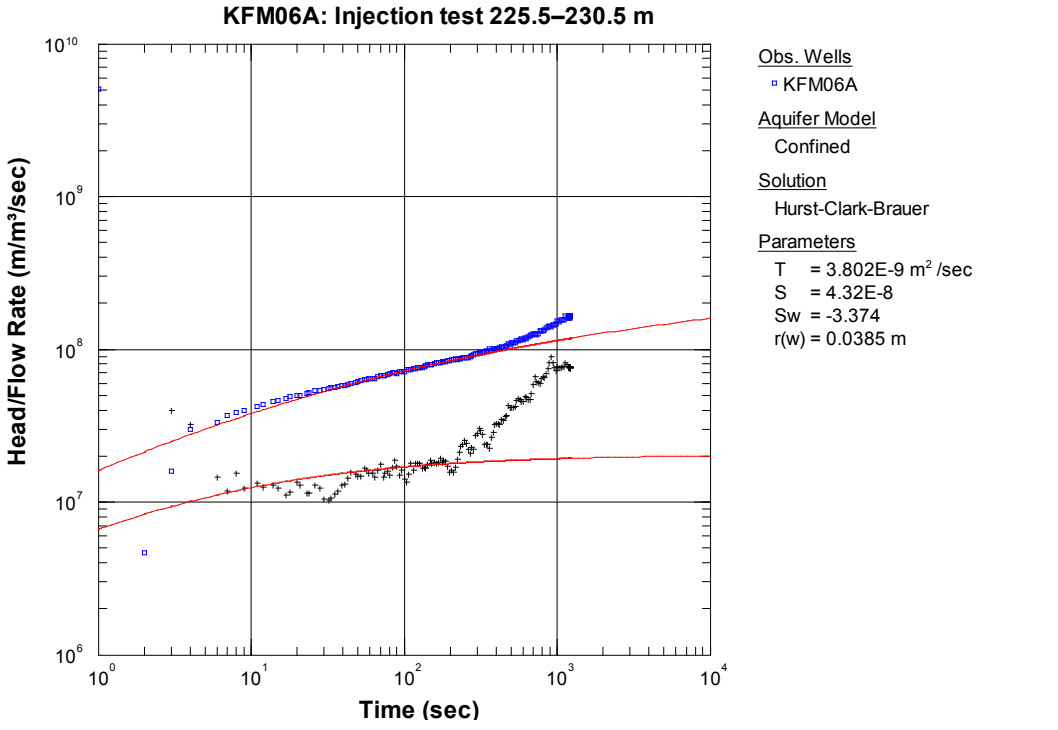

Figure 4-2d. *Example of a pseudo-radial flow regime transitioning to an apparent no-flow boundary (NFB) during the injection period of test section KFM06A:225.5–230.5 m (blue = head/flow rate and black = derivative.*

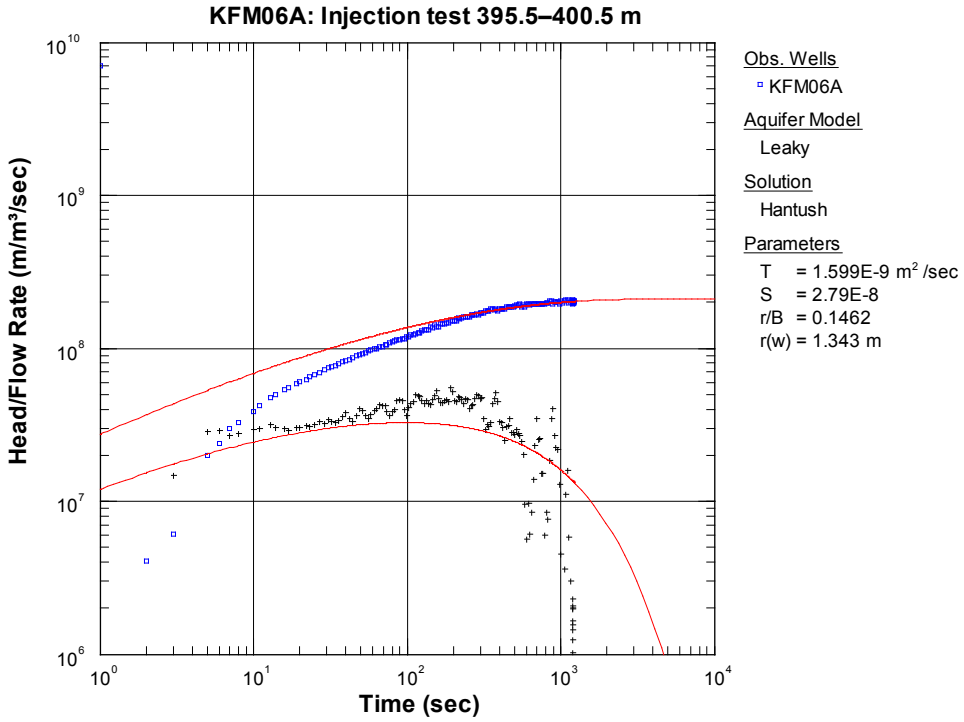

Figure 4-2e. *Example of a pseudo-radial flow regime transitioning to pseudo-stationary flow (PSS) caused by an apparent constant head boundary (CHB) during the injection period of test section KFM06A:395.5–400.5 m (blue = head/flow rate and black = derivative).*

4.1.3 Analysis using a prescribed storativity, deriving the skin factor

According to the Instruction for analysis of injection and single-hole pumping tests (SKB MD 320.004) the storativity is estimated at $1 \cdot 10^{-6}$ by the evaluation of the tests. However, in May, 2005 it was decided by SKB to estimate the storativity for each test by a certain regression formula, derived from previous injection tests at Simpevarp described in SKB (2006) /8/. At Forsmark, this procedure to estimate the storativity was firstly used in borehole KFM07A and in all subsequent boreholes.

In this procedure, the storativity is calculated using a combination of the fixed storativity approach and an empirical relationship between storativity and transmissivity according to Eqn. (4-3). Firstly, the transmissivity and skin factor are obtained by type curve matching using a fixed storativity value of 10^{-6} according to the instruction SKB MD 320.004. From the transmissivity value obtained, the storativity was then calculated according to Eqn. (4-3) and the type curve matching is repeated with the new storativity value as an input parameter, resulting in a new estimate of the skin factor.

$$S = 0.0007 \cdot T^{0.5} \qquad (4\text{-}3)$$

S = storativity (–).

T = transmissivity (m^2/s).

In most cases, the change of storativity does not significantly alter the calculated transmissivity in the repeated type curve matching. Instead, the estimated skin factor, which is strongly correlated to the storativity using the effective borehole radius concept according to Eqn. (4-1), was changed correspondingly.

4.1.4 Analysis examples

In Figure 4-2a-e examples of qualitative and quantitative evaluation of typical injection periods exhibiting different flow regimes.

4.1.5 Uncertainties

4.1.5.1 Poor pressure control

Two major sources of uncertainties related to the pressure control during the injection period can be defined:

- the stabilisation time to obtain a constant injection pressure in the test section,
- maintenance of a constant injection pressure during the injection period.

Both sources of uncertainty are mainly related to the performance and application of the automatic pressure control system in PSS. Available borehole information, e.g. from difference flow logging and borehole TV (BIPS), was used to select the most efficient way to achieve a constant injection pressure in the tests section. In very low-transmissive sections, the pressure vessel was used directly to control the injection pressure instead of using the automatic system. In Figures 4-3a and b the estimated stabilisation times for the injection pressure from previous tests in 5 m sections in boreholes KFM03A and KFM04A at Forsmark when using the automatic pressure control system or the pressure vessel directly, respectively are shown.

Figure 4-3a shows the total number of all analysable tests (N = 219) in KFM03A and KFM04A in different classes of stabilisation time before an injection pressure within ± 5 kPa of the final pressure was reached. The automatic flow regulation system was used as standard except in low-transmissive sections in which the pressure vessel was used directly. The figure shows that short stabilisation times (0–10 s) were achieved in all tests in the low-transmissive sections (N = 141) by using the pressure vessel directly. Figure 4-3b shows the stabilisation times of the remaining tests (N = 78) in which the automatic flow regulation system was used. For the majority of these tests the stabilisation times range between 10–50 s. Relatively long stabilisation times may occur in high-transmissive test sections, mainly due to the limitations of the injection flow rate in the PSS system.

The other source of uncertainty related to pressure control is the stability of the pressure during the injection period. Large pressure fluctuations or deviating trends of the pressure may cause corresponding fluctuations of the flow rate and thus more problematic to define flow regimes during this period. An example of cases that may lead to pressure control problems is when apparent no-flow boundaries (NFB) affect the test or other factors causing a rapid decrease of the flow rate. In addition, in very high-transmissive test sections only a low injection pressure (c. 10 kPa) may be achieved due to the limited flow rate capacity of the PSS-system. In such tests pressure control problems may also arise.

The stabilisation times and pressure control achieved by using the automatic system as well as the pressure vessel directly in low-transmissive sections are considered as sufficient to allow a representative transient evaluation of the injection (and subsequent recovery) period of the tests in most cases. The quality of the pressure control constitutes one of the items in Index 5: Ambiguous interpretation in the Statistics of the tests, which is further discussed in Chapter 6.

4.1.5.2 Noise in the flow rate data

Noise in the flow rate data frequently appear in low-transmissive sections due to noise from the flow meter. Noise in the flow rate data may also be present at certain flow rate ranges in relation to an unfavourable working (end) position of the control valves in the automatic system.

4.1.6 Flow rates below the measurement limit

The standard lower measurement limit for flow rate for injection tests with the PSS system is c. 1 mL/min ($1.7 \cdot 10^{-8}$ m^3/s), cf Table 3-2. However, if the flow rate for a test was close to, or below, the standard lower measurement limit, a test-specific estimate of the lower measurement limit of flow rate was attempted. The test-specific lower limit was based on the measurement noise level of the flow rate just before and after stop of the injection period. The decisive factor of the magnitude of the varying lower measurement limit for the tests is not identified, but it might be of both technical and hydraulic character. The estimated, test-specific lower measurement limit of flow rate of the injection tests performed at Forsmark generally ranges from c. $5–10 \cdot 10^{-9}$ m^3/s (c. 0.3–0.6 mL/min).

In some boreholes, pressure pulse tests have been performed in sections close to, or below the lower measurement limit. The results of these tests are presented in Section 4.3.

4.1.7 Estimation of the radius of influence

The equivalent radius of influence at a certain time may be roughly estimated from Jacob's approximation of the Theis' well function, Cooper and Jacob (1946) /9/:

$$r_i = \sqrt{\frac{2.25Tt}{S}} \qquad (4\text{-}4)$$

T= representative transmissivity from the test (m^2/s).

S= storativity estimated from Equation (4-3).

r_i= radius of influence (m).

t= time after start of injection (s).

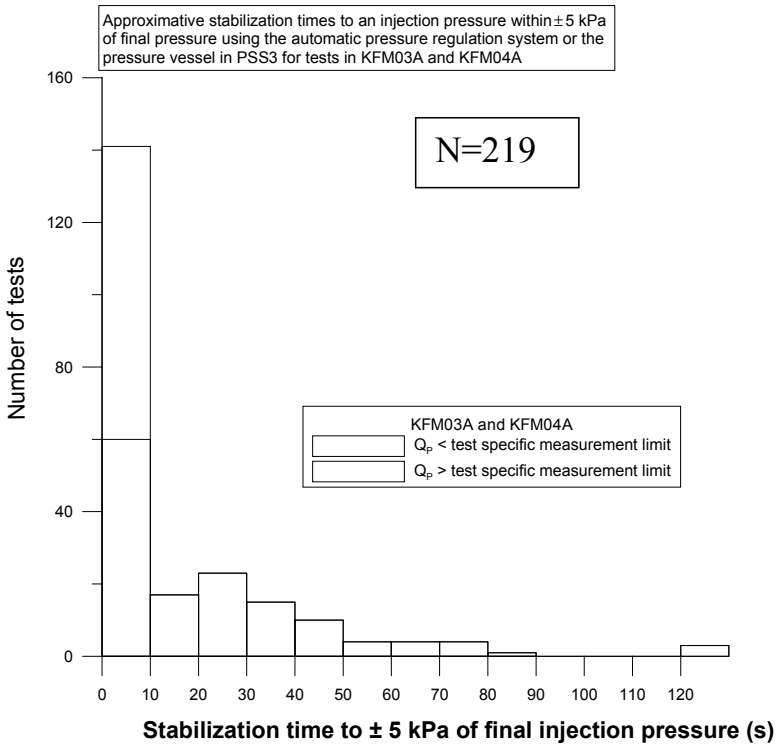

Figure 4-3a. *Number of tests in different stabilisation time intervals to achieve an injection pressure within ± 5 kPa of the final pressure for tests in boreholes KFM03A and KFM04A when using the automatic pressure control system or the pressure vessel directly.*

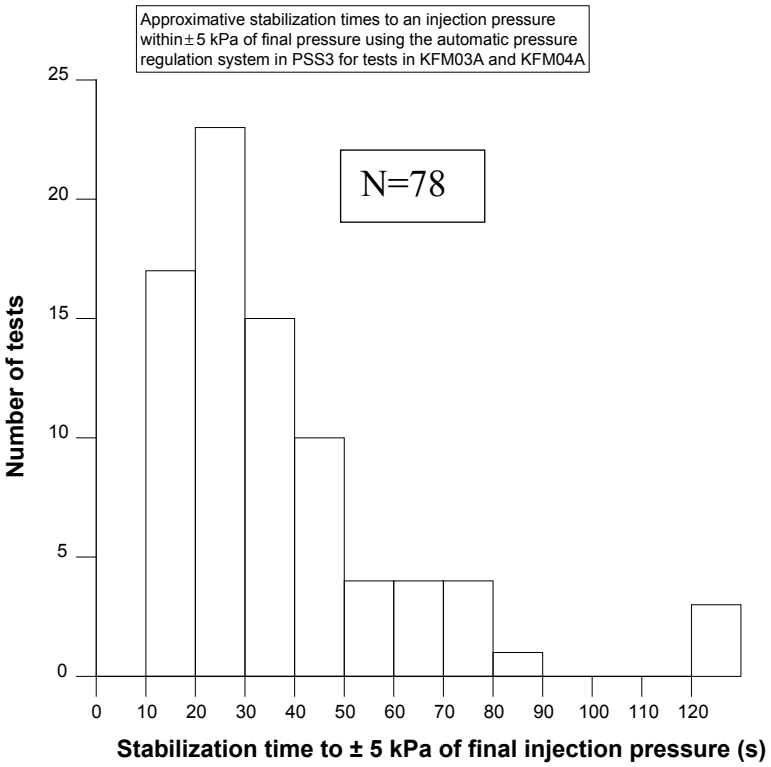

Figure 4-3b. *Number of tests in different stabilisation time intervals to achieve an injection pressure within ± 5 kPa of the final pressure for tests in boreholes KFM03A and KFM04A when using the automatic pressure control system.*

If a certain time interval of pseudo-radial flow (PRF) from time t_1 to t_2 can be identified during the test, the radius of influence is estimated using time t_2 in Equation (4-4). If no interval of PRF can be identified, the actual total flow time t_p is used. The estimated radius of influence may be used to roughly estimate the length of the hydraulic feature(s) tested.

Furthermore, an r_i-index (–1, 0 or 1) is defined to characterize the hydraulic conditions by the end of the test. The r_i-index is defined as shown below. It is assumed that a certain time interval with pseudo-radial flow (PRF) can be identified between t_1 and t_2 during the test.

- r_i-index = 0: The transient response indicates that the size of the hydraulic feature tested is greater than the radius of influence based on the actual test time ($t_2 = t_p$), i.e. the PRF is continuing at stop of the test. This fact is reflected by a flat derivative at this time.
- r_i-index = 1: The transient response indicates that the hydraulic feature tested is connected to a hydraulic feature with lower transmissivity or an apparent barrier boundary (NFB). This fact is reflected by an increase of the derivative. The size of the hydraulic feature tested is estimated as the radius of influence based on t_2.
- r_i-index = –1: The transient response indicates that the hydraulic feature tested is connected to a hydraulic feature with higher transmissivity or an apparent constant head boundary (CHB). This fact is reflected by a decrease of the derivative. The size of the hydraulic feature tested is estimated as the radius of influence based on t_2.

If a certain time interval of PRF cannot be identified during the test, the r_i-indices –1 and 1 are defined as above. In such cases the radius of influence is estimated using the actual flow time t_p in Equation (4-4).

4.2 Analysis of the recovery period

4.2.1 Brief theoretical background

4.2.1.1 Type curve analysis

For transient analysis of the recovery period, a theoretical solution presented by Dougherty and Babu (1984) /10/ was used when a certain period with pseudo-radial flow could be identified from the data curve. The same authors presented a variety of transient solutions for flow in fractured porous media, accounting for e.g. wellbore storage and skin effects, double porosity etc. The solution for wellbore storage and skin effects is analogous to the corresponding solution presented in Earlougher (1977) /11/ and based on the effective wellbore radius concept to account for non-zero (negative) skin factors as for the analysis of the injection period.

The model by Dougherty-Babu /10/ was used to estimate the transmissivity and skin factor from the recovery period for tests showing a pseudo-radial flow regime. The storativity was calculated using Eqn. (4-3) in the same way as described above for the transient analysis of the injection period. In addition, the wellbore storage coefficient was estimated, cf Section 4.2.3.

For tests showing pseudo-spherical (leaky) flow, eventually transitioning to pseudo-stationary flow, during the recovery period, the standard model by Hantush (1955) /12/ was used for the evaluation. As for the injection period, the skin factor is not estimated explicitly in this model but can be calculated from the simulated (effective) borehole radius according to Eqn. (4-1). The wellbore storage coefficient is calculated from the simulated radius of the fictive standpipe according to Eqn. (4-5). In addition, the apparent leakage coefficient K'/b' can be calculated from the simulated value on the leakage factor r/B.

For tests showing fracture responses (a straight line of slope of 0.5 or less in a log-log plot) models for equivalent single fractures were used for the transient analysis as a complement to the standard models described above. The models by Ozkan-Raghavan /6a/ and /6b/, respectively for a vertical fracture and the model by Gringarten-Ramey /7/ for a horizontal fracture were employed. Type curve matching provided values of the equivalent hydraulic conductivity of the rock K and the estimated extent of the equivalent fracture for a given value on the specific storativity S_s. The test section length was then used to convert K and S_s to T and S, respectively to be compared with corresponding estimates from other models. By the simulation, the ratio K_x/K_y of the hydraulic conductivity of the rock in the x and y-direction respectively was assumed to be 1.0 (one).

The same procedures were followed by the processing and evaluation of the test data from the recovery period as described in Section 4.1 for the injection period. The recovery data are plotted versus Agarwal equivalent time (Agarwal 1980) /13/ to account for remaining transients in flow rate and pressure in the rock created during the injection period. The calculation of the Agarwal equivalent time is based on the multi-rate approach, i.e. superposition of the flow rate history during the injection period. If the final flow rate data are scattered, e.g. in low-transmissive test sections, smoothing of the data may be nessecary to achieve a correct recovery curve for transient analysis.

A separate investigation of different ways to calculate the Agarwal equivalent time for the recovery period after constant head tests is presented in Appendix 5. Three different ways of calculation have been studied, i) based on the actual injection time t_p, ii) based on the pseudo-injection time t_{pp} and iii) based on the flow sequence during the injection period (multi-rate). These three ways have been examined in the analysis of selected injection tests in core boreholes at Forsmark. The results indicate that, in analyses of tests in sections with higher transmissivity than about $1 \cdot 10^{-8}$ m^2/s, the difference is small or insignificant in the shape of the recovery curve and for evaluated hydraulic parameters, regardless of which of the above-mentioned three ways of calculating the Agarwal equivalent time is used. However, for tests in sections with a transmissivity lower than about $1 \cdot 10^{-8}$ m^2/s, greater differences may occur in the appearance of the recovery curve and calculated hydraulic parameters.

It was concluded that the multi-rate assumption is the way that is most correct and theoretically most free from objection for calculating the Agarwal equivalent time after constant pressure tests. It is thus assumed that flow variations during the injection period will affect the pressure during the recovery period. In very low-transmissive test sections and in sections where incomplete recovery of the pressure is achieved during the recovery period (e.g. due to restrictions in the extension and/or aperture of fractures) the recovery curve can be of completely different shapes when using t_p or the multi-rate assumption respectively in the calculation of the Agarwal equivalent time. This fact may influence interpretation of flow regimes as well as calculation of hydraulic parameters from the recovery period. In such sections the interpretation is, however, uncertain regardless of which method is used.

4.2.1.2 Horner analysis

Conventional Horner analysis by extrapolation of the straight line for pseudo-radial flow to estimate the static pressure in semi-logarithmic diagrams was generally not performed for the injection tests at Forsmark. Although the corresponding analysis may be performed in recovery diagrams with Agarwal equivalent time on the time scale (Almén et al. 1986) /4/, determination of the static pressure was not done at Forsmark as a routine. However, in borehole KSH02 at Simpevarp Horner analysis of the static pressure was performed for tests exhibiting a well-defined straight line indicating pseudo-radial flow (Ludvigson et al. 2004) /14/.

4.2.2 Determination of the flow model

The determination of the flow model for the transient analysis of the recovery period is based on the same technique and criteria as described above for the injection period also including wellbore storage effects. Apparent no-flow- (NFB) and constant head boundaries (CHB), or equivalent boundary conditions of single fractures, are reflected by a rapid increase/decrease of the derivative, respectively.

Due to the limited resolution of the pressure sensor, the corresponding derivative may some times erroneously indicate a false horizontal line by the end of periods with pseudo-stationary flow, cf Section 6.5.

4.2.3 Determination of the wellbore storage coefficient

4.2.3.1 Type curve analysis

In the transient analysis of the recovery period wellbore storage is represented by a radius of a fictive standpipe, denoted fictive casing radius, r(c), and connected to the test section. This concept, which represents an equivalent open borehole test configuration, is equivalent to calculating the wellbore storage coefficient from the compressibility in an isolated test section according to Eqn. (4-7). In non-stiff test systems, the water compressibility should be replaced by the effective compressibility including packer compliance and other factors affecting the stiffness of the test system. This item is further discussed in Chapter 5.

The wellbore storage coefficient was calculated from the transient analysis of the recovery period according to Eqn. (4-5).

$$C = \frac{\pi \cdot r(c)^2}{\rho_w \cdot g} \qquad (4\text{-}5)$$

C = wellbore storage coefficient (m^3/Pa).
$r(c)$ = simulated radius of fictive standpipe (m).
ρ_w = density of water (kg/m^3).
g = acceleration of gravity (m/s^2).

4.2.3.2 From the initial straight line of slope 1:1

In addition, the wellbore storage coefficient was estimated from the initial straight line of slope 1:1 in the logarithmic diagram from the recovery period according to Eqn. (4-6), cf Almén et al. (1986) /4/:

$$C = \frac{Q_p \cdot dt_{e1}}{p_1} \qquad (4\text{-}6)$$

Q_p = final flow rate during the injection period (m^3/s).
dt_{e1} = Agarwal equivalent time at an arbitrary point on the straight line of slope 1:1 (s).
p_1 = pressure change at the same point (Pa).

In general, there is a good agreement between the C-values estimated from the transient analysis and those determined from the initial straight line of slope 1:1.

4.2.3.3 Comparison with the theoretical value

The theoretical, net borehole storage coefficient, C, may be estimated from the actual borehole geometrical data, test configuration and fluid properties for a perfectly stiff test system. For an isolated test section in a stiff system, the net wellbore storage coefficient may be calculated as Earlougher (Almén et al. 1986) /4/:

$$C_{net} = V_w \cdot c_w = L_w \cdot \pi \cdot r_w^2 \cdot c_w \qquad (4\text{-}7)$$

V_w = net water volume in test section (m^3).
r_w = nominal borehole radius (m).
L_w = section length (m).
c_w = compressibility of water (Pa^{-1}).

The calculated net values of C for standard injection tests with PSS are shown in Table 4-1. The net water volume in the test section, V_w, for the injection tests was calculated by subtracting the volume of equipment in the test section (pipes and thin hoses) from the total volume of the test section. The water compressibility is assumed at $4.6 \cdot 10^{-10}\ Pa^{-1}$. The net wellbore storage coefficient is constant for a given borehole diameter, section length, equipment configuration and fluid properties in the test section. C_{net} may be compared with the estimated, effective wellbore storage coefficient (C_{eff}) and estimated values on C from injection tests in different section length. Such a comparison is shown in Section 6.6. The estimation of C_{eff} is presented in Section 5.1.2.

4.2.4 Determination of the static formation pressure and the equivalent freshwater head

As discussed above, the static formation pressure has not been performed for the injection tests at Forsmark by routine. Neither, the equivalent freshwater head has been determined. However, in borehole KSH02 at Simpevarp (Ludvigson et al. 2004) /14/ analysis of the static pressure as well as equivalent freshwater head was performed. The hydraulic (freshwater) head distribution along the borehole was determined in the following way. Firstly, the measured atmospheric pressure (p_a) before the start of the flow period was subtracted from the pressure in the test section before the start of the flow period (p_i) or Horner pressure if such estimation was available. The freshwater head at a certain elevation (from ToC) was calculated according to the following expression:

$$h_{FWi} = (p_i - p_{atm})/(\rho_w \cdot g) + z \qquad (4\text{-}8)$$

h_{FWi} = freshwater head in test section before start of flow period (metres above sea level).
p_i = pressure in test section immediately before start of flow period (Pa). When the Horner pressure p* was estimated it was used instead of p_i.

p_{atm} = atmospheric pressure before start of flow period (Pa).
ρ_w = density of freshwater (kg/m^3), assumed to 1,000 kg/ m^3.
g = acceleration of gravity, g = 9.81 m/s^2 is assumed according to SKB MD320.004.
z = elevation of measurement point (metres above sea level).

4.2.5 Analysis using a prescribed storativity, deriving the skin factor

The transient analysis of the recovery period is similar to the analysis of the injection period, described in Section 4.1.3. Firstly, the transmissivity, skin factor and wellbore storage coefficient are obtained by type curve matching using a fixed storativity value of 10^{-6} according to the instruction SKB MD 320.004. From the transmissivity value obtained, the storativity is then calculated according to Eqn. (4-3) and the type curve matching is repeated with the new storativity value as an input parameter, resulting in a new estimate of the skin factor.

4.2.6 Analysis examples

In Figure 4-4a-g, examples of qualitative and quantitative evaluation of typical recovery periods exhibiting different flow regimes are presented.

Table 4-1. Calculated net values of the wellbore storage coefficient C for injection tests with different section length based on geometrical properties of the borehole and equipment configuration in the test section.

Borehole radius (m)	Section length (m)	Volume of test section (m^3)	Volume of equipment in test section (m^3)	Vw (m^3)	Cnet (m^3/Pa)
0.038	100	0.454	0.061	0.393	1.9·10–10
0.038	20	0.091	0.013	0.078	3.6·10–11
0.038	5	0.023	0.004	0.019	8.6·10–12

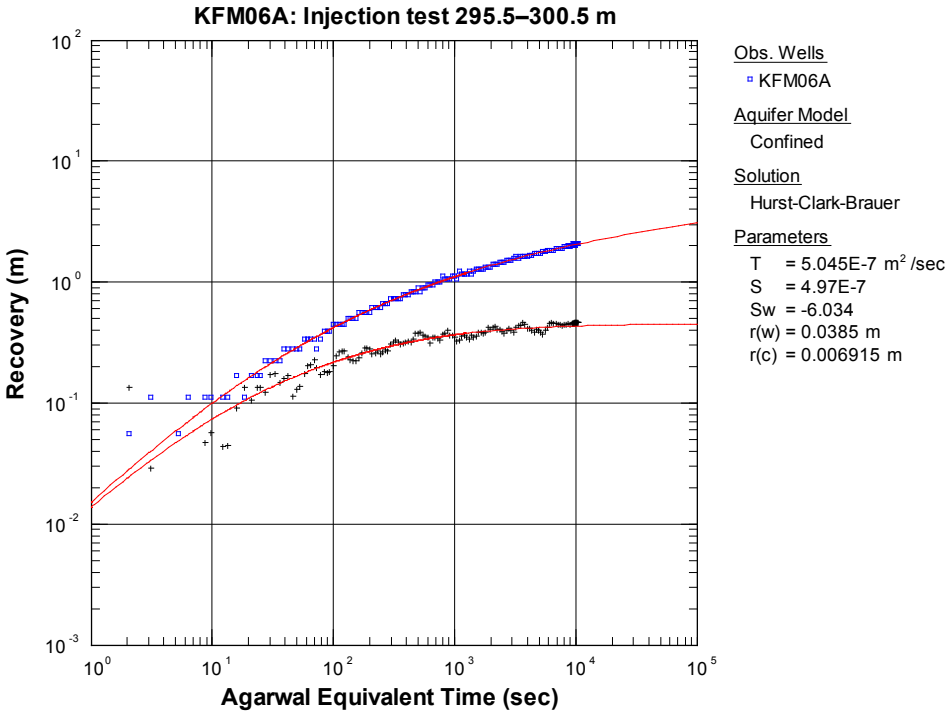

Figure 4-4a. *Example of a transition to a pseudo-radial flow regime (PRF) by the end of the recovery period of test section KFM06A:295.5–300.5 m (blue = head/flow rate and black = derivative).*

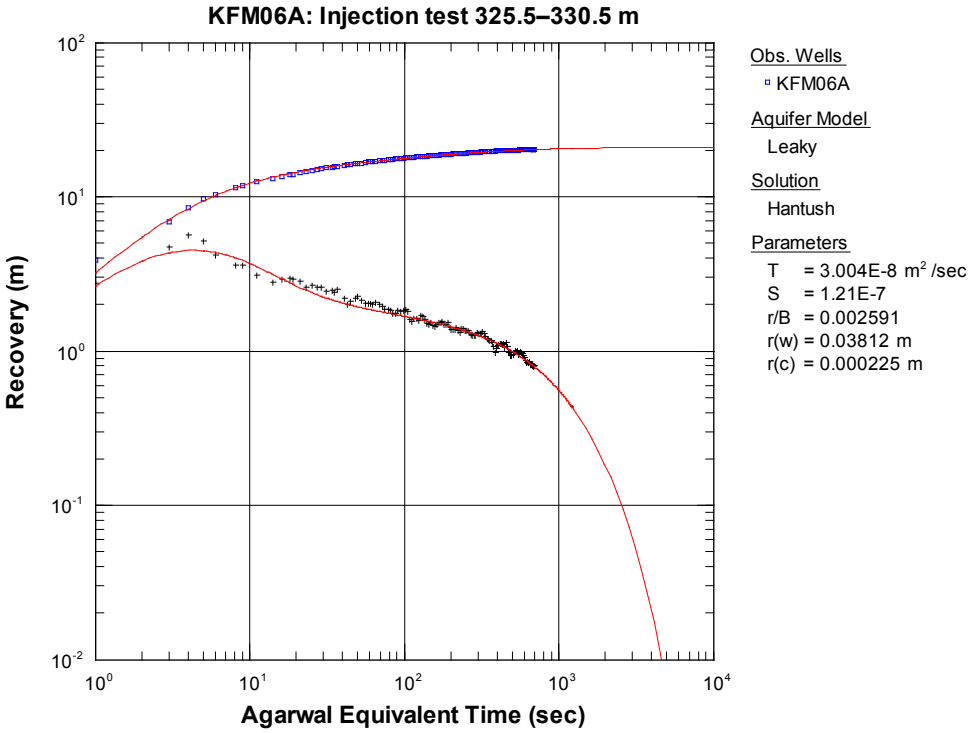

Figure 4-4b. *Example of a dominating pseudo-spherical flow regime (PSF) during the recovery period of test section KFM06A:325.5–330.5 m (blue = head/flow rate and black = derivative).*

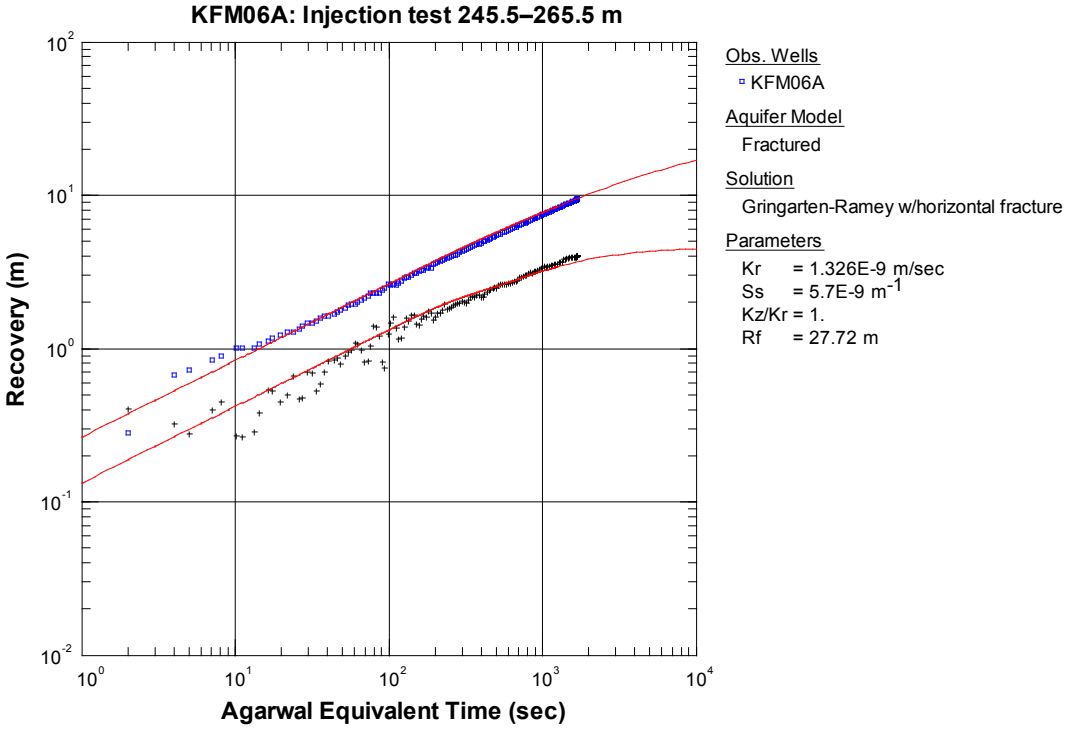

Figure 4-4c. *Example of a dominating pseudo-linear flow regime (PLF) during the recovery period of test section KFM06A:245.5–265.5 m (blue = head/flow rate and black = derivative).*

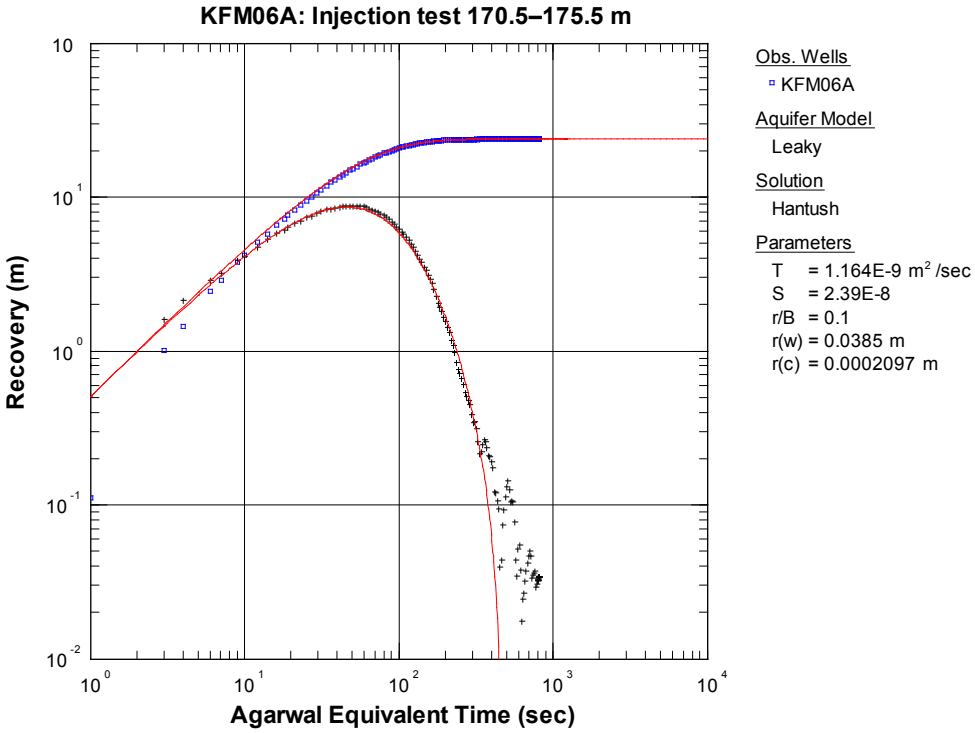

Figure 4-4d. *Example of a transition to a pseudo-stationary flow regime (PSS) during the recovery period of test section KFM06A:170.5–175.5 m (blue = head/flow rate and black = derivative).*

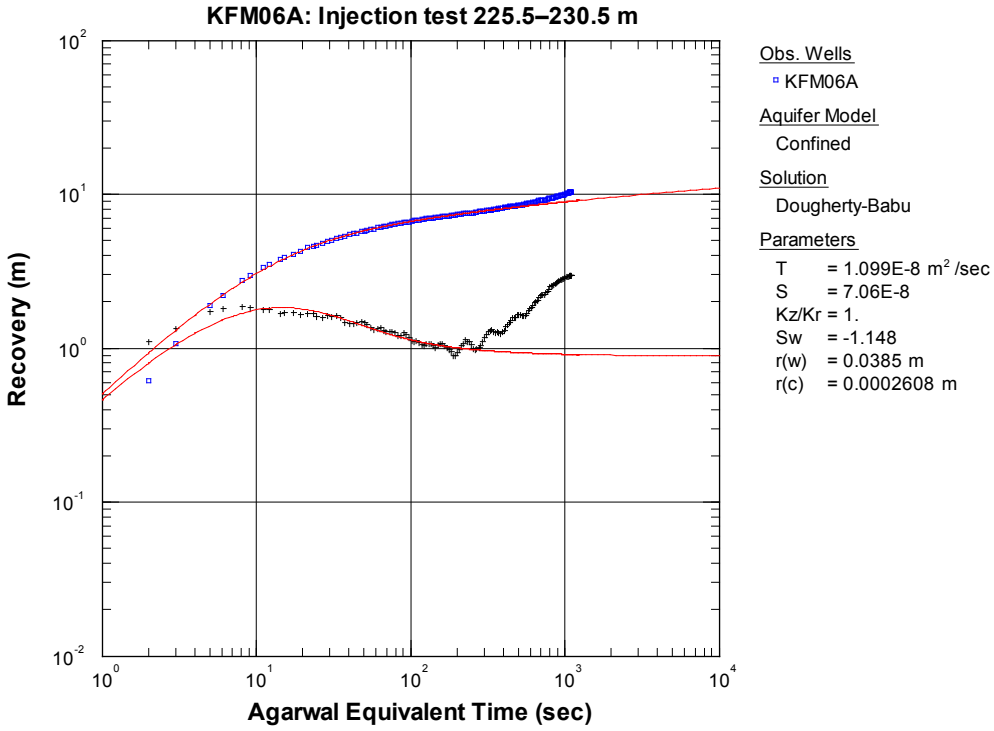

Figure 4-4e. *Example of an apparent no-flow boundary (NFB) by the end of the recovery period of test section KFM06A:225.5–230.5 m (blue = head/flow rate and black = derivative).*

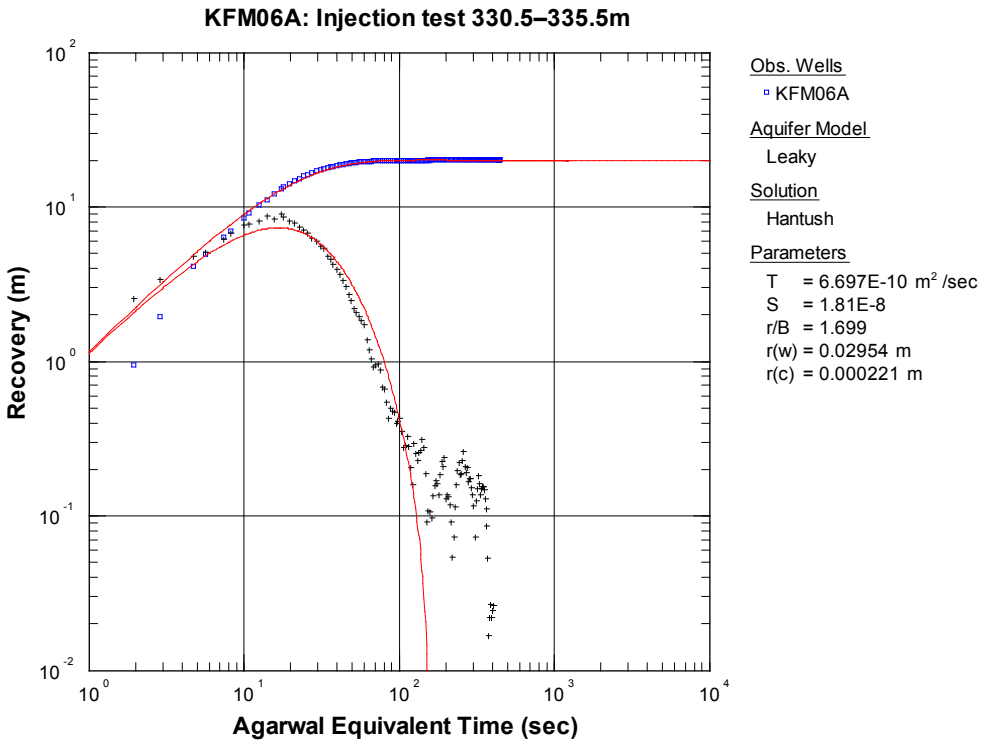

Figure 4-4f. *Example of a transition to a pseudo-stationary flow regime (PSS) during the recovery period of test section KFM06A:330.5–335.5 m (blue = head/flow rate and black = derivative).*

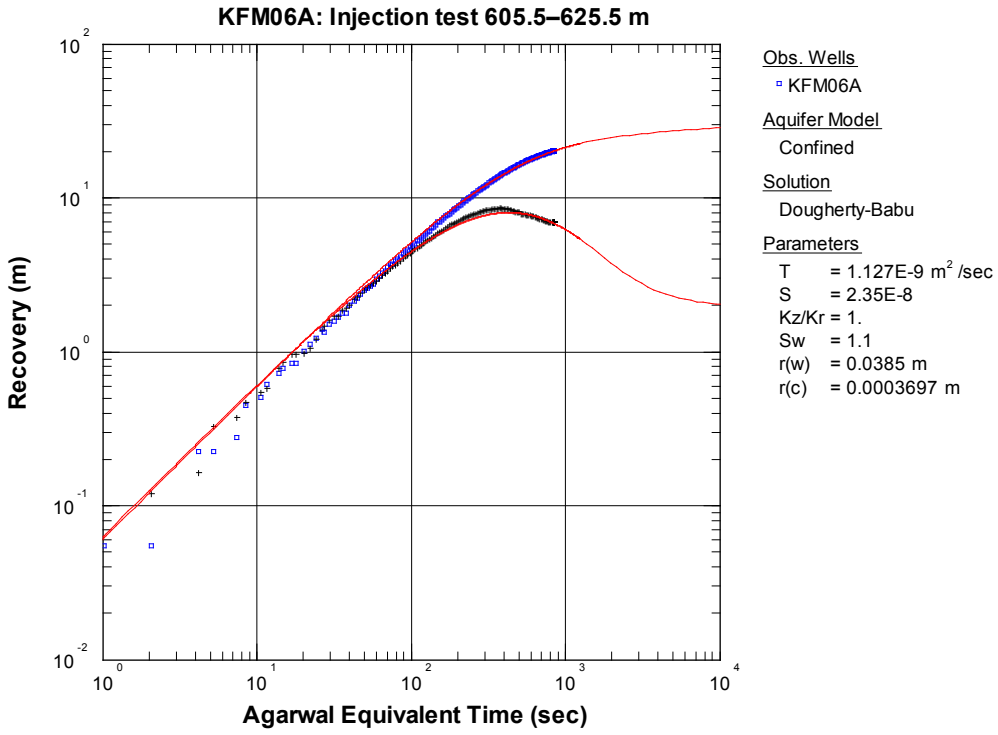

Figure 4-4g. *Example of dominating wellbore storage (WBS) during the recovery period of test section KFM06A:605.5–625.5 m (blue = head/flow rate and black = derivative).*

4.2.7 Uncertainties

4.2.7.1 Fast recovery

Some of the tests show a very fast pressure recovery, rapidly approaching a pseudo-stationary pressure during the recovery period. However, the previous injection period may often exhibit pseudo-radial flow with indications of an apparent no-flow boundary by the end in such cases. Examples of tests with fast recovery are shown in Figures 4-5a–d. Figure 4-5a and b show the responses during the injection- and recovery period, respectively, together with possible transient evaluations. The evaluation of the injection period was made on the first part with pseudo-radial flow before the apparent no-flow boundary effects by the end. An approximate evaluation was made of the recovery period using the Hantush´ model for pseudo-spherical (leaky) flow. The evaluations of the injection- and recovery period give hydraulic parameter values in the same order of magnitude.

Figure 4-5c shows the predicted recovery using the same hydraulic parameters as obtained from the evaluation of the injection period. The figure indicates that the observed recovery is much faster than predicted from the injection period resulting in inconsistent behaviour during the two periods of the test. Figure 4-5d shows a non-representative evaluation of the recovery period using a model assuming radial flow. This assumption may result in a significant over-estimation of both transmissivity, and particularly, the skin factor. A calculated very high positive skin factor using a model for radial flow may indicate a higher flow dimension, e.g. pseudo-spherical flow. It should be pointed out that the calculated pressure derivatives in Figures 4-5b–d suffer from limited resolution of the pressure gauge as discussed in Section 6-5. This fact makes the interpretation of flow regimes during the recovery period difficult.

The number of tests with fast recovery together with a discussion of possible reasons to the observed fast recovery in some tests is presented in Section 6.4.

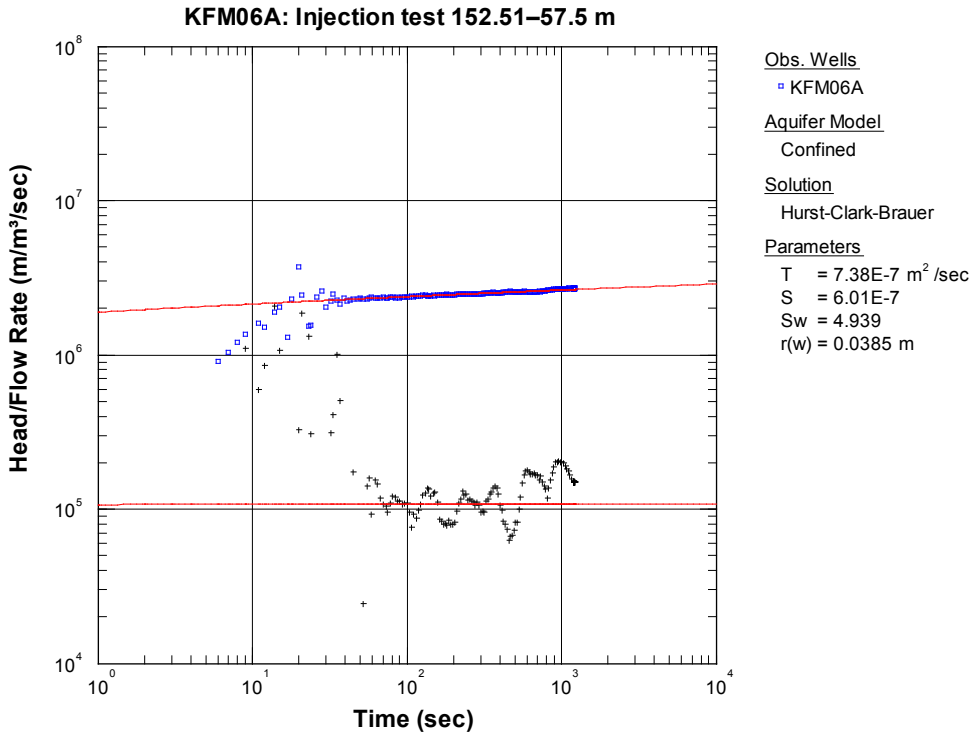

Figure 4-5a. *Log-log plot of head/flow rate (□) and derivative (+) versus time during the injection period of the injection test in section 152.5–157.5 m in KFM06A.*

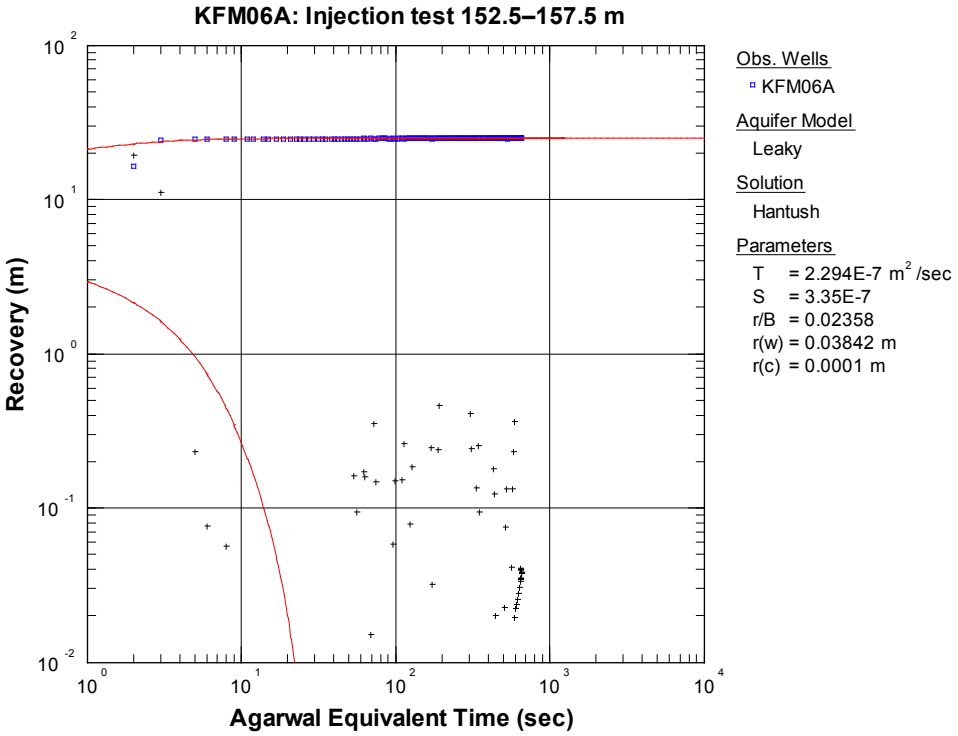

Figure 4-5b. *Log-log plot of recovery (□) and derivative (+) versus equivalent time during the recovery period of the injection test in section 152.5–157.5 m in KFM06A.*

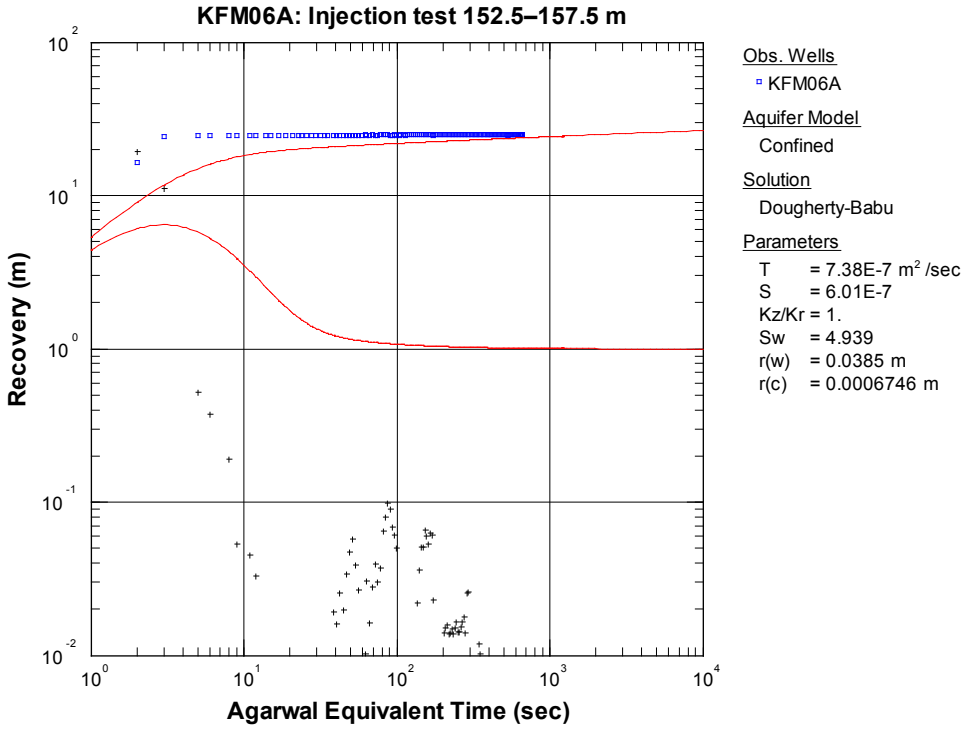

Figure 4-5c. *Log-log plot of predicted recovery and -derivative (red solid lines) versus equivalent time during the injection test in section 152.5–157.5 m in KFM06A, based on the estimated hydraulic parameters from the injection period of the test.*

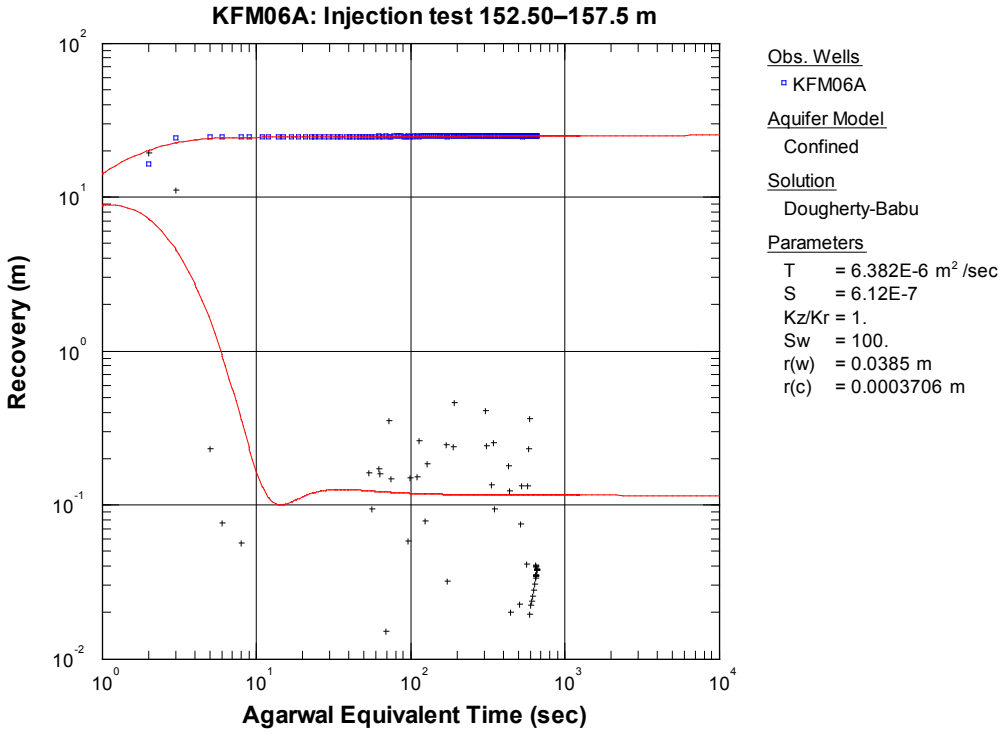

Figure 4-5d. *Example of non-representative transient evaluation of a test with fast recovery (red solid lines) using a model assuming pseudo-radial flow resulting in an extremely high, ambiguous skin factor (S_w) during the injection test in section 152.5–157.5 m in KFM06A.*

4.2.7.2 Ambiguous flow model identification

Ambiguous flow model identification may arise from a too short test time regarding wellbore storage resulting in that no well-defined flow regime is developed during the test. An example of such a case is shown in Figure 4-4g. Ambiguous flow model identification may also arise from poor resolution of the pressure sensor during the recovery period. Examples are shown in Figures 4-5b–d. The pressure derivative may in such cases be misinterpreted as indicating apparent pseudo-radial flow by the end of the test (flat derivative). Finally, ambiguous flow model identification may also be due to poor pressure control during the injection period. Table 6-1 shows that this is rather uncommon for the tests performed at Forsmark.

The number of tests with ambiguous flow model identification together with a discussion is presented in Section 6.1.

4.3 Analysis of pulse injection and slug injection tests

4.3.1 Brief theoretical background

A model described by Dougherty and Babu /10/ was used for standard evaluation of the pressure pulse tests performed at Forsmark. The model assumes radial flow in a porous medium. The normalized recovery H/H_0 is plotted versus elapsed time after stop of the pressure pulse in a lin-log diagram. In very low-transmissive sections, normally selected for pressure pulse tests, the recovery, H, is generally normalized with respect to H_0, which is the initial pressure in the borehole section before the packers are expanded to avoid substantial influence of packer compliance on the initial pressure in the test section. Furthermore, the model assumes that no effects of packer compliance are present on the measured recovery.

As for the injection tests, the effective borehole radius concept, Eqn. (4-1), was used for calculating the skin factor as well as the concept of a fictive standpipe connected to the test section representing wellbore storage according to Eqn. (4-5). With the above model, the transmissivity and skin factor was estimated from type curve matching for given values of storativity and wellbore storage coefficient (the latter represented by the radius of the fictive standpipe). The storativity was estimated from Eqn. (4-3) as for injection tests.

4.3.2 Determination of the flow model

Qualitative evaluation of flow regimes during pressure pulse tests can be made from the derivative in a similar manner as described for injection tests in Section 4.1.2. In low-transmissive sections, pseudo-radial flow is seldom reached during the test. For the pressure pulse tests performed at Forsmark, no qualitative evaluation of flow regimes or determination of flow model was made systematically. The model described by Dougherty and Babu /10/ was generally used for transient evaluation of pressure pulse tests performed at Forsmark.

In the preliminary analysis, the actual head change during the recovery period, H, was not corrected for effects of packer generated flow. As shown in Section 5.1.3 the generated flow may have a major impact on tests in very low-transmissive sections and result in an under-estimation of the transmissivity by standard analysis methods. Attempts were made to correct the head change during the recovery period for these effects, e.g. by extrapolating the increasing pressure trend due to packer compliance before the application of the pressure pulse and then superposing this pressure trend on the measured recovery. However, this technique was considered as unreliable since the calculated hydraulic parameters with the above model proved to be very sensitive to the shape of the transient H/H_0-curve and thus to the correction applied.

Whenever the transmissivity in the section was so low that the packer generated flow caused a pressure increase still after stop of the pressure pulse, the test was interrupted. For low-conductive sections when the packer generated flow significantly affects the pressure recovery a simple stationary method described in Section 5.2.3 was used to estimate the transmissivity. If the effects of packer compliance were considered as negligible, transient evaluation was performed according to the model described above.

4.3.3 Measuring the wellbore storage coefficient

By the analysis of the pressure pulse tests the estimated values of the effective wellbore storage coefficient for different section lengths listed in Table 5-1 from the laboratory measurements were generally used (or the corresponding radius of the fictive standpipe according to Eqn. (4-5)). The sensitivity of using the net wellbore storage C_w (based on only the water compressibility) in the transient analysis was also tested.

4.3.4 Analysis examples

Pressure pulse tests were performed in selected test sections in borehole KFM07A according to a modified test scheme which involved a diagnostic test whether a pressure pulse test was appropriate in the actual section (SKB P-05-133). In some of these sections, both pressure pulse tests and injection tests were made for comparison. The pressure pulse tests in KFM07A were performed according to the scheme in Table 4-2. The standard injection tests were performed according to Table 3-1a. Examples of transient evaluation of the pressure pulse tests are shown below. For comparison, the results of the pressure pulse tests and the previous injection tests in corresponding sections (KFM07A: 404–504 m and KFM07A: 154–159 m) are presented and discussed. The sensitivity of using the normalized head H/H_i and H/H_0, respectively in the analysis was also tested.

Table 4-2. Modified test scheme for pressure pulse tests applied at Forsmark.

Time (min)	Test phase	Activity	Comments
0	2	Start of packer sealing	Test valve is opened and the borehole pressure is registered
5	3	Test section is closed-in	Test valve is closed and the pressure behavior in the test section is observed
10	3	Check of pressure build-up at t = 10 min due to packer compliance	If the pressure in the test section is continuously increasing, the section is a candidate for a pressure pulse test (decision is taken)
11	(3)*	Preparation for pressure pulse test	Test valve is opened and the pressure is allowed to return to the borehole pressure
40	3	Pressurization (200 kPa) of the pipe string, de-aeration of the test system etc	Test valve is closed. Preparations for a pressure pulse test. Registration of the pressure in the test section.
60	4	Application of the pressure pulse	Test valve is opened at t = 60 min and closed at t = 62 min
62	5	Start of recovery of the pressure pulse – recovery period	Transient registration of the decay of the pressure pulse in the test section
c. 102	6	Stop of the recovery period of the pressure pulse. Packers are deflated. The test is finished	Test valve is opened and the packers are deflated, the pressure returns to the borehole pressure

* Test valve open.

Example 1. Pressure pulse test in section KFM07A: 404.00–504.00 m

The pressure history during the entire pressure pulse test, including the packer inflation period (test phase 2), shut-in of the test section (3), application of the pressure pulse (4), recovery of the pressure pulse (5) and the deflation of the packers (6) is shown in Figure 4-6. A detailed picture of the pressure behaviour during the packer inflation period and the shut-in pressure is shown in Figure 4-7. Figure 4-6 shows that a slow pressure recovery (p_p–p_F) of the applied pressure pulse occurred, indicating a rather tight section.

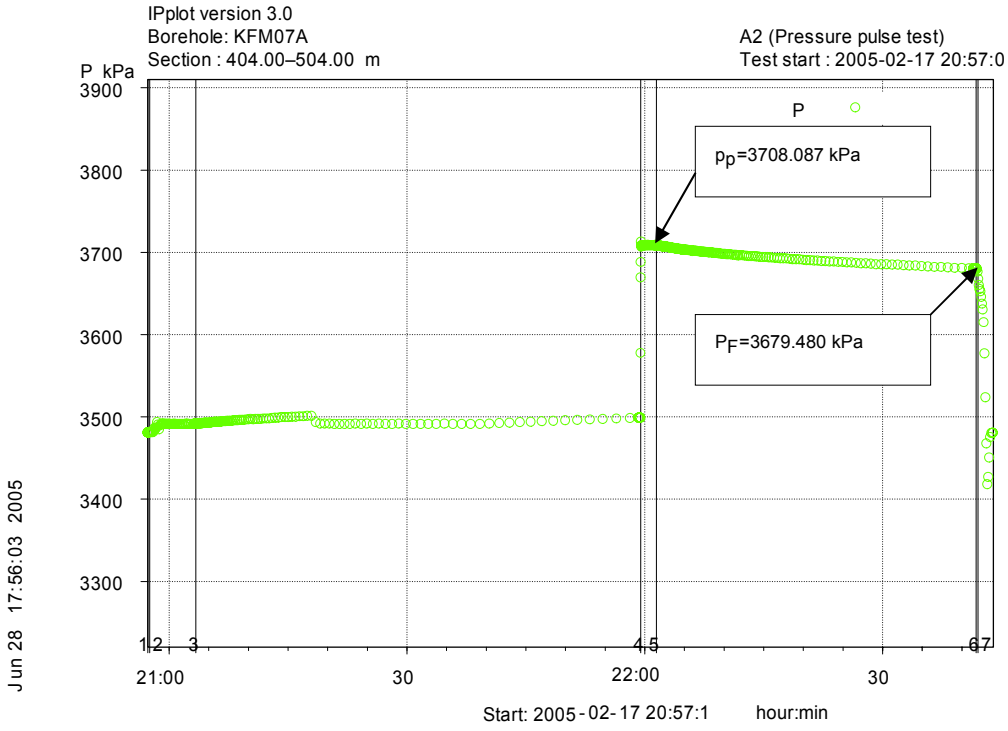

Figure 4-6. *Pressure history during the pressure pulse test in section KFM07A:404–504 m showing the different test phases on the time scale. A diagram with increased resolution of pressure during the packer sealing- and shut-in periods is shown in Figure 4-7.*

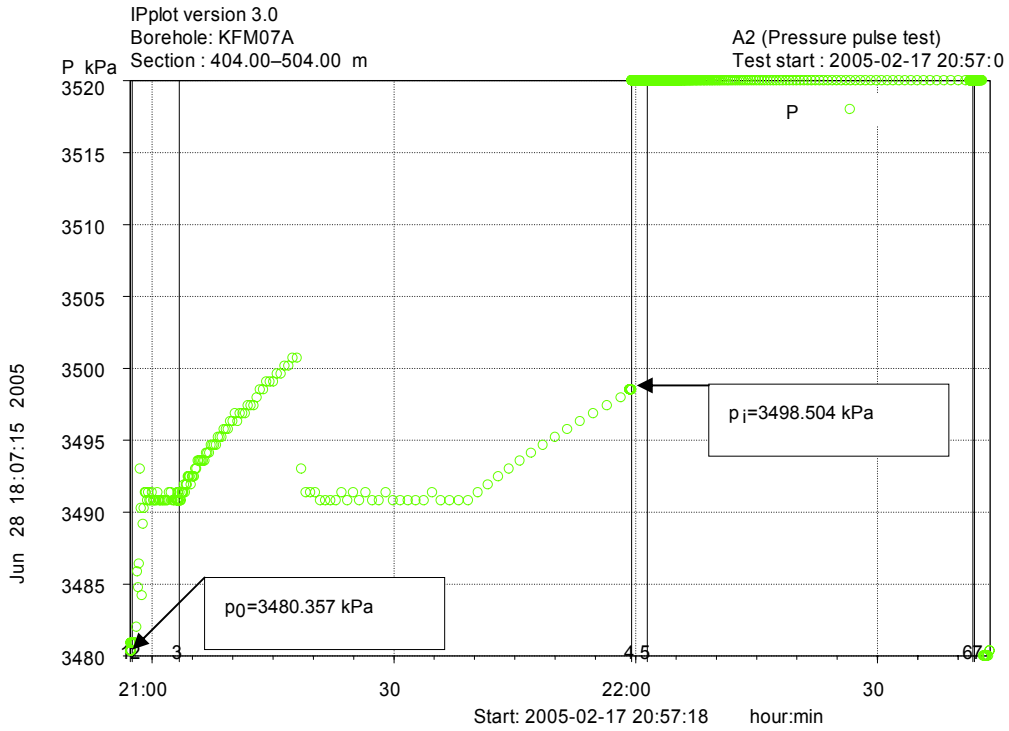

Figure 4-7. *Observed pressure during the packer sealing- and shut-in periods (test phase 2 and 3) of the pressure pulse test in section KFM07A:404–504 m. Expanded pressure scale.*

Figure 4-7 shows that the borehole pressure suddenly increased by c. 10 kPa at the start of packer sealing (test phase 2), mainly due to the rising water level in the pipe string at the surface due to the squeeze pressure from the packer inflation. At the shut-in of the test section (test phase 3) the pressure in the section started to increase due to the generated flow from the packers as described in Chapter 5.1. Therefore, the valve was opened at t = 11 min to allow the pressure to return to the actual borehole pressure. At t = 40 min the test valve was closed again and the pressure started to increase due to the generated flow from the packers but now at a slower rate.

At the start of the application of the pressure pulse (test phase 4) the rate of pressure increase in the test section was c. 3.5 kPa/min due to the generated flow from the packers. Although the generated flow is decreasing, the observed pressure decline during the recovery of the pressure pulse (test phase 5) is thus slightly underestimated due to this effect. By the end of the recovery of the pressure pulse (at t = c. 100 min) the generated flow is very small and probably negligible, cf Table 5-2.

The pressure pulse tests were evaluated according to the model described in Section 4.3.1. By the evaluation the estimated, effective borehole storage coefficient (C_{eff}) was used, cf Table 5-1. In a 100 m section, C_{eff} is the same as the net value of C, which is only based on the compressibility of the water volume in the test section (c_w). The corresponding fictive casing radius (r_c) was used by the evaluation of the tests. For comparison, the applied pressure pulse (dp) was based on both the borehole pressure before packer sealing ($dp_0 = p_p – p_0$) and on the pressure in the test section immediately before the application of the pulse ($dp_i = p_p – p_i$), respectively. By the evaluation, the pressure changes are converted to head H_0 and H_i, respectively (i.e. $H_0 = dp_0/\rho g$). The effects of packer compliance were not considered by the evaluation.

In Figure 4-8a and b) the transient evaluation of the pressure pulse test performed in section KFM07A: 404.00–504.00 m is shown. The normalized decline of head (H/H_0) is plotted versus time after stop of the pressure pulse in Figure 4-8a. The head H_0 corresponds to the applied pressure pulse using p_0 as reference pressure. For comparison, the corresponding plot with H/H_i

versus time, in which H_i is based on p_i as reference pressure, is shown in Figure 4-8b. H_0 is considered as the most representative value on the pressure pulse applied since H_i is affected by the pressure increase due to packer compliance. Figures 4-8a and b show that there is little difference in the estimated transmissivity and skin factor if the applied pressure pulse is based on p_0 or p_i. The storativity was estimated from Eqn. (4-3) as for the injection tests. Effects of packer compliance were not considered by the evaluation.

In order to roughly assess the effect of the generated flow by the packers on the evaluation of the pressure pulse test, the increasing pressure trend before the application of the pressure pulse (3.5 kPa/min) was added to the observed pressure change H during the recovery of the pressure pulse. This is considered as an extreme correction since the effect of the packer compliance decreases with time. Thus, this correction is assumed to represent an upper bound on the estimated transmissivity in this case. The evaluation with corrected normalized head H/H_0 is shown in Figure 4-9a and b to be compared with the corresponding plots with uncorrected pressures in Figure 4-8a and b.

Figures 4-8a-b and 4-9a-b show that the estimated transmissivity increases by a factor of c 3 in this case when the (extreme) correction of the pressure due to packer compliance effects is applied. The real transmissivity of the test section should thus fall within this interval. The effect of packer compliance can be regarded as limited in this case for the actual test performance and -design.

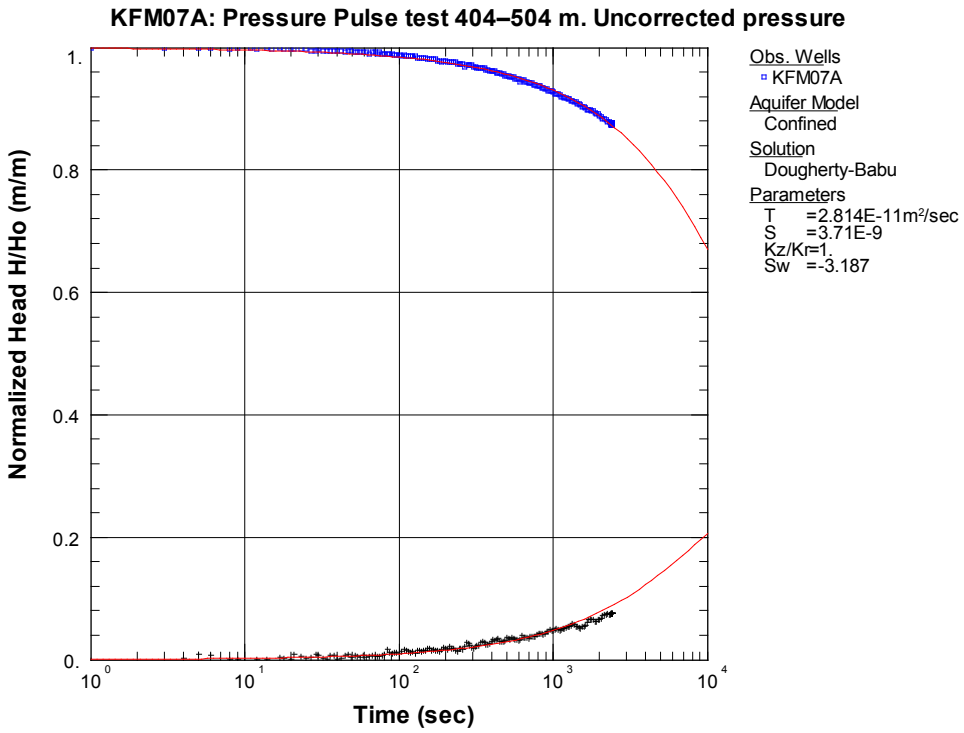

Figure 4-8a. *Normalized head H/H_0 versus time and corresponding derivative during the pressure pulse test in section KFM07A:404–504 m. H_0 is based on p_0 as reference pressure. Uncorrected pressure for packer compliance effects.*

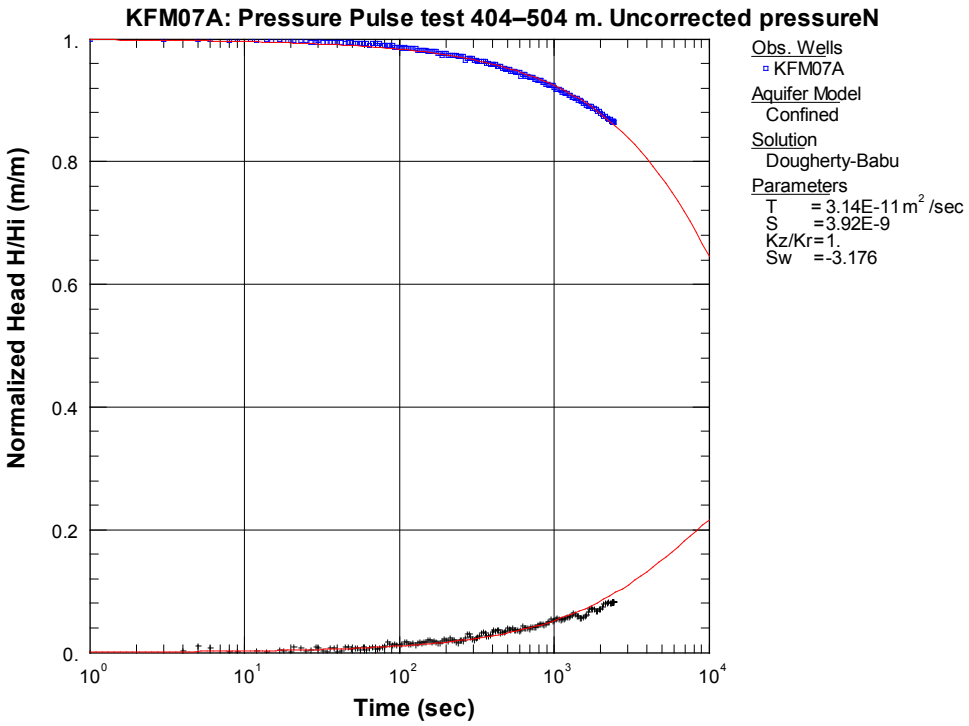

Figure 4-8b. *Normalized head H/H_i versus time and corresponding derivative during the pressure pulse test in section KFM07A:404–504 m. H_i is based on p_i as reference pressure. Uncorrected pressure for packer compliance effects.*

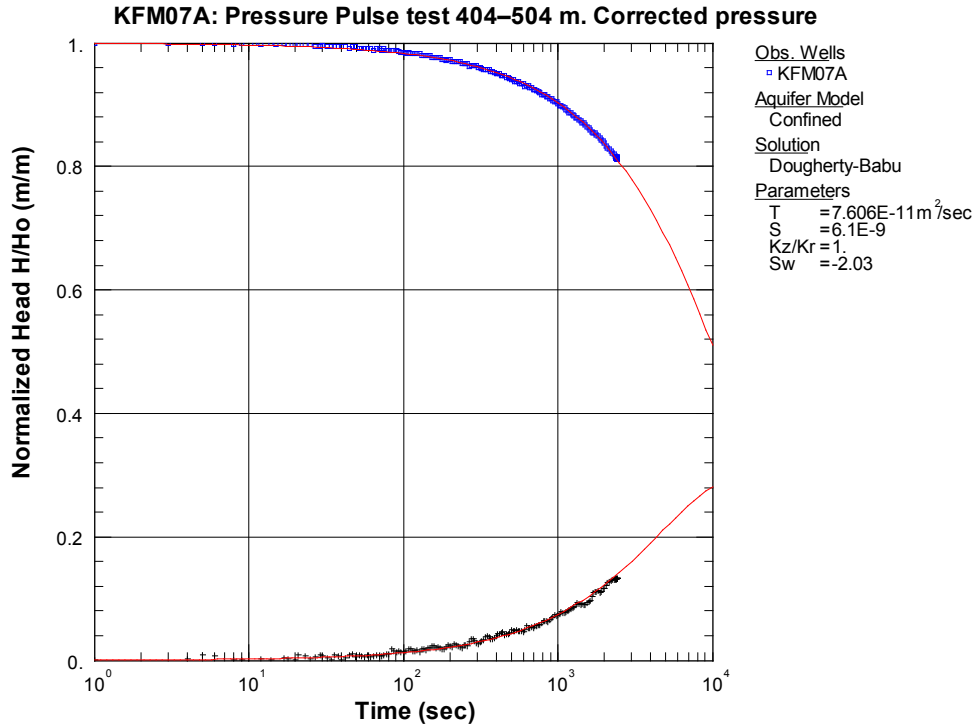

Figure 4-9a. *Corrected normalized head H/H_0 versus time and corresponding derivative during the pressure pulse test in section KFM07A:404–504 m. H_0 is based on p_0 as reference pressure. Corrected pressure for packer compliance effects (extreme case).*

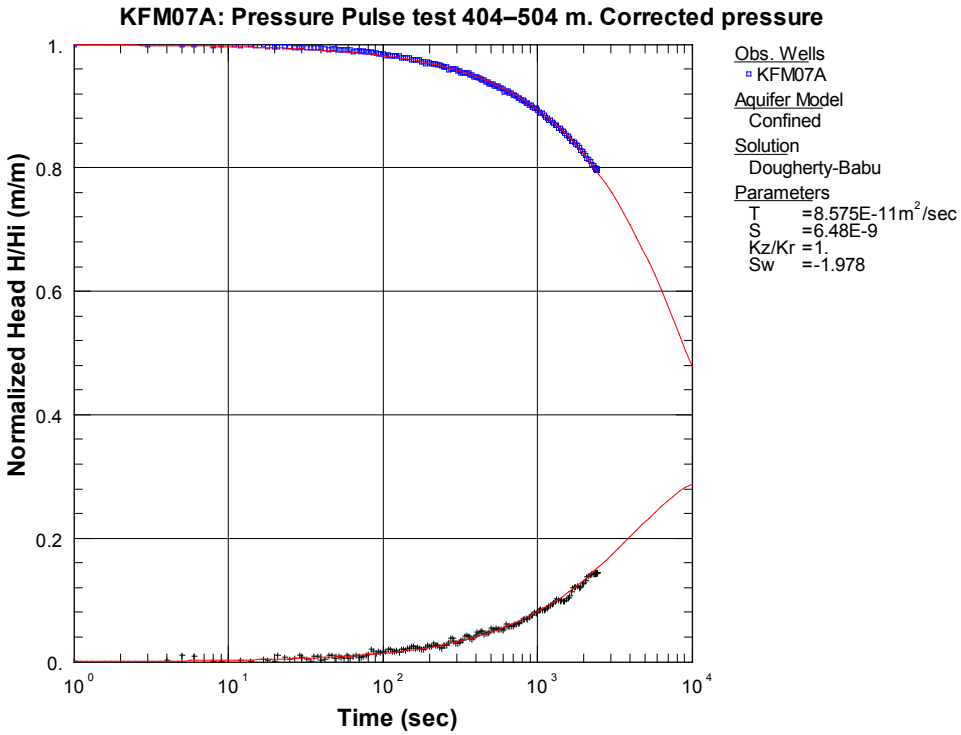

Figure 4-9b. *Corrected normalized head H/H_i versus time and corresponding derivative during the pressure pulse test in section KFM07A:404–504 m. H_i is based on p_i as reference pressure. Corrected pressure for packer compliance effects (extreme case).*

Example 2. Injection test in section KFM07A: 404.00–504.00 m

For comparison, the results of the previous injection test in this section, reported in SKB P-05-133, are presented and discussed. An overview of the pressure and flow rate during the entire test sequence is shown in Figure A2-1 in Appendix 2. A higher resolution of the pressure during the packer sealing and shut-in phases is shown in Figure A2-2. Comparison of Figure 4-7 and A2-2 shows that the pressure behaviour was quite different during the packer sealing period for the pressure pulse- and the injection test, respectively. The pressure pulse test was performed one day after the injection test. No increasing pressure trend was observed during this period of the injection test but instead, a decreasing pressure. No explanation has been found to this deviation so far.

Tests on the packers in the laboratory after the field tests showed no effects of leakage or other failures of the packers. Furthermore, the calculated hydraulic parameters from both tests showed very good agreement, indicating that the same section was tested, i.e. no depth shift between the tests was indicated, cf Table 4-3. Thus, the packers may perform differently in different tests.

The transient evaluation of the injection- and recovery period of the previous injection test in section KFM07A: 404.00–504.00 m is shown in Figure A2-3 and A2-4, respectively.

Comparison of results from the pressure pulse and injection test in KFM07A: 404–504 m

The results from the injection test and pressure pulse test in this section are similar and consistent, cf Table 4-3. The transmissivity from the injection test are within the estimated interval for transmissivity from the different types of evaluations of the pressure pulse test. This fact may indicate that the effects of packer compliance were rather small in this case.

Table 4-3. Comparison of results from the injection test and pressure pulse test in section KFM07A: 404–504 m. $C_{eff} = C_w = 1.9 \cdot 10^{-10}$ m³/Pa.

Test type	Transmissivity (m²/s)	Storativity*	Skin factor
Injection test			
–injection	$3.87 \cdot 10^{-11}$	$4.78 \cdot 10^{-9}$	–4.67
–recovery	$3.45 \cdot 10^{-11}$	$4.11 \cdot 10^{-9}$	–7.72
Pressure pulse test			
– H/H_0 and Ceff	$2.81 \cdot 10^{-11}$	$3.71 \cdot 10^{-9}$	–3.19
– H/H_i and Ceff	$3.14 \cdot 10^{-11}$	$3.92 \cdot 10^{-9}$	–3.18
– corrected H/H_0 and Ceff	$7.61 \cdot 10^{-11}$	$6.10 \cdot 10^{-9}$	–2.03
– corrected H/H_i and Ceff	$8.58 \cdot 10^{-11}$	$6.48 \cdot 10^{-9}$	–1.98

* Calculated from regression equation based on estimated T.

Example 3. Pressure pulse test in section KFM07A: 154.00–159.00 m

The pressure history during the entire pressure pulse test, including the packer inflation period (test phase 2), shut-in of the test section (3), application of the pressure pulse (4), recovery of the pressure pulse (5) and the deflation of the packers (6) is shown in Figure 4-10. A detailed picture of the pressure behavior during the packer inflation period and the shut-in pressure is shown in Figure 4-11. Figure 4-10 indicates that almost the entire pressure pulse declined during the recovery period, indicating a moderate transmissivity of the section.

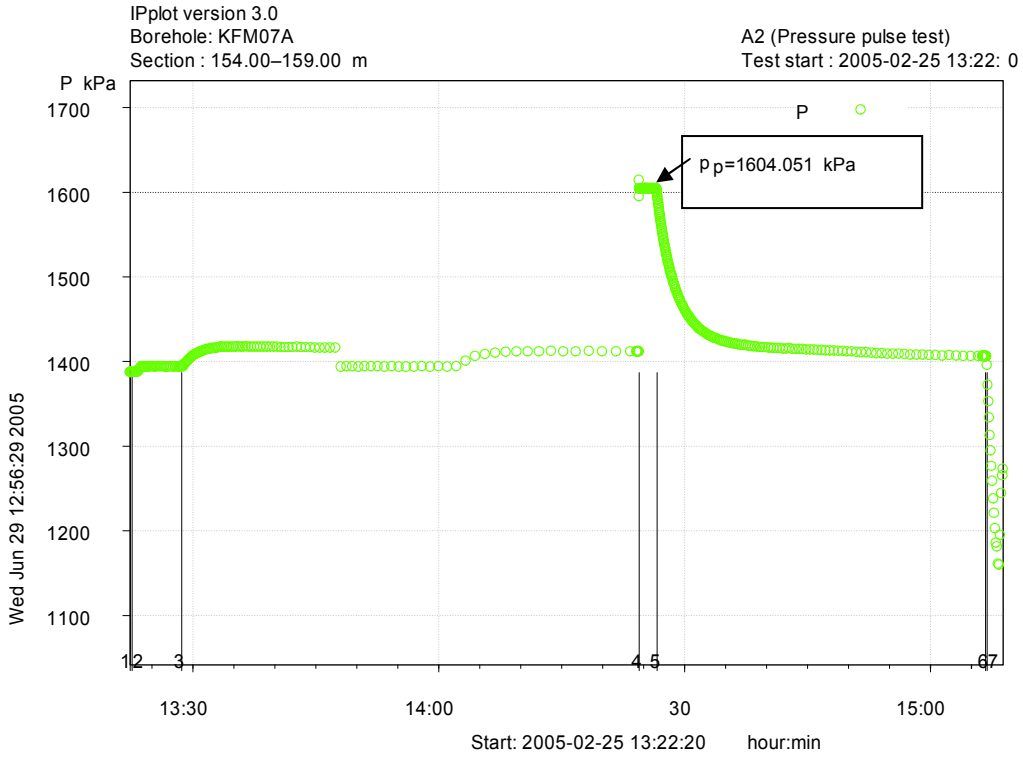

Figure 4-10. *Pressure history during the pressure pulse test in section KFM07A:154.00–159.00 m showing the different test periods on the time scale. A diagram with increased resolution of pressure during the packer sealing- and shut-in periods is shown in Figure 4-11.*

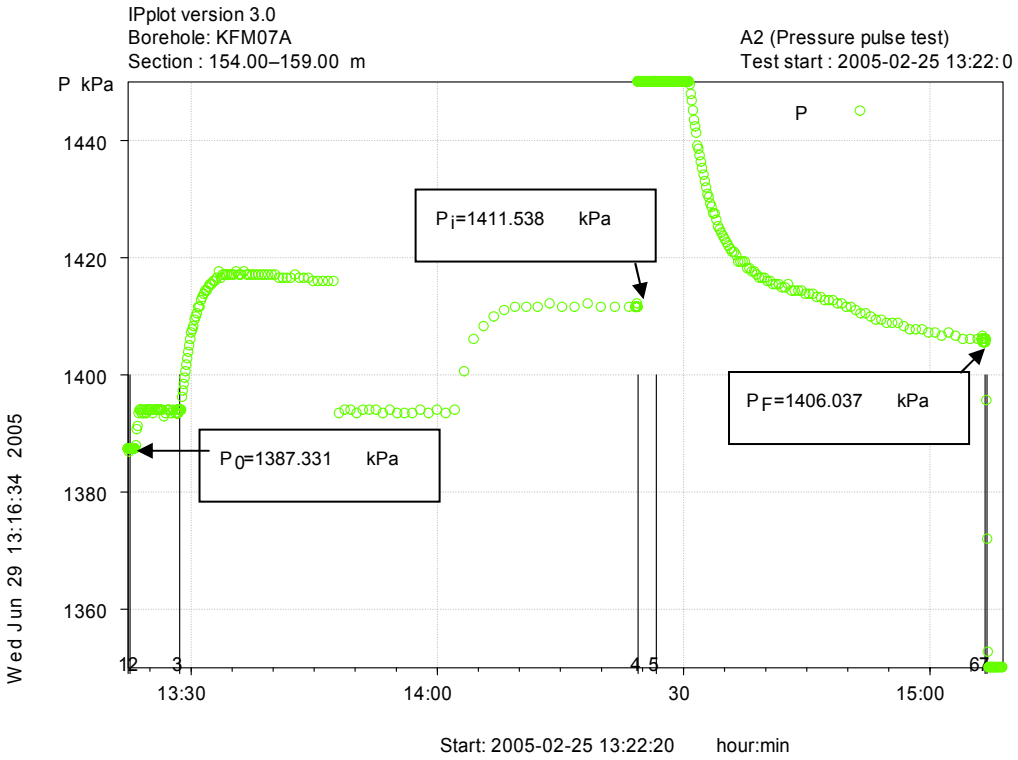

Figure 4-11. *Observed pressure with increased resolution during the packer sealing- and shut-in periods (test phase 2 and 3) of the pressure pulse test in section KFM07A:154.00–159.00 m.*

Figure 4-11 shows that the borehole pressure suddenly increased by c. 5 kPa at the start of packer sealing (test phase 2), mainly due to the rising water level in the pipe string at the surface due to the squeeze pressure from the packer inflation. When the test section was shut-in (test phase 3) the pressure in the section started to increase due to the generated flow from the packers as described in Chapter 5.1. Therefore, the test valve was opened to allow the pressure to return to the actual borehole pressure. At t = 40 min the test valve was closed again and the pressure started to increase again due to the generated flow from the packers but now at a slower rate. Then the pressure in the test section stabilised before the application of the pressure pulse.

The pressure pulse test was evaluated according to the model described in Section 4.3.1. By the evaluation the estimated, effective borehole storage coefficient (C_{eff}) was used, cf Table 5-1. For comparison, the net value C_w, based on only the compressibility of the water volume in the test section was also used. The corresponding fictive casing radius r(c) was applied by the evaluation of the tests. For comparison, the applied pressure pulse (dp) was based on both the borehole pressure before packer sealing ($dp_0 = p_p – p_0$) and on the pressure in the test section immediately before the application of the pulse ($dp_i = p_p – p_i$), respectively. By the evaluation, the pressure changes are converted to head H_0 and H_i, respectively (e.g. $H_0 = dp_0/\rho g$).

In Figure 4-12a and b) the evaluation of the pressure pulse test in section KFM07A: 154.00–159.00 m based on the effective borehole storage coefficient (C_{eff}) is shown for the normalized head H/H_0 and H/H_i, respectively. In Figure 4-12 b, the normalised head H/H_i falls below zero since the final pressure (p_F) is lower than p_i. Figure 4-12a and b) show that there is larger difference in the estimated transmissivity and skin factor in this case depending on if the pressure pulse is based on p_0 or p_i. The evaluation based on H/H_i shows a slightly better fit to the simulated curve and results in an estimated transmissivity c. 4 times higher than based on H/H_0. The storativity has been estimated from Eqn. (4-3) as for the injection tests.

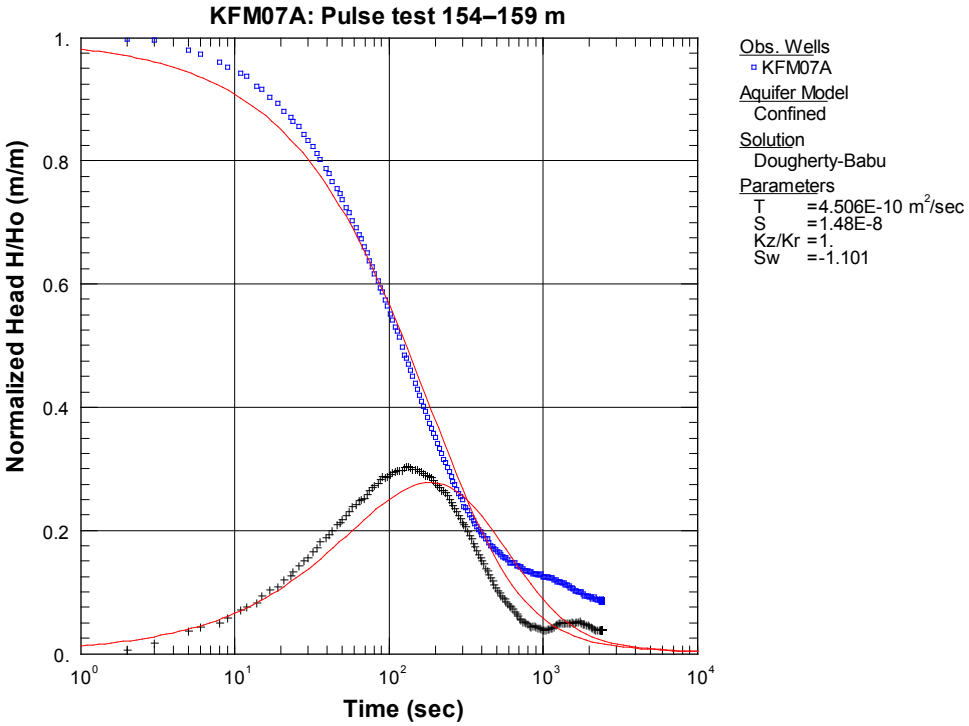

Figure 4-12a. *Normalized head H/H_0 versus time and corresponding derivative during the pressure pulse test in section KFM07A:154–159 m. H_0 is based on p_0 as reference pressure. Uncorrected pressure for packer compliance effects. The effective borehole storage coefficient C_{eff} is used by the calculation of transmissivity.*

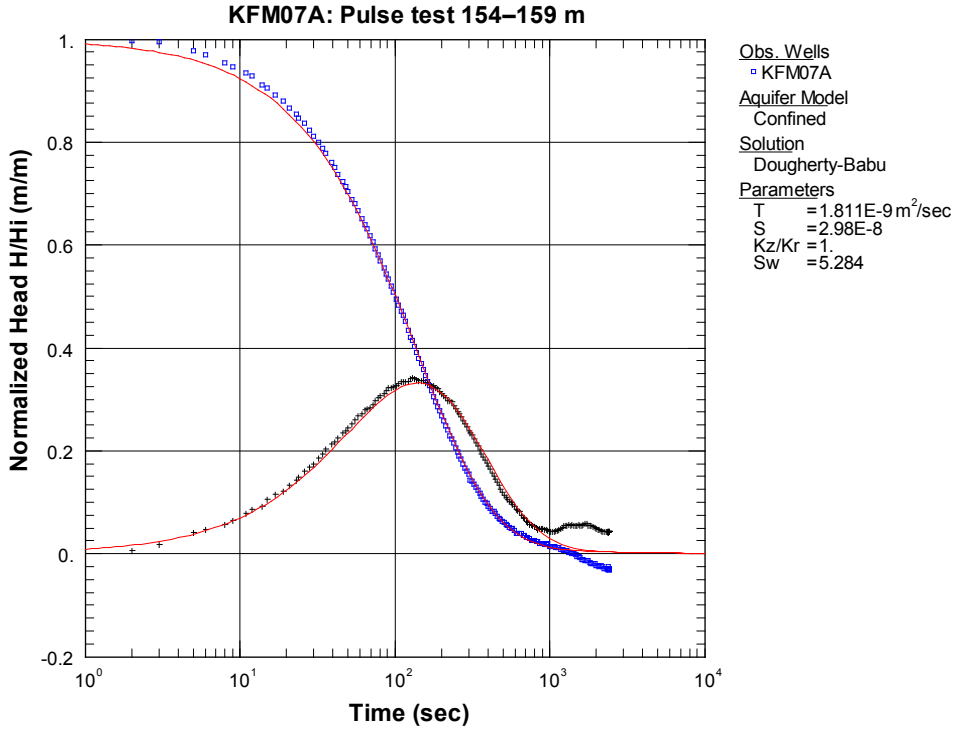

Figure 4-12b. *Normalized head H/H_i versus time and corresponding derivative during the pressure pulse test in section KFM07A:154–159 m. H_i is based on p_i as reference pressure. Uncorrected pressure for packer compliance effects. The effective borehole storage coefficient C_{eff} is used by the calculation of transmissivity.*

In Figure 4-13a and b) the evaluation of the same pressure pulse test in section KFM07A: 154.00–159.00 m based on the net borehole storage coefficient (C_w) is shown for the normalized head H/H_0 and H/H_i, respectively. The same pattern as in Figures 4-12a) and b) is maintained. There is little difference in estimated transmissivity and skin factor if C_{eff} or C_w is used in the evaluation. The differences are larger depending on if H/H_0 or H/H_i is used in this case.

No correction for packer compliance effects has been made for this test since no such effects were indicated before the application of the pressure pulse, cf Figure 4-11.

Example 4. Injection test in section KFM07A: 154.00–159.00 m

For comparison, the results of the previous injection test in this section, reported in SKB P-05-133, are presented and discussed. An overview of pressures and flow rate during the entire injection test sequence is shown in Figure A2-6 in Appendix 2. A higher resolution of the pressure during the packer sealing and shut-in period is shown in Figure A2-7. Comparison of Figure 4-11 and A2-7 shows that the pressure behaviour was rather similar during the packer sealing period before the pressure pulse- and the injection test, respectively. The pressure pulse test was performed c. 2 days after the injection test. The evaluation of the injection- and recovery period of the previous injection test in section KFM07A: 154.00–159.00 m is shown in Figure A2-13 and A2-14, respectively.

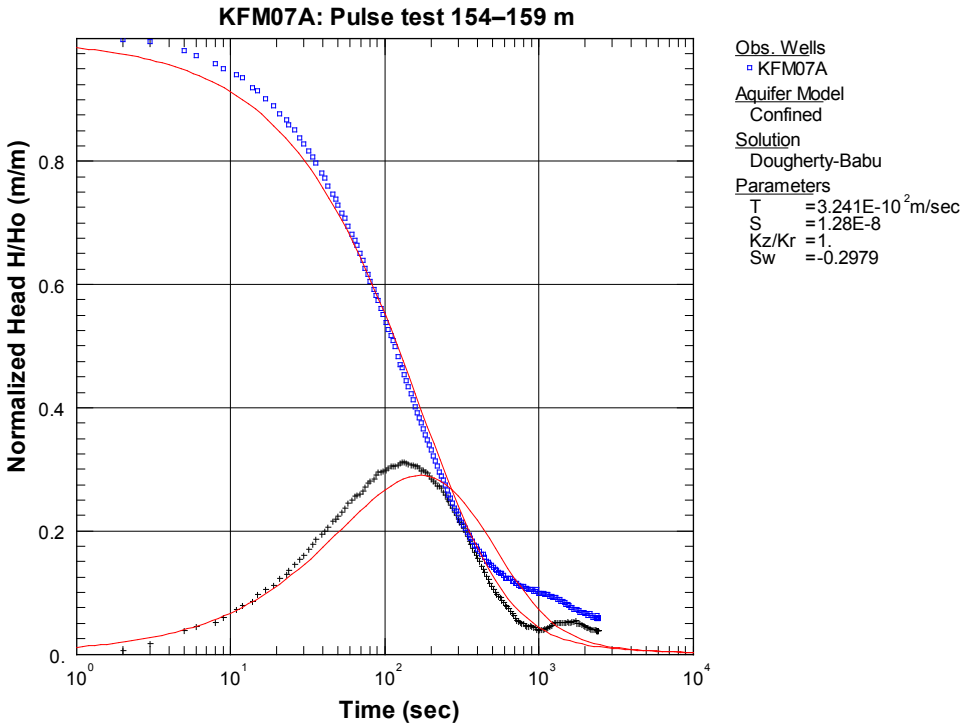

Figure 4-13a. *Normalized head H/H_0 versus time and corresponding derivative during the pressure pulse test in section KFM07A:154–159 m. H_0 is based on p_0 as reference pressure. Uncorrected pressure for packer compliance effects. The net borehole storage coefficient C_w is used by the calculation of transmissivity.*

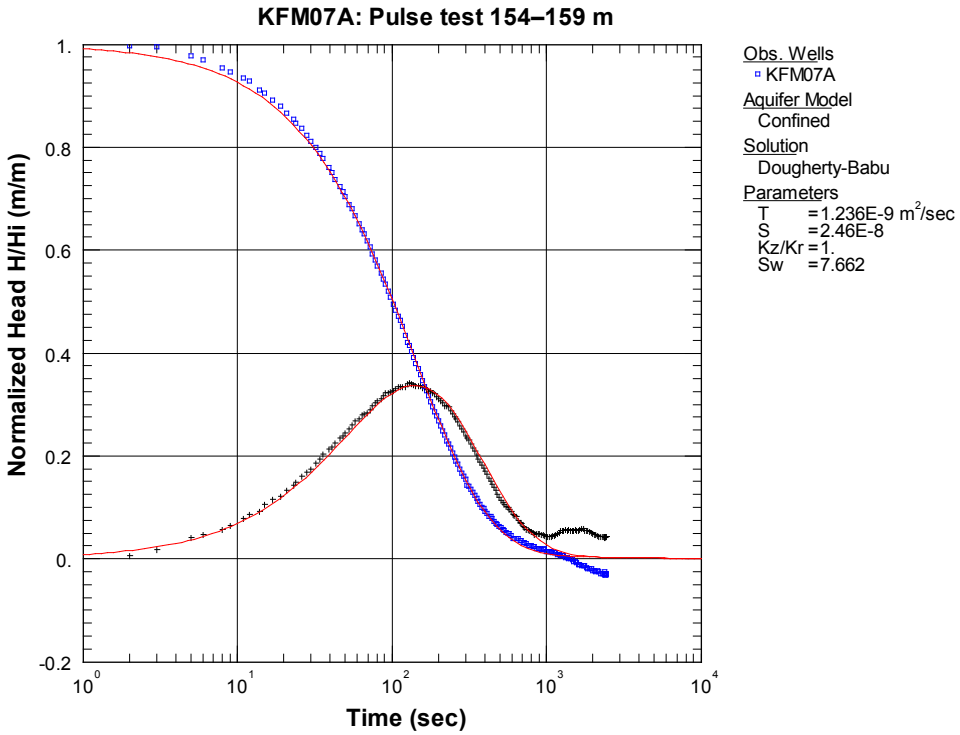

Figure 4-13b. *Normalized head H/H_i versus time and corresponding derivative during the pressure pulse test in section KFM07A:154–159 m. H_i is based on p_i as reference pressure. Uncorrected pressure for packer compliance effects. The net borehole storage coefficient C_w is used by the calculation of transmissivity.*

Comparison of results from the pressure pulse and injection test in KFM07A: 154–159 m

The results from the pressure pulse test and the injection test in this section are similar and consistent, cf Table 4-4. The transmissivity from the injection test are within the estimated interval for transmissivity from the pressure pulse test depending on if H/H_0 or H/H_i is used. The latter assumption causes the largest differences in results. Effects of packer compliance are assumed to be negligible in this section and are not considered by the transient analysis of the pressure pulse test.

Table 4-4. Comparison of results from the pressure pulse test and the injection test in section KFM07A: 154–159 m. $C_{eff} = 1.6 \cdot 10^{-11}$ m³/Pa and $C_w = 9.1 \cdot 10^{-12}$ m³/Pa.

Test type	Transmissivity (m^2/s)	Storativity* (–)	Skin factor (–)
Injection test			
–injection	$7.03 \cdot 10^{-10}$	$1.86 \cdot 10^{-8}$	–0.84
–recovery	$7.54 \cdot 10^{-10}$	$1.92 \cdot 10^{-8}$	0.12
Pressure pulse test			
– H/H_0 and Ceff	$4.50 \cdot 10^{-10}$	$1.48 \cdot 10^{-8}$	–1.10
– H/H_i and Ceff	$1.81 \cdot 10^{-9}$	$2.98 \cdot 10^{-8}$	5.28
– H/H_0 and Cw	$3.24 \cdot 10^{-10}$	$1.28 \cdot 10^{-8}$	–0.30
– H/H_i and Cw	$1.24 \cdot 10^{-9}$	$2.46 \cdot 10^{-8}$	7.66

* Calculated from regression equation based on estimated T.

4.3.5 Uncertainties

4.3.5.1 Determination of the wellbore storage coefficient

The determination of the effective wellbore storage C_{eff}, generally used by the evaluation of the pressure pulse tests, together with associated uncertainties, is discussed in Section 5.1.2. The consistency of the determined wellbore storage coefficient is checked against the results of the analysis of the recovery period of the injection tests as discussed in Section 6.6.

The sensitivity of using C_{eff} and C_w, respectively in the analysis of pressure pulse tests together with the sensitivity of using H/H_i and H/H_i, respectively can be seen in Table 4-4.

4.4 Derivation of recommended values and confidence ranges

4.4.1 Consistency between test periods

The consistency between the injection- and recovery period has only been checked in a qualitative way by comparison of the responses and the hydraulic parameters calculated from the different periods. Inconsistent behaviour has been observed in several tests in different section lengths. The most common feature leading to inconsistency is wellbore storage. For example, an approximate pseudo-radial flow regime may frequently be identified during the injection period but not during the recovery period due to wellbore storage at the short test times applied. Another rather frequent cause of inconsistent behaviour is fast recovery which is not consistent during the injection period. This item is further discussed in Section 6.4 based on the observations of the item “Fast recovery” in Table 6-1 (column N).

4.4.2 Recommended transmissivity

The basic decisive criterion applied by the evaluation of the injection tests at Forsmark was the possibility to identify a certain segment with pseudo-radial flow in the qualitative evaluation as discussed in Section 4.1.1.1 and 4.2.1.1 during the injection- and recovery period, respectively. If a certain interval with pseudo-radial flow could be identified from e.g. the injection period but not from the recovery period, the representative values on the hydraulic parameters were selected from the injection period. If such intervals could be identified from both test periods, the parameters from the period showing the best data quality and conformance to the model used for evaluation was selected.

If a pseudo-radial flow regime was not present during any of the periods, the representative parameters were selected on the basis of the quality of the data and conformance to other models, e.g. for pseudo-linear and pseudo-spherical flow. Occasionally, a representative transient evaluation was not possible on any period. In such cases, the steady-state transmissivity was selected as the representative parameter.

4.4.3 Transmissivity confidence range

In AQTESOLV, the conventional standard error as well as the approximate 95% confidence interval for each estimated parameter is calculated. Both these statistical measures could be assigned as the confidence range of the estimated transmissivity from a test evaluation point of view. However, there are several other potential factors which may cause errors in the determination of the transmissivity from injection tests to a varying degree, e.g.

- Instrumental malfunctions.
- Pressure not stabilized in the test section before injection.
- Packer compliance.
- Differences in temperature, density and viscosity of the injected water and water in the rock.

- Uncertain (low) injection pressure in high-transmissive sections due to flow restrictions of the equipment used.
- Rock leakage, e.g. by interconnecting fractures around the packers.
- Clogging of fractures during the drilling or testing operation.
- Scattered flow rate data in low-transmissive test sections.
- Incorrect model used for the evaluation.
- Inconsistent results from the injection- and recovery period.
- Strongly deviating test responses from expected.

Thus it may be difficult to derive a representative confidence range of transmissivity for each test. For the hydraulic tests performed at Forsmark, no transmissivity confidence range is reported.

4.4.4 Other consistency checks

For the hydraulic tests performed at Forsmark, other estimated parameters were used as qualitative consistency checks of the estimated transmissivity. In particular, the estimated wellbore storage coefficient and skin factor should fall within certain expected ranges constrained by the test configuration, rock conditions and experience from similar tests.

5 General uncertainties

5.1 Packer compliance

5.1.1 General

In conjunction with the construction of equipment for different kinds of hydraulic tests, prototypes are manufactured which are tested on the basis of the actual application. In general, tests are made on each component which implies that separate tests are made on the properties of the packers. Since the testing programme is governed by the actual application of the packer, the programme for e.g. a packer designed for piezometric measurements installed in boreholes drilled from a deep tunnel may differ from that for a packer to be used in hydraulic tests in boreholes drilled from the surface.

The processes of deformation of packers which may affect the evaluation of hydraulic tests in low-transmissive sections include:

1. Linear-elastic deformation of the packers constitutes one part of the *effective* wellbore storage coefficient (C_{eff}) in an isolated test section. This kind of deformation may depend i. a. on the properties of the rubber used and the relationship between the pressure in the packer and test section, respectively. These deformations are regarded as none time-dependent

2. Time-dependent deformation of packers is of two kinds:

a) **Material creeping** in e.g. the rubber at changes of pressure. These effects are reflected by a weakly decreasing pressure in the test section after an instantaneous pressure increase, even if the section is completely tight. Conversely, after an instantaneous pressure decrease, a weakly increasing pressure is obtained in the section. These pressure changes dissipate with time.
b) **Generated flow caused by the packer inflation.** Even after that the packers ”tighten”, they continue to expand slightly (“residual expansion”). The resulting decrease of the volume of the test section may in “tight” sections be treated as a fictive flow which affects the flow- as well as the recovery period of the test. The longer packer sealing time, the lower this effect.

Both of processes 1 and 2 are included in the term “packer compliance” used in this report. The performance of the testing of the packers is described in Appendix 1.

3. Other changes of the volume of the test section.

a) **Material** generated changes of the packer pressure caused by **temperature variations in the test container.** In hydraulic tests in the upper part of the borehole, apart from the pressure vessel, a major part of the expansion hose to the packers is located in the test container. Large temperature variations in the container may also create large variations of the packer pressure which may, in turn, create small pressure variations in short, “tight” sections. To distinguish such effects, both the packer pressure and the temperature in the test container are measured during the tests.
b) **Temperature variations in the test section.** Since the temperature in “tight” sections may be regarded as stable, this effect may be ignored in most cases.

5.1.2 Linear-elastic deformations

Based on the results of the laboratory tests in Appendix 1, the volume change of *two* packers per pressure change was estimated at 0.7 mL/100 kPa which corresponds to a packer-related wellbore storage coefficient $C_m = 7 \cdot 10^{-12}$ m^3/Pa. This value can be used to calculate the effective compressibility in test sections of different length.

The effective compressibility of a test section depends on the compression of:

- water volume in the test section,
- equipment (packers etc),
- rock.

In the estimation of the effective compressibility below, the rock is assumed as in-compressible. In addition, any volume changes in the cable and the hose in the test section have been ignored. The total change of volume in a test section may thus be calculated as:

$$\Delta V = \Delta V_w + \Delta V_m = \Delta p \cdot V_w \cdot c_w + \Delta V_m = \Delta p \cdot V_w \cdot c_w + C_m \cdot \Delta p \quad (5\text{-}1)$$

ΔV = total change in volume of water and packers (m^3).
ΔV_w = change of volume of water (m^3).
ΔV_m = change of volume of packers (m^3).
C_m = packer-related wellbore storage coefficient (m^3/Pa).
V_w = volume of water in the test section (m^3).
Δp = pressure change (Pa).
c_w = compressibility of water (Pa^{-1}).

The effective compressibility (c_{eff}) of the test section may be calculated as:

$$c_{eff} = \Delta V / \Delta p \cdot 1 / V_w \quad (5\text{-}2)$$

The effective borehole storage coefficient (C_{eff}) of the test section may be calculated as:

$$C_{eff} = V_w \cdot c_{eff} \quad (5\text{-}3)$$

The changes of volume in the test section that can be expected for hydraulic tests with a pressure change of 200 kPa in the section together with the estimated effective compressibility and effective borehole storage coefficient of the test section are presented in Table 5-1. The compressibility of water is assumed to $c_w = 4.6 \cdot 10^{-10}$ Pa^{-1} and the rock is assumed to be virtually incompressible in the calculations. Any volume changes of the cable and hose through the section have been ignored. The values on the effective borehole coefficient (C_{eff}) in Table 5-1 can be compared with the corresponding values on this parameter from the test evaluation, cf Section 4.2.3.

Table 5-1. Estimated volume changes in test sections of different length for hydraulic tests at a pressure change of 200 kPa together with the estimated effective compressibility c_{eff} and effective borehole storage coefficient C_{eff}. Borehole diameter = 76 mm.

Parameter	Section length (m)		
	5	20	100
Net water volume in test section, Vw (L)	c. 19	c. 78	c. 393
Change of the water volume in the test section at a pressure change of 200 kPa, ΔVw (mL)	c. 1.8	c. 7.2	c. 36
Volume change of 2 packers at a pressure change of 200 kPa, ΔVm (mL)	c. 1.4	c. 1.4	c. 1.4
Volume change of water and 2 packers at a pressure change of 200 kPa, ΔV (mL)	c. 3.2	c. 8.6	c. 37.4
Effective compressibility of test section, ceff (Pa–1)	$8.4 \cdot 10^{-10}$	$5.5 \cdot 10^{-10}$	$4.8 \cdot 10^{-10}$
Effective borehole storage coefficient of test section, Ceff (m^3/Pa)	$1.6 \cdot 10^{-11}$	$4.3 \cdot 10^{-11}$	$1.9 \cdot 10^{-10}$

5.1.3 Time-dependent deformations

Material creeping due to instantaneous pressure changes

The laboratory tests exhibited small pressure changes after large pressure disturbances which probably are caused by material creeping. In field tests, the effective compressibility is much higher than in the laboratory tests, why these effects can be ignored by the evaluation of transmissivity from field tests.

Generated flow caused by packer sealing

The generated flows from packer sealing by one packer have been measured at different times after start of sealing at two different pressures, i.e. at atmospheric pressure and at 200 kPa, see Tables A1-1 and A1-2 in Appendix 1, respectively. The calculated packer generated flows are presented for selected test times in Table 5-2 below. The selected times refer to different phases in the current scheme of the performance of hydraulic injection tests of different section lengths, cf Section 3.1.2. The number of figures of the values in the table is presented without considering the actual measurement accuracy.

The measured packer generated flows at different test times in Table A1-2 in Appendix 1 are shown in Figures 5-1 and 5-2, respectively, together with the interpolated curve between the measurement points. In the latter diagram, the measured average flow rate value at t = 60 min for one packer (0.005 mL/min) was omitted since it is regarded as uncertain. It should also be pointed out that the estimated flow rates below c. 0.1 mL/min are very uncertain.

The selected times in the figures refer to the following activities of the constant head injection tests:

t = 0 start of packer sealing.

t = 30 min start of injection period (5 and 20 m tests).

t = 45 min start of injection period (100 m tests).

t = 50 min stop of injection period/start of recovery period (5 and 20 m tests).

t = 70 min stop of recovery period (5 and 20 m tests).

t = 75 min stop of injection period/start of recovery period (100 m tests).

t = 105 min stop of recovery period (100 m tests).

If the estimated packer generated flows in Table 5-2 are assumed at injection tests in the field, the real flow into the formation at the end of the injection period (t = 50 min) is c. 0.08 mL/min higher than the actually measured flow by the flow meter at the surface in 5 m and 20 m test sections. This value can be compared with the lower standard measurement limit for flow rate of 1 mL/min for the PSS system. The effect of the generated flow will disappear if sufficient time is allowed between start of packer sealing and the start of subsequent hydraulic tests. In Section 5.2, estimations of the packer generated flow are made for a few selected field tests in very low-transmissive sections.

Table 5-2. Estimated flow generated by two packers at selected times after start of packer sealing (t = 0) at atmospheric pressure and an overpressure of 200 kPa in the test section, respectively.

Pressure in test section (kPa)	Flow rate (mL/min)					
	t = 30 min	t = 45 min	t = 50 min	t = 70 min	t = 75 min	t = 105 min
0 (atmospheric pressure)	0.50	0.26	0.18	0.05	0.037	0.0067
200	0.48	0.16	0.08	0.005	0.0039	0.001

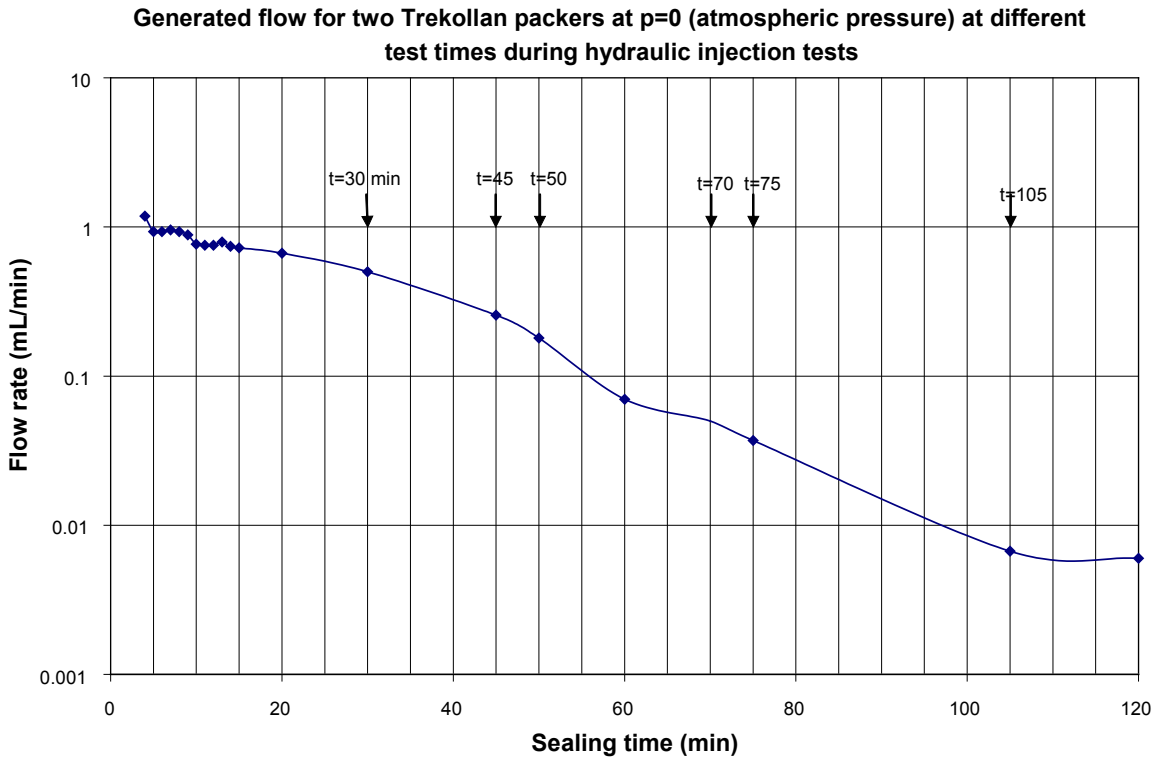

Figure 5-1. *Generated flow of* ***two*** *Trekollan packers at p = 0 (atmospheric pressure) at different times during the hydraulic injection tests.*

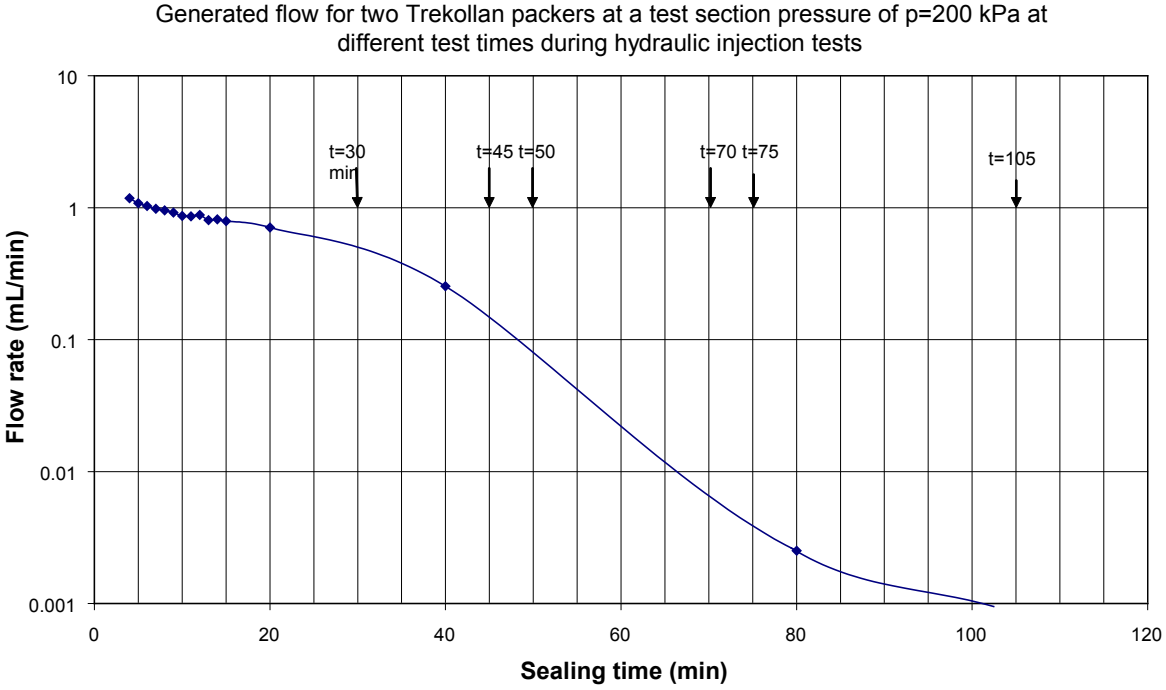

Figure 5-2. *Generated flow of* ***two*** *Trekollan packers at p = 200 kPa at different times during the hydraulic injection tests.*

5.2 Effects of packer compliance on testing

5.2.1 Generated flow by the packers

From measured pressure changes during the packer sealing period of tests in very tight sections (below the measurement limit), consistency checks of C_{eff} and the generated flow by the packers may be made. The results can be compared with the corresponding estimations from the laboratory tests described in Section 5.1. However, no independent estimations of C_{eff} and the generated flow can be made from the field tests.

Below, some examples of such estimations of the flow generated by the packers from tests in very low-transmissive test sections at Forsmark exhibiting the highest observed pressure increase after the application of the pressure pulse during the recovery period due to packer compliance. These sections are considered as virtually tight, i.e. the flow into the rock is assumed to be extremely small and negligible in relation to the flow generated by the packers. The estimations of the packer generated flow were made according to Eqn. (5-4) from the pressure increase in virtually tight test sections during the first 10 mins of the recovery period due to the generated flow together with the estimated value of C_{eff} from the laboratory tests described above:

$$C_{eff}\frac{dp_{packer}}{dt} = Q_{packer} \qquad (5\text{-}4)$$

Q_{packer} = packer generated flow (m^3/s).
C_{eff} = effective borehole storage coefficient of test section (m^3/Pa).
dp_{packer} / dt = pressure increase in virtually tight test section per time unit (Pa/s).

5.2.1.1 Field test examples

Example 1. Injection test in KFM06A: 450.50–455.50 m

The packer sealing time was c. 30 min. Figure 5-3 shows the flow rate and pressure history during the entire test in a linear diagram. The figure shows that the pressure build-up is similar before (test phase 3) and after the application of the pressure pulse (test phase 5). The estimations of the packer generated flow are made from the first part of the recovery period.

dp_{packer} /dt = 429 Pa/s.
Q_{packer} = $6.86 \cdot 10^{-9}$ m^3/s = 0.41mL/min.

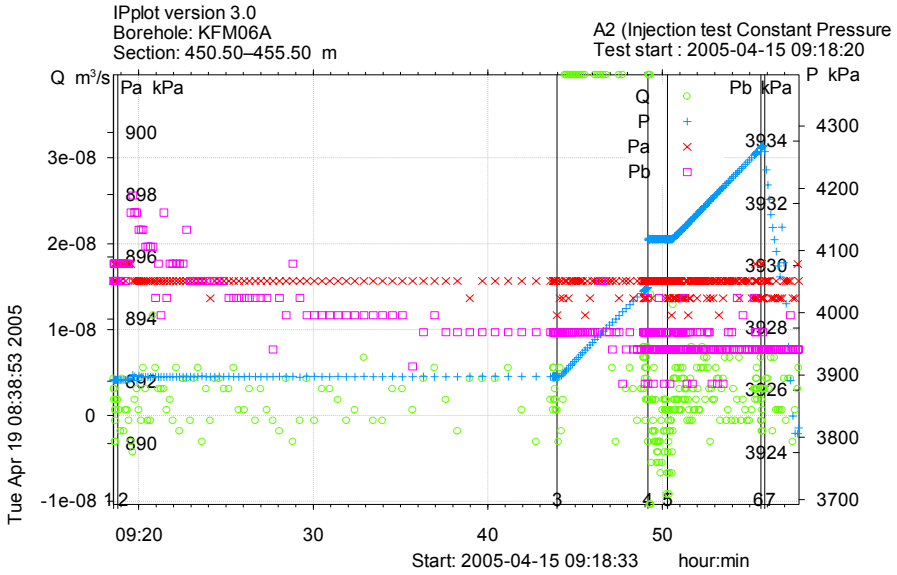

Figure 5-3. *Linear graph of flow rate and pressure during the injection test in section KFM06A:450.50–455.50 m.*

Example 2. Injection test in KFM06A: 460.50–465.50 m

The packer sealing time was c. 30 min. Figure 5-4 shows the flow rate and pressure history during the entire test in a linear diagram. The figure shows that the pressure build-up deviates before (test phase 3) and after the application of the pressure pulse (test phase 5). The calculations are made from the first part of the recovery period.

dp_{packer}/dt = 488 Pa/s.

Q_{packer} = $7.82 \cdot 10^{-9}$ m^3/s = 0.47 mL/min.

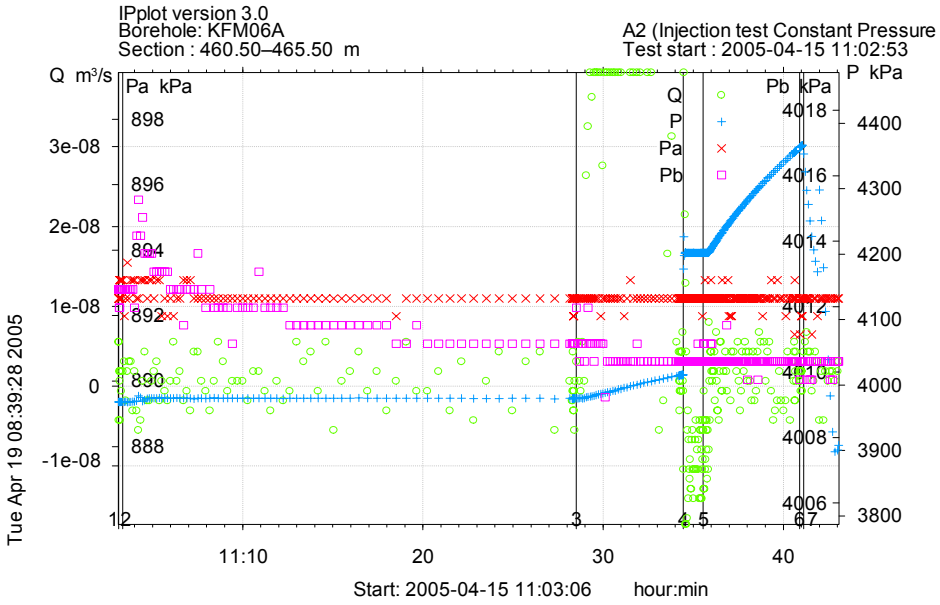

Figure 5-4. *Linear graph of flow rate and pressure during the injection test in section KFM06A:460.50–465.50 m.*

Example 3. Pressure pulse test in KFM08B: 149–154 m

The packer sealing time was c. 60 min. Figure 5-5 shows the pressure history during the entire test in a linear diagram. The figure shows that the pressure build-up deviates before (test phase 3) and after the application of the pressure pulse (test phase 5). The calculations are made from the first part of the recovery period.

$dp_{packer}/dt = 83.5$ Pa/s.

$Q_{packer} = 1.35 \cdot 10^{-9}$ m³/s = 0.081 mL/min.

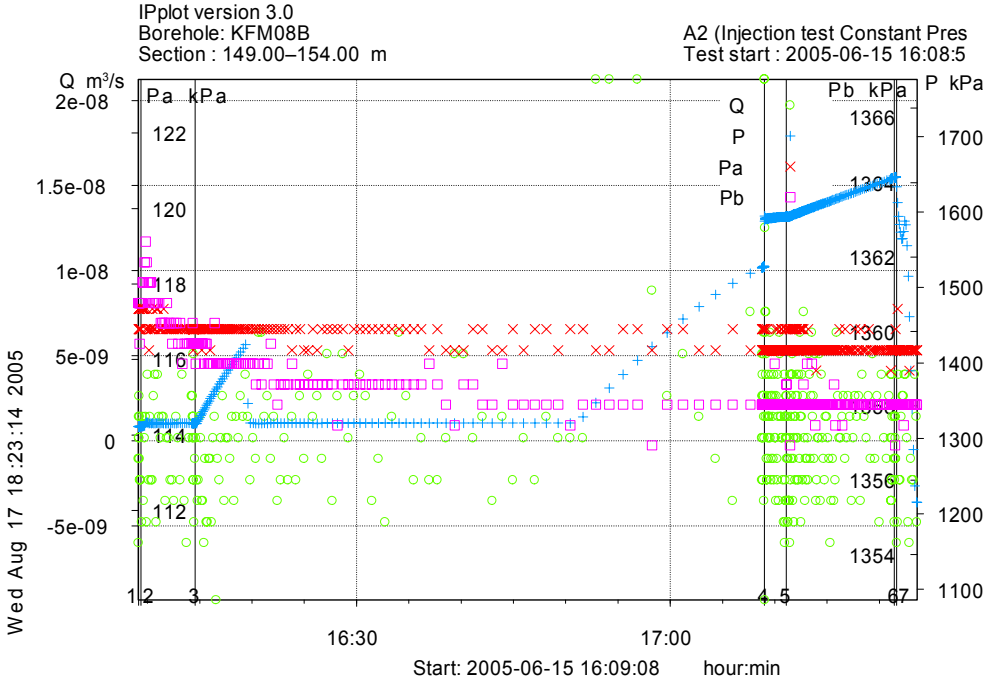

Figure 5-5. *Linear graph of flow rate and pressure during the pressure pulse test in section KFM08B:149.00–154.00 m.*

5.2.1.2 Comparison of results from the laboratory measurements

The results from the estimations of the generated flow by the two packers in selected, ”tight” 5 m sections at different sealing times (30 min and 60 min, respectively) from the first c. 10 mins of the recovery period were compared with the corresponding flows (for one packer) estimated from the laboratory tests in Table A1-2 in Appendix 1. The results from the selected sections are presented in Table 5-3.

The higher value from the field tests (0.47 mL/min) is considered as more uncertain than the lower value (0.41 mL/min). The agreement between the field- and laboratory tests is very good for the injection tests with 30 min packer sealing time. However, there is a relatively large deviation between the field- and laboratory values for the pressure pulse test with 60 min packer sealing time. The deviation in estimated flow rates though only corresponds to approximately one drop of water per minute. The value from the field tests are considered as more correct.

It appears that the packer generated flow in field tests in almost impermeable test sections generally shows good agreement with the laboratory measurements for times up to c. 30 min after start of packer sealing, cf Figure 5-2. For longer times, it appears that the packer generated flow from field tests is higher than the laboratory measurements, cf section KFM08B: 149–154 m.

Deviations in results from field- and laboratory tests may be caused by the following factors:

- the selected section is not completely impermeable,
- the formation pressure in the test section deviates from the hydrostatic pressure in the borehole at the actual depth,
- the two packers do not seal at exactly the same time,
- sealing of the packers does not start at exactly the same point on the rubber at all tests,
- the elastic properties of the rubber may have changed after long time of application (aging),
- the borehole diameter deviates slightly from the diameter of the steel pipe in the laboratory measurements,
- the packer compliance under down-hole conditions is different from the one measured at surface (in laboratory).

Caution should be exercised whenever estimated packer generated flows are used to determine very low transmissivities of the rock. The packer generated flows should be determined by the same equipment and at the same time as the actual field test. Since the relative errors of low packer generated flows are higher, the lower limit for evaluation of transmissivity and associated significant figures should be based on this fact.

Table 5-3. Comparison of the estimated packer generated flow from field tests and laboratory measurements.

Borehole section	Test type	Packer sealing time (mins)	Packer generated flow (mL/min)	
			Field tests	Laboratory tests
KFM06A: 450.50–455.50	Injection	30	0.41	0.4
KFM06A: 460.50–465.50	Injection	30	0.47	0.4
KFM08B: 149.00–154.00	Pressure pulse	60	0.081	0.012

5.2.2 Rough estimation of the transmissivity of tight sections

There is sometimes an interest of estimations of transmissivity below the actual measurement limit of the PSS system. Below, a simple, rough method to estimate the transmissivity of almost tight sections is proposed. The method is based on stationary evaluation of the pressure behaviour during the recovery period of short injection tests or pressure pulse tests. With this method, the transmissivity may be roughly estimated even if the pressure is still increasing during the recovery period.

The average flow rate into the rock is calculated according to Eqn. (5-5) from the previously estimated packer generated flow for tight sections according to Eqn. (5-4) and the change of borehole storage (water and packers) with time (dV/dt) in the test section. The average flow rate into the rock may, for example, be determined during the first 10 mins of the recovery period. The change of borehole storage with time (dV/dt) in the test section may be calculated from the observed pressure change during the actual time interval of the recovery period (dp/dt) and the estimated effective borehole storage coefficient from the laboratory tests, see below. The pressure may either decrease during this period (positive dp/dt) or still increase (negative dp/dt) after the application of the pressure pulse.

$$Q_{ave\ (formation)} = Q_{ave\ (packer)} + dV/dt \qquad (5\text{-}5)$$

$Q_{ave\ (formation)}$ = average flow rate into the rock (m^3/s).
$Q_{ave\ (packer)}$ = average packer generated flow rate (m^3/s).
dV/dt = change of borehole storage with time = $C_{eff}\ \frac{dp}{dt}$ (m^3/s).
C_{eff} = effective borehole storage coefficient of test section (m^3/Pa).
dp/dt = pressure change during the actual time interval of the recovery period (Pa/s). Decreasing pressure corresponds to a positive pressure change dp/dt.

The transmissivity is calculated from the stationary evaluation according to Eqn. (5-6), based on the estimated average flow rate into the rock and the applied differential pressure. If the pressure change during the recovery period is large compared to the applied pressure increase during the pressure pulse test an average differential pressure may be used in Eqn. (5-6).

$$T = Q_{ave\ (formation)} / dh_f \qquad (5\text{-}6)$$

T= transmissivity (m^2/s).
dh_f =applied differential pressure during the (pulse) injection period (m).

The following assumptions are made:

- the transmissivity of the selected section used for estimation of the packer generated flow from field tests is much lower compared to the actual test to be evaluated,
- the packer generated flow rate is assumed to be the same in all test sections, independently on the depth to the test section. This assumption may not always be full-filled in the field,
- the estimated effective borehole storage coefficient from laboratory tests is assumed to also be valid for field tests.

Below, some examples are shown of the application of the method described above.

Example 1. Pressure pulse test in section KFM06A: 455.50–460.50 m

The flow rate and pressure history during the pressure pulse test in section KFM06A: 455.50–460.50 m is shown in a linear diagram in Figure 5-6.

Packer sealing time: 30 min.

$Q_{ave(packer)}$ = $6.86 \cdot 10^{-9}$ m³/s = 0.41mL/min.
C_{eff} = $1.6 \cdot 10^{-11}$ m³/Pa.
dp/dt = –122.8 Pa/s.
$Q_{ave\ (formation)}$ = $4.90 \cdot 10^{-10}$ m³/s = 0.29 mL/min.
dh_f = c. 20 m.
T = $2.4 \cdot 10^{-11}$ m²/s.

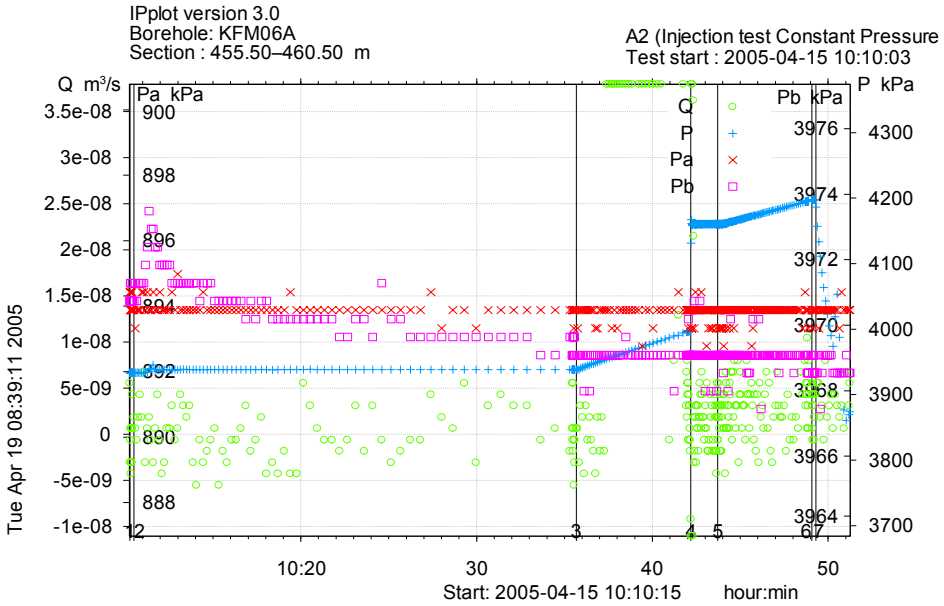

Figure 5-6. *Linear diagram of flow rate and pressure during pressure pulse test in section KFM06A:455.50–460.50 m.*

Example 2. Pressure pulse test in section KFM08B: 79.00–84.00 m

The flow rate and pressure history during the pressure pulse test in section KFM08B: 79.00–84.00 m is shown in a linear diagram in Figure 5-7.

Packer sealing time: 60 min.

$Q_{ave(packer)}$ = $1.35 \cdot 10^{-9}$ m³/s = 0.41mL/min.

C_{eff} = $1.6 \cdot 10^{-11}$ m³/Pa.

dp/dt = 19.3 Pa/s.

$Q_{ave(formation)}$ = $1.66 \cdot 10^{-9}$ m³/s = 0.1 mL/min.

dh_f = c. 20 m.

T = $8.3 \cdot 10^{-11}$ m²/s.

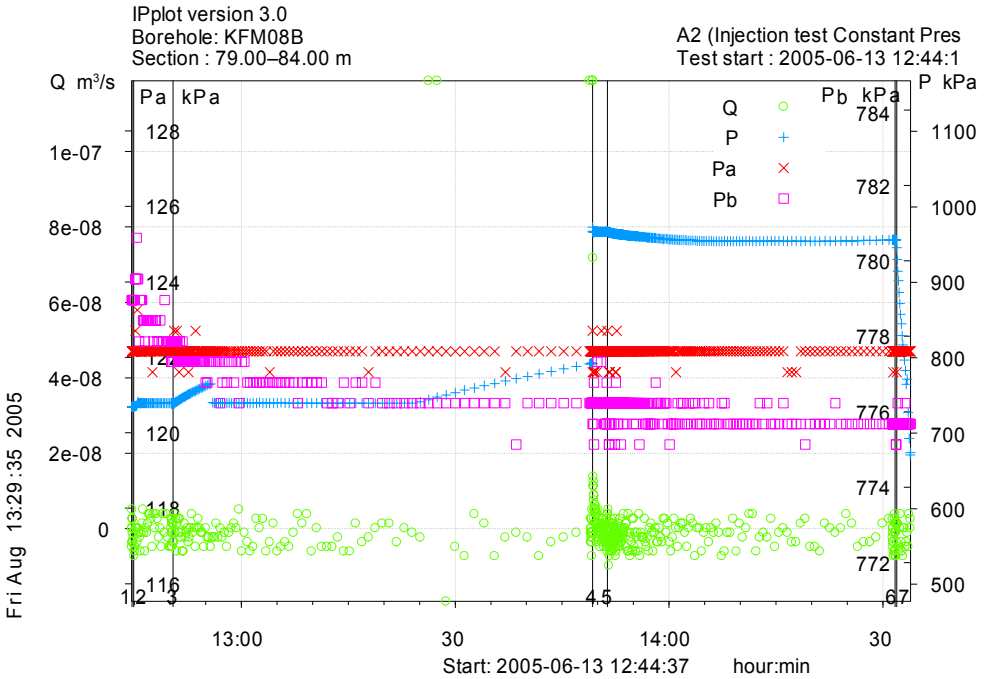

Figure 5-7. *Linear diagram of flow rate and pressure during pressure pulse test in section KFM08B:79.00–84.00 m.*

Example 3. Pressure pulse test in section KFM08B: 109.00–114.00 m

The flow rate and pressure history during the pressure pulse test in section KFM08B: 109.00–114.00 m is shown in a linear diagram in Figure 5-8.

Packer sealing time: 60 min.

$Q_{ave(packer)}$ = $1.35 \cdot 10^{-9}$ m³/s = 0.41mL/min.

C_{eff} = $1.6 \cdot 10^{-11}$ m³/Pa.

dp/dt = –74.5 Pa/s.

$Q_{ave(formation)}$ = $1.58 \cdot 10^{-10}$ m³/s = 0.009 mL/min.

dh_f = c. 20 m.

T = $7.9 \cdot 10^{-12}$ m²/s.

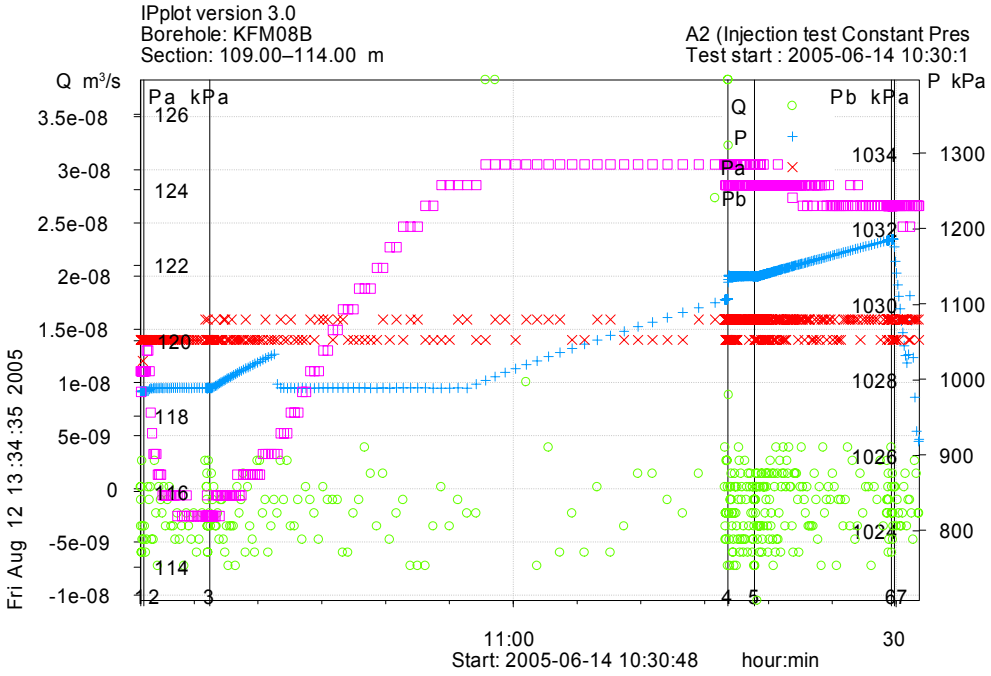

Figure 5-8. *Linear diagram of flow rate and pressure during pressure pulse test in section KFM08B:109.00–114.00 m.*

Example 4. Pressure pulse test in section KFM08B: 119.00–124.00 m

The flow rate and pressure history during the pressure pulse test in section KFM08B: 119.00–124.00 m is shown in a linear diagram in Figure 5-9.

Packer sealing time: 60 min.

$Q_{ave(packer)}$ = $1.35 \cdot 10^{-9}$ m^3/s = 0.41mL/min.

C_{eff} = $1.6 \cdot 10^{-11}$ m^3/Pa.

dp/dt = 207.7 Pa/s.

$Q_{ave(formation)}$ = $4.67 \cdot 10^{-9}$ m^3/s = 0.280 mL/min.

dh_f = c. 20 m.

T = $2.3 \cdot 10^{-10}$ m^2/s.

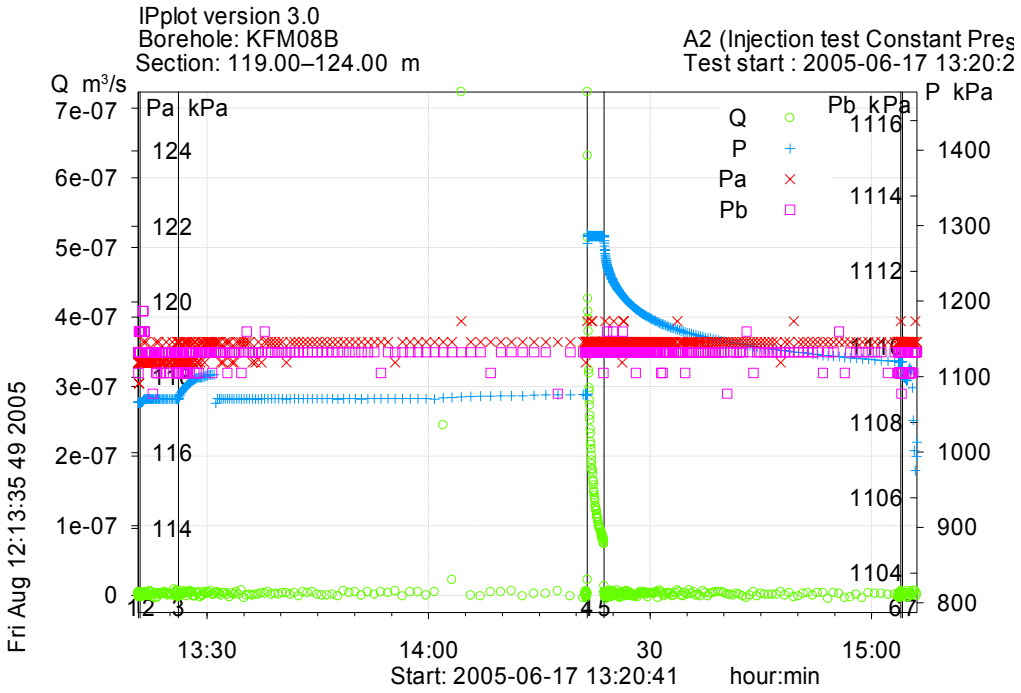

Figure 5-9. *Linear diagram of flow rate and pressure during pressure pulse test in section KFM08B:119.00–124.00 m.*

5.2.2.1 Discussion

The PSS system is designed for a lower measurement limit of flow rate of 1 mL/min. The flow rate generated by the packers at the end of the injection period is c. 0.10–0.15 mL/min. The latter flow rate is considered to be included in the accuracy of the lower limit of flow rate. If it is desired to lower the measurement limit for flow rate by some fractions of 1 mL/min, either the allowed uncertainty of the measured flow must be extended or alternatively, the flow generated by the packers must be taken into account and corrected for in very low-transmissive test sections. As discussed above, the compensation for the flow generated by the packers may sometimes be problematic.

The estimations of transmissivity by the simple method described above are below the measurement limit of the PSS system. The method assumes that packers and other test equipment perform identically during each test. However, based on current experience, there are indications that the equipment does not perform quite identically during all tests. The packer compliance effects may possibly decrease with depth due to increased water pressures but this hypothesis has not been confirmed by field tests. In addition, the packer compliance effects may decrease with time due to aging of the packers and number of inflations.

For a packer sealing time of 60 min, used by the pressure pulse tests at Forsmark, it may be possible to estimate transmissivities in the interval c. $5 \cdot 10^{-11}$ to $5 \cdot 10^{-10}$ m^2/s with this method. However, the uncertainty of such estimates is high. If the packer sealing time was increased, the packer generated flow would decrease significantly according to Figure 5-1 and 5-2. However, in practise other factors may dominate the test results, e.g. the lower measurement limit of the flow meter, background pressure variations etc.

5.2.3 Numeric simulation of packer compliance effects (prepared by Golder)

The present section describes an example of the influence of packer compliance (as described by laboratory measurements) on the response of pulse injection tests. The simulation results were organized in an Excel spreadsheet (SIMS_PackerCompliance.xls). The spreadsheet allows the user to compare three simulations with different parameter sets (L, T, S) at the choice of the user. More detailed description of the spreadsheet is given further below. The main question asked in this section is: "How good is our ability to derive the formation transmissivity correctly by using pulse test deconvolution analysis, while neglecting the packer compliance?"

Simulations

The simulations were calculated using nSIGHTS. The simulated sequence was:

- Packer inflation (at time = 0).
- Pressure measurement with test valve open (duration 30 min).
- Pressure measurement with test valve closed (duration 20 min).
- Pulse injection with pressure difference of 200 kPa measured from the last pressure of the previous phase (duration 40 min).

The test sequence described above roughly resembles the current testing procedure in Oskarshamn when pulse tests were conducted. The simulations were conducted for an array of parameters as listed below:

- Transmissivity (T) = 1E–8, 1E–9, 1E–10, 1E–11, 1E–12 and 1E–13 m^2/s.
- Storativity (S) = 1E–5, 1E–6 and 1E–7.
- Section length (L) = 5, 20 and 100 m.

The wellbore storage coefficient was calculated from the actual interval volume and a test zone compressibility of 2E–9 1/Pa[1] (this is how L influences the simulations).

All simulations were started at an initial formation pressure of 5,000 kPa. During the simulation, the interval volume decreases at a rate described by the packer compliance measurements from the laboratory.

Presentation of results

Figure 5-10 presents a snapshot from the spreadsheet showing three simulations conducted for a section length of 20 m, a storativity of 1E–6 and transmissivities of 1E–9, 1E–10 and 1E–11 m^2/s, respectively. The upper graph compares the simulations in Cartesian coordinates together with the packer displacement rate. The lower graph shows the normalized deconvolution derivative of the simulated pulse tests (dots) together with the ideal response derived from the type curve derivative (solid line). The data in the yellow area would not be available in the case of a real test, because it corresponds to sample rates lower than 1 reading/second. Generally, the difference between the simulated response (the dots) and the ideal type curve (the solid line) is a measure for the error introduced by packer compliance. Note that the Y-axis is plotted in transmissivity units (m^2/s), such that vertical differences between the dots and the corresponding solid line can be directly quantified in terms of transmissivity error.

Summary

- Packer compliance (i.e. decreasing interval volume during the test) in the magnitude described by the laboratory measurements influences the ability of deriving the formation transmissivity correctly when the true formation transmissivity is 1E–11 m^2/s or lower. In this case, a transmissivity lower than the correct one would be derived.
- Larger formation storativity (1E–5) improves the situation at transmissivities in the range 1E–11 m^2/s.
- A lower wellbore storage coefficient (i.e. smaller section length) improves the situation at transmissivities in the range 1E–11 m^2/s.
- The situation would change considerably in case the actual packer compliance under down-hole conditions is different than the one measured under surface conditions. Generally, it can be expected that under down-hole conditions the effect of packer compliance would decrease. Also as addressed by Geosigma, the effect of packer aging was not considered. It can be expected that the magnitude of the compliance would decrease with the age of the packer (i.e. number of inflations).

5.3 Background pressure gradients

5.3.1 General

Hydraulic test responses may sometimes be affected by other (external) factors which are not related to the test itself. Such factors include:

- Tidal effects.
- Precipitation.

[1] It should be observed that the test zone compressibility is defined slightly different than the effective compressibility of the test section used by Geosigma in this report, cf Section 5.1.2.

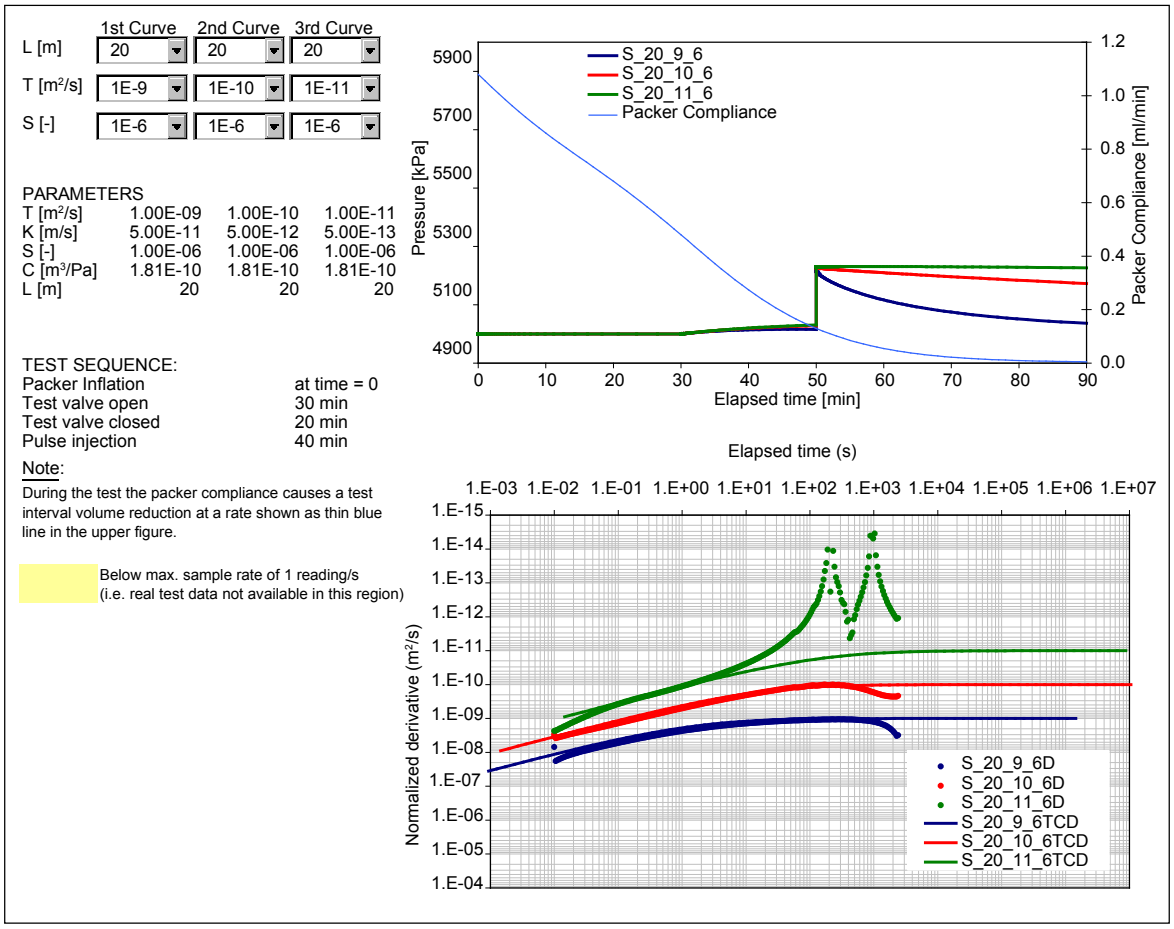

Figure 5-10. *Presentation of simulation results.*

- Barometric pressure changes.
- Sea level fluctuations.
- Earth quakes.
- Drilling and other activities in surrounding boreholes.
- Re-establishment of section pressure to formation pressure after packer sealing.

The influence of such factors can, in general, be neglected by the evaluation of short-time tests.

Below, some (randomly) selected examples of pressure histories from the Forsmark and Simpevarp area exhibiting different types of external “disturbances” are shown. Since several of the disturbances interact with each other, it is difficult to find clear examples of isolated disturbances. For comparison, examples of the rate of pressure changes due to different external factors are presented below.

5.3.2 Tidal effects

In Figure A3-1a in Appendix 3 examples of pressure variations along borehole KSH01 due to tidal effects are shown. Figure A3-1b shows the same effects in the isolated, deepest section KLX02_1: 256.4–1,700 m. During the actual time period, the scanning frequency of pressure was increased in this borehole. In the figures shown, the pressure decreases/increases by a rate of c. 0.09–0.1 kPa/20 min due to tidal effects.

5.3.3 Precipitation

The effects of precipitation (snow melting etc) on the pressure in isolated borehole sections may depend on many factors, e.g. the degree of saturation in the un-saturated zone together with duration and intensity of precipitation. Rapid responses on intensive rainfalls have been registered in shallow borehole sections. The pressure history in a percussion borehole (HAV08) together with the precipitation is shown in Figure A3-2a. During the period 25–26/11, 2004, a maximal rate of pressure increase of c. 2.2 kPa/20 min was observed in this borehole due to precipitation. On the other hand, in deeper sections in an arbitrarily selected, cored borehole only a faint response on precipitation, less than 0.01 kPa/20 min, was observed during the same time period.

Pressure responses due to precipitation are in general much lower in deep sections than in shallow sections. However, in conjunction with prolonged, continuous rainfall, pressure responses may also be observed in relatively deep borehole sections. A time lag between precipitation and pressure responses is generally observed in such cases. The magnitude of the time lag depends on a. o. the transmissivity of the section and its depth below the ground surface.

In Figure A3-2b, the observed pressure responses in isolated sections in borehole KLX02 in conjunction with an interference test with constant flow rate in HLX10 (Gustafsson and Ludvigson, 2005 /15/ are shown. Heavy rainfalls affected the test response during the two flow periods and subsequent recovery periods. A rainfall caused a significant recovery of the pressure during the first flow period. The maximal rate of pressure increase in section KLX02_1: 256.4–1,700 m during the later part of the first flow period was c. 0.04 kPa/20 min.

5.3.4 Sea water level

In boreholes at SFR, located close to the Forsmark candidate area, pressure changes corresponding to c. 70% of the change of the sea level in the Baltic Sea have been observed in some sections. The example shown in Figure A3-3 is derived from borehole KFM03A at Forsmark in conjunction with a pumping test with constant head in an isolated section of the borehole (Ludvigson et al. 2004) /16/. The observed flow rate variations from the pumped section thus reflect the natural pressure variations in the section. To be able to easier compare the flow rate variations with the corresponding sea level fluctuations the time scales of sea water level and atmospheric pressure have been shifted in the horizontal direction. The maximal rate of change of sea level in Figure A3-3 is c. 0.1 kPa/20 min.

5.3.5 Atmospheric pressure

The effects of the atmospheric pressure in the test section depend on a. o. if the section is confined or (partly) unconfined, depth to the section etc. The pressures (and groundwater levels) presented from the data acquisition system for observation boreholes as well as from the PSS system are given relative to the atmospheric pressure. The pressure in the section is measured by an absolute pressure sensor. The section pressure is calculated by subtraction of the observed atmospheric pressure at the surface from the measured absolute pressure. In general, the effect of the atmospheric pressure is relatively small for such short times (c. 20 min) as for an injection test. Sometimes, the pressure changes caused by the changes of the atmospheric pressure coincide with the tidal variations which may result in a relatively large superimposed response.

In Figures A3-4a and -b, the pressure history in observation borehole KSH01 during a 10 days period is presented. The calculated water levels in Figure A3-4a are adjusted for changes in atmospheric pressure. In Figure A3-4b, the absolute pressure at sensor depth in the different sections, expressed in m water column, is presented. The variations of the atmospheric pressure in the area during the same time period are shown in Figure A3-4c. If the part of the curve beginning the 8/1 and ending the 10/1 is considered, the maximal decrease/increase in atmospheric pressure is c. 2.5 kPa and c. 3.5 kPa, respectively. These variations of the atmospheric pressure correspond to a rate of 0.04 kPa/20 min.

Based on Figure A3-4a, an estimation of the total effect of the atmospheric pressure changes and the tidal in borehole section 3 during the first two hours on the 10/1 results in a rate of change of pressure of c. 0.20 kPa/20 min. This value may be compared with the estimated value above of c. 0.1 kPa/20 m for tidal effects only. By comparison of the pressure in the deepest section (section 1) in Figures A3-4a and -b at the time of the low atmospheric pressure (by the end of 05-09), it may be assumed that only part of the atmospheric pressure should be subtracted by the calculation of the groundwater level in this section.

In Figure A3-4d the effect of the atmospheric pressure in three sections of an arbitrarily selected percussion borehole is shown. Inspection of the section pressure and atmospheric pressure shows that these pressures are not completely correlated. It can not be excluded that also the variation of the sea level may have affected the observed water levels. The pressure variations during the time period 03-19 to 03-21 correspond to a rate of decline of the atmospheric pressure by c. 0.025 kPa/20 min. The change of the piezometric level in the borehole corresponds to a rate of change of the pressure of c. 0.013 kPa/20 min which means that the barometric efficiency is relatively large.

5.3.6 Earth quakes

Pressure responses caused by earth quakes have been observed in boreholes within SKB's study sites, e.g. earth quakes at Turkey (1999), Greece (2000) and South East Asia (2004). Such strong earth quakes are, however, not so frequent. Sometimes, small disturbances which may appear as earth quakes are registered but not reported in news media. From the recent earth quake at South East Asia, pressure changes with amplitudes of c. 16 kPa were registered in a borehole drilled from the Äspö Tunnel, cf Figure A3-5a. In a borehole drilled from the ground surface, amplitudes of c. 8 kPa were registered at the same time, cf Figure A3-5b. However, such disturbances are generally high, only during such short periods of c. 10 min.

5.3.7 Drilling

In Figure A3-6, an example of the effect in an observation borehole, caused by drilling of the borehole KFM01B at Forsmark is shown. The boreholes presented in the figure are located c. 120–150 m from the active borehole. According to the figure, the rate of change of pressure is c. 0.08 kPa/20 min. In previous investigations, pressure disturbances have been observed at larger distances.

5.3.8 Re-establishment of the section pressure to formation pressure

Some boreholes exhibit differences of c. 50–80 kPa in the formation pressure along the boreholes. This means that the formation pressure may deviate up to c. 40–50 kPa from the open borehole pressure. If the test section includes such a formation with higher pressure than in the open borehole, the section pressure will increase after the packer sealing. Sometimes it may be difficult to distinguish between effects generated by the packers from this type of responses. On the other hand, if a decrease of the pressure is obtained during packer sealing, it is probably caused by an under-pressure in the formation relative the open borehole pressure. Data from e.g. difference flow logging may provide information of differences in the formation pressue along the borehole. For example, in borehole KLX02, there are several indications of under-pressure in the middle and lower part of the borehole (Ekman, ed. 2001) /17/. From inspection of the recovery period of hydro-tests, the estimated rate of pressure decrease due to "under-pressure in formation" is sometimes c. 1–2 kPa/20 min. In Figure A3-7, an example from KLX02 is presented.

5.3.9 Conclusions

The ”environmental” impact on short-time hydraulic tests is generally so small that it can be neglected by the evaluation of the tests. The current standard data acquisition system of PSS has an estimated resolution in pressure of 0.7 kPa. For example, for injection tests showing fast recovery the pressure may thus appear virtually constant during almost the entire recovery period (c. 20 min). Theoretically, improved resolution of pressure may improve the possibility to extract more information from this period and thus refine the evaluation of the test. However, external factors may reduce this possibility. This is more discussed in Section 6.5.

Below, some estimated rate of pressure changes, expressed in kPa/20 min, due to external effects from randomly selected boreholes at Forsmark and Simpevarp are presented.

- Tidal effects: c. 0.1 kPa/20 min.
- Precipitation: c. 0.05 kPa/20 min. Much higher rates in shallow sections.
- Changes of atmospheric pressure: c. 0.015 kPa/20 min. Higher rates in shallow sections.
- Changes of the sea level: Visible effects but no rates are estimated.
- Earth quakes: Non-frequent. Strong earth quakes may have large effects during short times, even if occurring on the other side of the globe.
- Drilling and other activities in surrounding boreholes: c. 0.08 kPa/20 min.
- Re-establishment of the section pressure to formation pressure after packer sealing: c. 1–2 kPa/20 min.

If possible, test procedures and associated evaluations should be performed in such a way that the effects of above mentioned external factors are minimized.

The sensitivity to background natural pressure trends as presented in Section 5.3 (and external pressure trends) on the results on pressure pulse tests is discussed in Chapter 8.6.

6 Test statistics

Statistics of the results of all injection tests performed in seven of the cored boreholes at Forsmark is shown in Table 6-1 together with a description of the definition of the columns. The information in the table is retrieved from data presented in the Primary data reports from the actual boreholes listed in Section 1.2 in this report. Columns A–E in Table 6-1 show the actual borehole, total number of sections of different length in the boreholes, the number of tests performed and the number of tests below the standard (1 mL/min) and test-specific measurement limit (t-s.m.l), respectively. Columns F–S are related to the qualitative and quantitative evaluation of both the injection (Chi) – and recovery period (CHir) of the tests.

Columns F–S can be divided in seven major groups including tests with:

- Ambiguous interpretation of the injection- and/or recovery period (columns F–G).
- Inconsistent responses during the injection- and recovery period (columns H–J) and inconsistent results between test sections of different length (column K).
- Gauge resolution problems during the injection- and recovery period (columns L–M).
- Fast recovery (column N).
- No formation flow during the injection- and recovery period (columns O–P).
- Not analysable injection- and/or recovery period (columns Q–R).
- Clearly analysable injection- and recovery period (column S).

It should be born in mind that the individual number of tests assigned to the different columns in the table is subjective and should only be used in a statistical sense. In addition, some of the columns may represent similar or associated information which thus causes some redundancy in the table. For example, tests exhibiting fast recovery (column N) may also lead to inconsistent responses during the injection- and recovery period (columns H–J) and resolution problems of the pressure gauge (column M). Such tests are scored in all of these columns (and possibly also in further columns). In the sections below, the specific items of the test results in Table 6-1 are discussed.

6.1 Ambiguous responses

Ambiguous responses are defined if no clear identification of the flow model could be made due to

- test time too short,
- poor gauge resolution (mainly during the recovery period),
- poor pressure control during the injection period.

Examples of ambiguous responses are shown in Section 4.2.7.2. In Table 6-1, column F reflects the number of tests with poor control of the injection pressure in the different boreholes. The selection was made by manual inspection of the plots showing the injection pressure versus time. Tests, for which the evaluation was considered as ambiguous, were included in column F.

Column G includes tests for which the recovery period was considered as too short to make an unambiguous transient evaluation due to wellbore storage effects. In addition, tests with potential resolution problems during pressure recovery when the pressure approaches pseudo-stationary conditions, e.g. tests with fast recovery as identified from the pressure derivative in log-log plots were included in column G. Limited resolution of pressure may in some cases affect the shape of the pressure derivative curve and give the appearance of a false pseudo-radial flow regime in log-log plots when the pressure is close to stationary with a certain scatter (the derivative is changing around zero), cf Section 6.4.1. Many of the latter tests are also included in Column N (Fast recovery).

Table 6-1. Compilation of results from constant head injection tests in boreholes KFM01A–KFM07A at Forsmark.

A	B	C	D	E	F	G	H	I	J	K	L	M	N	O	P	Q	R	S
Borehole Seclength	Total no of sections	No of sections tested	No of sections < 1mL/min	No of sections below tsml	Ambiguous interpretation		Inconsistency between				Gauge resolution problem		Fast recovery	No formation flow (test too short)		Not analysable		Clearly analysable
					CHi	CHir	Chi and Chir (T-value)	Chi and Chir (Flow regime)	Chi and Chir (total)	Sections	CHi	CHir	Chir	CHi	CHir	CHi	CHir	CHi and Chir
KFM01A																		
100 m	9	9	5	4	1	4	2	0	2	0	–	0	0	–	4	0	2	3
20 m	45	15	3	3	1	7	7	0	7	0	–	0	0	–	11	0	7	5
5 m	178	51	28	26	1	9	13	3	14	–	–	1	0	–	20	2	12	12
Total:	232	75	36	33	3	20	22	3	23	0	–	1	0	–	35	2	21	20
KFM02A																		
100 m	9	8	2	0	2	5	7	2	7	1	–	1	1	–	4	1	7	1
20 m	45	22	3	2	2	12	16	10	17	0	–	9	9	–	3	1	15	3
5 m	178	74	22	18	3	34	47	39	48	–	–	22	24	–	12	2	45	8
Total:	232	104	27	20	7	51	70	51	72	1	–	32	34	–	19	4	67	12
KFM03A																		
100 m	9	8	0	0	1	2	2	3	3	0	–	2	2	–	3	1	2	5
20 m	45	46	22	13	0	11	14	5	16	0	–	3	2	–	18	2	12	17
5 m	178	103	61	51	1	15	25	15	28	–	–	8	6	–	15	3	20	24
Total:	232	157	83	64	2	28	41	23	47	0	–	13	10	–	36	6	34	46
KFM04A																		
100 m	9	9	2	1	0	3	4	1	5	0	–	1	1	–	4	1	4	3
20 m	43	22	5	3	1	4	7	4	10	0	–	1	1	–	4	1	6	9
5 m	171	32	15	13	2	7	11	7	11	–	–	5	2	–	5	0	9	8
Total:	223	63	22	17	3	14	22	12	26	0	–	7	4	–	13	2	19	20
KFM05A																		
100 m	9	10	4	3	0	6	5	0	5	0	–	0	0	–	6	1	5	2
20 m	44	16	8	6	1	4	4	0	4	0	–	0	0	–	7	1	4	6
5 m	174	29	14	10	1	6	9	4	10	–	–	1	0	–	9	2	8	9
Total:	227	55	26	19	2	16	18	4	19	0	–	1	0	–	22	4	17	17
KFM06A																		
100 m	9	9	2	2	0	0	0	0	0	0	–	0	0	–	3	0	0	7
20 m	45	35	12	11	3	0	5	4	7	0	–	0	1	–	6	2	1	17
5 m	177	71	20	13	6	5	18	17	27	–	–	2	1	–	9	6	3	31
Total:	231	115	34	26	9	5	23	21	34	0	–	2	2	–	18	8	4	55
KFM07A																		
100 m	9	8	6	5	0	2	0	0	0	1	–	1	0	–	2	0	0	3
20 m	45	9	3	3	0	3	2	1	3	0	–	3	0	–	1	1	0	4
5 m	178	29	13	13	0	4	2	8	8	–	–	4	2	–	4	0	1	9
Total:	232	47	22	21	0	9	4	9	11	1	–	8	2	–	7	1	1	17

tsml = test specific measurement limit

Criteria used for retrieval of the information in Table 6-1.

Column A	Borehole and section length.
Column B	Tested interval with a certain section length.
Column C	Total number of tested sections (including pressure pulse tests).
Column D	Total number of tested sections with a final flow rate below 1 mL/min (including pressure pulse tests).
Column E	Total number of tested sections with a final flow rate below the estimated test-specific lower measurement limit (including pressure pulse tests).
Column F	Poor Chi control: Tests with such a noisy data due to poor control of the injection pressure making an unambiguous interpretation difficult or impossible (subjective).
Column G	Poor gauge resolution: The pressure derivative by the end of the recovery period is highly affected by the step length (filter factor) used Test time considered too short, making an unambiguous interpretation difficult or impossible due to i) wellbore storage (tests classified as WBS or WBS- >) or ii) Poor gauge resolution (defined as if the pressure derivative is non-representative by the end of the recovery period).
Column H	Tests for which Ts and Tf differs by a factor of 3 or more and/or if either Ts or Tf is missing (tests below the test-specific measurement limit are excluded).
Column I	Tests exhibiting inconsistent responses during the injection- and recovery period. Defined as if any of the flow regimes PLF, PRF, PSF or PSS is present during the injection period at least one of them must be present during recovery (tests exhibiting only WBS during recovery and tests below the test-specific measurement limit are excluded).
Column J	The union of the number of tests in columns H and I.
Column K	Number of tests containing at least one shorter section with an estimated T-value more than 3 times higher than the actual longer section. Results from 100 m sections were only compared with 20 m sections and 20 m sections compared with 5 m sections.
Column L	Not applicable.
Column M	The same criteria as Poor gauge resolution in column G.
Column N	Number of tests exhibiting PSS or PSF during the recovery period but not during the injection period.
Column O	Not applicable.
Column P	Number of tests exhibiting WBS or WBS- > (WBS+transition period).
Column Q	Number of tests with no Tf reported. (tests below the test-specific measurement limit are excluded). Depends on both evaluation- and instrumental problems.
Column R	Number of tests with no Ts reported. (tests below the test-specific measurement limit are excluded). Depends on both evaluation- and instrumental problems.
Column S	Number of tests exhibiting the same flow regime (PRF, PLF, PSF or the recovery period only exhibits WBS) and/or Ts and Tf deviate by a factor of 3 or more.

Nomenclature.

CHi	Flow period of a constant head injection test.
CHir	Recovery period of a constant head injection test.
Tf	Transmissivity estimated from the flow period.
Ts	Transmissivity estimated from the recovery period.
PLF	Pseudo-linear flow regime.
PRF	Pseudo-radial flow regime.
PSF	Pseudo-spherical (leaky) flow regime.
PSS	Pseudo-stationary flow regime.
WBS	Wellbore storage.

Column F in Table 6-1 shows that rather few tests have been identified with such a poor pressure control to make the evaluation of the tests ambiguous, although the number of such tests varies from borehole to borehole. On the other hand, column G shows that several tests are considered too short to make a clear identification of the flow model or are affected by poor pressure resolution during the recovery period, respectively. Tests considered too short for an unambiguous transient evaluation in column G are also included in column P (No formation flow) whereas tests with gauge resolution problems also are included in columns M and N and (partly) in columns H–J.

The increased number of tests in column G for borehole KFM02A is probably a result of the increased number of tests showing fast recovery in this borehole (column N) with associated pressure resolution problems as discussed in Section 6.4.1. After subtracting such tests in column G, the remaining number of tests with ambiguous interpretation seems to be rather similar for the different boreholes.

6.2 Inconsistent results from the flow- and recovery period

Inconsistent results from the flow- and recovery period are defined if criterion i) and/or ii) below are true.

i) different flow models are used for interpretation of the flow- and recovery period of the same section,

ii) different transmissivities are derived (deviation of more than ± 30% of a log cycle corresponding to a factor of c. ± 3 or more).

Possible reasons to inconsistent behaviour during the flow- and recovery period of the tests may be, for example:

- dominating wellbore storage effects during the recovery period but a certain flow regime could be interpreted during the flow period,
- turbulent flow in fractures, predominantly during the flow period,
- factors related to the drilling operation, e.g. flushing pressure etc,
- (hydro)geological factors, e.g. wide fracture zones with interconnected fractures,
- flow features of limited extension (showing apparent NFB) or decreasing aperture away from the borehole.

In Table 6-1, the number of tests satisfying condition i) is shown in column I whereas the number of tests satisfying condition ii) is shown in column H. Column J shows the union of tests in columns H and I. Column H also includes tests for which the transmissivity was not estimated from either the flow or recovery period (Columns Q and R), cf KFM02A.

In several of the tests in low-transmissive sections, wellbore storage (WBS) dominated the recovery period and no clear flow regime was developed. For many of these tests an apparent pseudo-radial flow regime could though be identified during the flow period. Thus, such tests are classified as “Inconsistent” and included in column I in Table 6-1. However, tests exhibiting *only* WBS during the recovery period are not included in this column. Instead, such tests are included in column G in Table 6-1 (Ambiguous responses).

By comparing columns H and I in Table 6-1 it is evident that, in most boreholes, more tests show inconsistency regarding calculated transmissivities than regarding interpreted flow regimes. This fact is to some extent due to that the transmissivity was not estimated from the recovery period in some boreholes if a pseudo-stationary flow regime (e.g. fast recovery) dominated the period, particularly in boreholes KFM01A–KFM03A, see below. Such tests are also classified as “Inconsistent” and included in column H in Table 6-1. It should be pointed out that in borehole KFM01A mainly the pseudo-radial flow regime was considered by the evaluation.

Table 6-1 (columns H and I) indicates that the highest number of inconsistent tests is found in borehole KFM02A, both regarding calculated transmissivity (H) and interpreted flow regimes (I), particularly the tests in 5 m sections. This fact is partly explained by the increased number of tests exhibiting pseudo-stationary flow (fast recovery) during the recovery period in this borehole. As discussed above, the transmissivity was not estimated from the recovery period in such cases in KFM02A (column H). Borehole KFM02A intersects several deformation zones together with an interval of porous granite, cf Table 6-2.

For several tests a pseudo-radial flow regime could be defined during the flow period but not during the recovery period. In boreholes KFM06A and KFM07A the number of inconsistent tests regarding transmissivity decreases. Tests exhibiting pseudo-stationary flow (e.g. fast recovery) during the recovery period, but not during the flow period, are also listed in column N (Fast recovery) in Table 6-1 and further discussed in Section 6.4.

Finally, inconsistent responses and/or results between the flow and recovery period may occur if the test section is intersected by flow feature(s) of limited extension or decreasing aperture away from the borehole. Such sections may indicate the presence of apparent no-flow boundary (NFB) but a relatively high transmissivity ($T_M > 1 \cdot 10^{-7}$ m^2/s) during the flow period but exhibit a slow and small pressure recovery (c. 10–20 % of the applied injection pressure). An example of such behaviour is shown in Figure 6-1a and b.

Column K in Table 6-1 shows the number of tests for which the calculated transmissivity is inconsistent between sections of different length. The column shows that there are very few tests with significantly higher transmissivities in shorter sections than in the corresponding longer section in all boreholes tested.

6.3 Tests not analysable

Non-analysable tests are defined as tests for which no results of the quantitative evaluation of the flow- and/or recovery period are reported, cf columns Q and R, respectively in Table 6-1. For such tests no unambiguous transient evaluation is possible. Tests below the test-specific lower measurement limit (column E) are excluded in these columns. Column Q shows that there are rather few tests with no reported evaluated parameters from the injection period. The majority of such tests are likely to be due to poor pressure control during the injection period (cf column F). Not analysable flow period of a test may also arise if the period is dominated by apparent no-flow boundary (NFB), possibly indicating a flow feature of limited extension or decreasing aperture away from the borehole, cf Figure 6-1a.

Several tests with no reported parameters from the recovery period in column R are also classified as ambiguous interpretations due to too short test times considering WBS and thus included in column G in Table 6-1 (together with additional tests). In addition, tests with fast recovery, rapidly approaching a pseudo-stationary flow regime (PSS) were sometimes not analysed. These tests are also included in Column N (fast recovery) in Table 6-1.

In boreholes KFM01A–KFM03A, no parameters from quantitative evaluation of tests with fast recovery was, in general, reported for the recovery period provided that a pseudo-radial flow regime (PRF) could be identified during the injection period of the test. The parameters evaluated from the latter period were, in most cases, selected as representative from such tests. However, for borehole KFM04A and subsequent boreholes, evaluated parameters from the recovery period are generally also reported for such tests. This fact partly explains the significantly lower number of tests in column R (not analysable during recovery period) for the latter boreholes in Table 6-1 in comparison to boreholes KFM01A–KFM03A.

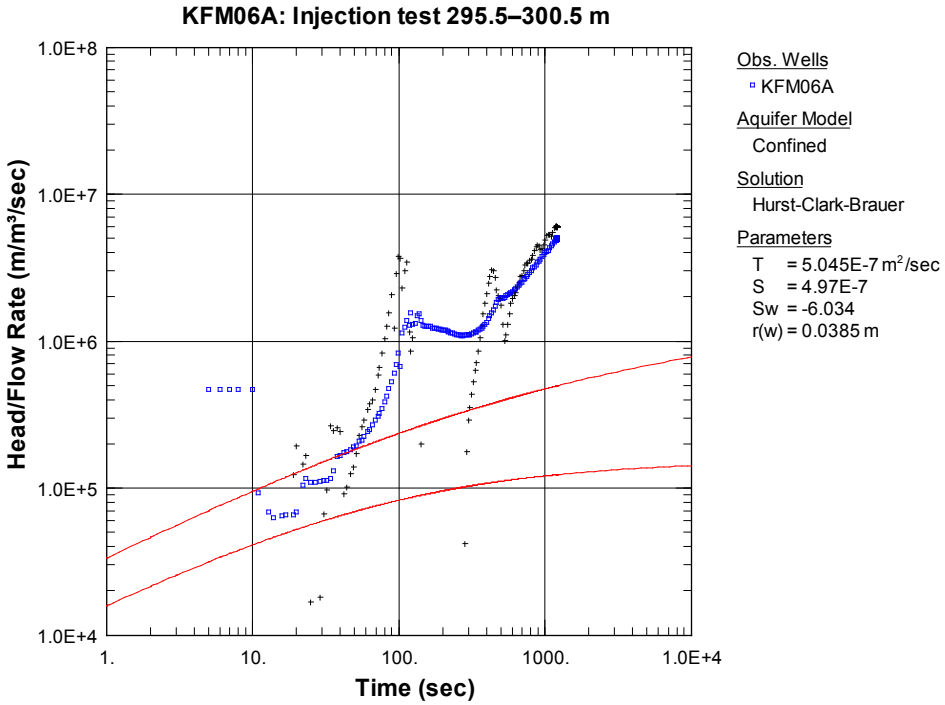

Figure 6-1a. *Head/flow rate (□) and derivative (+) versus time during the flow period of constant head injection test in section KFM06A:295.5–300.5 m showing effects of apparent no-flow boundary. No unambiguous transient evaluation is possible. The simulated responses with red lines (head/flow rate and its derivative) correspond to the hydraulic parameters derived from the recovery period of the test in Figure 6-1b for comparison.* $T_M = 1.6 \cdot 10^{-7}$ *m²/s.*

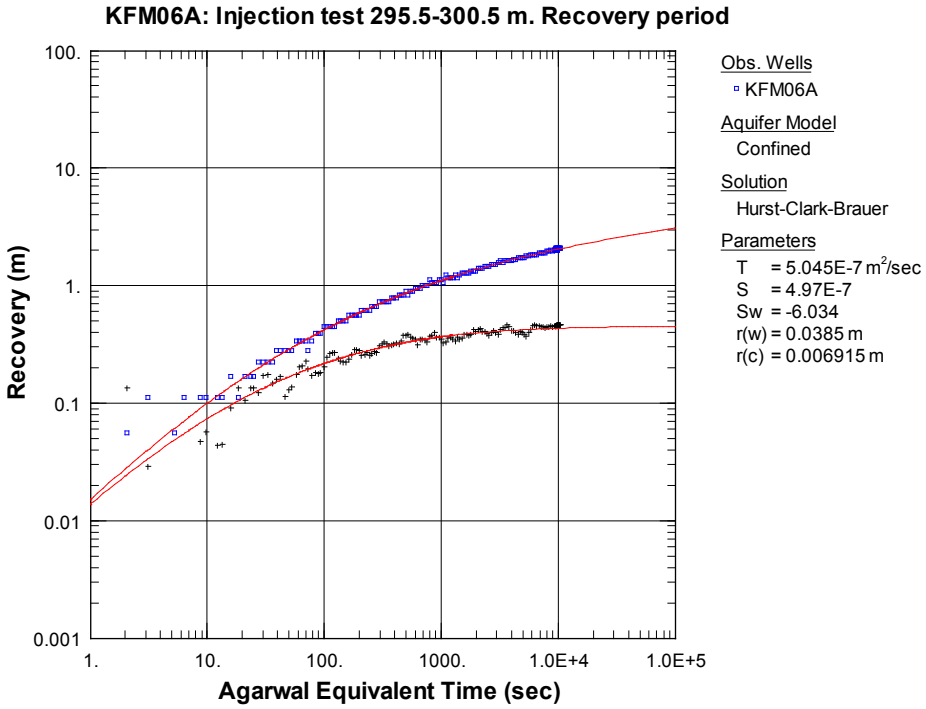

Figure 6-1b. *Pressure (□) and pressure derivative (+) versus Agarwal equivalent time during the recovery period of constant head injection test in section KFM06A:295.5–300.5 m showing inconsistent responses. The recovery is only c. 13% of the applied injection head of c. 14 m. The simulated responses (pressure and pressure derivative) are shown as red lines. From SKB P-05-165.*

6.4 Fast recovery

6.4.1 Correlation to geological conditions

Tests exhibiting fast recovery, reflected by a fast transition to a pseudo-stationary (PSS) or pseudo-spherical flow regime (PSF) after stop of injection but a different flow regime during the flow period, are listed in column N in Table 6-1. As discussed above, the dominating number of such tests occurs in KFM02A. To investigate possible reasons for the increased number of tests showing fast recovery in borehole KFM02A, mainly tests exhibiting pseudo-stationary flow (PSS) during the recovery period are listed in Table 6-2. In addition, the calculated transmissivities and interpreted flow regimes for these tests as reported in the actual SKB P-report (P-04-100), cf Section 1.2, together with the interpreted geological units in the sections are included in the table.

Table 6-2 indicates that almost all test sections with fast recovery can be correlated to interpreted deformation zones and to the interval with porous granite in KFM02A. Most of these intervals have a rather high transmissivity. In addition, several tests exhibit a pseudo-radial flow regime (PRF) during the injection period but a pseudo-stationary flow regime (PSS) during the recovery period, even in rather low-transmissive sections, e.g. 496–501 m. These tests thus show both inconsistent responses during the injection and recovery period and unexpectedly fast recovery.

In the geological units included in Table 6-2, pseudo-radial flow might be expected. On the other hand, pseudo-spherical flow (PSF), eventually approaching pseudo-stationary (PSS), may occur in short test sections in thick formations with interconnecting fractures. An alternative explanation to the fast recovery observed in many sections would be turbulent flow in fractures (or other head losses) during the injection period which possibly might affect the subsequent recovery period. In some tests with fast recovery, effects of apparent no-flow boundaries (NFB) are observed during the preceding flow period.

6.4.2 Step injection test at different pressures

In conjunction with the ordinary injection test campaign in KFM05A, reported in SKB P-05-56, special tests with different injection pressures were performed in section 284–289 m. This section was selected due to the observed fast recovery during the standard injection test, which fact may possibly indicate turbulent flow in fractures intersecting the section, cf Figure A4-1 and -2 in Appendix 4. Figure A4-3 shows the flow rate during the standard injection test.

During the step injection test the injection pressure was increased in steps with subsequent recovery after each injection period. The transient responses during the step injection tests are shown in Appendix 3 in SKB P-05-56. All recovery plots show a fast pressure recovery towards a stable pressure by the end of the recovery period for this rather low-transmissive section, similar to the responses during the standard injection test in this section. Similar transmissivities were calculated from the injection periods for the different pressure steps. However, no unambiguous evaluation could be made from the recovery periods due to the fast recovery. The transient flow rate curves during the different pressure steps of the step injection tests are shown in Figures A4-4 to A4-7 in Appendix 4. A slight jump in flow rate occurred in the beginning of the last pressure step (300 kPa). The reasons are not clear.

As discussed in Section 4.2.7.1, the limited resolution of the pressure gauge may cause distortions on the pressure derivative when the pressure is approaching a near steady-state. The derivative sometimes becomes very scattered with an apparent segment of a flat derivative by the end of the recovery. This segment may erroneously be interpreted as a pseudo-radial flow regime.

To investigate possible effects of turbulent flow, the linearity between the measured final flow rates at each step and the corresponding pressure was studied. In Figure 6-2, the measured final flow rate versus the injection pressure for the step injection test is shown. In addition, the theoretically predicted flow rates at each pressure step, assuming a constant specific flow (Q_p/dp) based on the test at the lowest injection pressure, are shown. Figure 6-2 indicates that

the flow rate does not increase proportionally with the injection pressure as expected theoretically. The deviation between the measured and theoretical flow rate can be explained by various head losses in the borehole, including skin effects and turbulence etc (Atkinson et al. 1994) /18/. However, the deviation is rather small in this case which means that the specific flow rate is rather constant for each step, cf Figure 6-3.

Table 6-2. Tests exhibiting fast recovery in borehole KFM02A. After SKB P-04-100.

Borehole	Borehole secup (m)	Borehole seclow (m)	Dominating flow regime Injection	Recovery	TR (m^2/s)	Geological unit (m^2/s)
KFM02A	103.5	108.5	PRF1->PRF2	WBS->PSS	2.25E–09	Deformation zone
KFM02A	106	111	PRF/PSF	PSS	3.88E–05	Deformation zone
KFM02A	111	116	PRF->PSF	PSS	6.04E–05	Deformation zone
KFM02A	116	121	PRF/PSF?	PSF	1.31E–04	Deformation zone
KFM02A	121	126	PRF/PSF?	PSF	6.90E–05	Deformation zone
KFM02A	161	166	PRF	PSF	4.11E–07	Deformation zone
KFM02A	166	171	PRF	PSF	4.27E–07	Deformation zone
KFM02A	171	176	PRF/PSF?	PSF	3.35E–06	Deformation zone
KFM02A	176	181	PRF	PSS	3.31E–08	Deformation zone
KFM02A	264.5	269.5	PRF/PSF?	PSS	1.13E–06	Porous granite
KFM02A	269.5	274.5	PRF	PSS	1.54E–07	Porous granite
KFM02A	271	276	PRF->NFB?–>PSF?	PSS	1.13E–06	Porous granite
KFM02A	276	281	PLF->PRF?	PSS	2.78E–07	Porous granite
KFM02A	281	286	PRF->PLF	PSS	2.58E–06	Porous granite
KFM02A	286	291	PRF1->PLF–>PRF2	PSS	1.82E–06	Porous granite
KFM02A	291	296	PRF	PSS	3.64E–06	Porous granite
KFM02A	296	301	PRF	PSS	2.05E–06	Porous granite
KFM02A	421	426	PRF->NFB?	PSS	2.30E–07	
KFM02A	426	431	PRF	PSS	1.15E–06	Deformation zone
KFM02A	431	436	PRF?	WBS->PSS	3.56E–09	
KFM02A	436	441	PRF	PSS	1.06E–07	
KFM02A	446	451	PRF->NFB	WBS->PSS	9.15E–09	
KFM02A	451	456	PRF	PSF	2.05E–08	
KFM02A	476	481	PRF	PSF	2.58E–07	Deformation zone
KFM02A	481	486	PRF	PSF	1.03E–08	Deformation zone
KFM02A	486	491	PRF	PSS	8.14E–08	Deformation zone
KFM02A	491	496	PRF	WBS->PSS	6.47E–09	Deformation zone
KFM02A	496	501	PRF	PSS	1.63E–08	Deformation zone
KFM02A	501	506	PRF	WBS->PSF	1.03E–09	
KFM02A	511	516	PSF	WBS->PSS	2.03E–06	Deformation zone

The specific flow rate, which is directly proportional to the transmissivity of the section, decreased from c. $4.3 \cdot 10^{-9}$ m^2/s for the lowest injection pressure (50 kPa) to c. $2.8 \cdot 10^{-9}$ m^2/s for the highest pressure (300 kPa), i.e. only by a factor of 1.5 as shown in Figure 6-3. Thus, the head losses, e.g. due to turbulence during the injection period, are assumed to be small and can probably not fully explain the fast recovery observed in this case.

6.5 Gauge resolution problem

Gauge resolution problems (shown in columns L and M in Table 6-1) may arise during the recovery period when very small pressure changes occur by the end, e.g. in sections showing fast recovery. Table 6-1 shows that potential gauge resolution problems were only observed during the recovery period of the tests performed at Forsmark. As discussed above, the number of such tests was increased in borehole KFM02A.

As mentioned earlier, the data acquisition system has a standard resolution of pressure of c. 0.7 kPa. The pressure control system includes a data logger with an AD converter. To be able to detect any errors on the control system and to improve the function of the system, the current status of valves and data records from the flow meters and pressure sensors in the test sections are stored each second. The stored values are overwritten when the memory is full. The resolution of the control system regarding the pressure sensor in the test section is 0.005 kPa. An attempt was made to dump data from the control computer to further study this issue. The actual data record retrieved involved data from the flow period of a previous rinse pumping activity before hydro-chemical sampling in borehole KFM03A, i.e. the section pressure, which is continuously controlled by the control computer. The recorded pressures each second show a large noise which partly is assumed to be due to the pressure control. The noise can though be reduced by filtering of the data.

It should be pointed out that the reported accuracies for pressure in Section 3.2.3 will not be improved if the data are collected from the control computer instead of the data acquisition system. It is very hard to assess the noise level during e.g. the recovery period of an injection test without using regulation of the pressure. Filtering of such data may possibly reduce the noise of the data to c. ± 0.1 kPa. To confirm the magnitude of the noise level, data must be extracted from the recovery period of a few tests which have achieved a rather constant pressure level. However, it is not possible to confirm that the calculated pressure variations represent real pressure fluctuations. The eventually improved resolution of pressure data (including noise) may possibly be used to improve the evaluation of some of the flat recovery curves. However, care should be exercised by the evaluation of very flat pressure curves during the recovery period if:

- data may be affected by natural and external pressure variations, cf Section 5.3,
- data calculated from filtered measurement data have not been confirmed by pressure calibrations.

6.6 Wellbore storage coefficient

Figures 6-4a-c shows the estimated wellbore storage coefficient C from the analysis of the recovery periods of the injection tests as described in Section 4.2.3 versus the representative transmissivity for tests in different section lengths at Forsmark. Estimated C-values, reported from boreholes KFMA01A–07A at Forsmark are included in the figures. Although similar values on C were obtained from the simulation of the transient test responses by type curve matching and from the initial straight line of slope 1:1, only the latter values were reported.

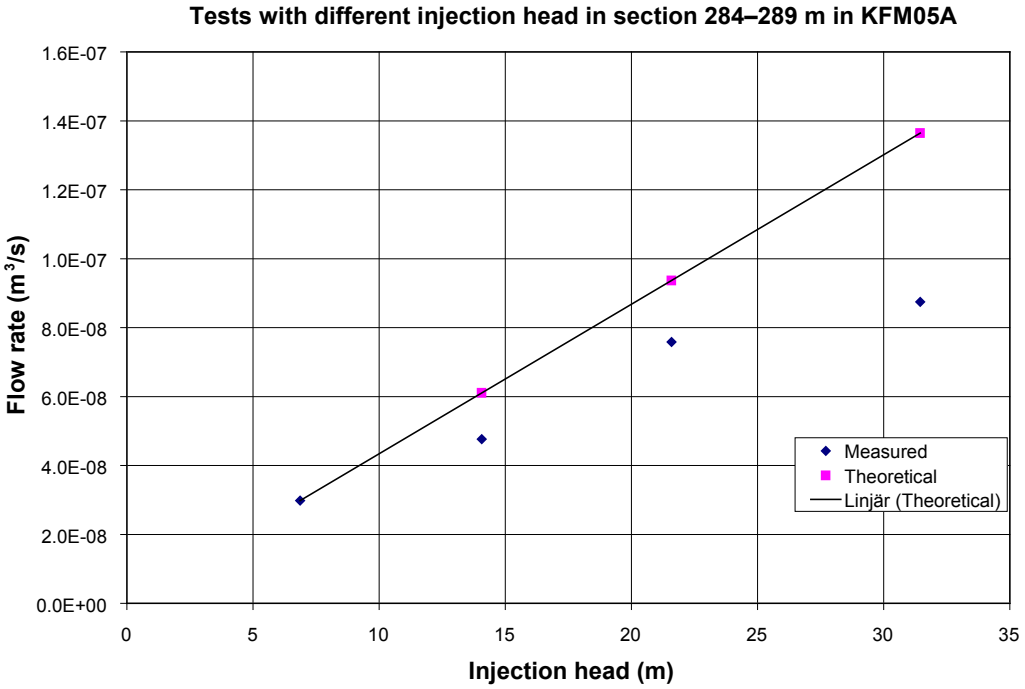

Figure 6-2. *Linear plot of measured final flow rates (Q_p) versus injection head for the step injection tests in section 284–289 m in KFM05A together with theoretically predicted flow rates assuming a constant specific flow (Q_p/dp) based on the measured specific flow at the lowest injection pressure step.*

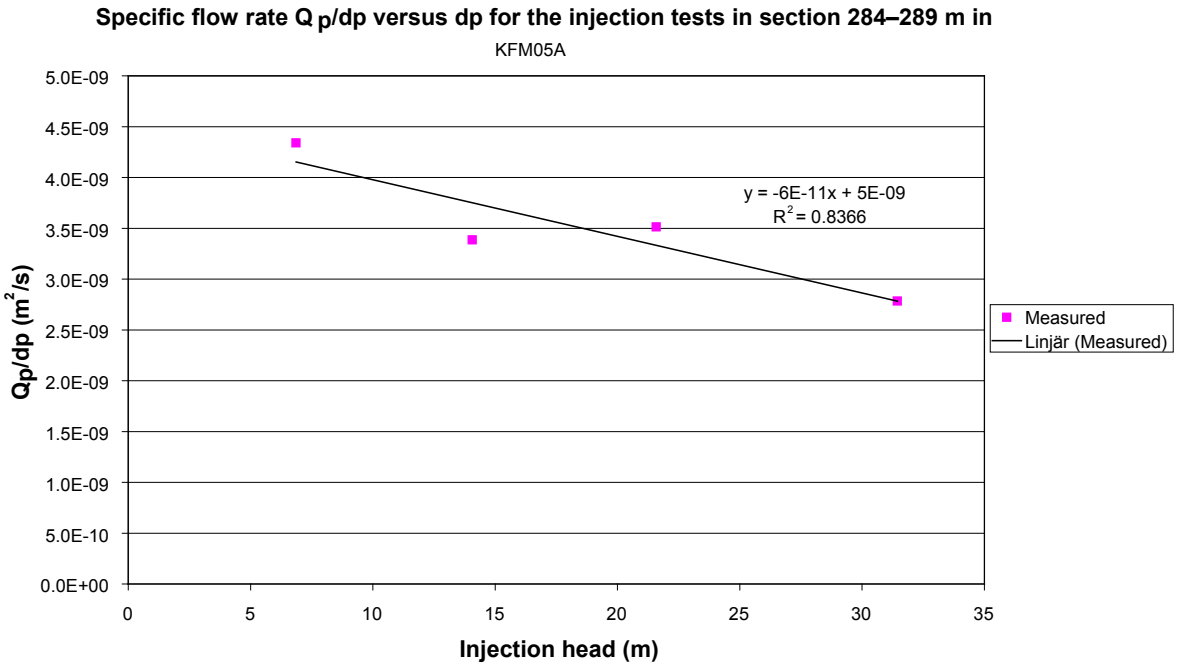

Figure 6-3. *Linear plot of measured specific flow rate (Q_p/dp) versus injection head for the step injection tests in section 284–289 m in KFM05A together with a linear regression line of the measured data.*

C was only calculated for tests with a well-defined slope of 1:1 in the beginning of the recovery. This means that only tests with transmissivities less than c. $1 \cdot 10^{-7}$ m^2/s are included since no well-defined straight line of such a slope generally is visible in sections with higher transmissivity in the actual time interval of the tests. In fact, calculated C-values in sections of higher transmissivity than c. $1 \cdot 10^{-8}$ m^2/s are considered as increasingly uncertain due to this fact. In the figures below the estimated, effective borehole storage coefficient from laboratory tests for the corresponding section lengths as described in Section 5.1.2 and the net values on C based on borehole geometry are shown for comparison.

Figure 6-4a shows that there is a good agreement between estimated C-values from the tests, the net value of C (C_{net}) and the calculated effective wellbore storage coefficient (C_{eff}) for the 100 m sections. In 100 m sections, the net values of C are the same as the effective C_{eff}, i.e. no effects of packer compliance are observed.

In shorter test sections the estimated C-values from the tests are, in general, slightly higher than the corresponding net- and effective values on C due to the increasing effect of packer compliance in shorter sections, cf Figures 6-4b and c. For test sections with transmissivities higher than about $1 \cdot 10^{-8}$ m^2/s, reliable estimates of C may not be obtained due to virtual absence of wellbore storage effects in such sections during the times sampled.

It should be noted that a few outliers are present in the above figures with significantly deviating C-values. Some of these may be real, e.g. one section in KFM05A appearing in all test section lengths, due to e.g cavities or presence of gas in the water in the borehole sections whereas others, particularly for transmissivities above $1 \cdot 10^{-8}$ m^2/s, may be non-representative for the test.

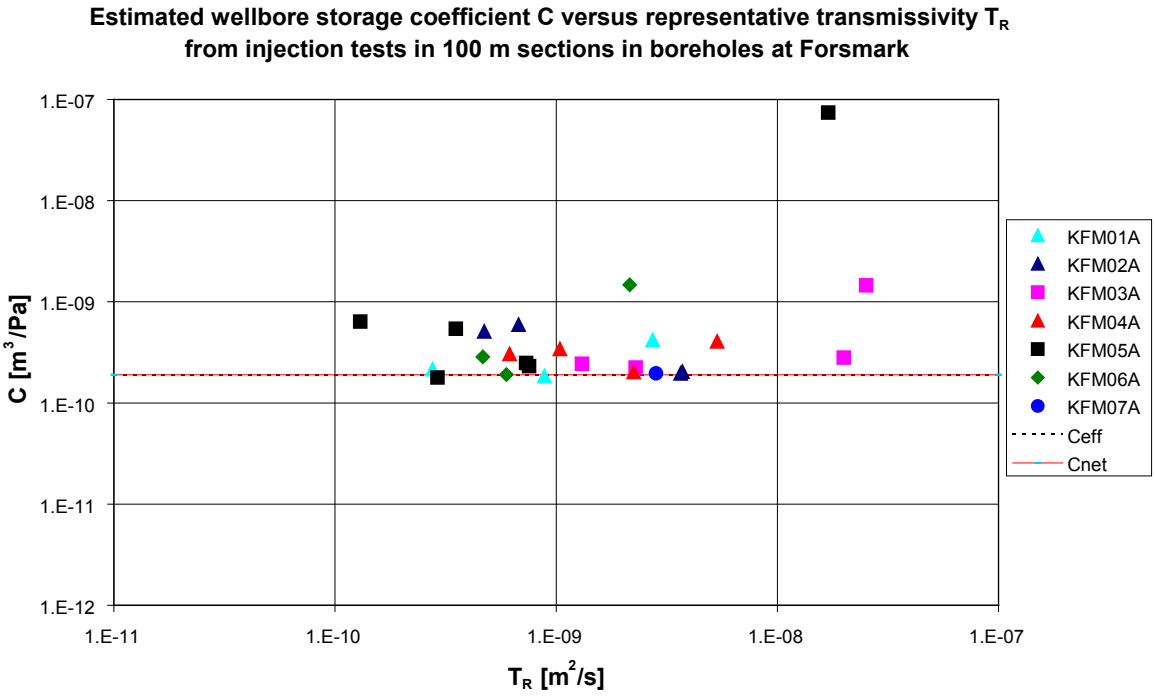

Figure 6-4a. *Estimated wellbore storage coefficient C versus representative transmissivity T_R from injection tests in 100 m sections in different boreholes at Forsmark. For comparison, the calculated values of effective (Ceff) and net wellbore storage coefficient (Cnet) are shown.*

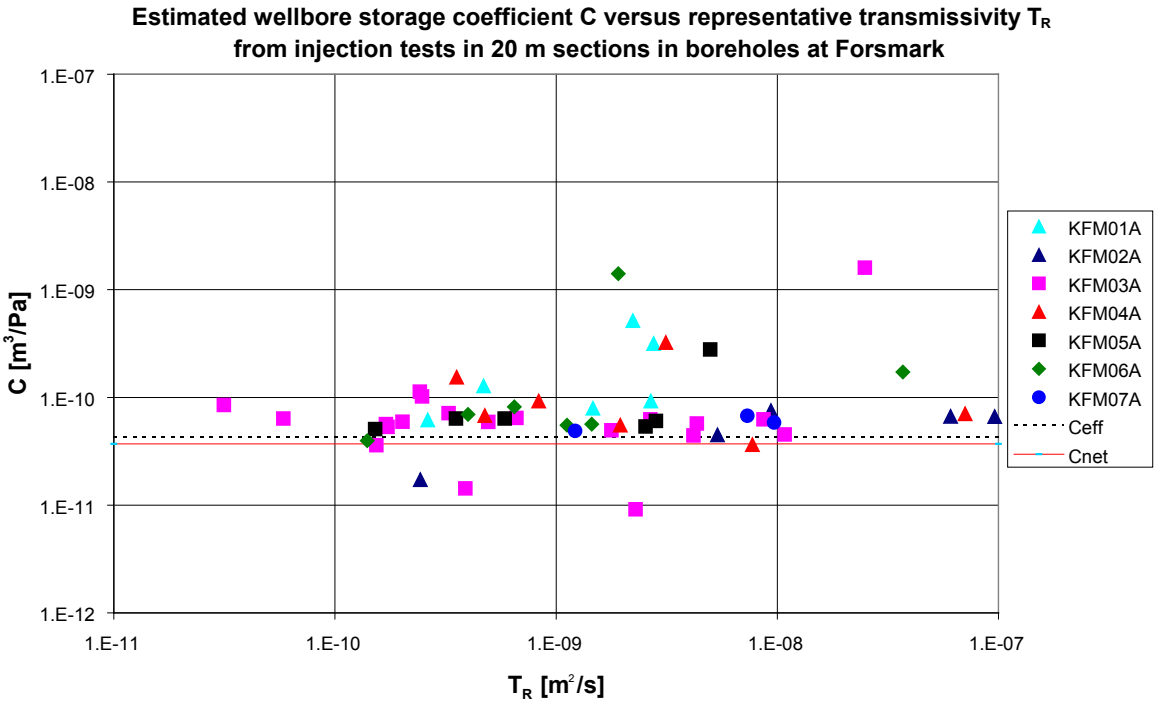

Figure 6-4b. *Estimated wellbore storage coefficient C versus representative transmissivity T_R from injection tests in 20 m sections in different boreholes at Forsmark. For comparison, the calculated values of effective (Ceff) and net wellbore storage coefficient (Cnet) are shown.*

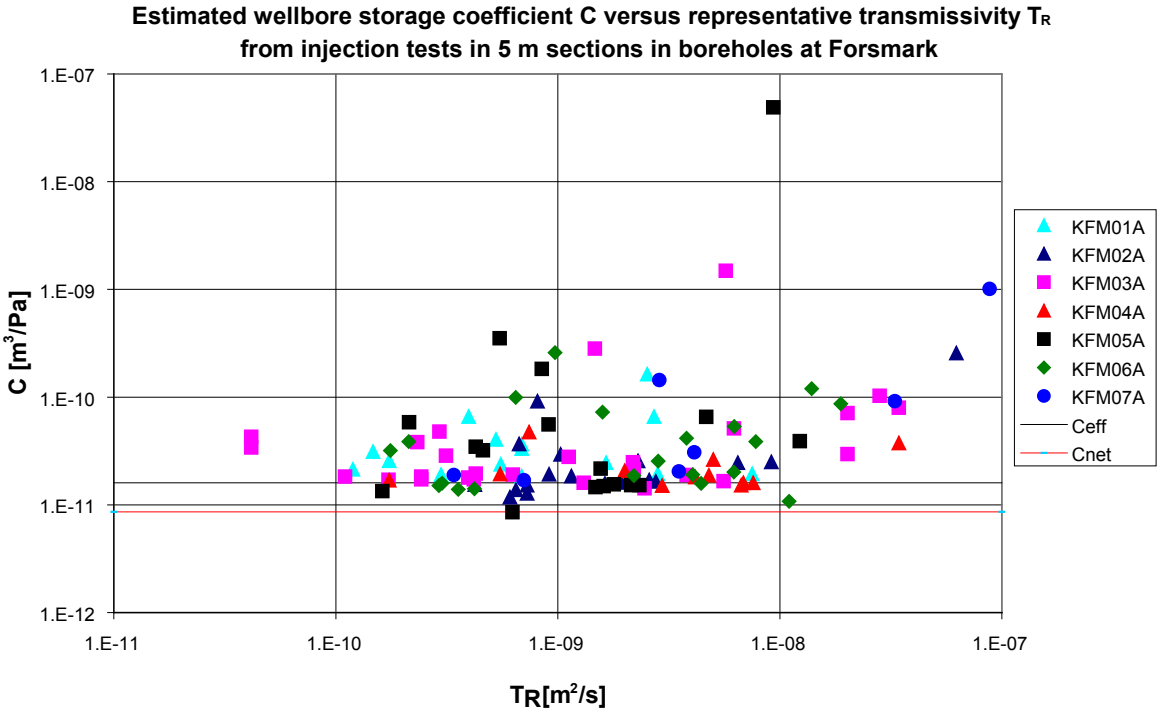

Figure 6-4c. *Estimated wellbore storage coefficient C versus representative transmissivity T_R from injection tests in 5 m sections in different boreholes at Forsmark. For comparison, the calculated values of effective (Ceff) and net wellbore storage coefficient (Cnet) are shown.*

7 Differences in analysis methodology between Golder and Geosigma

Below, a summary of the test analysis methodologies used by Golder and Geosigma in selected main items together with a comparison and conclusions is presented. Any differences and their implications, with emphasis on the results presented to the Sicada data base, are discussed.

7.1 Software used

7.1.1 Geosigma

The test analysis software Aqtesolv, extended for constant pressure tests, was used for test analysis. The software contains a suite of analytical solutions (models) of different types of tests (constant rate, constant pressure, slug- and pressure pulse tests) and flow characteristics. Both manual analysis and automatic simulation by non-linear regression technique can be performed. The software simulates the response in real time according to a certain analytical model for a given set of hydraulic parameters and compares with the observed response. The associated derivatives may be calculated according to the algorithms by Bourdet et al. (1989) /19/ and/or Spane and Wurstner (1993) /20/.

7.1.2 Golder

The Golder in-house test analysis program FlowDim V2.14b was used for the analysis. FlowDim allows the analysis of constant rate, constant pressure, slug and pulse tests both in source and observation boreholes. The program uses manual and automated (non-linear regression) type curve and derivative analysis. The flow models available include homogeneous, two-zone composite and dual porosity for any flow dimension between 1 and 3. FlowDim uses one step superposition for the analysis of constant rate and recovery tests and deconvolution as well as RAMEY analysis for the analysis of slug and pulse tests. The program has been widely used in the frame on radioactive waste projects since 1994.

7.1.3 Comparison and conclusions

Both software programs used implement state of art test analysis methods and have been validated in the frame of past testing projects. It can be assumed that the analysis programs produce compatible results.

7.2 Models used for transient analysis of the injection period of the injection tests

7.2.1 Geosigma

Models based on Hurst, Clark and Brauer (1969) /3/ for radial flow and Hantush (1959) /5/ for pseudo-spherical (leaky) flow in an equivalent porous medium were used. Both models include the inverse flow rate derivative and skin according to the effective wellbore radius concept. The models by Ozkan and Raghavan (1991) /6a and 6b/ were used for linear flow in single fractures.

The evaluation of the hydraulic parameters is made on the time interval representing the rock conditions close to the borehole (inner region) or outside the skin zone if such a zone is present. In some cases the properties of an outer zone with different transmissivity were also calculated.

The presence of apparent outer hydraulic boundaries (no-flow and constant pressure) was only evaluated qualitatively.

From borehole KFM05A and onward, the storativity was estimated from a regression relationship between T and S presented in SKB (2006) /8/. For previous boreholes the storativity was assumed at $1 \cdot 10^{-6}$, independently of the transmissivity.

7.2.2 Golder

Golder uses a generic two-zone composite fractional dimension model in the analysis. According to the observed behaviour, the model was configured in most cases to a flow dimension of two (radial flow). Linear and spherical flow can be simulated as well as changes of flow dimension at some distance from the borehole. All models account for borehole effects (i.e. wellbore storage and skin).

In cases when only one parameter zone was seen by the tests, a homogeneous (one zone) flow model was used. Constant pressure boundaries were modelled as an increase of transmissivity in the outer composite zone, no flow boundaries were modelled as a decrease of transmissivity in the outer composite zone.

The storativity was assumed known and constant at $1 \cdot 10^{-3}$ (above 100 m depth) and $1 \cdot 10^{-6}$ (below 100 m depth). The evaluation of the hydraulic parameters is made on the time interval representing the rock conditions close to the borehole (inner zone) or outside the skin zone if such a zone is present. If seen by the test, the properties of an outer zone were also calculated.

7.2.3 Comparison and conclusions

Although the two analysis approaches use a slightly different flow model philosophy, the differences are in terms of nomenclature and not in the description of the flow phenomena actually occurring. Each of the flow models used in one of the approaches can be translated into the other model system, respectively.

The two analysis approaches use different assumptions for storativity, which leads to incompatible calculation of skin factors and distances.

7.3 Models used for transient analysis of the recovery period of the injection tests

7.3.1 Geosigma

The models by Dougherty and Babu (1984) /10/ for radial flow and Hantush (1955) /5/ for pseudo-spherical (leaky) flow in an equivalent porous medium were used by the evaluation of the recovery period. Both models include the pressure derivative together with skin according to the effective wellbore radius concept and wellbore storage represented by a fictive standpipe connected to the test section. The models by Ozkan and Raghavan (1991) /6a and b/ and Gringarten and Ramey (1974) /7/ were used for linear flow in single fractures.

The evaluation of the hydraulic parameters is made on the time interval representing the rock conditions close to the borehole (inner region) outside the zone affected by skin and wellbore storage. In some cases the properties of an outer zone with different transmissivity were also calculated. The presence of apparent outer hydraulic boundaries (no-flow and constant pressure) was only evaluated qualitatively.

The analysis of the recovery period was made on the pressure recovery plotted versus the Agarwal equivalent time using the multi-rate approach, i.e superposition of the flow rates during the injection period (Agarwal 1980) /13/. The wellbore storage coefficient C was determined

from the recovery period by type curve matching as well as from the initial straight line with slope 1:1. C was only determined for tests with a well-defined slope of 1:1 in the beginning of the recovery period.

The storativity was estimated from a regression relationship between T and S according to SKB (2006) /8/ from borehole KFM05A and onward. For previous boreholes the storativity was assumed at $1 \cdot 10^{-6}$, independently of the transmissivity.

7.3.2 Golder

Golder uses a generic two-zone composite fractional dimension model in the analysis. According to the observed behaviour, the model was configured in most cases to a flow dimension of two (radial flow). Linear and spherical flow can be simulated as well as changes of flow dimension at some distance from the borehole. All models account for borehole effects (i.e. wellbore storage and skin).

In cases when only one parameter zone was seen by the tests, a homogeneous (one zone) flow model was used. Constant pressure boundaries were modelled as an increase of transmissivity in the outer composite zone, no flow boundaries were modelled as a decrease of transmissivity in the outer composite zone.

The pressure recovery was analysed using Bourdet superposition (Bourdet, 1989).

The storativity was assumed known and constant at $1 \cdot 10^{-3}$ (above 100 m depth) and $1 \cdot 10^{-6}$ (below 100 m depth). The evaluation of the hydraulic parameters are made on the time interval representing the rock conditions close to the borehole (inner zone) or outside the skin zone if such a zone is present. If seen by the test, the properties of an outer zone were also calculated.

7.3.3 Comparison and conclusions

As in the previous paragraph, although the two analysis approaches use a slightly different flow model philosophy, the differences are in terms of nomenclature and not in the description of the flow phenomena actually occurring. Each of the flow models used in one of the approaches can be translated into the other model system, respectively.

The two analysis approaches use different assumptions for storativity, which leads to incompatible calculation of skin factors and distances.

7.4 Steady-state analysis

7.4.1 Geosigma

The steady-state transmissivity was calculated according to Moye (1967) /21/ for all tests for comparison.

7.4.2 Golder

The steady-state transmissivity was calculated according to Moye (1967) /21/ for all tests for comparison.

7.4.3 Comparison and conclusions

Both analysis approaches use the same steady-state analysis.

7.5 Assumed conceptualisation of the rock

7.5.1 Geosigma

By the evaluation of the injection tests, the rock at Forsmark is assumed to be represented by a network of sparsely connected fractures forming an equivalent fractured porous medium or alternatively, by single fractures in a very low-conductive rock matrix with no hydraulic interaction between the fractures and rock matrix. A certain interval with pseudo-radial flow may be identified in most of the tests. Apparent pseudo-spherical (leaky) flow, reflected by a higher flow dimension, may represent intersection by fractures of higher transmissivity or flow in a wide, well-connected fracture zone. Apparent no-flow boundaries may reflect flow in fractures of limited extent.

7.5.2 Golder

The granite formation at the Oskarshamn site can be described from a hydraulic point of view as a sparsely connected fracture network. The matrix is expected to have extremely low conductivity and storativity, such that hydraulic interaction between fractures and matrix is not expected. Therefore, the tests conducted at Oskarshamn are expected to reveal fracture transmissivities. The derived transmissivities will reflect the properties of fractures intersecting the test zone. Also, the transmissivity may vary with the distance from the borehole to the extent further fractures are intersected. Conceptually, the flow dimension displayed by the tests can vary between linear and spherical. However, as the experience of the tests conducted so far shows, the majority of the tests display radial flow geometry.

7.5.3 Comparison and conclusions

The assumed conceptualization of the rock is compatible for both analysis approaches.

7.6 Determination of the flow model

7.6.1 Geosigma

From qualitative analysis of the semi-log derivative in log-log diagrams the dominating flow regimes during the tests were determined, e.g. pseudo-radial, pseudo-spherical (leaky) and pseudo-linear flow. The models for analysis were selected accordingly. Increases or decreases in the derivative may be assumed to be due to the presence of hydraulic features with higher and lower transmissivity, respectively away from the borehole. In addition, apparent outer boundary effects, e.g. no-flow boundaries and constant pressure boundaries were identified.

7.6.2 Golder

The determination of flow model was based on the qualitative analysis of the semi-log derivative plotted in log-log coordinates. The characteristic flow regimes were determined using the shape of the derivative. Typical flow regimes considered were:

- wellbore storage,
- skin-dominated transition period,
- infinite acting flow of a given flow dimension (typically radial),
- transition to a second composite zone with increase or decrease of transmissivity (also interpreted as constant pressure or no-flow boundaries).

7.6.3 Comparison and conclusions

Both analysis approaches use the semi-log derivative for flow model identification. Differences are only in nomenclature and caused by the different flow model philosophy used (see above).

7.7 Flow rates below the measurement limit

7.7.1 Geosigma

For all injection tests with a final flow rate below 1 mL/min a test-specific lower measurement limit was estimated based on the observed background level of flow rate before and after the injection period. The test-specific lower measurement limit, which ranges from c. 0.3–0.6 mL/min, does not account for the flow generated by the packers (packer compliance). The latter flow is assumed to constitute between c. 0.1–0.2 mL/min.

In some boreholes at Forsmark pressure pulse tests were performed in low-transmissivity sections.

7.7.2 Golder

In cases when the flow rate was below measurement limit from the beginning of the test pulse tests were performed. In cases when the flow rate fell below measurement limit during the CHi phase, the analysis was conducted using the normal derivative type curve matching procedure. However, the early test data was emphasized in the analysis, which accounts for the fact that the late time data may not be as accurate due to the measurement limit.

7.7.3 Comparison and conclusions

Both analysis approaches recognise the need of additional measures in case the injection rate falls below measurement limits. While Geosigma re-defines the measurement limits of the injection tests on an individual case basis, Golder bases their strategy on the conduction of alternative test types (i.e. pulse tests). Both methods successfully push the detectable transmissivity limit down by approx. one order of magnitude. Geosigma also performs pressure pulse tests in selected boreholes.

7.8 Determination of the static formation pressure and freshwater head

7.8.1 Geosigma

The static formation pressure and freshwater head using the Horner method was only determined in borehole KSH02 at Simpevarp (Ludvigson et al. 2004) /14/. In boreholes at Forsmark, no determination of the static formation pressure and freshwater head according to the Horner method was made. The static pressure may be estimated from the initial pressure in the tests section immediately before the injection period.

7.8.2 Golder

The static formation pressure and equivalent freshwater head was determined from the pressure recovery phases with the HORNER extrapolation method by using the HORNER straight line or the type curve, depending on whether the infinite acting radial flow period was reached at the late times of the test.

7.8.3 Comparison and conclusions

Both analysis approaches use the same method for determining the static formation pressure. The static formation pressure and freshwater head in the boreholes will also be measured in the subsequent monitoring program at the two sites.

7.9 Analysis of pressure pulse tests

7.9.1 Geosigma

The standard model by Dougherty and Babu (1984) /10/ assuming radial flow was used for analysis of all the pressure pulse tests performed at Forsmark. No determination of flow regimes during the tests was made for these tests.

The effective borehole storage used in the analyses was determined from laboratory measurements of the total compressibility of the test system (PSS) used.

A new simple method was derived for estimation of the transmissivity accounting for the estimated packer compliance effects in very low-conductive test sections.

7.9.2 Golder

Pulse tests were analysed using both the RAMEY method and the pressure deconvolution method (Peres et al. 1989, Chakrabarty and Enachescu et al. 1997) /22, 23/. The flow model determination was made using the pressure deconvolution method. All flow models available in FlowDim can also be used for pulse test analysis. The wellbore storage coefficient was directly measured in the field using the dV/dp method (see description in the text).

7.9.3 Comparison and conclusions

The pressure deconvolution method used by Golder allows flow model identification for pulse tests, which is an advantage in cases of very low transmissivity. Further, the method allows the use of a large variety of flow models for analysis. It should be emphasised that this difference will not typically influence the recommended transmissivity.

The wellbore storage coefficient used by the two analysis approaches was derived differently. While Geosigma bases their analysis on values derived in the laboratory, Golder measures the wellbore storage coefficient in situ for each test. None of the methods is completely accurate; however, discrepancies should be expected in the results (i.e. transmissivity) due to the different inputs.

7.10 Derivation and use of the wellbore storage coefficient

7.10.1 Geosigma

The wellbore storage coefficient C was determined from the simulation of the transient test responses during the recovery period of the injection tests by type curve matching and from the initial straight line of slope 1:1, respectively. Consistent values on C were generally obtained with the two methods but only values from the latter method were reported. C was only reported for tests with a reasonably well-defined slope of 1:1 in the beginning of the recovery period. In fact, calculated C-values in sections of higher transmissivity than c. $1 \cdot 10^{-8}$ m^2/s are considered as increasingly uncertain due to lack of a well-defined line of slope 1:1.

For comparison, the borehole storage coefficients, based on the estimated (total) effective compressibilities from laboratory tests for corresponding section lengths, were calculated as

described in Section 5.1.2. In addition, the net values on C based on borehole geometry (volume of test section) and the compressibility of water are also shown for comparison. The estimated C-values from the injection test responses were generally in good agreement (or only slightly higher) with the C-values from the laboratory tests and the net values of C for test sections with a transmissivity less than c. $1 \cdot 10^{-8}$ m^2/s. Some test sections with significantly deviating (high) C-values were however observed. Some of these values may be real due to e.g cavities or presence of gas in the water in the borehole sections whereas others, particularly for transmissivities above $1 \cdot 10^{-8}$ m^2/s, may be non-representative for the test (poorly defined due to lack of character from WBS).

In the analysis of the pressure pulse tests, the estimated wellbore storage coefficient from the laboratory tests was used. C was not estimated from the pulse test responses.

7.10.2 Golder

The theoretical value of the wellbore storage coefficient was used just as a reference for comparison with the values derived from testing. The theoretical value was calculated as the product of total compressibility and volume of the test section. The total compressibility is calculated as the sum of the compressibilities of the individual system components: (a) water compressibility = 5E–10 1/Pa (from physics), (b) rock compressibility 1E–10 1/Pa (estimated) and (c) packer compressibility on average 5E–11 1/Pa (from laboratory measurements). The sum of these three components is approximately 7E–10 1/Pa with the largest component being the water. If the packer compressibility is accepted to be small (in the order of 5E–11 1/Pa) it follows that the value of the total compressibility is not controlled by the packers but by the water. So the influence of the packer compressibility can basically be neglected. Based on the above, a total compressibility of 7E–10 1/Pa is approx. the minimum to be expected if considering that water alone is 5E–10 1/Pa. The theoretical value of the wellbore storage coefficient was not used for the analysis of pulse tests (see additional comments below). In conclusion, the theoretical compressibility (or wellbore storage coefficient) does not influence the analysis results.

The wellbore storage coefficient derived from the recovery phases (CHir) is a result of the analysis. Two methods were used to derive it. The first method was type curve matching and the second method was to calculate the wellbore storage coefficient from the linear portion of the pressure recovery at early times. In effect, both methods are the same, and if discarding the subjectivity inherent to the analysis they should give the same C-values. A correlation analysis of the C-values derived using the two methods shows very good agreement. However, the C-values derived using these two methods are often much larger than the theoretical C-value. This has been frequently observed but the reason for this is not clear. Up to this point, the only plausible explanation for this phenomenon was found in SPIVEY's paper on turbulent flow (2002) /24/. This does not necessarily mean that turbulent flow exists; this hypothesis is just the only plausible explanation currently available.

The wellbore storage coefficient used for the analysis of pulse tests is a result of direct measurements. The C-value is calculated as $\Delta V/\Delta p$ where ΔV is measured as the volume of water needed to elevate the pressure in the test section by Δp (usually 200 kPa). The measured values are more consistent showing discrepancies of maximum one order of magnitude to the theoretical values. Considering how the volume difference (and hence the C-value) is measured, the derived C-value should be regarded as an upper bound for the true C-value of the system. The reason for this assessment is twofold: (1) the volume difference is measured using the entire column of water in the test tubing and (2) it cannot be excluded that small volumes of water flow into the formation, so the volume difference may also have a formation flow component.

Because of the above, the C-value can be bounded between the theoretical value and the measured value during the pulse. The C-value matched from the CHir phase is often larger, but it may not reflect the actual storage conditions in the test section (perhaps due to turbulent flow).

7.10.3 Comparison and conclusions

The theoretical value of the wellbore storage coefficient was determined in different ways by Geosigma and Golder. Geosigma determined slightly different values on the effective (total) compressibility for test sections in 100 m, 20 m and 5 m, respectively from laboratory tests ($4.8 \cdot 10^{-10}$, $5.5 \cdot 10^{-10}$ and $8.4 \cdot 10^{-10}$ 1/Pa, respectively).

Golder estimated the total (effective) compressibility of the test system as c. 7E–10 1/Pa with the largest component being the compressibility of water, independently of the section length. The theoretical value of the wellbore storage coefficient was calculated as the product of total (effective) compressibility and volume of the test section by both Geosigma and Golder.

For the actual test section lengths, the differences in the theoretical values of C used by Geosigma and Golder are considered of minor importance since these values were only used as reference values in the analysis of the injection tests.

In the analysis of pressure pulse tests, Geosigma used the estimated theoretical values on C while Golder estimated C from each test. The actual C-value is assumed to be bounded between the theoretical value and the measured value. Both approaches are uncertain which may affect the estimated transmissivities from the pressure pulse tests.

7.11 Derivation of recommended values and confidence ranges

7.11.1 Geosigma

In general, both the injection-and recovery period of the injection tests were evaluated by transient methods. The hydraulic parameters from the period exhibiting the most well-defined period with pseudo-radial flow, or other flow regime, were selected as the representative ones. The parameters from the inner region were selected if more than one region was evaluated. In most cases the parameters from the injection period were selected as the representative. If no transient evaluation could be made, the steady-state transmissivity was selected.

No confidence interval for the estimated parameters was reported for the tests at Forsmark. The approximate 95% statistical confidence range for each estimated parameter is calculated by the software from the regression analysis. In addition, there are several other uncertainties which may affect the confidence range of the estimated parameters.

7.11.2 Golder

In most of the cases more than one analysis was conducted on a specific test. Typically both test phases were analyzed (CHi and CHir) and in some cases the CHi or the CHir phase was analyzed using two different flow models. The parameter sets (i.e. transmissivities) derived from the individual analyses of a specific test usually differ. In the case when the differences are small (which is typically the case) the recommended transmissivity value is chosen from the test phase that shows the best data and derivative quality.

In cases when the difference in results of the individual analyses was large (more than half order of magnitude) the test phases were compared and the phase showing the best derivative quality was selected.

The confidence range of the transmissivity was derived using expert judgment. Factors considered were the range of transmissivities derived from the individual analyses of the test as well as additional sources of uncertainty such as noise in the flow rate measurement, numeric effects in the calculation of the derivative or possible errors in the measurement of the wellbore storage coefficient. No statistical calculations were performed to derive the confidence range of transmissivity.

In cases when changing transmissivity with distance from the borehole (composite model) was diagnosed, the inner zone transmissivity (in borehole vicinity) was recommended.

In cases when the infinite acting radial flow (IARF) phase was not supported by the data the additional uncertainty was accounted for in the estimation of the transmissivity confidence ranges.

While the recommended transmissivity was derived using type curve analysis methods, the confidence range of transmissivity was derived from the comparison of the analysis results of the two phases. In many cases Transmissivity Normalized Plots (TNP) were used to compare the derivatives of the two test phases in a normalized fashion. This way the amount of uncertainty was derived graphically as presented in the report.

7.11.3 Comparison and conclusions

Both approaches use “best data quality” test phases for the derivation of the recommended transmissivity. In both cases the transmissivity confidence range is derived using “expert judgement”; however Geosigma does not report these values.

Golder uses the TNP method to identify compatibility (or incompatibility) between the individual test phases and translates this information into transmissivity confidence ranges.

8 Conclusions and recommendations

The following main conclusions may be drawn from the performance and evaluation of injection tests and pressure pulse tests at the Forsmark site:

8.1 Injection period

- The injection period considered as more appropriate for transient evaluation due to, in general, longer analyzable and representative part of the inverse flow rate data curve (1–2 log cycles of time).
- The average stabilization time to get a constant pressure in the test section was 20–30 s for most tests using the automatic flow regulation system. Lower times (0–10 s) were achieved in low-transmissivity tests using the pressure vessel directly.
- During the injection period, tests exhibiting an approximate pseudo-radial flow regime (PRF) dominate in relation to other flow regimes.
- Possible to identify a representative pseudo-radial flow regime (PRF) during the injection period for most of the tests on which transient evaluation was made.
- The estimated skin factors are in general close to zero or negative which can be expected in fractured crystalline rock.
- Occasionally, high positive skin factors are estimated for pseudo-radial flow conditions which possibly may reflect turbulent flow in fractures or other head losses or flow restrictions.
- Effects of apparent no-flow boundaries, e.g. flow features of limited extension or decreasing aperture further away from the borehole, may strongly affect the injection period but cause an inconsistent behaviour during recovery, see below.
- A test-specific lower measurement limit for flow rate and transmissivity can be estimated for each test from the background level of the flow rate before and after the injection period, respectively. The lowest evaluated flow rate limit was c. 0.3 mL/min using this approach, corresponding to a steady-state transmissivity of c. $3 \cdot 10^{-10}$ m^2/s.
- In general, good agreement between the estimated transmissivity from transient evaluation of the injection period and the stationary transmissivity T_M. Discrepancies may arise when the estimated skin factor deviates significantly from zero, e.g. pseudo-linear (fracture) flow and when effects of apparent no-flow boundaries are present.

8.2 Recovery period

- The beginning of the recovery period is frequently disturbed by wellbore storage (WBS) which decreases the analyzable, representative part of the recovery data curve (in general less than one log cycle of time).
- Only effects of wellbore storage can, in general, be identified during the recovery period in low-transmissive test sections ($T <$ c. 10^{-9} m^2/s).
- In general, only occasionally possible to identify a representative pseudo-radial flow regime (PRF) during the recovery period.
- Sometimes difficult to obtain an unambiguous transient evaluation of the recovery period due to fast pressure recovery and inconsistent behaviour between injection- and recovery period.

- In test sections showing major effects of apparent no-flow boundaries (NFB) during the injection period, a slow and incomplete pressure recovery was generally observed , also in relatively transmissive sections, e.g. $T >$ c. 10^{-7} m^2/s.
- In general, good agreement between the calculated wellbore storage coefficient from test analysis and the estimated effective wellbore storage coefficient C_{eff} from laboratory tests for sections with $T <$ c. 10^{-8} m^2/s.

8.3 Representative injection test results

- The representative hydraulic parameters from the tests were in general selected from the transient evaluation of the test period showing the best data quality and derivative. In most cases the results from the injection period were selected as representative for the test section.

8.4 Pressure pulse tests

- Pressure pulse tests were evaluated with standard methods (including WBS and skin) when effects of packer compliance were limited.
- Consistent estimates of transmissivity from pressure pulse- and injection tests were obtained when effects of packer compliance during the tests were limited.
- Difficult to correct the transient pressure behavior during the recovery period after the pressure pulse when significant effects of packer compliance are present (i.e. insufficient packer sealing times) which makes transient evaluation with standard methods very uncertain or impossible.
- A simple stationary method was derived for estimating the transmissivity from pressure pulse tests in low-transmissive sections from the pressure behavior during the recovery period after the pressure pulse. For a packer sealing time of 60 minutes, it may be possible to estimate transmissivities in the interval c. $5{\cdot}10^{-11}$ m^2/s to c. $5{\cdot}10^{-10}$ m^2/s with this method. However, the uncertainty of such estimates is high.

8.5 Test statistics

The test statistics from the injection tests and pressure pulse tests performed in boreholes KFM01A–KFM07A at Forsmark indicates:

- The increased number of ambiguous responses during the recovery period of the injection tests in KFM02A is probably due to the increased number of test showing fast recovery (pseudo-stationary flow). The majority of these tests correspond to geological deformation zones and the interval with the porous granite formation.
- Fast recovery may possibly be caused by certain geological factors or alternatively, by turbulent flow in fractures intersecting the borehole.
- The increased number of inconsistent behavior between the injection- and flow period and tests not analysable in borehole KFM02A is also explained by fast recovery tests in this borehole.
- Inconsistent behavior between the flow and recovery period may be caused for tests showing effects of apparent no-flow boundaries during the flow period. The subsequent recovery may be slow and incomplete.
- Ambiguous responses during recovery and non-analysable tests may be caused by dominating wellbore storage effects during the tests.
- Gauge resolution problems were only noticed during the pressure recovery period, particularly in borehole KFM02A due to fast recovery.

8.6 Natural background pressure gradients

In order to test the sensitivity to background natural pressure trend as presented in Section 5.3 or other external pressure trends on the results on pressure pulse tests, responses of such tests were simulated according to the model described in Section 4.3.1 assuming a certain ongoing background pressure trend during the test. These responses were compared with the corresponding responses with no background pressure trend. No effects of packer compliance were assumed to influence the responses in the simulations.

Examples of simulated responses are shown in Figures 8-1a-b. The examples are based on a test section of L = 5 m in a borehole of diameter of 0.076 m in a synthetic formation with a transmissivity $T = 1 \cdot 10^{-11}$ m^2/s, storativity $S = 1 \cdot 10^{-7}$, skin factor = 0 and an effective wellbore storage $C_{eff} = 1.6 \cdot 10^{-11}$ m^3/Pa. The latter value is taken from Table 5-1. In Figure 8-1a, no background pressure trend is assumed whereas in Figure 8-1b, a linearly increasing pressure trend of c. 0.3 m/h is assumed to prevail during the entire recovery period after the application of a pressure pulse of c. 20 m in the test section. The assumed pressure trend is higher than the background trends discussed in Section 5.3 (with the exception of a possible trend due to re-establishment of the section pressure).

Comparison of Figures 8-1a) and b) shows that the assumed background pressure trend only affects the later part of the recovery curve (after c. 5,000 s). Furthermore, Figure 8-1b demonstrates that the assumed pressure trend only resulted in a change of c. 20% of transmissivity in this case which is considered as relatively small in relation to other uncertainties in this range of transmissivity. However, in practise, effects of packer compliance are likely to affect such a test significantly, thus introducing higher uncertainty.

Figure 8-1b indicates that background pressure trends of c. 0.3 m/h or lower (in the absence of packer compliance effects) are not likely to significantly affect the results of transient evaluation of most pressure pulse tests for transmissivities in the order of $1 \cdot 10^{-11}$ m^2/s or higher, provided that the evaluation is based on the entire recovery curve. However, if only the later part of the

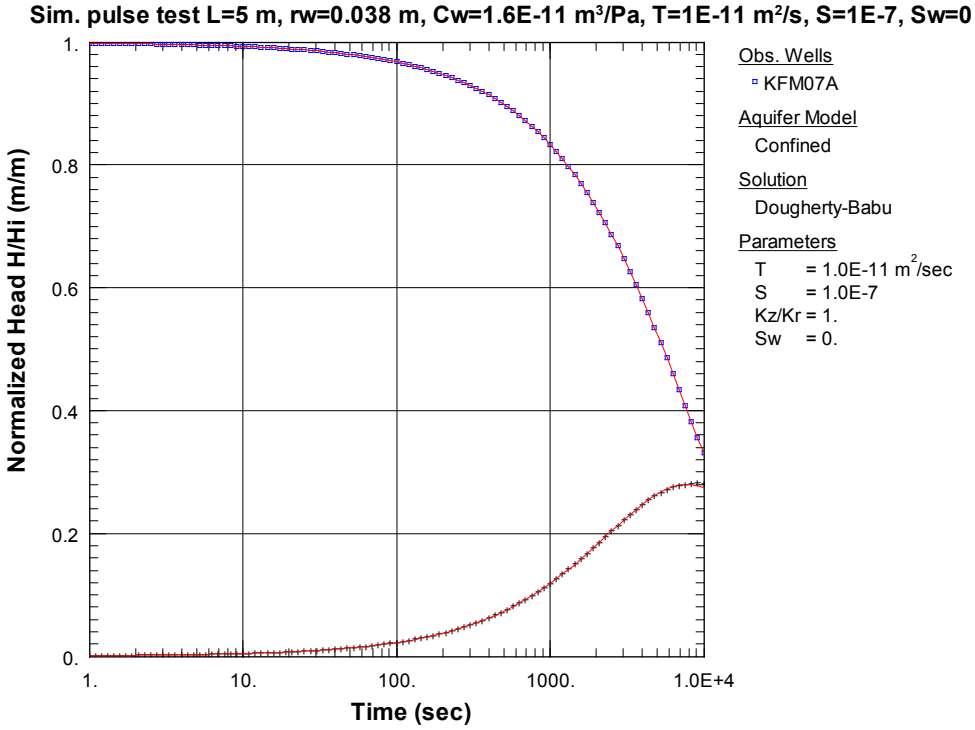

Figure 8-1a. *Simulated responses of a pressure pulse test in a 5 m low-transmissive test section for assumed hydraulic parameters (blue = normalized head and black = derivative). No background pressure trend is assumed during the test.*

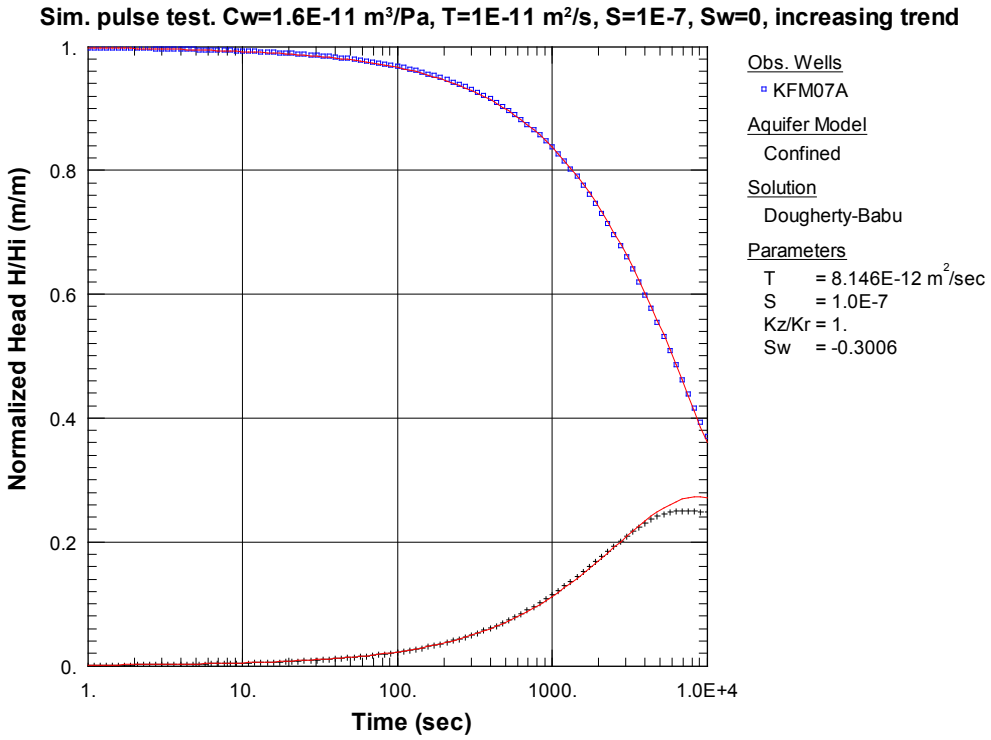

Figure 8-1b. *Simulated responses of a pressure pulse test in the same test section as above but with an assumed linearly increasing background pressure trend of c. 0.3 m/h during the recovery period of the test (blue = normalized head and black = derivative).*

recovery curve is used for evaluation, or a lower pressure pulse is applied, background pressure trends may have a significant effect on the tests. This is also true for injection tests if the evaluation is based on the later part of the recovery period with small pressure changes as discussed in Section 5.3. If effects of packer compliance occur during the test, such effects are likely to dominate the uncertainties, see Section 5.2.3.

8.7 Comparison of estimated transmissivities from injection tests and difference flow logging

In general, good agreement between the estimated transmissivity from the injection tests and difference flow logging was obtained. The latter method is described in Morosini et al. (2001) /1/. In some boreholes, higher transmissivities are estimated from the injection tests. In such boreholes the number of tests with effects of apparent no-flow boundaries (NFB) seems to be increased. This fact is likely to reflect the differences in pre-conditions for the tests. While the injection tests are short (c. 20 min) and thus also may sample transmissive, single flow features of limited extension close to the borehole, difference flow logging predominantly samples interconnected flow features of larger extension since the borehole is continuously pumped during several days before the flow measurements.

8.8 Recommendations

Comparisons should be made of the results from the injection tests in 5 m section length with complementary GRF-analysis regarding the interpreted flow dimension and transmissivity in corresponding sections. The results should be correlated with the geological conditions in the sections (e.g. fracture frequency together with interpreted rock units and fracture zones). The results should also be compared with the results of the difference flow logging in corresponding 5 m sections.

9 References

/1/ **Morosini M, Almén K-E, Follin S, Hansson K, Ludvigson J-E, Rhén I, 2001.** Djupförvarsteknik. Metoder och utrustningar för hydrauliska enhålstester. Metod och programaspekter för geovetenskapliga platsundersökningar. SKB TD-01-63, Svensk Kärnbränslehantering AB (In Swedish).

/2/ **Jacob C E, Lohman S W, 1952.** Nonsteady flow to a well of constant drawdown in an extensive aquifer. Trans., AGU (Aug. 1952), pp 559–569.

/3/ **Hurst W, Clark J D, Brauer E B, 1969.** The skin effect in producing wells. J. Pet. Tech., Nov 1969, pp 1483–1489.

/4/ **Almén K-E, Andersson J-E, Carlsson L, Hansson K, Larsson N-Å, 1986.** Hydraulic testing in crystalline rock. A comparative study of single-hole test methods. SKB TR 86–27, Svensk Kärnbränslehantering AB.

/5/ **Hantush M S, 1959.** Non-steady flow to flowing wells in leaky aquifer. Jour. Geophys. Research, v. 64, no 8, pp 1043–1052.

/6a/ **Ozkan E, Raghavan R, 1991.** New solutions for well test analysis; Part 1, Analytical considerations. SPE Formation Evaluation vol 6, no 3, pp 359–368.

/6b/ **Ozkan E, Raghavan R, 1991.** New solutions for well test analysis; Part 2, Computational considerations and applications. SPE Formation Evaluation vol 6, no 3, pp 369–378.

/7/ **Gringarten A C, Ramey H J, 1974.** Unsteady state pressure distributions created by a well with a single horizontal fracture, partial penetration or restricted entry. Soc. Petrol. Engrs. J., pp 413–426.

/8/ **SKB, 2006.** Preliminary site description. Laxemar subarea – version 1.2. SKB R 06-10, Svensk Kärnbränslehantering AB.

/9/ **Cooper H H, Jacob C E, 1946.** A generalized graphical method for evaluating formation constants and summarizing well field history. Am. Geophys. Union Trans., v 27 no 4 pp 526–534.

/10/ **Dougherty D E, Babu D K**, **1984.** Flow to a partially penetrating well in a double-porosity reservoir. Water Resour. Res., 20 (8), 1116–1122

/11/ **Earlougher R C Jr, 1977.** Advances in well test analysis. Monogr. Ser., vol. 5, Soc. Petrol. Engrs., Dallas, 1977.

/12/ **Hantush M S, 1955.** Non-steady radial flow in an infinite leaky aquifer. Am. Geophys. Union Trans., v. 36, no 1, pp 95–100.

/13/ **Agarwal R G, 1980:** A new method to account for producing time effects when drawdown type curves are used to analyze pressure build-up and other test data. Soc. Pet. Eng. Paper 9289.

/14/ **Ludvigson J-E, Levén J, Källgården J, Jönsson S, 2004.** Oskarshamn site investigation. Single-hole injection tests in borehole KSH02. SKB P-04-247, Svensk Kärnbränslehantering AB.

/15/ **Gustafsson E, Ludvigson J-E, 2005.** Oskarshamn site investigation. Combined interference test and tracer test between KLX02 and HLX10. SKB P-05-20, Svensk Kärnbränslehantering AB.

/16/ **Ludvigson J-E, Jönsson S, Levén J, 2004.** Forsmark site investigation. Hydraulic evaluation of pumping activities prior to hydro-geochemical sampling in borehole KFM03A – Comparison with results from difference flow logging. SKB P-04-96, Svensk Kärnbränslehantering AB.

/17/ **Ekman L (ed), 2001.** Project Deep Drilling KLX02- Phase 2. Methods, scope of activities and results. Summary report. SKB TR-01-11, Svensk Kärnbränslehantering AB.

/18/ **Atkinson L E, Gale J E, Dudgeon C R, 1994.** New insight into the step drawdown test in fractured-rock aquifers. Applied Hydrogeology 1/94, pp 9–18.

/19/ **Bourdet D, Ayoub J A, Pirard Y M, 1989.** Use of Pressure Derivative in Well-Test Interpretation. SPEFE (June 1989). Pp 293–302. Trans., AIME, 287.

/20/ **Spane F A, Wurstner S K, 1993.** DERIV: A computer program for calculating pressure derivatives for use in hydraulic test analysis. Ground Water, vol. 31, no. 5, pp 814–822.

/21/ **Moye D G, 1967.** Diamond drilling for foundation exploration. Civil Eng. Trans., Inst. Eng. Australia, pp 95–100.

22/ **Peres A M M, Onur M, Reynolds A C, 1989.** A new analysis procedure for determining aquifer properties from slug test data. Water Resour. Res., v. 25 (7), pp. 1591–1602.

/23/ **Chakrabarty C, Enachescu C, 1997.** Using the Deconvolution Approach for Slug Test Analysis: Theory and Application. Ground Water. vol. 35, no. 5, pp. 797–806.

/24/ **Spivey J P, Brown K G, Sawyer W K, Frantz J H, 2002.** Estimating Non Darcy Flow Coefficient from Buildup Test Data with Wellbore Storage. Soc. Pet. Eng. Paper SPE 77484.

/25/ **Levén J, Ludvigson J-E, 2004.** Hydraulic interferences during the drilling of borehole KFM01B. Boreholes HFM01, HFM02, HFM03 and KFM01A. SKB P-04-135, Svensk Kärnbränslehantering AB.

/26/ **Rahm N, Enachescu C, 2004.** Oskarshamn site investigation. Hydraulic injection tests in borehole KLX02, 2003. SKB P-04-288, Svensk Kärnbränslehantering AB.

In addition, the following test reports are cited in this report:

SKB P-04-95: Forsmark site investigation. Single-hole injection tests in borehole KFM01A, April 2004.

SKB P-04-100: Forsmark site investigation. Single-hole injection tests in borehole KFM02A, May 2004.

SKB P-04-194: Forsmark site investigation. Single-hole injection tests in borehole KFM03A, July 2004.

SKB P-04-293: Forsmark site investigation. Single-hole injection tests in borehole KFM04A, January 2005.

SKB P-05-56: Forsmark site investigation. Single-hole injection tests in borehole KFM05A, March 2005.

SKB P-05-165: Forsmark site investigation. Single-hole injection tests in boreholes KFM06A and KFM06B, June 2005.

SKB P-05-133: Forsmark site investigation. Single-hole injection tests in borehole KFM07A, May 2005.

10 Nomenclature and glossary of abbreviations

Symbol	Description	Unit
L_w	Test section length	m
r_w	Nominal radius of borehole or well	m
r_{wf}	Effective radius of borehole or well in the test section. (Considering of skin factor)	m
r_i	Influence radius	m
z	Level above (+)/below (–) reference point. Positive upward	m
Q	Flow rate	m^3/s
Q_p	Flow rate at the end of flow period	m^3/s
Q_{packer}	Generated flow by the packers due to packer compliance	m^3/s
Q_{ave}	Average flow	m^3/s
V	Volume	m^3
V_w	Water volume in test section	m^3
V_p	Total water volume pumped or injected during flow period	m^3
ΔV	Total change in volume of water and packers	m^3
ΔV_w	Change in volume of water	m^3
ΔV_m	Change in volume of packers	m^3
ΔV	Total change in volume of water and packers	m^3
t	Time from start of flow period	s
t_p	Duration of flow period	s
t_{pp}	Pseudo-duration of flow period for constant head test ($t_{pp} = V_p/Q_p$)	s
t_F	Duration of recovery period	s
dt	Time from start of recovery period	s
dt_e	Agarwal equivalent time during the recovery period	s
p	Water pressure at certain depth below ground surface in open borehole or sealed-off test section	kPa
p_{atm}	Atmospheric pressure	kPa
p_0	Groundwater pressure in open borehole (before packer sealing)	kPa
p_i	Groundwater pressure in test section at start of flow period	kPa
p_f	Groundwater pressure in test section during flow period	kPa
p_p	Groundwater pressure in test section at stop of flow period	kPa
p_F	Groundwater pressure in test section at stop of recovery period	kPa
p_a	Groundwater pressure above test section	kPa
p_b	Groundwater pressure below test section	kPa
p*	Horner extrapolated pressure (used as an estimation of natural pressure of the test section)	kPa
Δp	Pressure change	kPa
dp	Absolute pressure difference	kPa
dp_{packer}	Pressure increase in test section due to packer compliance	kPa
dp_f	$dp_f = p_f – p_i$ pressure difference between pressure at start of flow period and pressure during flow period	kPa

Symbol	Description	Unit
dp_p	$dp_p = p_p - p_i$ pressure difference between pressure at start of injection period and pressure at stop of injection period	kPa
dp_0	$dp_0 = pp - p_0$ applied pressure difference during pressure pulse test	kPa
dp_i	$dp_i = pp - p_i$ applied pressure difference during pressure pulse test	kPa
H	Head in test section during pressure pulse test	kPa
H_0	$H_0 = dp_0/\rho wg$ applied head during pressure pulse test	kPa
H_i	$H_i = dp_i/\rho wg$ applied head during pressure pulse test	kPa
h	Hydraulic head (piezometric head) at certain depth below ground surface in open borehole or sealed-off test section	m
h_{FW}	Freshwater head	m
h_i	Hydraulic head in test section at start of flow period	m
h_f	Hydraulic head in test section during flow period	m
dh	Absolute hydraulic head difference	m
dh_f	$dh_f = h_f - h_i$ hydraulic head difference between pressure at start of flow period and pressure during flow period	m
T	Transmissivity of formation, based on 2D radial flow model.	m^2/s
T_M	Transmissivity, based on Moye (1967)	m^2/s
T_T	Transmissivity of formation, based on 2D radial flow model. Considered best estimate from transient evaluation of flow period or recovery period.	m^2/s
T_R	Representative transmissivity (T_T, T_Q, T_M) for the borehole section from the routine evaluation.	m^2/s
K	Hydraulic conductivity of formation.	m/s
K´/b´	Leakage coefficient evaluated from 2D radial flow model. K´ = hydraulic conductivity across the aquitard, b´ = water saturated thickness of aquitard (leaky formation).	1/s
S	Storativity (Storage coefficient) of formation based on 2D radial flow model.	–
S_s	Specific storativity of formation based on 2D radial flow model.	
ξ	Skin factor	–
ρ_w	Density of water	kg/m^3
Te_w	Temperature of water in the test section	°C
c_w	Compressibility of water	1/Pa
c_{eff}	Effective compressibility	1/Pa
g	Acceleration of gravity	m/s^2
C_M	Geometric factor in Moye's formula, $C = [1+\ln(L_w/2r_w)]/2\pi$	–
C	Wellbore storage coefficient	m^3/Pa
C_{net}	Net wellbore storage coefficient based on geometrical borehole properties	m^3/Pa
C_{eff}	Effective wellbore storage coefficient	m^3/Pa

Nomenclature used in test diagrams using the AQTESOLV software:

T = transmissivity (m^2/s).
S = storativity (–).
K_z/K_r = ratio of hydraulic conductivities in the vertical and radial direction (set to 1).
Sw = skin factor.
r(w) = borehole radius or effective borehole radius (m).
r(c) = effective casing radius or radius of fictive standpipe in test section (m).
r/B = leakage factor (–).

Appendix 1

Laboratory tests of packers

The performance of the packer tests in the laboratory together with the test set-up generally used for some of the prototypes of the packers is presented below.

A1.1 Linear-elastic deformation

The elasticity of packers is measured from tests of a sealed packer in a steel pipe, see Figure A1-1. The steel pipe which should simulate the borehole has the dimensions (OD/ID) of 80/76 mm and supplied with a strong end of steel. The test section constitutes of the volume in front of the packer and the end of the steel pipe. To minimize the movement of the frame of the packer in the test pipe during tests the frame is anchored to the test pipe by a yoke. The confined water volume in the test section is c. 2.3 L and the section length is 550 mm. The packer is expanded by nitrogen gas which pressurizes a pressure vessel containing water.

A1.1.1 Test set-up

The test set-up is shown in Figure A1-1 below.

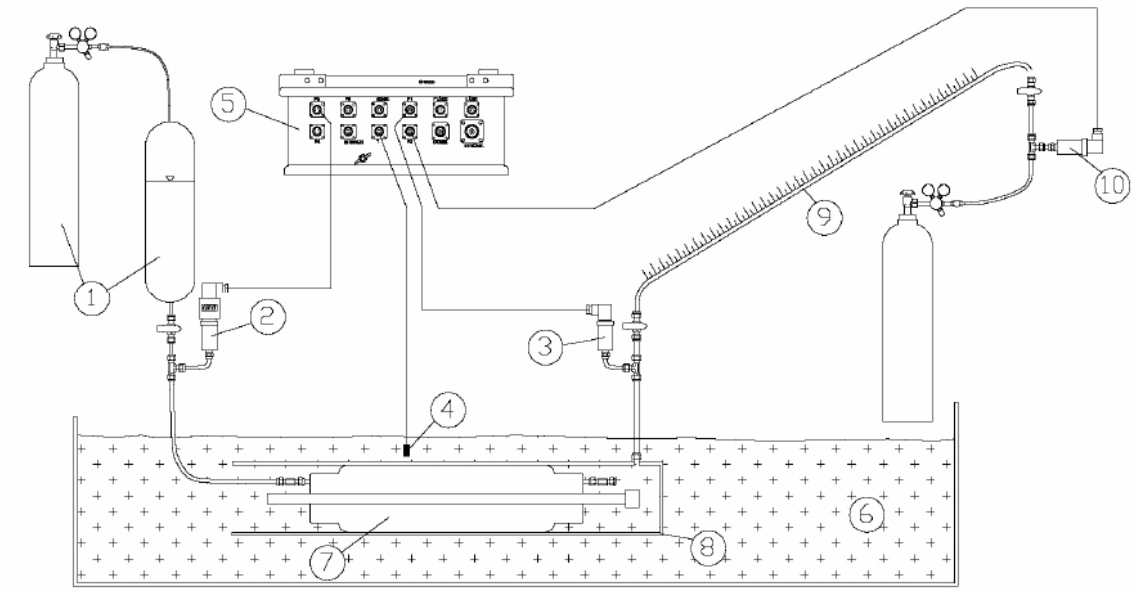

Figure A1-1. *Test set-up for measuring the linear-elastic deformation of packers. Legend, see below.*
Legend to Figure A1-1:

1. *Pressure regulation system for packer.*
2. *Pressure transmitter for packer.*
3. *Pressure transmitter for test section.*
4. *Temperature transmitter for water tank.*
5. *Data logger.*
6. *Water tank.*
7. *Packer.*
8. *Steel pipe.*
9. *Piston used for pressure change in section and volume measurement.*

The pressurization of the test section is made by a manually operated piston, by which water may be injected or extracted to/from the test section. By means of the piston volumes can also be measured. One rotation of the handle corresponds to c. 0.7 mL. To the handle a protractor is attached by which a rotation of 1/40 may be read, corresponding to a volume slightly less than 0.02 mL. The equipment is lowered into a water bath adjusted to room temperature in order to minimize the temperature variations during the test. The temperature should be constant at c. 20°C.

The packer pressure and section pressure are registered by a data logger. The packer pressure is measured by an absolute pressure transducer of type Druck PTX 1400 with a measuring range of 0–6,000 kPa and accuracy (linearity, hysteresis and repeatability) of ± 0.25% BSL (Best Straight Line). The section pressure is measured by an absolute pressure transducer of type Druck 639–1,138 with a measuring range of 0–6,000 kPa and accuracy (linearity, hysteresis and repeatability) of ± 0.15% BSL (Best Straight Line).
The water temperature is measured by a temperature sensor of type Inor with an adjusted measurement range of 0–50°C and an accuracy of ± 0.3°C.

A1.1.2 Test performance

To minimize creeping effects of the material, the packer is sealed during c. 12 hours before the start of the test. The test section is pressurized by the piston in steps of 200 kPa up to maximally 600 kPa. Then the pressure was lowered in corresponding steps. During the pressure increase the pressure was held constant during c. 15 s after which time the pressure was shut-in. The shut-in pressure was measured during 5 minutes. The registered volumes also included the volume changes in the steel pipe and of the water in the section.

The proportion of the volume changes of the steel pipe was calculated from a separate pressure test of only a steel pipe furnished with strong ends at both sides. The volume changes due to only the steel pipe was calculated to c. 0.03 mL/100 kPa. The proportion of the volume changes of the water was calculated based on the compressibility of water (assumed to $4.6 \cdot 10^{-10}$ Pa^{-1}) and the water volume in the test section. With the actual volume of 2.3 L in the test section the volume changes of water was calculated to 0.11 mL/100 kPa.

A1.2 Time-dependent deformation of packers

A1.2.1 Material creeping due to pressure changes

No separate tests were made to study this effect. However, this effect is demonstrated in the previous test.

A1.2.2 Generated flow caused by the packer expansion

The test set-up is shown in Figure A1-2.

To a large extent the test set-up is identical with the one used in the previous test. The piston has though been exchanged by a transparent hose with a slight upward incline (0.25 m/4 m). The diameter of the hose is 6/4 mm. The squeezed out water column by the end of the hose was measured by means of a steel scale and vernier callipers. For some prototypes the test has been done at both atmospheric pressure and at an overpressure of 200 kPa. If the squeezed out water volume is measured at an overpressure in the section, the hose is pressurized by nitrogen gas, see point 10 in Figure A1-2.

The starting point of the water level is marked at the hose and the packer is then expanded. At the hose marks are made of the movement of the water column each minute (up to 15 minutes, then more sparsely. The length of the water column in the section hose is measured by steel scale/vernier callipers and noted against the time marks on the hose. Based on these data the volume (mL) versus time (min) and flow rate (mL/min) versus time (min) are calculated.

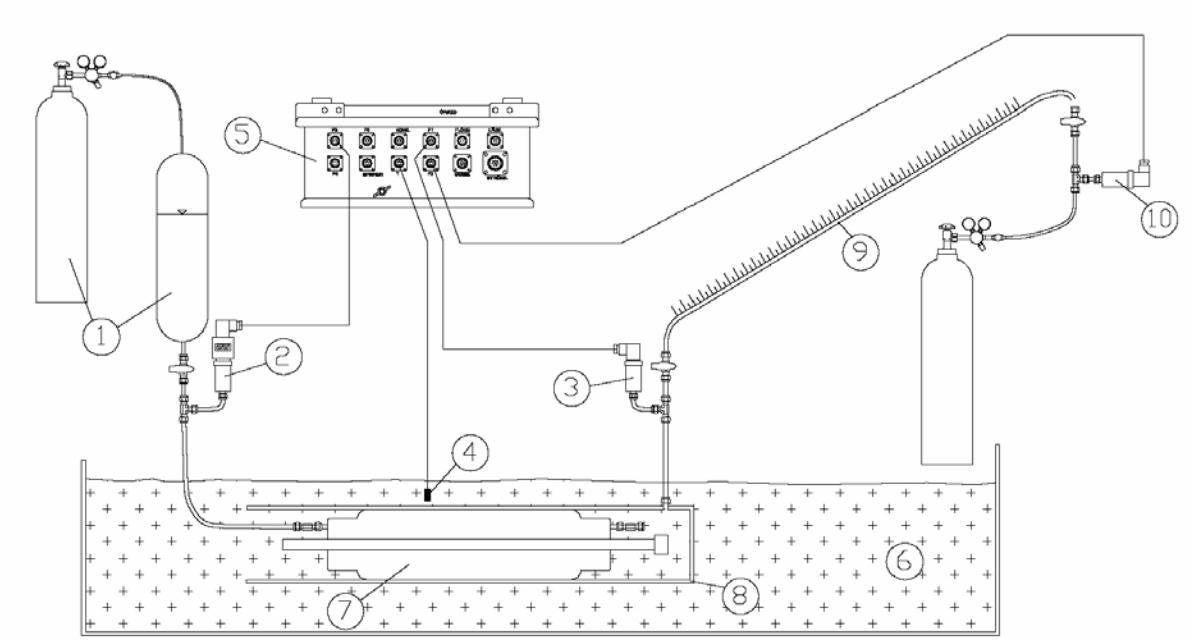

Figure A1-2. *Test set-up for measuring the generated flow caused by the packer expansion.*
Legend to Figure A1-2:

1. *Pressure regulation system for packer.*
2. *Pressure transmitter for packer.*
3. *Pressure transmitter for test section.*
4. *Temperature transmitter for water tank.*
5. *Data logger.*
6. *Water tank.*
7. *Packer.*
8. *Steel pipe.*
9. *Tubing for measuring the generated flow.*
10. *Equipment for pressurizing the test section.*

A1.3 Results and comments

As mentioned above, different types of packers have been tested regarding their intended application at the time of manufacturing. This means that the corresponding testing programmes have been slightly different. For packers to be installed in both PSS units, rubber from two different suppliers has been used. Both rubber types are made of polyurethane and constructed with strength of shore 90. Tests of the rubber types show rather good agreement. The deviations are likely to be in the same order of magnitude as the deviations obtained from tests of two prototypes from the same supplier. Below, tests on packers with rubbers supplied from the company Trekollan are presented (Packer PU 72).

A1.3.1 Linear-elastic deformation

During testing, the packer was expanded by a pressure of 2,016 kPa. The test section pressure versus time for the different pressure steps (injection/withdrawal) is shown in Figure A1-3. The corresponding injected/extracted water volume versus pressure is shown in Figure A1-4.

The curves in Figure A1-4 are rather straight which indicates that the system exhibits a near-linear-elastic performance. The curves are somewhat more flat at lower pressures. In the pressure range from atmospheric pressure to 200 kPa overpressure a total volume change of 0.48 mL/100 kPa is obtained. If this value is reduced for the volume changes of water (0.11 mL/100 kPa) and the steel pipe (0.03 mL/100 kPa) a resulting volume change of 0.34 mL/100 kPa, caused by one packer, is obtained. Thus, for two packers a volume change of 0.7 mL/100 kPa is obtained.

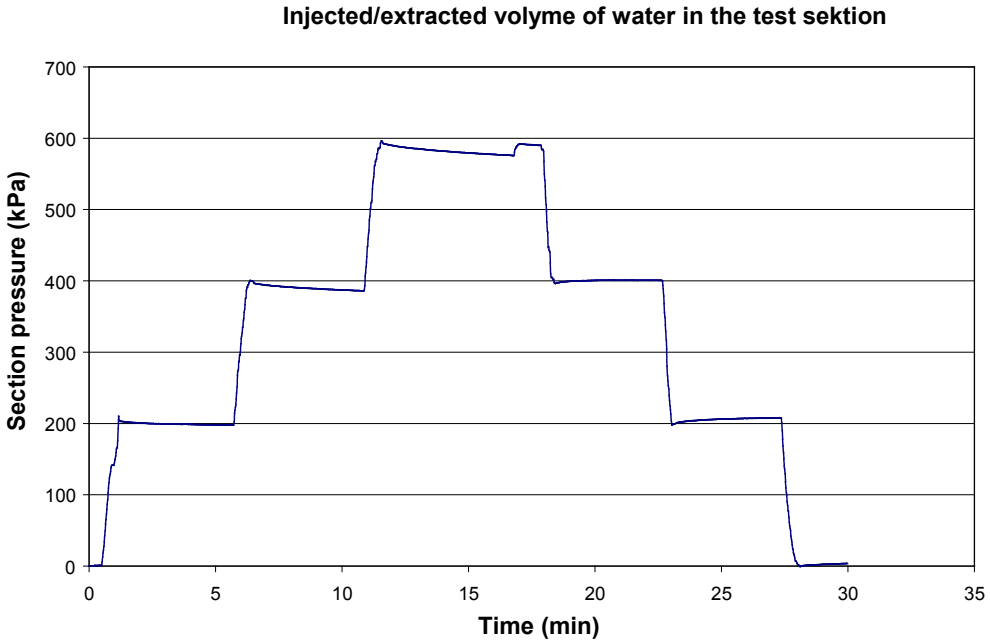

Figure A1-3. *Pressure in the test section versus time at injected/extracted water volumes in the test section. The corresponding water volume changes at each pressure step are shown in Figure A1-4.*

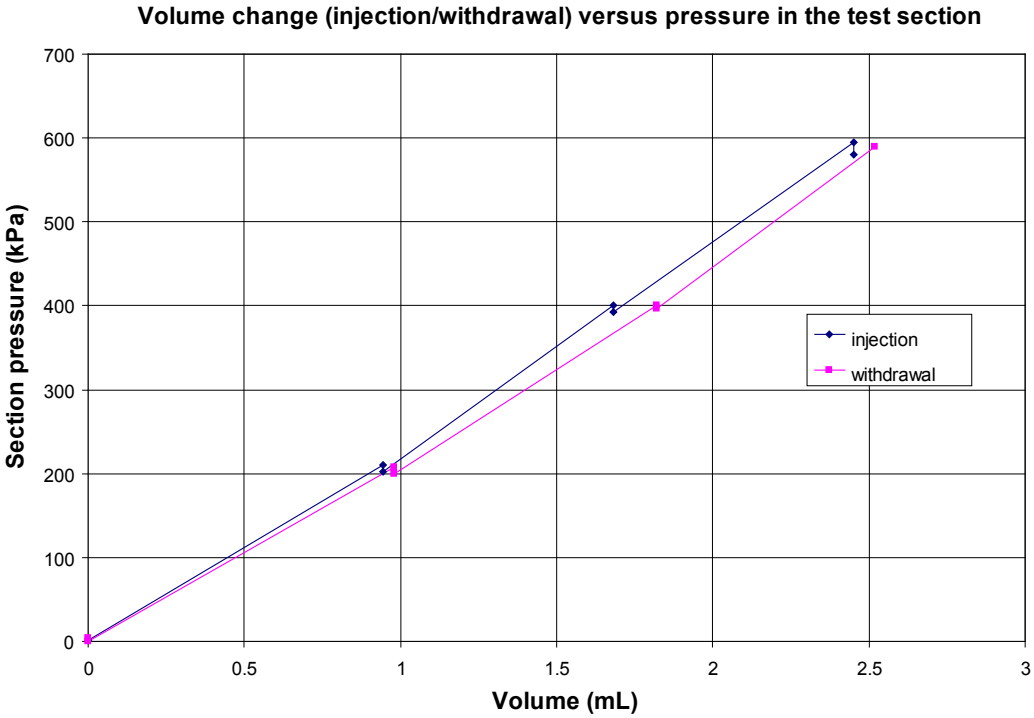

Figure A1-4. *Water volume changes versus pressure in the test section reflecting the total elasticity including one packer, c. 2.3 L of water and a steel pipe with a length of 0.55 m.*

A1.3.2 Time-dependent deformation

Material creeping due to pressure changes

The estimation of material creeping is based on the results from the previous test of linear-elastic deformations in Figure A1-3. When the pressure was increased in steps of 200 kPa and was shut-in, the pressure decreased c. 7 kPa during the actual period of 5 minutes. About the same increase of pressure was obtained when the pressure was lowered in steps of 200 kPa. It can be assumed that the material creeping in the steel pipe is much lower than the material creeping caused by the packer. It should be born in mind that the effective borehole storage coefficient for the test set-up is small in relation to the test sections in field tests.

Generated flow caused by the packer expansion

The squeezed out water volumes from the test section were registered versus time at two different pressure, i.e. atmospheric pressure and 200 kPa overpressure. The results presented in Tables A1-1 and A1-2 corresponds to volumes generated by one packer inflated at 2,016 kPa.

Table A1-1. Generated flow by one packer at no overpressure in the test section and hose.

Total time (min)	Time since previous measurement (min)	Change of water column (cm)	Height of water column (cm)	Change of volume (mL)	Total volume (mL)	Average flow rate (mL/min)
0	0	0	0	0	0	0
0.5	0.5	241	241	30.285	30.285	60.5699
1	0.5	4.85	245.85	0.609	30.894	1.2189
2	1	5.7	251.55	0.716	31.611	0.7163
3	1	4.7	256.25	0.591	32.201	0.5906
4	1	4.7	260.95	0.591	32.792	0.5906
5	1	3.7	264.65	0.465	33.257	0.4650
6	1	3.7	268.35	0.465	33.722	0.4650
7	1	3.8	272.15	0.478	34.199	0.4775
8	1	3.7	275.85	0.465	34.664	0.4650
9	1	3.52	279.37	0.442	35.107	0.4423
10	1	3.05	282.42	0.383	35.490	0.3833
11	1	3	285.42	0.377	35.867	0.3770
12	1	3	288.42	0.377	36.244	0.3770
13	1	3.15	291.57	0.396	36.640	0.3958
14	1	2.95	294.52	0.371	37.010	0.3707
15	1	2.88	297.4	0.362	37.372	0.3619
20	5	13.25	310.65	1.665	39.037	0.3330
45	25	25.5	336.15	3.204	42.242	0.1282
105	60	1.6	337.75	0.201	42.443	0.0034
1,085	980	10.7	348.45	1.345	43.788	0.0014

Test start: 2004-09-01 13:35.
Volume of 6/4 mm hose: 0.126 mL/cm.

Table A1-2. Generated flow by one packer at 200 kPa overpressure in the test section and hose.

Total time (min)	Time since previous measurement (min)	Change of water column (cm)	Height of water column (cm)	Change of volume (mL)	Total volume (mL)	Average flow rate (mL/min)
0	0	0	0	0.000	0.000	0.0000
1	1	17.1	17.1	2.149	2.149	2.1488
2	1	6.15	23.25	0.773	2.922	0.7728
3	1	6.1	29.35	0.767	3.688	0.7665
4	1	4.7	34.05	0.591	4.279	0.5906
5	1	4.3	38.35	0.540	4.819	0.5404
6	1	4.1	42.45	0.515	5.334	0.5152
7	1	3.9	46.35	0.490	5.825	0.4901
8	1	3.8	50.15	0.478	6.302	0.4775
9	1	3.65	53.8	0.459	6.761	0.4587
10	1	3.45	57.25	0.434	7.194	0.4335
11	1	3.42	60.67	0.430	7.624	0.4298
12	1	3.51	64.18	0.441	8.065	0.4411
13	1	3.2	67.38	0.402	8.467	0.4021
14	1	3.25	70.63	0.408	8.876	0.4084
15	1	3.15	73.78	0.396	9.271	0.3958
20	5	14.1	87.88	1.772	11.043	0.3544
40	20	20.2	108.08	2.538	13.582	0.1269
60	20	0.8	108.88	0.101	13.682	0.0050
80	20	0.2	109.08	0.025	13.707	0.0013
120	40	0.1	109.18	0.013	13.720	0.0003

Test start: 2004-09-03 07:24.

Volume of 6/4 mm hose: 0.126 mL/cm.

Appendix 2

Injection tests in sections KFM07A: 404–504 m and KFM07A: 154–159 m

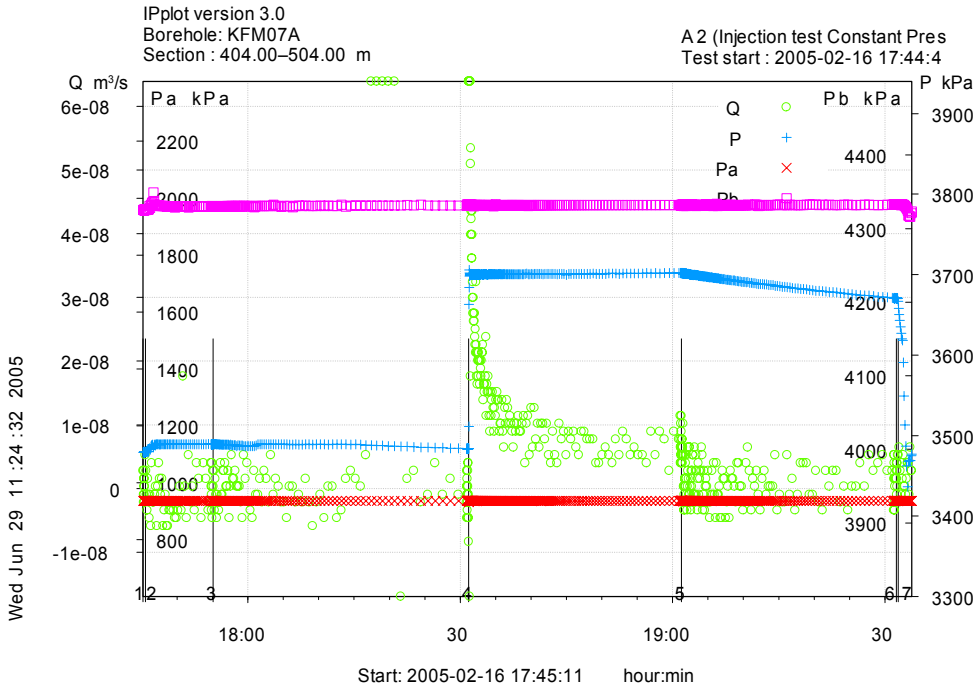

Figure A2-1. *Pressure history during the injection test in section KFM07A:404–504 m showing the different test phases on the time scale. A diagram with increased resolution of pressure during the packer sealing- and shut-in periods is shown in Figure A2-2.*

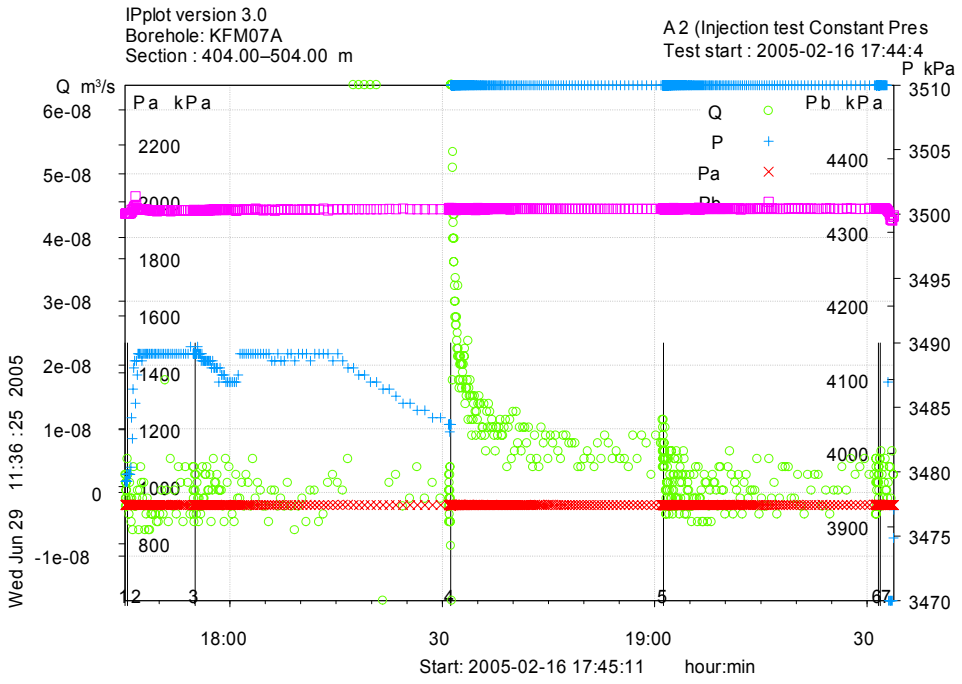

Figure A2-2. *Pressure in the test section during the packer sealing- and shut-in period (test phase 2 and 3) of the injection test in section KFM07A:404–504 m shown with higher resolution.*

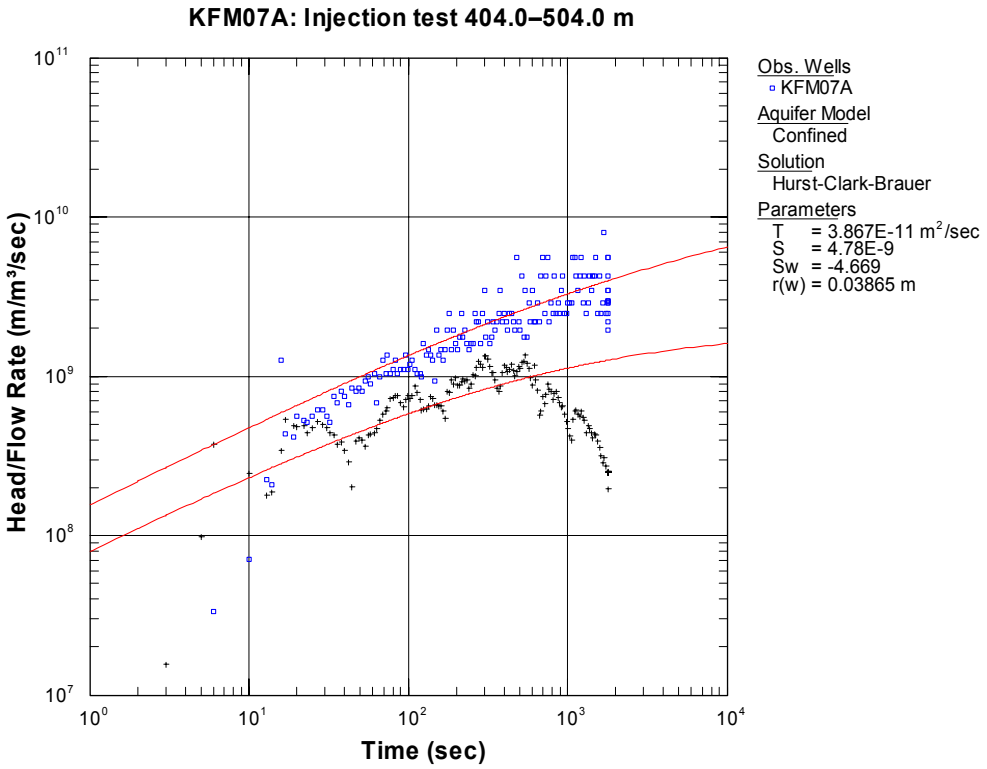

***Figure* A2-3.** *Log-log plot of head/flow rate (□) and derivative (+) versus time, from the injection test in section 404.0–504.0 m in KFM07A. From SKB P-05-133.*

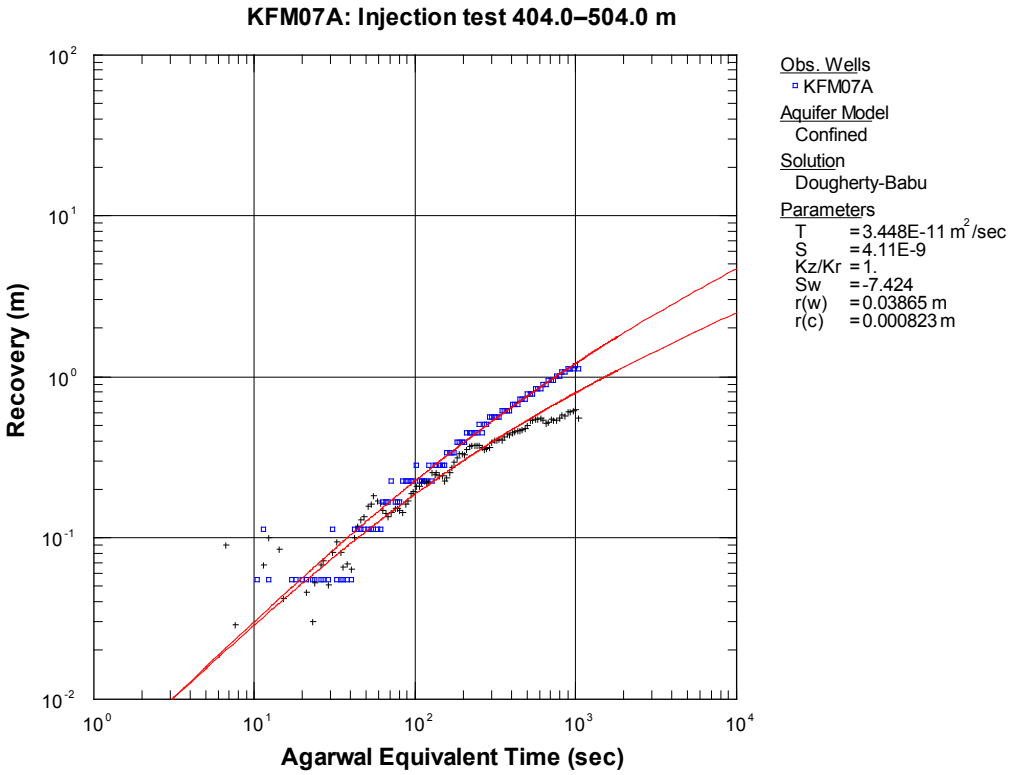

***Figure* A2-4.** *Log-log plot of recovery (□) and derivative (+) versus equivalent time from the injection test in section 404.0–504.0 m in KFM07A. From SKB P-05-133.*

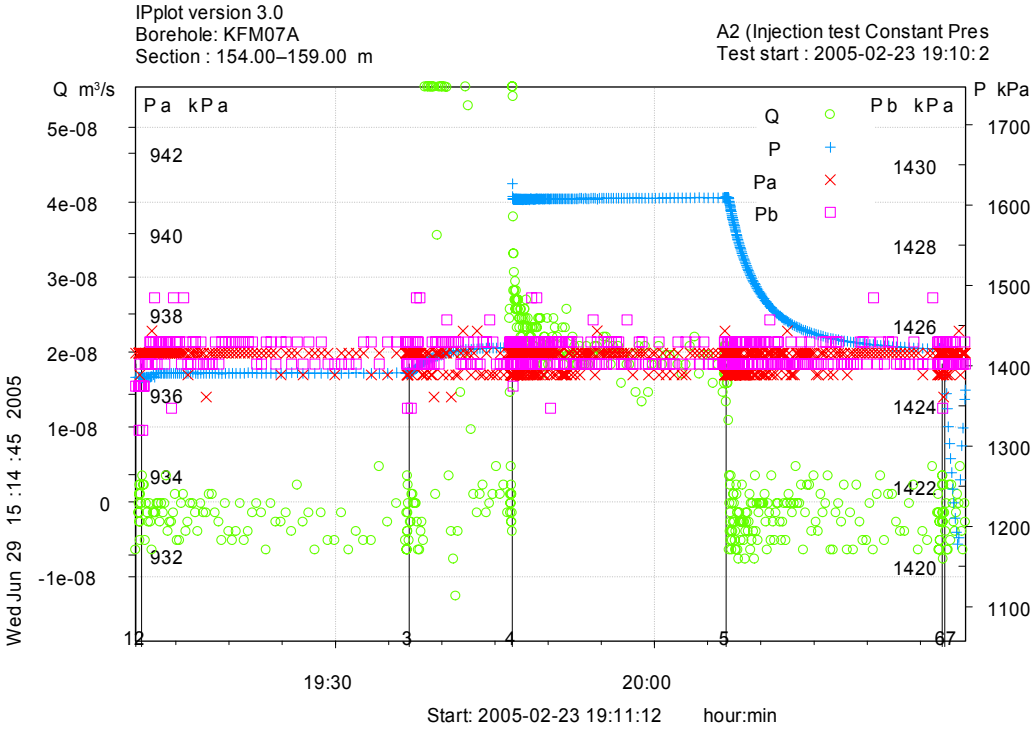

Figure A2-5. *Pressure history during the injection test in section KFM07A:154–159 m showing the different test periods on the time scale. A diagram with increased resolution of pressure during the packer sealing- and shut-in periods is shown in Figure A2-7.*

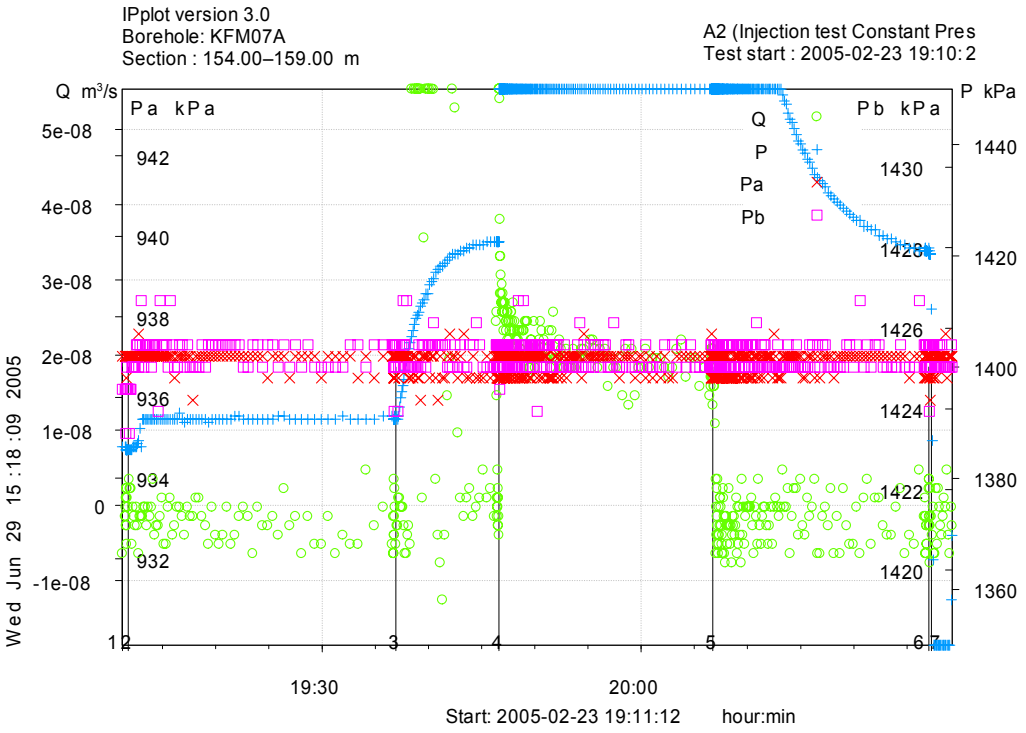

Figure A2-6. *Pressure in the test section during the packer sealing- and shut-in period (test period 2 and 3) of the injection test in section KFM07A:154–159 m shown with higher resolution.*

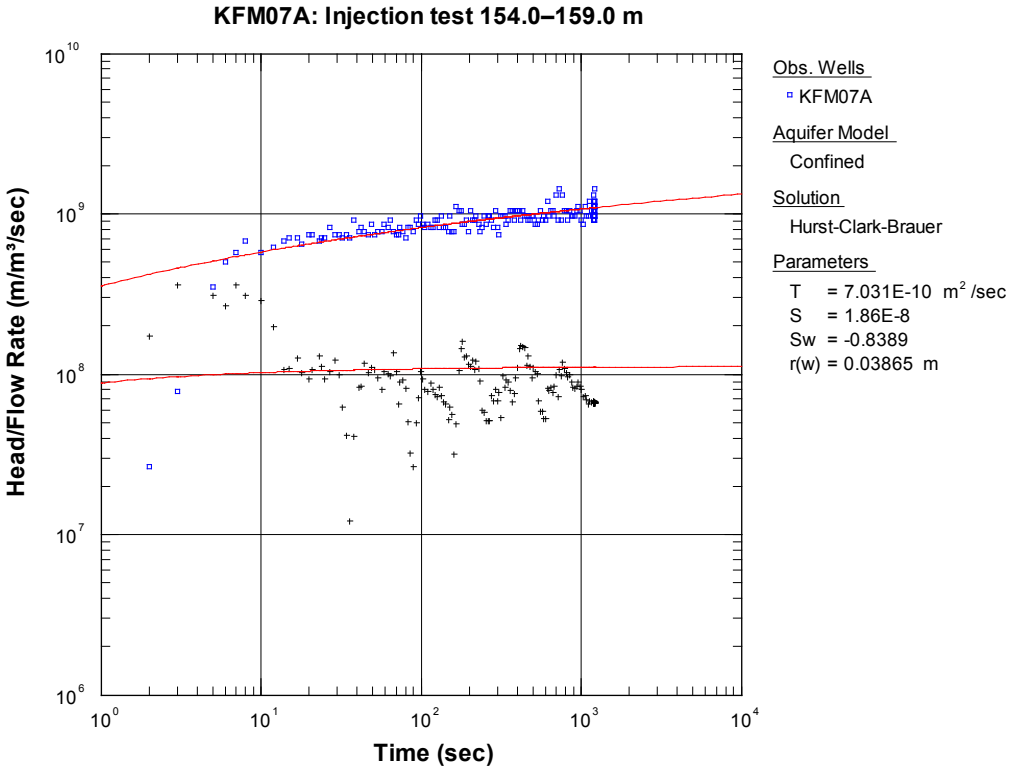

***Figure* A2-7.** *Log-log plot of head/flow rate (□) and derivative (+) versus time, from the injection test in section 154.0–159.0 m in KFM07A.From SKB P-05-133.*

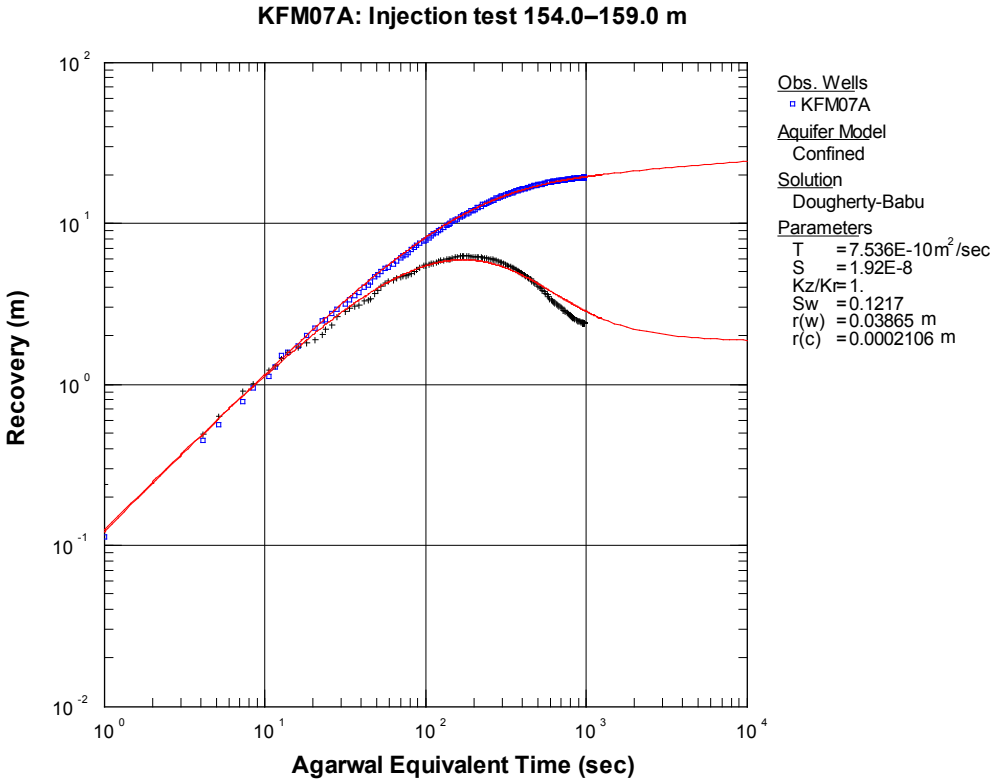

***Figure* A2-8.** *Log-log plot of recovery (□) and derivative (+) versus equivalent time from the injection test in section 154.0–159.0 m in KFM07A. SKB P-05-133.*

Examples of natural background pressure gradients

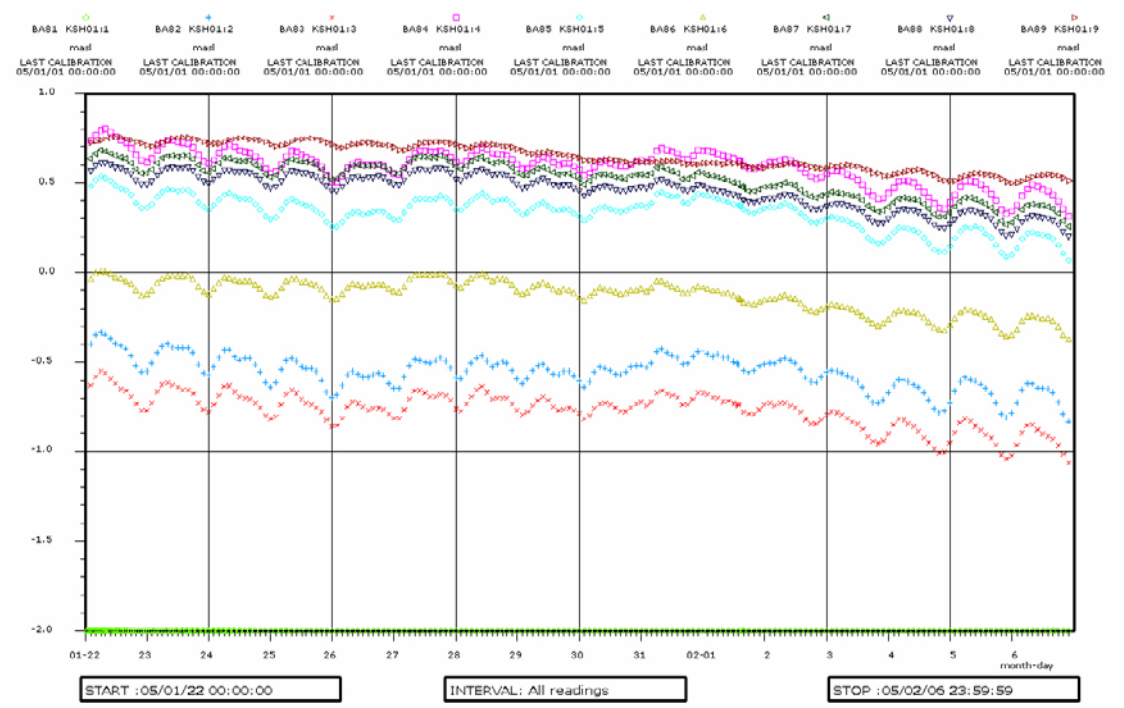

Figure A3-1a. *Piezometric level (metres above sea level) versus absolute time in isolated sections in borehole KSH01 during the time period 2005-01-22 to 2005-02-07 showing tidal effects.*

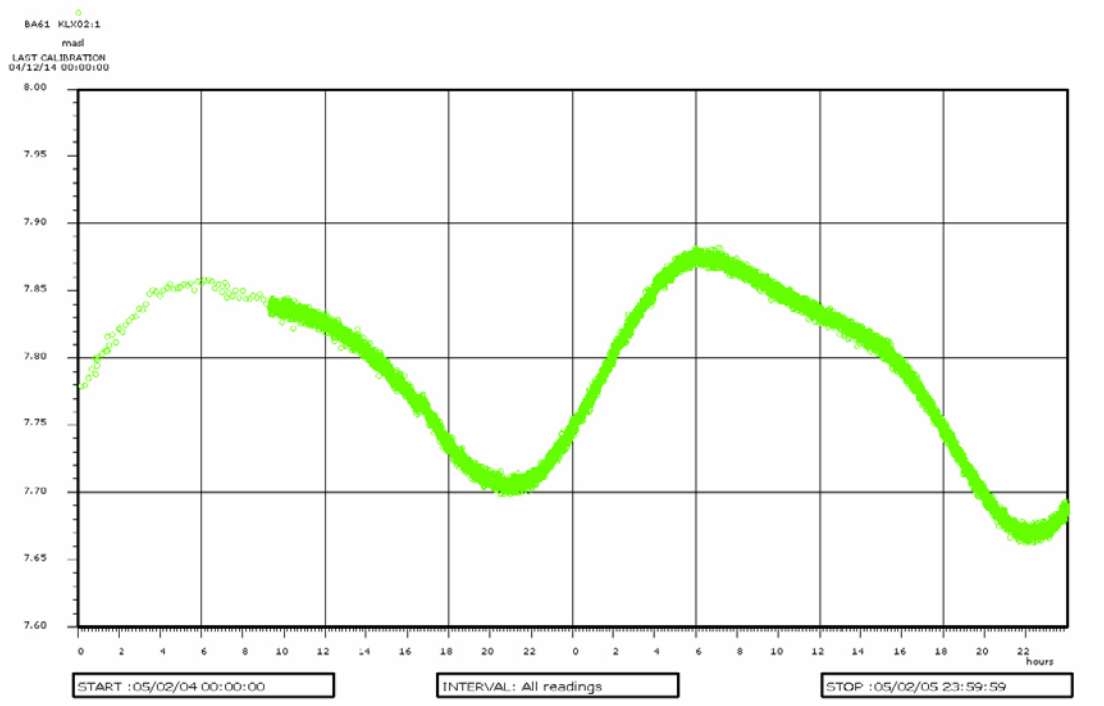

Figure A3-1b. *Detail of the piezometric level (metres above sea level) versus absolute time in deepest section in borehole KLX02 (256.4–1,700 m) during the time period 2005-02-04 to 2005-02-06 showing tidal effects.*

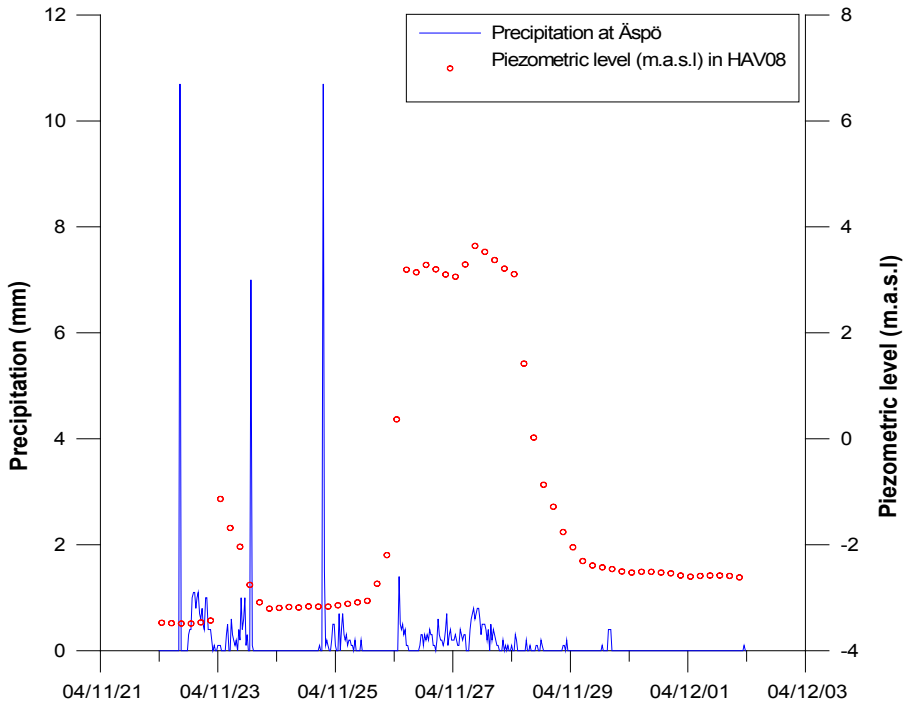

Figure A3-2a. *Piezometric level (metres above sea level) versus absolute time in percussion borehole HAV 08 together with observed precipitation at Äspö during the time period 2004-11-21 to 2004-12-03.*

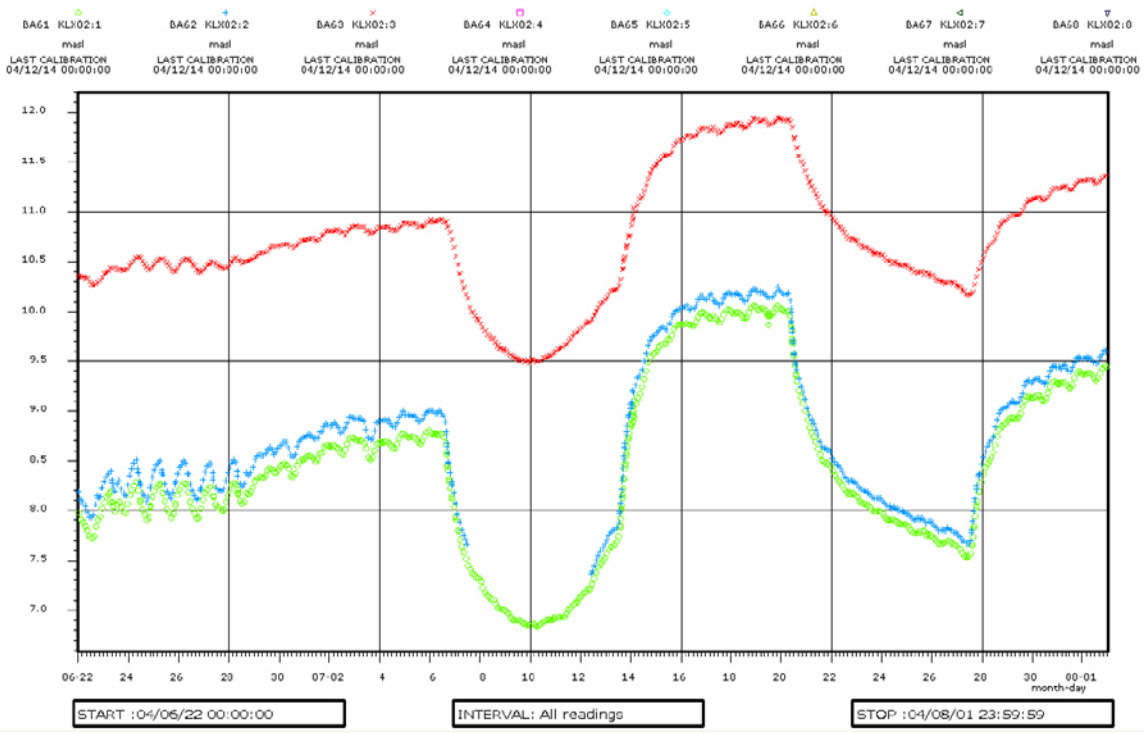

Figure A3-2b. *Piezometric level (metres above sea level) versus absolute time in isolated sections in borehole KLX02 strongly affected by precipitation during two flow periods with subsequent recovery of the interference test in HLX10. (KLX02_1: 256.4–1,700 m, KLX02_2: 207.9–255.4 m, KLX02_3: 0–206.9 m).*

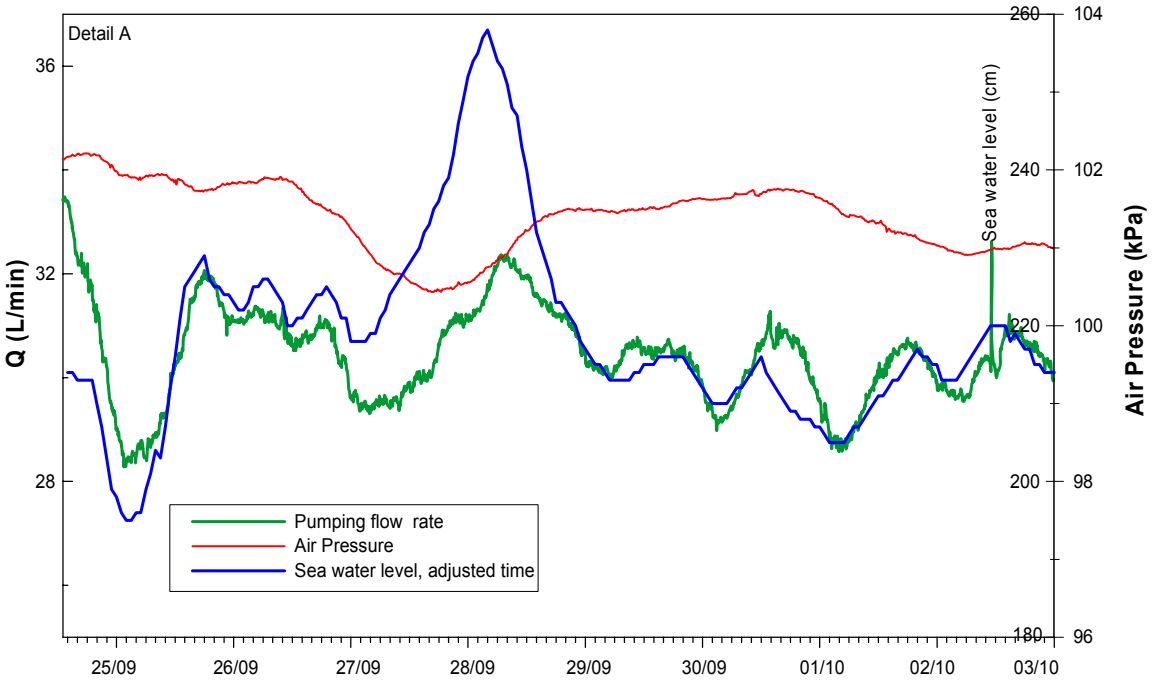

Figure A3-3. *Recorded flow rate during the time period 2003-09-25 to 2003-10-03 of the pumping with constant pressure in borehole KFM03A in conjunction with hydro-chemical sampling. Variations of the atmospheric pressure are affecting the flow rate at the high peak. From Ludvigson et al. (2004) /16/.*

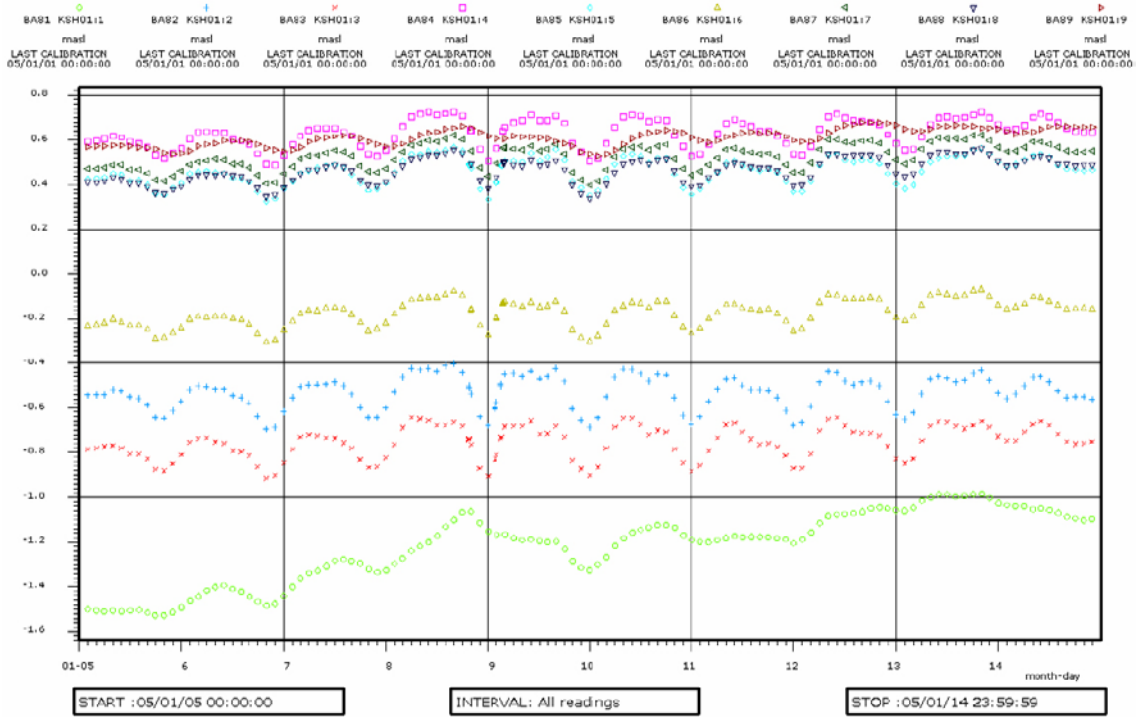

Figure A3-4a. *Piezometric level in metres above sea level (relative to the atmospheric pressure) versus absolute time in isolated sections in borehole KSH01 during the time period 2005-01-05 to 2005-01-15.*

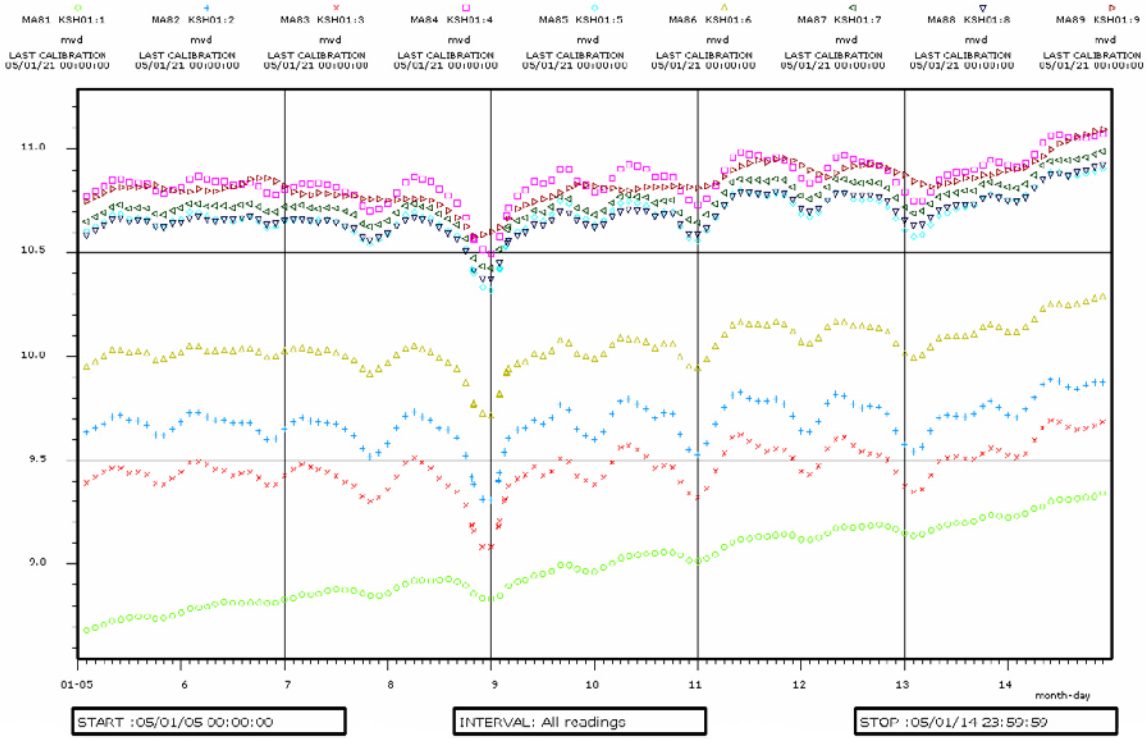

Figure A3-4b. *Piezometric level (m), based on the absolute pressure at the gauge level, in the same sections as in Figure A3-4a (uncorrected relative to the atmospheric pressure) during the time period 2005-01-05 to 2005-01-15.*

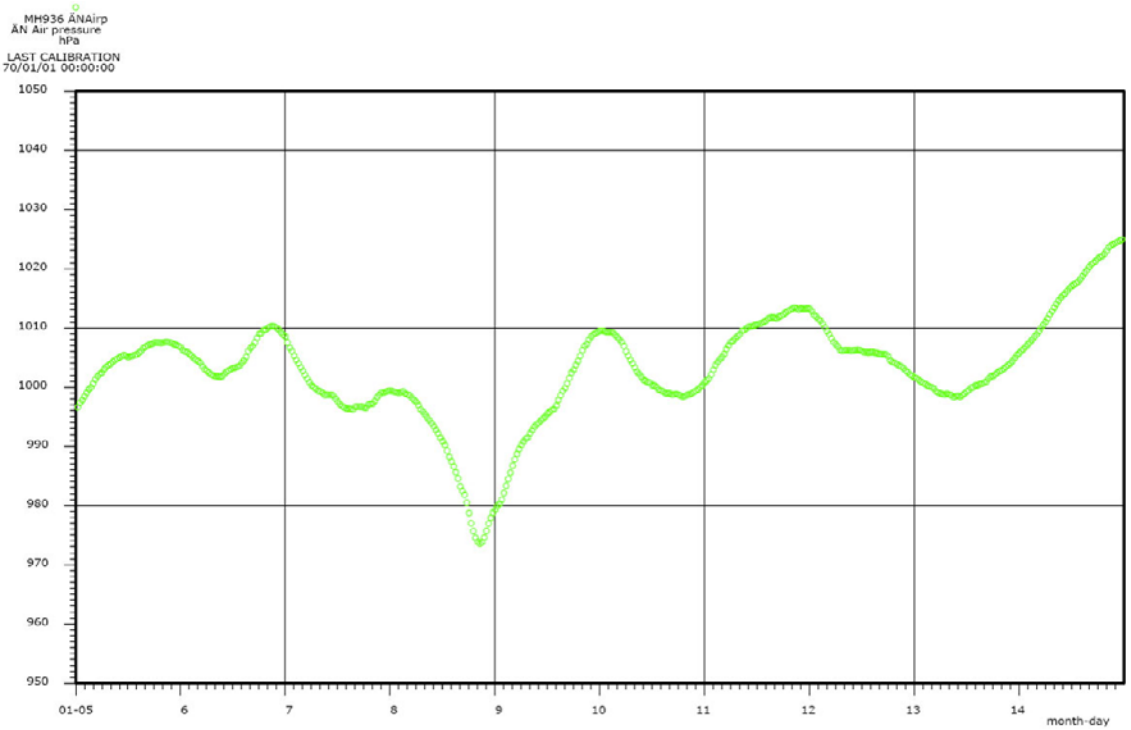

Figure A3-4c. *Recorded atmospheric pressure (mbar) at Äspö during the time period 2005-01-05 to 2005-01-15.*

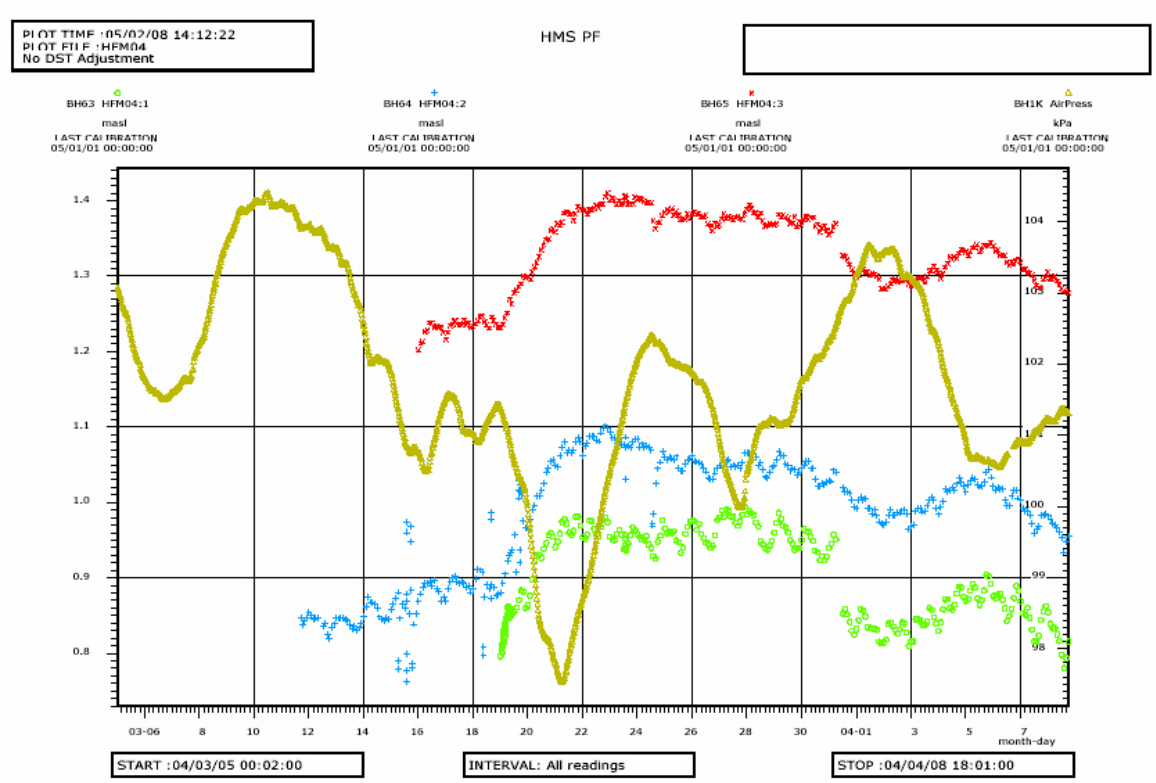

Figure A3-4d. *Piezometric level (metres above sea level) versus absolute time in three different sections in borehole HFM04 (red, blue, green) together with the atmospheric pressure (yellow) during the period 2004-03-05 to 2004-04-08.*

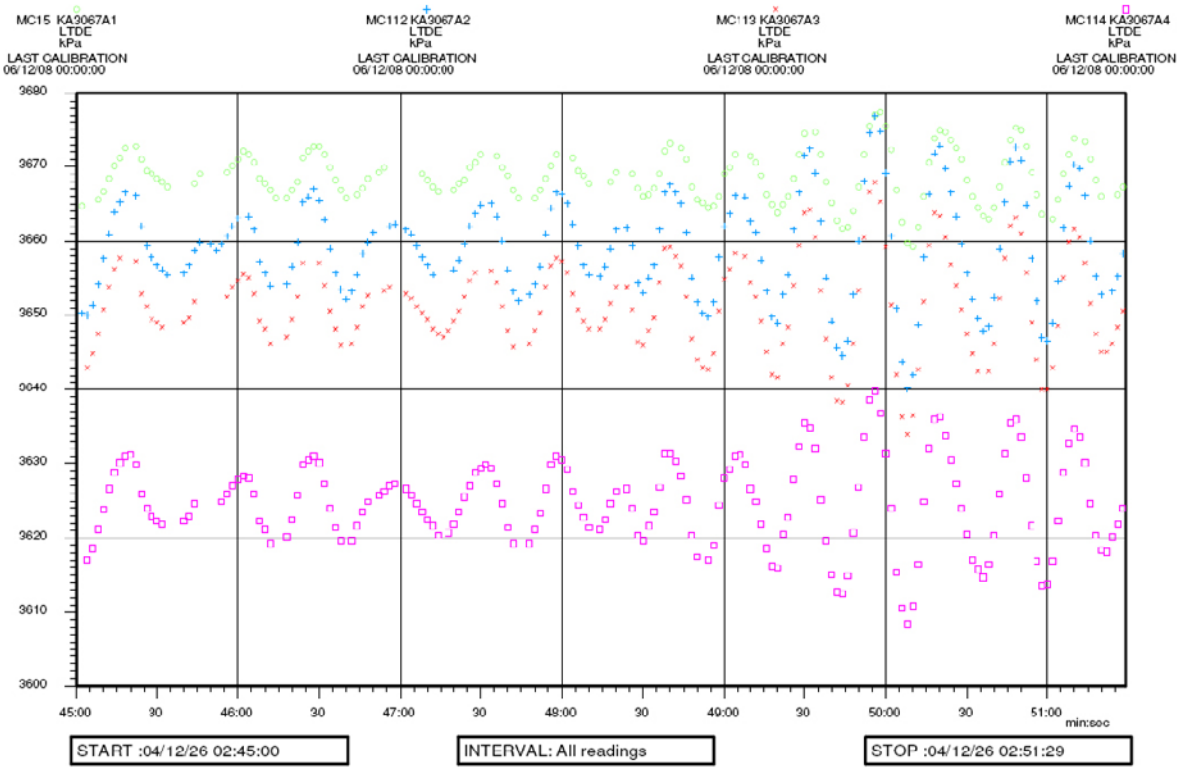

Figure A3-5a. *Detail of recorded absolute pressure (kPa) in different sections in the tunnel borehole KA3067A during the earth quake in South East Asia in 2004.*

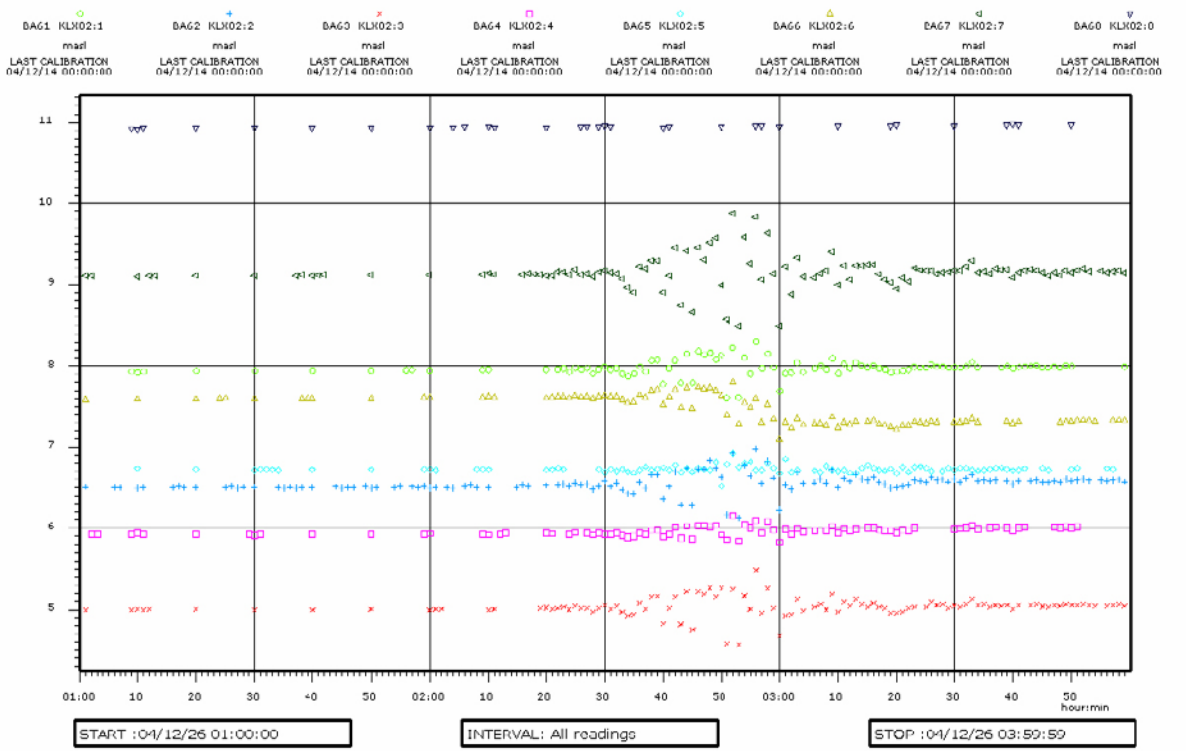

Figure A3-5b. *Piezometric level (metres above sea level) versus absolute time in sections in the surface borehole KLX02 during the earth quake in South East Asia in 2004.*

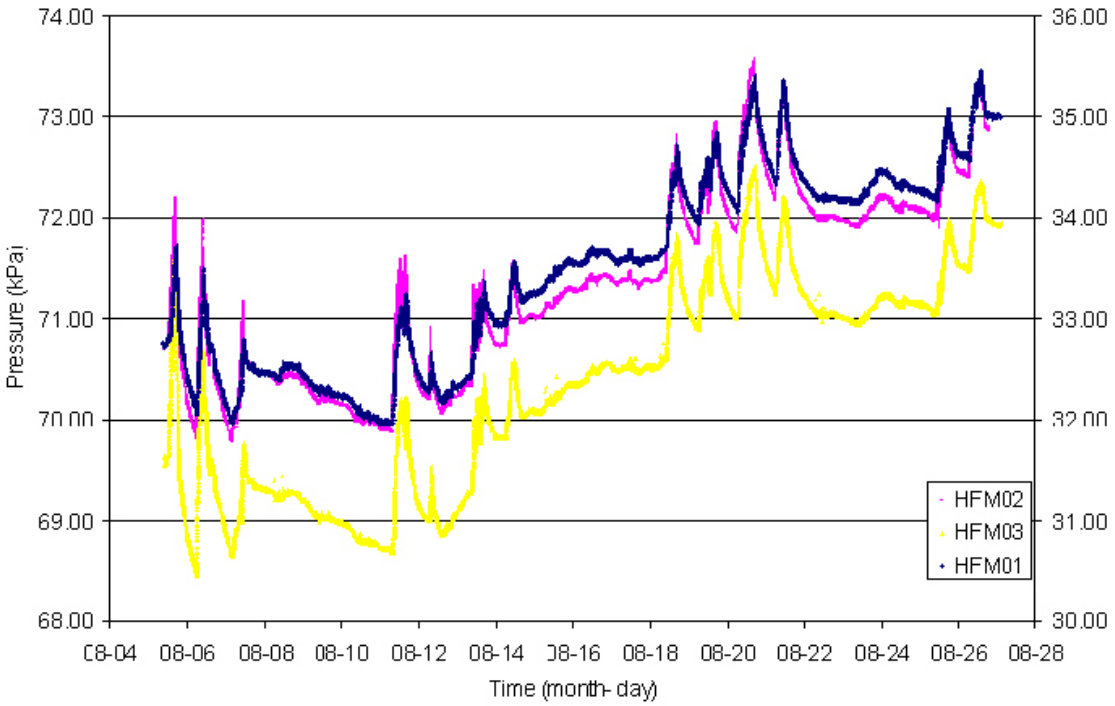

Figure A3-6. *Observed pressure responses in the boreholes HFM01-03 during drilling of borehole KFM01B (17–235 m). Drilling is performed during the periods with pressure peaks. The distances to KFM01B are estimated to c. 120 m, c. 140 m and c.140 m respectively. From Levén and Ludvigson (2004) /25/.*

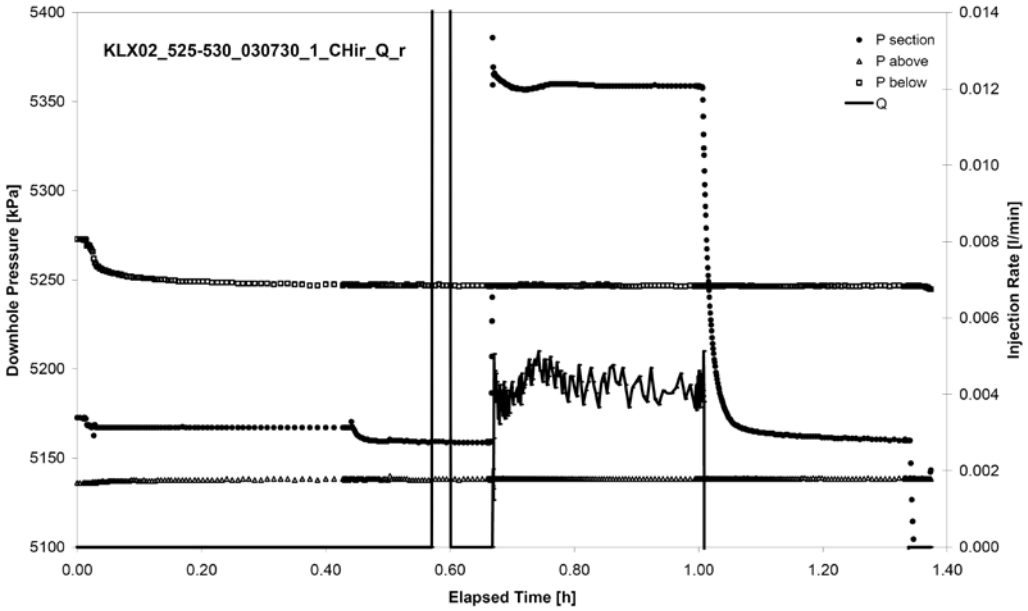

Figure A3-7. *Example of constant head injection test and subsequent pressure recovery in section KLX02:525–530 m showing a formation pressure below the average borehole pressure. In the figure, the formation pressure has been extrapolated from the pressure trend prevailing before start of injection (dashed line). After Rahm and Enachescu (2004) /26/.*

Appendix 4

Step injection tests in section KFM05A: 284–289 m

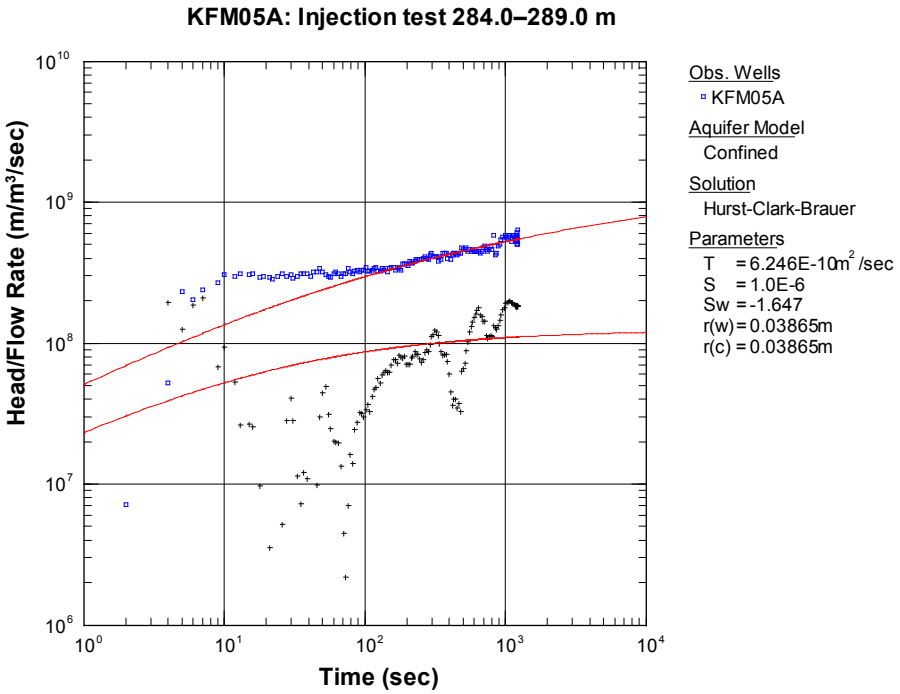

Figure A4-1. *Log-log plot of head/flow rate (□) and derivative (+) versus time from the standard injection test in section 284.0–289.0 m in KFM05A. From SKB P-05-56.*

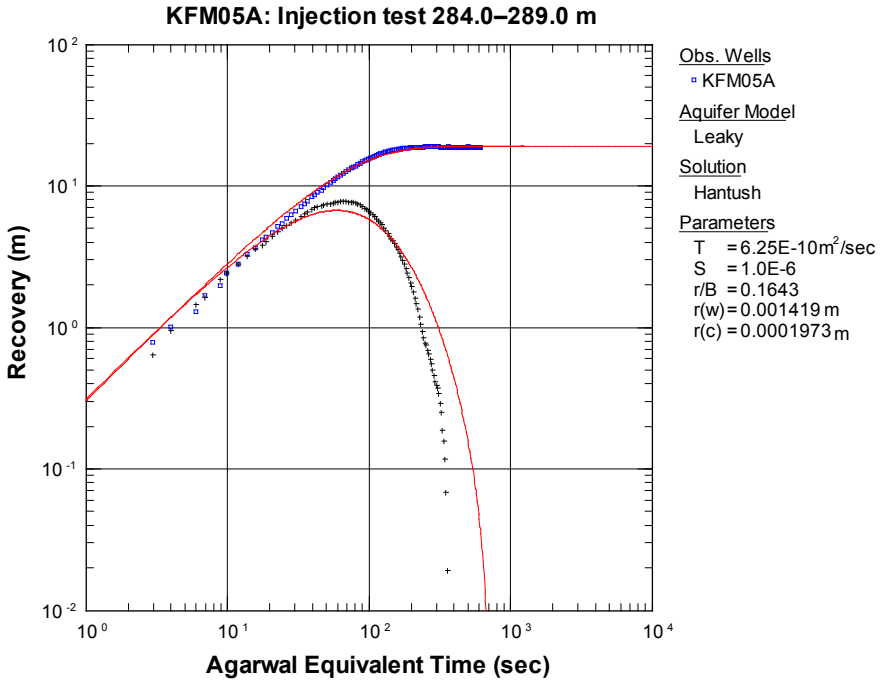

Figure A4-2. *Log-log plot of recovery (□) and derivative (+) versus equivalent time from the standard injection test in section 284.0–289.0 m in KFM05A. From SKB P-05-56.*

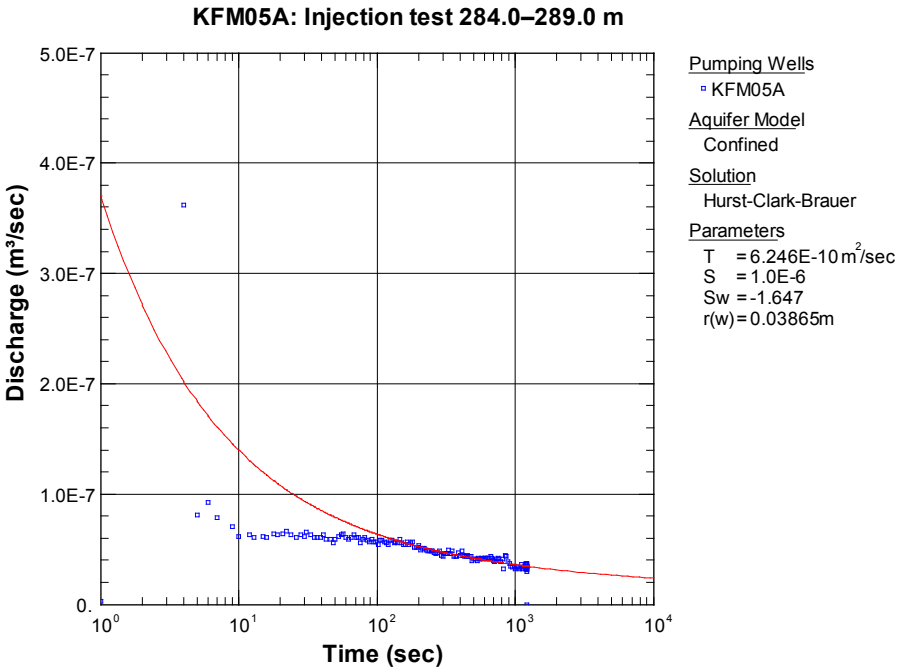

Figure A4-3. *Lin-log plot of flow rate versus time from the standard injection test in section 284.0–289.0 m in KFM05A. 200 kPa injection pressure.*

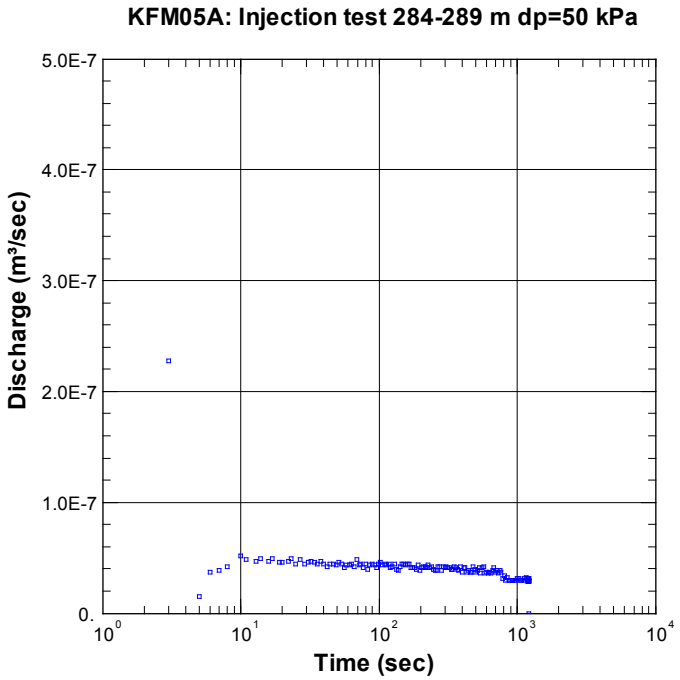

Figure A4-4. *Lin-log plot of flow rate versus time from the step injection test in section 284.0–289.0 m in KFM05A. 50 kPa injection pressure.*

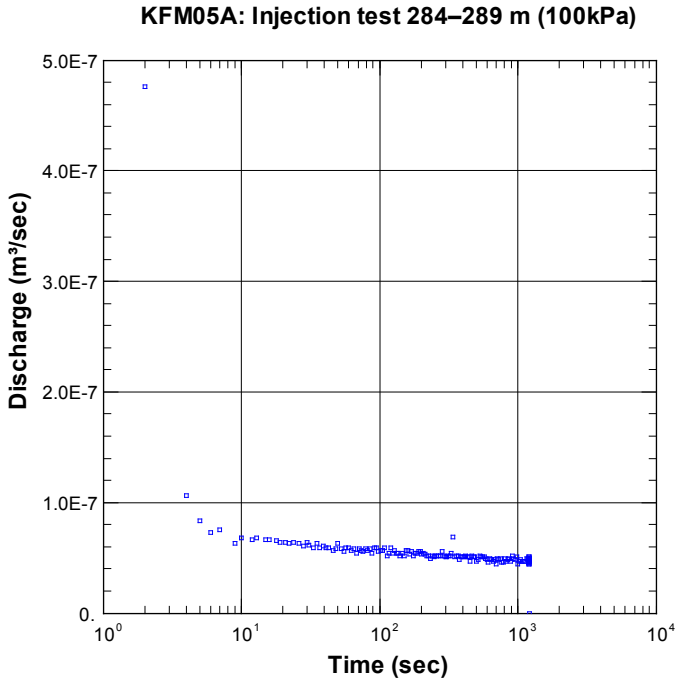

Figure A4-5. *Lin-log plot of flow rate versus time from the step injection test in section 284.0–289.0 m in KFM05A. 100 kPa injection pressure.*

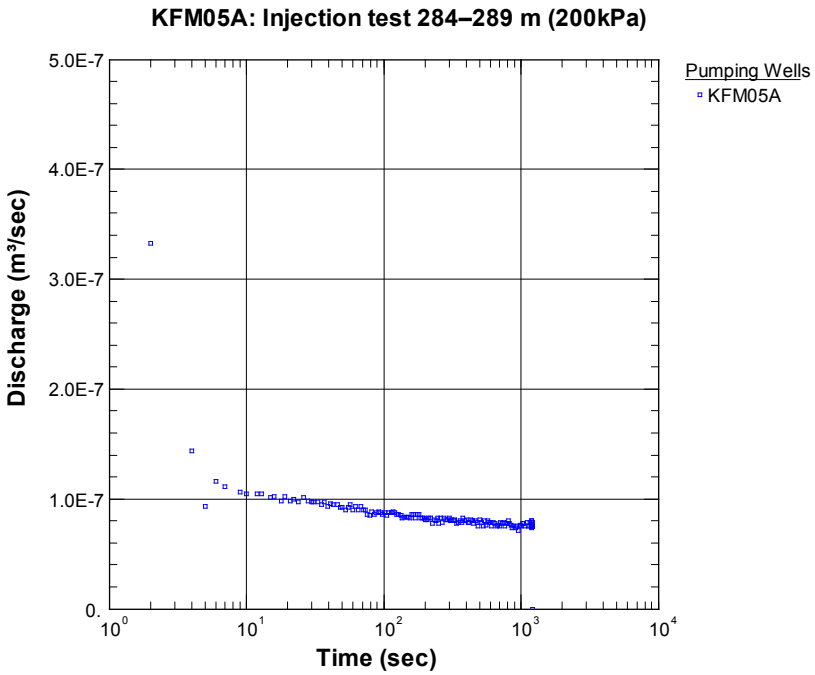

Figure A4-6. *Lin-log plot of flow rate versus time from the step injection test in section 284.0–289.0 m in KFM05A. 200 kPa injection pressure.*

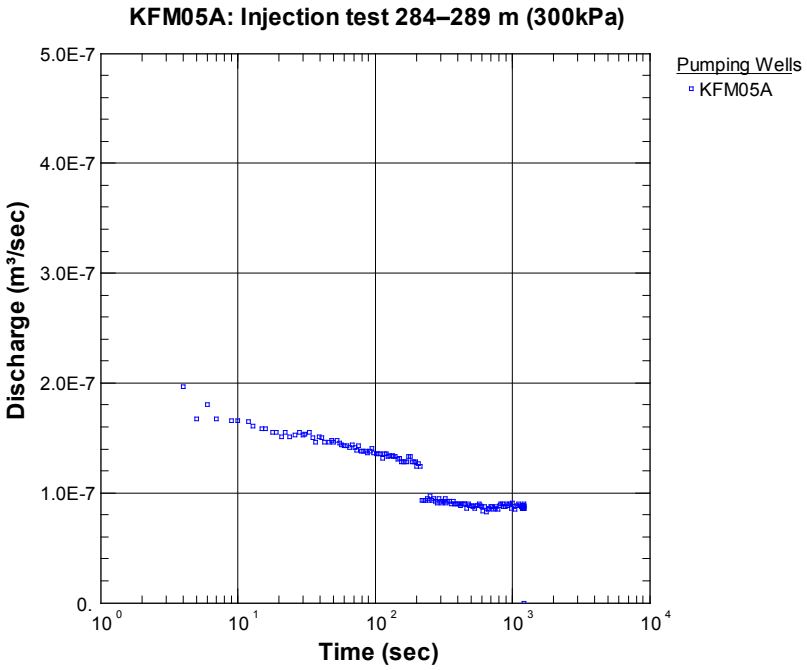

Figure A4-7. *Lin-log plot of flow rate versus time from the step injection test in section 284.0–289.0 m in KFM05A. 300 kPa injection pressure.*

Appendix 5

Calculation of Agarwal equivalent time in analysis of the recovery period following injection tests at constant pressure

Examples from injection tests in core boreholes at Forsmark

Jan-Erik Ludvigson, GEOSIGMA AB

January 2006

Summary

The purpose of this study is to examine different ways of calculating Agarwal equivalent time in the analysis of the recovery period following injection tests at constant pressure and its effect on the shape of the recovery curve and on the evaluated hydraulic parameters. Three different ways have been studied, i) based on the actual injection time $t_{p,}$ ii) based on the pseudo-injection time t_{pp} and iii) based on the flow sequence during the injection period (multi-rate). These three ways have been examined in the analysis of injection tests in core boreholes at Forsmark.

The results indicate that, in analyses of tests in sections with greater transmissivity than about $1 \cdot 10^{-8}$ m^2/s, the difference is small or insignificant in the shape of the recovery curve and for evaluated hydraulic parameters, regardless of which of the above-mentioned three ways of calculating the Agarwal equivalent time is used. The difference between t_p and calculated t_{pp} is usually also small in this case. However, it is considered that the Agarwal time based on the multi-rate assumption is the way that is most correct and theoretically most free from objection for calculating the equivalent time for constant pressure tests. It is assumed here that all flow variations during the injection period also will affect the recovery period.

However, for tests in sections that have transmissivity lower than about $1 \cdot 10^{-8}$ m^2/s, greater differences may occur in the appearance of the recovery curve and the calculated related hydraulic parameters depending if t_p or t_{pp} is used. This is because relatively large differences can occur between actual t_p and calculated t_{pp} due to large fluctuations of flow, mainly at the beginning but also towards the end of the injection period, which can result in the calculated total injected volume of water V_p not being representative for the test. For example, large initial flow peaks while regulating to a constant pressure can significantly affect V_p in low-transmissive sections. Furthermore, determining the final flow Q_p could be uncertain due to scatter in the flow rate. This implies especially that Agarwal equivalent time based on t_{pp} could be non-representative and thus affect the recovery curve negatively.

The actual flow time t_p is judged accordingly as being more robust and representative than t_{pp} when calculating the Agarwal time in sections having a transmissivity smaller than about $1 \cdot 10^{-8}$ m^2/s, and also simpler. The Agarwal time based on t_p is not affected by the flow sequence during the injection period. It is considered, however, that the Agarwal time based on the multi-rate assumption is more correct also in these cases.

In calculating the Agarwal equivalent time based on the multi-rate assumption it is important that excessive fluctuations in the flow do not occur, especially towards the end of the injection period because the equivalent time and the shape of the recovery curve are very sensitive to such fluctuations. Extremely high flow peaks while regulating at the beginning of the injection period can also affect the recovery curve. In such cases some form of smoothing of flow data is necessary and also to allow the final flow value of the data file to be always identical to the interpreted final flow Q_p. In very low-transmissive sections ($T < 1–5 \cdot 10^{-9}$ m^2/s) the Agarwal time should therefore also be evaluated on the basis of t_p for comparison and control. In sections

where full recovery of the pressure is not achieved during the recovery period the recovery curve can be of completely different shapes when using t_p or the multi-rate assumption respectively, which can influence interpretation of flow regimes as well as calculation of hydraulic parameters. In such sections the interpretation is however uncertain regardless of which method is used.

A5.1 Introduction

When plotting and evaluating the recovery period following injection tests at constant pressure the Agarwal equivalent time (dt_e) on the time scale is normally used instead of the actual recovery time (dt). For tests at constant pressure and decreasing flow during the injection period the Agarwal equivalent time can be calculated in different ways. The equivalent time can be based either on the *actual* flow time for the injection period (t_p) or on the pseudo-flow time (t_{pp}) according to Equation (1a) or (1b) below. When using Agarwal equivalent time based on t_p the flow is assumed to be constant throughout the entire injection period (= final flow Q_p). When the time is based instead on t_{pp} a constant mean flow is assumed during a pseudo-flow time (t_{pp}) which is calculated as the quotient of the total injected volume of water during the injection period (V_p) and the final flow Q_p.

$$dt_e = (t_p \cdot dt) / (t_p + dt) \quad (1a)$$

$$dt_e = (t_{pp} \cdot dt) / (t_{pp} + dt) \quad (1b)$$

t_p = actual flow time (s).
t_{pp} = pseudo-flow time (s) [= V_p/Q_p].
dt = running recovery time (s).

A third, more rigorous way of calculating Agarwal equivalent time is through step-by-step superposition of the varying flow during the injection period (i.e. multi-rate approach), see the Equation (1c). For a test with varying flow divided into n steps the Agarwal equivalent time dt_e is calculated according to the following formula /Agarwal 1980/:

$$dt_e = \left[\prod_{j=1}^{n-1} \left(\frac{t_{n-1} - t_{j-1}}{dt + t_{n-1} - t_{j-1}} \right)^{\frac{Q_j - Q_{j-1}}{Q_{n-1} - Q_n}} \right] * dt \quad (1c)$$

t = run time during the flow time (s) and $t_0 = 0$.
Q = flow during the flow period (m^3/s), $Q_0 = 0$ and $n > 1$.
dt = running recovery time (s).

Alternatively the pressure recovery can be plotted as a function of the Horner time (t_H) or its inverse /Earlougher 1977/:

$$t_H = (t_p + dt)/dt \quad (2)$$

Even in this time transform one can choose to use actual flow time (t_p) or the pseudo-flow time (t_{pp}) in analysing the pressure recovery following tests at constant pressure. All of the time transforms mentioned above are based on approximations of exact analytical solutions for the recovery period.

/Uraiet and Raghavan 1980/ recommend using Horner time based on actual flow time (t_p) when interpreting the recovery period following tests at constant pressure. However, in later articles /e.g. Rosato et al. 1982/ they recommend the use of Agarwal equivalent time based on the pseudo-flow time (t_{pp}) for interpreting the recovery period.

An exact analytical solution for the recovery following tests at constant pressure was presented by /Ehlig-Economides and Ramey 1981/. This is based on superposition of continually varying flows during the flow period, cf the multi-rate approach described above. Approximate solutions were derived from the exact solution for different types of fringe conditions, e.g. for analysis in Horner diagram. They ascertained, for example, that for dimensionless flow times $t_{pD} = T \cdot t / S \cdot r_w^2$

$> 10^4$ the error of the slope in the straight line in a Horner diagram is negligible (< 1.5 %) if one uses the actual flow time t_p instead of t_{pp} when analysing the recovery. However, for dimensionless flow times $t_{pD} < 10^4$ the error increases and the straight line in the Horner diagram is not developed fully in the recovery at short flow times.

For short injection tests as in PLU it can be assumed that $t_{pD} < 10^4$ in many cases, especially for low-conductive sections. Accordingly, it is uncertain whether one should use the actual flow time (t_p) or the pseudo-flow time (t_{pp}) when calculating Agarwal equivalent time (or Horner time) in analysing the recovery following tests at constant pressure and what consequences this may imply on evaluated hydraulic parameters from the recovery period.

A5.2 Evaluating the pseudo-flow time t_{pp} for injection tests in KFM02A and KFM04A

From injection tests performed earlier with PSS in KFM02A and KFM04A in 100 m, 20 m and 5 m sections a check was made first of the uncertainty in t_{pp}, calculated as V_p/Q_p, where V_p is the total injected volume during the injection period (test phase 4) and Q_p is the final flow during this phase. It can be assumed that Q_p is very uncertain at low rates of flow close to the lower measurement limit for flow. The volume V_p can be affected by the test procedure, especially the adjustment to constant pressure at the beginning, due to the possible presence of gas in the test system, etc. During the very first seconds after starting the injection a certain amount of water is expended to increase the pressure in the test section at 200 kPa, due to compressibility of water in the section and of the packers that limit the test section (wellbore storage). This can result in high flow peaks occurring while adjusting, especially in low-conductive sections, which can affect V_p and thus t_{pp}. Furthermore, a comparison was made between calculated t_{pp} and actual t_p for the tests mentioned above. The main purpose of the study is an assessment of the relevance of calculated t_{pp} from IPPLOT for the injection tests in KFM02A and KFM04A.

A5.2.1 Prerequisites

The data material that is analysed in this chapter consists of measured and interpreted data that is presented in the SKB P-data reports for the injection tests in KFM02A /Källgården et al. 2004/ and KFM04A /Hjerne and Ludvigson, 2005/. Data for the final flow Q_p that is presented in the P-reports was checked in the transient flow diagrams in connection with the normal test evaluation. This resulted for example in some of the Q_p values derived from diagram A0 in IPPLOT being corrected because they were judged as not being representative for the test, e.g. due to large variations in the flow at the end, especially in low-transmissive sections.

It was also judged that some of the flows can be regarded as significant (i.e. above background fluctuations in flow before and after the injection period), despite the fact that they were sometimes below the general lower measurement limit for PSS at 1 mL/min ($1.7 \cdot 10^{-8}$ m^3/s), cf Figure A5-1. This means that some values for t_{pp} from diagram A0 were adjusted in consideration of the updating of Q_p. The values for V_p however are taken directly from diagram A0 in IPPLOT. Accordingly, only checked values of t_{pp}, based on an interpreted, representative Q_p, are used in this study.

In the presented analysis only tests with a final flow Q_p that have been interpreted as significant (i.e. above the background flow) are used because no transient interpretation is made for injection tests with an interpreted non-significant final flow Q_p, neither for the injection period nor the recovery period. The values of the actual flow time t_p are taken directly from diagram A0.

The injection period is usually interrupted after about 5 min (300 s) in very low-transmissive sections. In these tests Q_p (as anticipated) has been interpreted as non-significant (non-definable) in almost all cases. Tests with an interpreted non-significant final flow Q_p have not been included in this study.

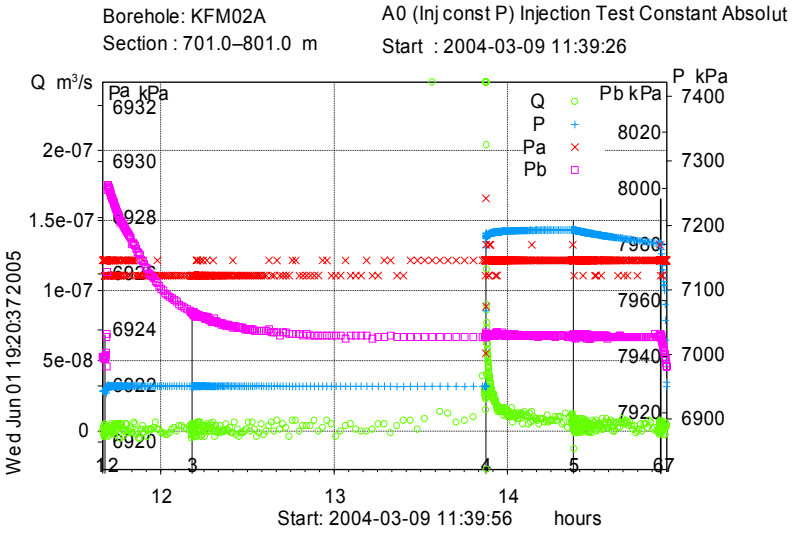

Figure A5-1. *Key diagram for pressure in the test section (P) and surrounding sections (P_a and P_b) and also flow (Q) for injection test at constant pressure in section 701.0–801.0 m in KFM02A.*

A5.2.2 Results

To study the difference between calculated t_{pp} and actual t_p as a function of transmissivity the calculated t_{pp} values in KFM02A were plotted versus T-moye (T_M) in Figure A5-2. The tests were arranged in different colours with regard to section length. Even the actual flow time t_p for tests with different section length are marked in the figure. Only tests with a definable final flow Q_p have been included in the figure. For the tests in 20 m and 5 m sections with an actual flow time of t_p = about 1,200 s the calculated t_{pp} varies between about 1,200–10,000 s while for the 100 m tests with t_p = about 1,800 s the calculated t_{pp} varied between about 1,800-25,000 s. Figure A5-2 shows that the difference between t_{pp} and t_p is greatest for 100 m sections. This is natural because greater deviations in the flow (inertia) can be anticipated when adjusting to a constant pressure in 100 m sections than in shorter sections.

The corresponding deviation between t_{pp} and t_p as a function of calculated T_M values in KFM04A are shown in Figure A5-3. Only tests with a definable final flow Q_p are included in the figure. In KFM04A, the calculated t_{pp} varied between about 1,200-5,000 s for the 20 m and 5 m sections with an actual flow time of t_p = about 1,200 s while for the 100 m tests with t_p = about 1,800 s the calculated t_{pp} varied between about 1,800–10,000 s.

Figure A5-2 and A5-3 clearly show that t_{pp} only differs markedly from t_p for tests with T_M less than about $1 \cdot 10^{-8}$ m²/s. However, t_{pp} differs markedly from t_p in only a few of the tests. Consequently, examining the cause of the big difference between t_{pp} and t_p for these tests is of interest. The difference between t_{pp} and t_p can be of significance in calculating Agarwal equivalent time and in the hydraulic evaluation of the recovery period. In other cases (T_M > about $1 \cdot 10^{-8}$ m²/s) it can be assumed that the difference between t_{pp} and t_p has no practical significance. In these cases it is probable that the difference will be small between calculated Agarwal equivalent time and interpreted hydraulic parameters of the recovery period, regardless of whether t_p or t_{pp} is used. Examples of test interpretations from KFM04A are presented in Chapter 3.

Tests where t_{pp} and t_p deviate most in Figures A5-2 and A5-3 are presented in Table A5-1. For several of these tests the interpreted final flow Q_p is smaller than the lower standard measurement limit for PSS of 1 mL/min ($1.7 \cdot 10^{-8}$ m³/s) but the flow has nevertheless been interpreted as significant (definable).

Transient flow curves during the injection period for selected tests from KFM02A and KFM04A that have a big difference between t_{pp} and t_p are shown in Sub-appendix A5:1. Also the simulated flow curves for these sections according to interpreted hydraulic parameters from the flow period are presented in the plots. The results of these tests are commented below.

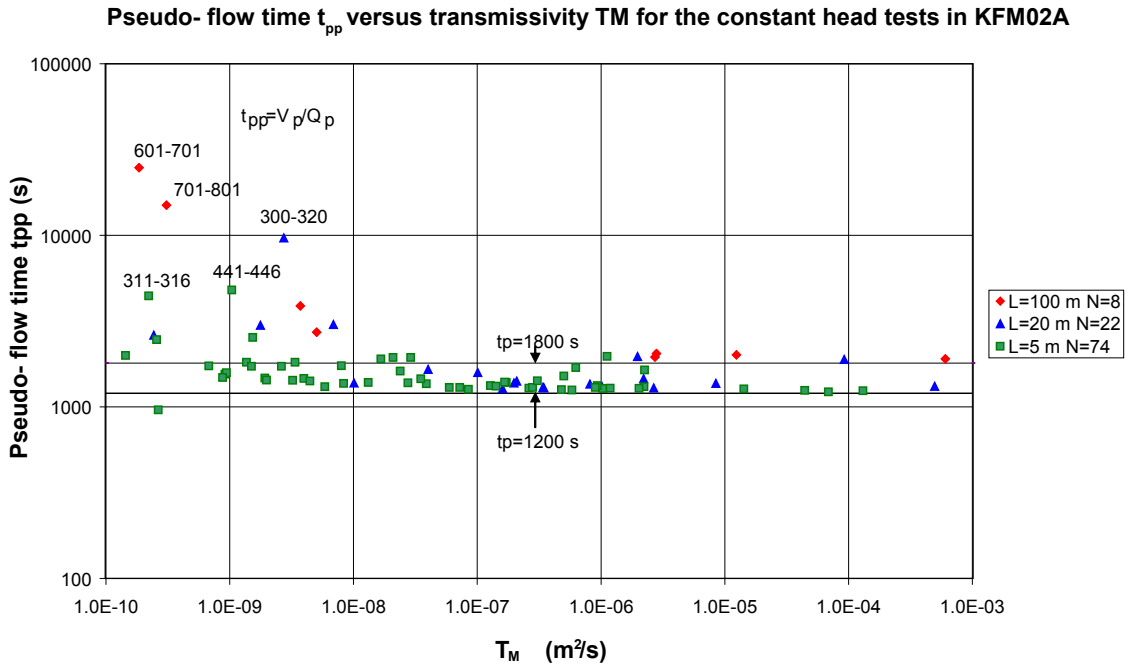

Figure A5-2. Calculated pseudo-flow time t_{pp} as function of calculated stationary transmissivity T_M for injection tests at constant head in KFM02A.

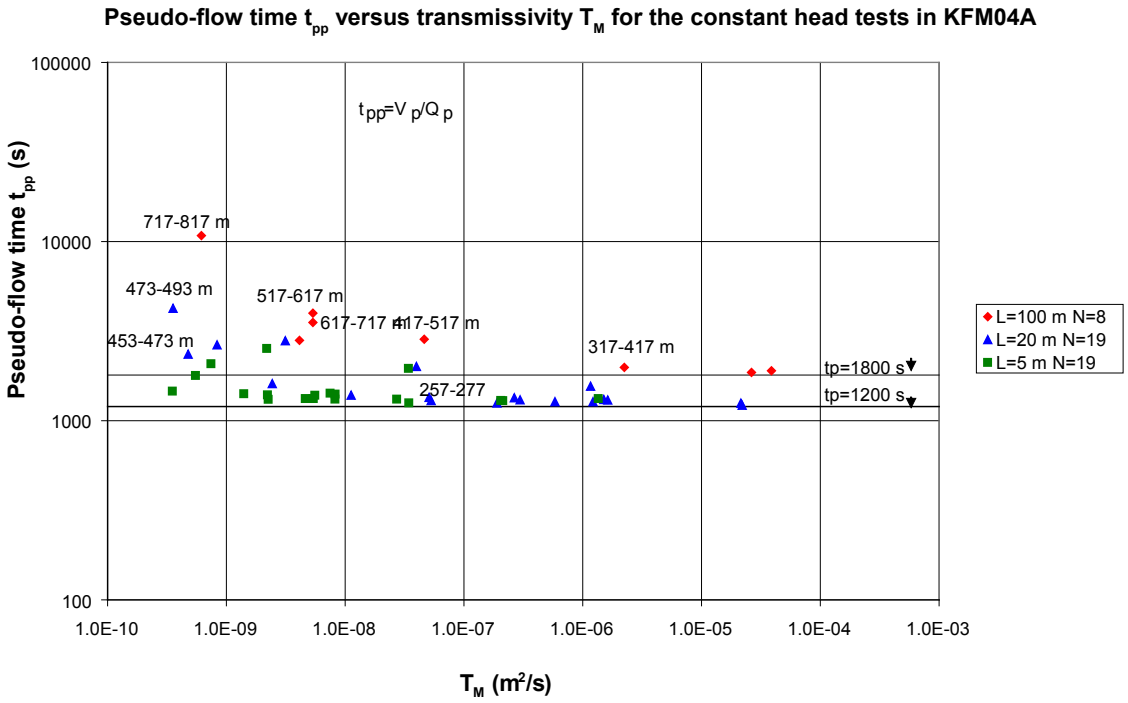

Figure A5-3. Calculated pseudo-flow time t_{pp} as function of calculated stationary transmissivity T_M for injection tests at constant head in KFM04A.

Table A5-1. Comparison between calculated pseudo-flow time t_{pp} and the actual flow time t_p for selected injection tests in KFM02A and KFM04A.

Borehole	Section (m)	Length (m)	Interpreted Qp (m^3/s)	Vp (m^3)	tp (s)	tpp (s)	tpp/tp	TM (m^2/s)
KFM02A	601–701	100	$5.00 \cdot 10^{-9}$	$1.24 \cdot 10^{-4}$	1,805	24,820	13.8	$1.85 \cdot 10^{-10}$
KFM02A	701–801	100	$5.83 \cdot 10^{-9}$	$8.73 \cdot 10^{-5}$	1,819	14,989	8.2	$3.08 \cdot 10^{-10}$
KFM02A	300–320	20	$5.21 \cdot 10^{-8}$	$5.04 \cdot 10^{-4}$	1,228	9,672	7.9	$2.73 \cdot 10^{-9}$
KFM02A	311–316	5	$1.06 \cdot 10^{-8}$	$4.68 \cdot 10^{-5}$	1,206	4,425	3.7	$2.22 \cdot 10^{-10}$
KFM02A	441–446	5	$4.39 \cdot 10^{-8}$	$2.10 \cdot 10^{-4}$	1,223	4,788	3.9	$1.04 \cdot 10^{-9}$
KFM04A	317–417	100	$3.94 \cdot 10–^{5}$	$7.83 \cdot 10^{-2}$	1,817	1,986	1.1	$2.24 \cdot 10^{-6}$
KFM04A	517–617	100	$1.20 \cdot 10^{-7}$	$4.78 \cdot 10^{-4}$	1,822	3,987	2.2	$5.34 \cdot 10^{-9}$
KFM04A	617–717	100	$8.41 \cdot 10^{-8}$	$2.97 \cdot 10^{-4}$	1,821	3,534	1.9	$5.36 \cdot 10^{-9}$
KFM04A	717–817	100	$9.00 \cdot 10^{-9}$	$9.70 \cdot 10^{-5}$	1,829	10,786	5.9	$6.16 \cdot 10^{-10}$
KFM04A	257–277	20	$9.95 \cdot 10^{-7}$	$1.34 \cdot 10^{-3}$	1,221	1,349	1.1	$5.08 \cdot 10^{-8}$
KFM04A	377–397	20	$1.82 \cdot 10^{-8}$	$4.83 \cdot 10^{-5}$	1,220	2,654	2.2	$8.34 \cdot 10^{-10}$
KFM04A	453–473	20	$1.00 \cdot 10^{-8}$	$2.35 \cdot 10^{-5}$	1,222	2,351	1.9	$4.76 \cdot 10^{-10}$
KFM04A	473–493	20	$7.56 \cdot 10^{-9}$	$3.21 \cdot 10^{-5}$	1,223	4,245	3.5	$3.55 \cdot 10^{-10}$

KFM02A: 601–701 m

Figure A5:1-1 in Sub-appendix A5:1 shows that the flow varied considerably at the beginning of the test in section 601–701 m leading to a greater injected volume (V_p) than expected (compare the simulated transient flow curve) and thereby a greater calculated value for t_{pp}. This is probably the explanation of the greater difference between t_{pp} and t_p in this case. However, t_{pp} is not considered representative in this case and is probably the result of practical difficulties in regulating the flow during the injection period and probably does not depend solely on hydraulic characteristics of the formation; compare simulated flow curve. For example it takes a volume of water of about 37 mL in a 100 m long test section to increase the pressure in the section by 200 kPa during the very first seconds when starting the injection, i.e. due to compressibility of the water and of the packers that limit the test section. After that a real flow will be obtained inside the formation in connection to the test section.

KFM02A: 701–801 m

Figure A5:1-2 shows that also for section 701–801 m there is a big difference between t_{pp} and t_p probably caused by an increased flow at the beginning of the test that can be related to problems in adjusting to a constant pressure. To test the sensitivity of the calculation for t_{pp} the test-data file (the ht2 file) for the test was modified by removing the first seven flow values in Figure A5:1-2 (about the first 15 s) after which the file was again converted in IPPLOT. This gave a new $V_p = 2.27 \cdot 10^{-5}\ m^3$ (previously $8.73 \cdot 10^{-5}\ m^3$) which with unchanged Q_p gives t_{ppcorr} = 3,900 s, i.e. about a fourth, see Table A5-1.

The subsequent analysis shows that t_{pp} (and V_p) are very sensitive to variations in flow at the beginning of the injection period, resulting from problems in adjusting to constant pressure. The corrected value of t_{pp} is considered more representative. It is however doubtful whether one should make such corrections of flow in the test evaluation.

KFM02A: 300–320 m

Figure A5:1-3 shows the transient flow curve during the injection period. The flow regime was interpreted as pseudo-spherical at the beginning with transition to an apparent negative hydraulic boundary (probably some sort of geometric limitation in the formation/fracture)

towards the end of the test. The same behaviour of the flow occurred during the corresponding test in the 5 m section 301–306 m but in that test the difference between t_{pp} and t_p was not so big. The final flow Q_p was interpreted as $5.21 \cdot 10^{-8}$ m^3/s (Table A5-1) although smaller flow was measured at the end.

In this case the difference between t_{pp} and t_p resulted mainly from characteristics of the formation (hydraulic boundary), rather than test-related causes. In this case it can be considered uncertain whether t_{pp} or t_p is most representative.

KFM02A: 311–316 m

Figure A5:1-4 shows the flow versus time during the injection period. It is probable that the relatively big difference between t_{pp} and t_p was caused by the large variations in flow at the beginning of the injection period that were probably related to problems in adjusting to constant pressure. Accordingly, t_p is judged as most representative for this test.

KFM02A: 441–446 m

Figure A5:1-5 shows the flow versus time during the injection period. Also in this test it is probable that the difference between t_{pp} and t_p was caused mainly by the large variations in flow at the beginning of the injection period that were probably related to problems in adjusting to constant pressure. Accordingly, t_p is judged as most representative for this test.

KFM04A: 317–417 m

Figure A5:1-6 shows the flow versus time during the injection period. This is a high-transmissive section. The difference between t_{pp} and t_p is rather small and is probably caused by variations in flow at the beginning of the injection period in connection with adjusting to constant pressure. The multi-rate assumption has also been considered for this test, see Chapter 3.

KFM04A: 617–717 m

Figure A5:1-7 shows the flow versus time during the injection period. This is a low-transmissive section. Also in this test it is probable that the difference between t_{pp} and t_p was caused mainly by the large variations in flow at the beginning of the injection period in connection with adjusting to constant pressure. Accordingly, t_p is judged as most representative for the test. The multi-rate assumption has also been considered for this test, see Chapter 3.

KFM04A: 257–277 m

Figure A5:1-8 shows the flow versus time during the injection period. This is a medium-transmissive section. The difference between t_{pp} and t_p is rather small and is probably caused by variations in flow at the beginning of the injection period in connection with adjusting to constant pressure. The multi-rate assumption has also been considered for this test, see Chapter 3.

KFM04A: 517–617 m, 717–817 m, 377–397 m, 453–473 m and 473–493 m

Figure A5:1-9-13 shows the flow versus time during the injection period for these sections. The difference between t_{pp} and t_p is probably caused by variations in flow at the beginning of the injection period in connection with adjusting to constant pressure.

A5.3 Comparison of evaluated hydraulic parameters in the different ways of determining Agarwal equivalent time

Of the sections in Table A5-1, three sections were selected in KFM04A for quantitative evaluation of hydraulic parameters from the recovery period in the three different ways for calculating the Agarwal equivalent time on the time scale according to Equation (1a-c). One high-transmissive section (KFM04A: 317–417 m), one medium-transmissive section (KFM04A: 257–277 m) and one low-transmissive section (KFM04A: 617–717 m) were selected. The transient interpretations of these sections are shown in Sub-appendix A5:2. The results of interpretation of the tests are presented in Table A5-2. The interpretation is based mainly on models for radial flow with effects of wellbore storage (WBS) and skin according to Instructions for analysis of injection and single-hole pump tests (SKB MD 320.004). The present report does not deal with interpretation of models for fractional flow. In analyses of most tests in this report the storage coefficient S is assumed as $1.0 \cdot 10^{-6}$.

The intention is that the tests shall illustrate possible differences in calculating hydraulic parameters from transient evaluation of the recovery period for these tests for different ways of calculating the Agarwal equivalent time. As comparison the results of interpretation of the injection period are also presented. All tests are shown in log-log diagrams.

For the above-mentioned tests three optional recovery diagrams are presented in Sub-appendix A5:2 with Agarwal equivalent time calculated in different ways:

- based on t_p = duration of the injection period according to Equation (1a),
- based on $t_{pp} = V_p/Q_p$ according to Equation (1b),
- based on the multi-rate approximation according to Equation (1c).

The diagrams with the Agarwal time based on t_p on the time axis (Agarwal Equivalent Time_tp) are presented at the top and based on t_{pp} (Agarwal Equivalent Time_tpp) in the centre of the page while the Agarwal time based on the multi-rate assumption (Agarwal Equivalent Time_m-rate) is presented at the bottom of the page in the diagrams in Sub-appendix A5:2 for direct comparison.

For calculation of the hydraulic parameters to be as objective as possible an automatic curve matching according to non-linear regression was made in AqteSolv of the recovery period in all the tests. The same convergence criteria for matching have been used in all the tests. Table A5-1 shows that interpretation of the recovery period for both of the two first tests (high-transmissive and medium-transmissive respectively) are mainly identical, regardless of whether the Agarwal time is based on t_{pp} or t_p or multi-rate. The small differences in calculated parameters can be regarded as insignificant. Accordingly, in these two cases it is of no practical significance which of the three ways that the Agarwal time for the recovery period is based on. However, for the low-transmissive section 617–717 m in KFM04A a somewhat bigger difference is obtained for calculated parameters in the different ways of calculating the Agarwal time for the recovery and even from the injection period.

As indicated by the measured transient flow curves during the injection period of the respective section (and comparison with simulated flow curves) the difference in calculated parameters from the various recovery curves is probably caused by varying flow at the beginning of the injection period while adjusting to constant pressure in the section; see corresponding flow curves in Sub-appendix A5:1. This has the greatest significance in low-transmissive sections.

Table A5-2. Comparison of calculation of hydraulic parameters from the recovery period for selected injection tests in KFM04A in different ways of calculating the Agarwal time. Interpreted parameters from the injection period are also shown as comparison.

Borehole	Section (m)	Parameter	Parameter calculated from test period/method			
			Injection	Rec_tp	Rec_tpp	Rec_m–rate
KFM04A	317–417	T (m^2/s)	$2.0 \cdot 10^{-6}$	$3.77 \cdot 10^{-6}$	$3.81 \cdot 10^{-6}$	$3.86 \cdot 10^{-6}$
		S* (–)	$1.0 \cdot 10^{-6}$	$1.0 \cdot 10^{-6}$	$1.0 \cdot 10^{-6}$	$1.0 \cdot 10^{-6}$
		Skin	–0.54	4.84	4.98	5.09
		rw (m)	0.0385	0.0385	0.0385	0.0385
		rc (m)	–	–	–	–
		C (m^3/Pa)*	–	–	–	–
KFM04A	257–277	T (m^2/s)	$4.89 \cdot 10^{-8}$	$4.01 \cdot 10^{-8}$	$4.10 \cdot 10^{-8}$	$4.13 \cdot 10^{-8}$
		S* (–)	$1.0 \cdot 10^{-6}$	$1.0 \cdot 10^{-6}$	$1.0 \cdot 10^{-6}$	$1.0 \cdot 10^{-6}$
		Skin	0.6	–0.17	–0.10	–0.08
		rw (m)	0.0385	0.0385	0.0385	0.0385
		rc (m)	–	0.0006077	0.0006115	0.0006122
		C (m^3/Pa)	–	$1.2 \cdot 10^{-10}$	$1.2 \cdot 10^{-10}$	$1.2 \cdot 10^{-10}$
KFM04A	617–717	T (m^2/s)	$8.95 \cdot 10^{-10}$	$2.24 \cdot 10^{-10}$	$6.03 \cdot 10^{-10}$	$5.44 \cdot 10^{-10}$
		S* (–)	$1.0 \cdot 10^{-6}$	$1.0 \cdot 10^{-6}$	$1.0 \cdot 10^{-6}$	$1.0 \cdot 10^{-6}$
		Skin	–2.92	–3.20	–3.09	–3.61
		rw (m)	0.0385	0.0385	0.0385	0.0385
		rc (m)	–	0.00110	0.00107	0.00102
		C (m^3/Pa)	–	$3.9 \cdot 10^{-10}$	$3.7 \cdot 10^{-10}$	$3.3 \cdot 10^{-10}$

* No representative value for r_c can be obtained in high-transmissive test sections.

Rec_t_p = calculated from the recovery period with Agarwal time based on t_p.

Rec_t_{pp} = calculated from the recovery period with Agarwal time based on t_{pp}.

Rec_m-rate = calculated from the recovery period with Agarwal time based on the multi-rate approach.

A5.4 Specific characteristics for the Agarwal multi-rate method

For the injection tests in KFM05A, KFM06A and KFM07A the Agarwal equivalent time calculated according to the multi-rate assumption has been examined more routinely and compared with the Agarwal time based on t_p. Some experience of these tests is described below and shown in Sub-appendix A5:3.

A5.4.1 Varying flow at the beginning of the injection period

The Agarwal equivalent time based on the multi-rate assumption according to Equation (1c) is also influenced by variations in flow at the beginning of the injection period while adjusting to constant pressure in the test section. An example of a low-conductive section (KFM06A: 805–905 m) in which the flow varies at the beginning of the injection period (about 30 s) is shown in Figures A5:3-1-4 in Sub-appendix A5:3. Figure A5:3-1 and A5:3-2 show measured flow during the injection period and the subsequent pressure recovery based on the multi-rate assumption (Agarwal_mrate). The Figures A5:3-3 and A5:3-4a show two corresponding plots in which the two highest flow values (c $1 \cdot 10^{-5}$ m^3/s) at the beginning of the injection period are deleted because they were probably caused by adjusting to constant pressure in the section, compare Figure A5:3-1 and A5:3-3. Deleting these two flow values results in a slight change in the recovery curve, compare Figure A5:3-2 and A5:3-4a. Automatic matching of the recovery curve now gave T = $1.74 \cdot 10^{-10}$ m^2/s compared to T = $3.44 \cdot 10^{-10}$ m^2/s, i.e. factor two lower.

The above test was performed using a pressure vessel instead of the automatic pressure regulating system. Bigger variations in the flow usually occur at the beginning of the injection period in tests performed using the later system. Especially in tests at great depth it is however doubtful whether these initial flow values (measured at ground level) are relevant for the section down at great depth (it is probable that flow evens out in the test section).

Figure A5:3-4b shows a corresponding interpretation of the recovery period but plotted versus the Agarwal time based on t_p according to Equation (1a) instead of multi-rate. The problem of varying flow during the injection period is thus avoided but no distinct automatic matching of the recovery period could be made in this case. The interpretation in the figure is shown as an example only.

The preceding example shows that the appearance of the flow curve at the beginning of the injection period has some significance for Agarwal_mrate and accordingly interpreted parameters from the recovery period. It is however uncertain which of the interpretations in Figure A5:3-2 and A5:3-4a respectively is most relevant. It depends mainly on whether the changes in flow registered at ground level (e.g. during adjustment to constant pressure) are assumed to be transmitted instantaneously to the test section which sometimes lies at great depth and the effect that deviating values of flow at the beginning of the injection period can be assumed to have in practice on the recovery sequence (through the principle of superposition).

In the interpretation principle used in Figure A5:3-4a it may be necessary to correct certain flow values at the beginning of the injection period that are judged as non-representative for the test section, before interpreting the recovery period based on the multi-rate assumption. Alternatively the interpretation in Figure A5:3-2 is chosen, based on the original flow curve. A third option is to use Agarwal_tp based on manual interpretation according to Figure A5:3-4b with increased uncertainty regarding its representativeness. The disadvantage of this option is that no unambiguous calculation of the hydraulic parameters can be made in this case. The interpretation shown in Figure A5:3-4b is only an example of possible interpretation.

A5.4.2 Varying flows at the end of the injection period

The Agarwal time based on the multi-rate assumption according to Equation (1c) is also sensitive to variations in flow at the end of the injection period, especially if the final flow value deviates somewhat from the interpreted final flow Q_p, compare Equation (1c). An example of this is shown for section 617–717 m in KFM04A. In the original data file for flow during the injection period the final flow value ($6.6 \cdot 10^{-8}$ m^3/s) deviates moderately from the interpreted stable final flow $Q_p = 8.4 \cdot 10^{-8}$ m^3/s, see Figure A5:1-7. To test sensitivity of the Agarwal time the final flow value was deleted from the data file. The recovery diagrams with Agarwal time according to the multi-rate assumption based on the original and on the modified flow curve respectively are shown in the Figures A5:3-5 and A5:3-6 in Sub-appendix A5:3. The figures indicate that removal of the final flow value has significant influence on the shape of the recovery curve based on Agarwal time according to the multi-rate assumption (the time scale changes) and also some influence on evaluation of hydraulic parameters from the curve. On the other hand the Agarwal time based on t_p and t_{pp} respectively are not affected by removing the final flow value.

This example shows that Agarwal time calculated according to the multi-rate assumption can be very sensitive to changes in flow at the end of the injection period, regardless of whether these are representative for the test or simply caused by normal fluctuations (noise) in the recording of flow that occur at low rates of flow. It is therefore recommended that some form of flow data smoothing should be made towards the end of the injection period,e.g. by always allowing the final flow value in the data file to be the same as the interpreted value of the final flow Q_p.

A5.4.3 Interpreting flow regimes

On comparing recovery plots with Agarwal time based on t_p or the multi-rate assumption it is evident that the curves can sometimes appear different in shape (the multi-rate curve becomes more extended in time). This occurs particularly in tests in very low-transmissive sections where full recovery of the pressure is not attained during the recovery period. This implies that the interpretation of flow regimes as well as evaluation of hydraulic parameters from the recovery period can be different in such cases. It appears as if the curve based on t_p maintains the classical curve shape better, i.e. WBS has slope 1:1, etc, which does not always apply for the multi-rate curve in very low-transmissive sections. However, when evaluating hydraulic parameters a better apparent matching is obtained with the latter curve. In low-transmissive sections no distinct matching can normally be obtained from the recovery curve based on t_p due to strong influence of WBS and consequently no unambiguous calculation of the hydraulic parameters. Even the results based on the multi-rate assumption are also considered uncertain in such cases.

The first example is from the injection test in KFM05A:436.5–456.5 m which is a very low-transmissive section. Interpretation of the injection period is shown in Figure A5:3-8. Matching was made on the first part of the curve because an apparent no-flow boundary (NFB) is assumed to influence the later part of the curve. The stationary transmissivity T_M is calculated as $3.9 \cdot 10^{-10}$ m^2/s. Even if the flow varies somewhat towards the end of the injection period the Agarwal time, based on the multi-rate assumption, is fairly stable. Figure A5:3-9a shows the recovery based on Agarwal_t_p and Figure A5:3-9b based on Agarwal_multi-rate (m-rate). The pressure recovery reaches only about 5 m of the applied injection pressure at about 20 m. The previous curve maintains more the characteristic 1:1 slope feature of WBS while the curve based on multi-rate is more extended in time and there is no marked 1:1 slope at the beginning. Reasonable automatic matching and calculations of hydraulic parameters are obtained both with the t_p and with the multi-rate assumption but the matching will normally be better with multi-rate. No unambiguous matching can usually be obtained with the Agarwal_t_p-curve in low-transmissive sections that are dominated by WBS.

The second example shows a test in KFM06A: 310.5–315.5 m that is very difficult to interpret. The Figures A5:3-10 and A5:3-11 show flow and pressure/flow-rate curves respectively for the injection period. These imply that apparent hydraulic boundaries (no-flow boundary, NFB) dominate this period. The stationary transmissivity is calculated as $T_M = 3.3 \cdot 10^{-9}$ m^2/s. The difference flow logging in KFM06A showed that no conductive fractures with measurable flow could be detected in this section /Rouhiainen and Sokolnicki, 2005/. No representative transient interpretation of the injection period can be made. In the Figures A5:3-10-11 simulated curves have been included based on approximated hydraulic parameters from the recovery period to enable comparison.

The Figures A5:3-12a-b show recovery with Agarwal time based on t_p and on multi-rate assumption respectively for this section. The figures show that only about 1 m of the applied injection head of about 20 m is recovered, which may imply a very low-transmissive section or alternatively, a flow anomaly of limited extent. The recovery curves in these two figures are of a completely different appearance and the flow regimes can be interpreted quite differently in the two figures. The curve in Figure A5:3-12a is dominated completely by WBS while the curve in Figure A5:3-12b indicates an apparent transition to pseudo-radial flow (PRF) at the beginning followed by a possible apparent NFB at the end. No distinct matching can be obtained from the curve in Figure A5:3-12a while an apparently relatively distinct matching can be obtained from the curve in Figure A5:3-12b. The evaluated hydraulic parameters are however probably not representative for the test due to little recovery. Results of matching from the later figure had been entered in Figure A5:3-12a for comparison.

A5.5 Conclusions

This study of results from the injection tests with PSS in boreholes at Forsmark shows primarily that the calculated values for the pseudo-flow time t_{pp} from IPPLOT in most of the cases are representative, on condition that the final flow Q_p is controlled and judged as being representative in each test. The calculation of the pseudo-flow time as $t_{pp} = V_p/Q_p$ is however sensitive to variations

of flow, e.g. while adjusting to constant pressure at the beginning of the tests. This can lead to the calculated, total injected volume of water V_p not being representative for the test and consequently not t_{pp} either. This applies especially for tests in low-conductive sections where large variations of flow can occur at the beginning. Even variations of flow towards the end of the injection period can influence the pseudo-flow time and lead to big differences between t_p and t_{pp} in such sections. Formation characteristics (e.g. effects of apparent negative hydraulic boundaries) can in certain cases also result in large changes of flow and differences between calculated t_{pp} and t_p.

The uncertainty in calculated t_{pp} increases usually for tests in low-conductive sections. Fairly low difference is obtained between calculated t_{pp} and actual flow time t_p for tests in sections with T_M > about $1 \cdot 10^{-8}$ m^2/s. This difference probably lacks practical significance in most cases when calculating Agarwal equivalent time and the calculation of hydraulic parameters from the recovery, i.e. t_p can probably be used equally well as t_{pp} when evaluating tests in such sections.

However, for sections where T_M < about $1 \cdot 10^{-8}$ m^2/s relatively big differences can be obtained between calculated t_{pp} and actual t_p. In most cases the difference is probably caused by large variations in flow while adjusting to constant pressure at the beginning of the test. In such cases the actual flow time t_p is usually judged as being more robust and representative than t_{pp} in calculating hydraulic parameters from this period and also simpler than the pseudo-flow time t_{pp}.

Routine calculation of the Agarwal time with multi-rate assumption and comparison with Agarwal time based on t_p was made in the normal interpretation of the tests in boreholes KFM05A, KFM06A and KFM07A. Favourable correspondence between evaluated hydraulic parameters was obtained from both of the methods. However, differences can occur in the results from low-conductive sections, both with regard to calculation of hydraulic parameters and with regard to interpretation of flow regimes.

Based on the results from these boreholes it is recommended that the Agarwal equivalent time is calculated routinely according to the multi-rate assumption for analysis of recovery following tests at constant pressure. This assumption presupposes that the existing changes of flow at the beginning of the injection period, e.g. by building up to constant pressure, influence the subsequent recovery procedure (principle of superposition). Moreover, it is assumed that changes in flow (that are measured at ground level) are transmitted instantaneously to the borehole section being tested. Some delay and evening out of the flow can however occur in test sections at great depth. Ideally the flow should be measured in the test section like the pressure.

The Agarwal equivalent time calculated according to the multi-rate assumption can be very sensitive to changes in the rate of flow both at the beginning and at the end of the injection period, regardless of whether these are representative for the test or resulting from adjusting to constant pressure or normal fluctuations in recording of flow (noise) that normally occur at low rates of flow. It is recommended therefore that some form of flow data smoothing should be made, especially towards the end of the injection period and by always allowing the final flow value in the data file to be the same as the interpreted value of the final flow Q_p.

However, in very low-conductive sections (T_M < about $1–5 \cdot 10^{-9}$ m^2/s) the actual flow time t_p should also be used as comparison and control when calculating the Agarwal equivalent time. In such sections the shape of the recovery curve can change in the multi-rate assumption which could result in a different interpretation of transient flow regimes and calculations of hydraulic parameters from this curve. This can occur especially in sections where low recovery of the applied injection pressure is achieved during the recovery period.

Approximate methods based on Agarwal equivalent time or Horner time can be uncertain in low-conductive sections. In thorough transient analysis of such tests the exact analytical solutions of the recovery period following tests at constant pressure should therefore be used e.g. /Ehlig-Economides and Ramey, 1981/. It is however not known whether such software is commercially available. Furthermore, the question is whether or not the interpretation due to other factors,e.g. well-bore storage effects, skin effects, etc, limits the usefulness of this option too much for tests in very low-conductive sections.

A5.6 References

Agarwal R G, 1980. A new method to account for producing time effects when drawdown type curves are used to analyze pressure buildup and other test data. Soc. Pet. Eng. Paper 9289.

Ehlig C A, Ramey Jr H J, 1981. Pressure buildup for wells produced at a constant pressure. Soc. Pet. Eng. J., Feb. 1981, pp 105–114.

Earlougher R C Jr, 1977. Advances in well test analysis. Monogr. Ser, vol. 5, Soc. Petrol. Engrs, Dallas, 1977.

Gokall-Norman K, Ludvigson J-E, Hjerne C, 2005. Single-hole injection tests in borehole KFM05A. Forsmark site investigation. SKB P-05-56, Svensk Kärnbränslehantering AB.

Gokall-Norman K, Svensson T, Ludvigson J-E, 2005. Single-hole injection tests in borehole KFM07A. Forsmark site investigation. SKB P-05-133, Svensk Kärnbränslehantering AB.

Hjerne C, Ludvigson J-E, 2005. Single-hole injection tests in borehole KFM04A. Forsmark site investigation. SKB P-04-293, Svensk Kärnbränslehantering AB.

Hjerne C, Ludvigson J-E, Lindquist A, 2005. Single-hole injection tests in boreholes KFM06A and KFM06B. Forsmark site investigation. SKB P-05-165, Svensk Kärnbränslehantering AB.

Källgården J, Ludvigson J-E, Jönsson J, 2004. Single-hole injection tests in borehole KFM02A. Forsmark site investigation. SKB P-04-100, Svensk Kärnbränslehantering AB.

Rouhiainen P, Sokolnicki M, 2005. Difference flow logging in borehole KFM06A. Forsmark site investigation. SKB P-05-15, Svensk Kärnbränslehantering AB.

Rosato N D, Bennet C O, Reynolds A C, Raghavan R, 1982. Analysis of short-time buildup data for finite-conductivity fractures. J. Pet.Tech., Oct. 1982, pp 2413–2422.

Uraiet A A, Raghavan R, 1980. Pressure buildup analysis for a well produced at constant bottomhole pressure. J. Pet. Tech., Oct. 1980, pp 1813–1824.

Sub-appendices

Test data diagrams

Sub-appendix A5:1. Discharge versus time in selected sections in KFM02A and KFM04A.

Sub-appendix A5:2. Head/flow rate versus time and recovery versus Agarwal equivalent time based on tp and tpp, respectively in selected sections in KFM04A.

Sub-appendix A5:3. Head/flow rate versus time and recovery versus Agarwal equivalent time based on tp, tpp and multi-rate, respectively in selected sections in KFM05A and KFM06A.

Nomenclature in AQTESOLV in the test data diagrams:

T = transmissivity (m^2/s).

S = storativity (–)

K_z/K_r = ratio of hydraulic conductivities in the vertical and radial direction (set to 1).

Sw = skin factor.

r(w) = borehole radius (m).

r(c) = effective casing radius or radius of fictive standpipe (m).

r/B = leakage factor (–).

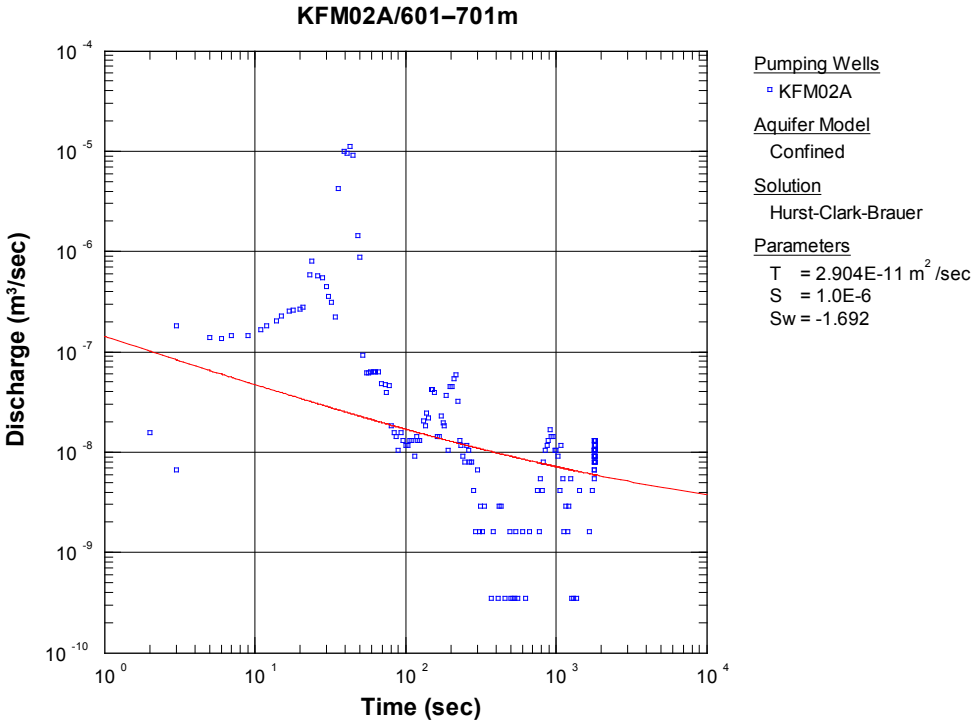

Figure A5:1-1. *Flow rate (blue) versus time during the flow period in section 601–701 m in KFM02A together with simulated flow rate (red) based on the evaluated hydraulic parameters from this period.*

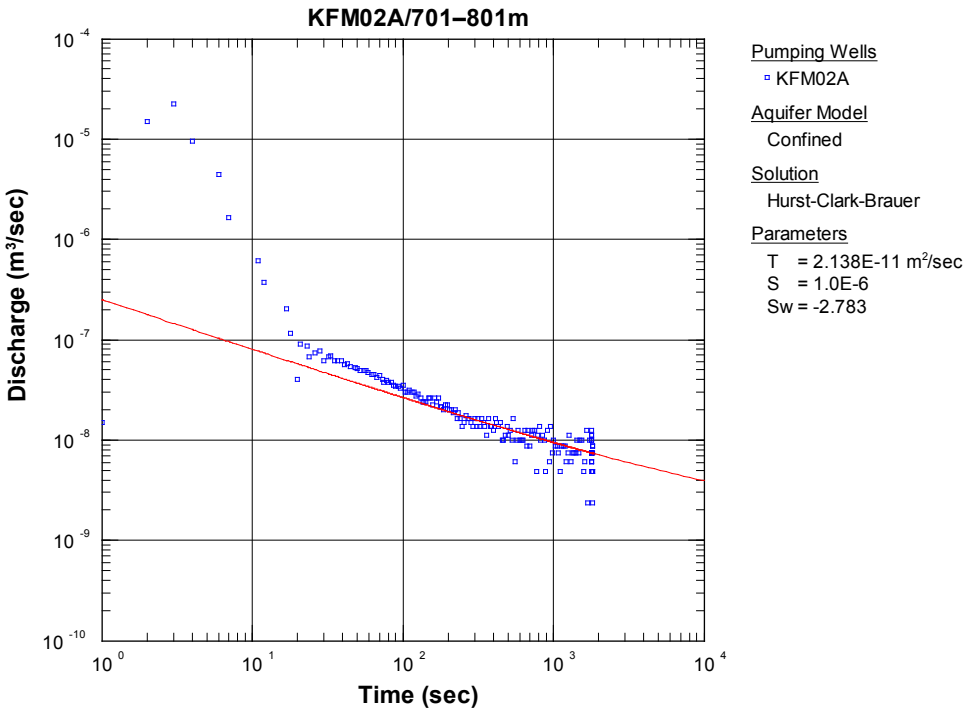

Figure A5:1-2. *Flow rate (blue) versus time during the flow period in section 701–801 m in KFM02A together with simulated flow rate (red) based on the evaluated hydraulic parameters from this period.*

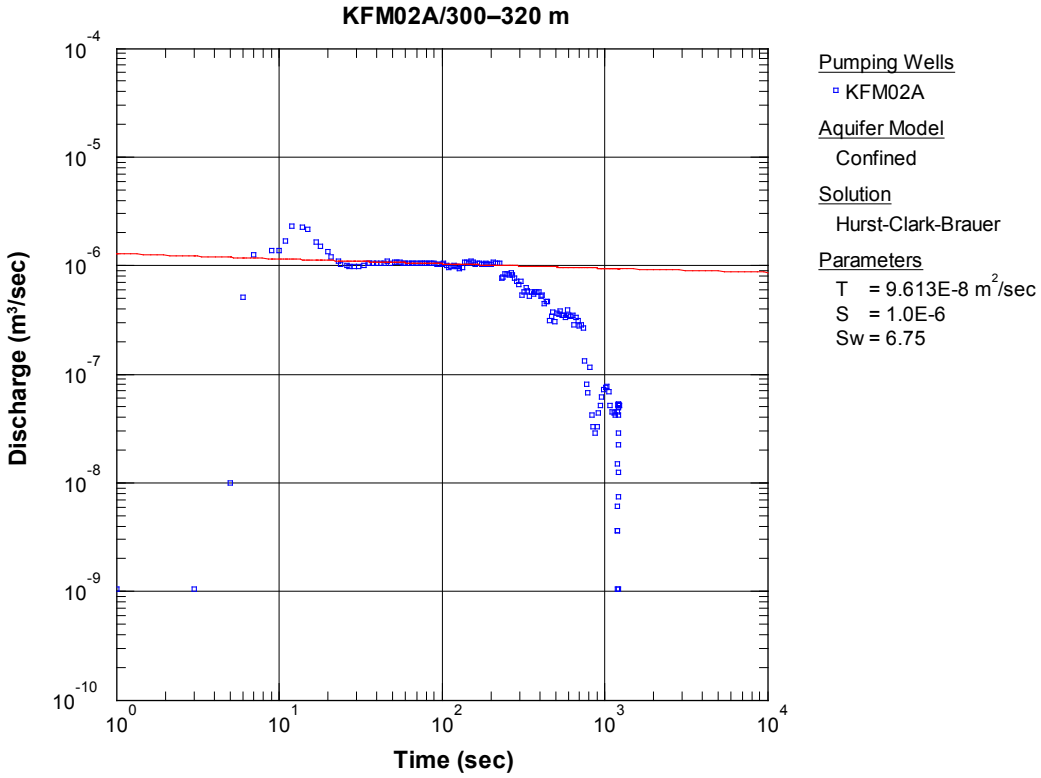

Figure A5:1-3. *Flow rate (blue) versus time during the flow period in section 300–320 m in KFM02A together with simulated flow rate (red) based on the evaluated hydraulic parameters from this period.*

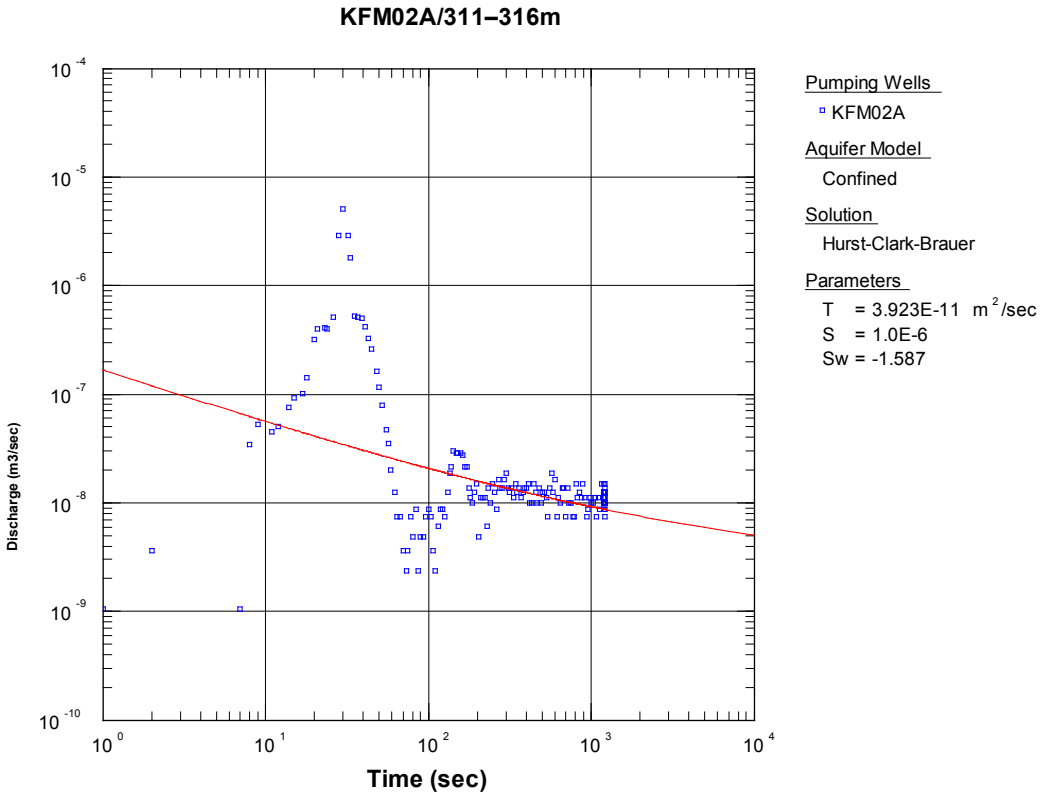

Figure A5:1-4. *Flow rate (blue) versus time during the flow period in section 311–316 m in KFM02A together with simulated flow rate (red) based on the evaluated hydraulic parameters from this period.*

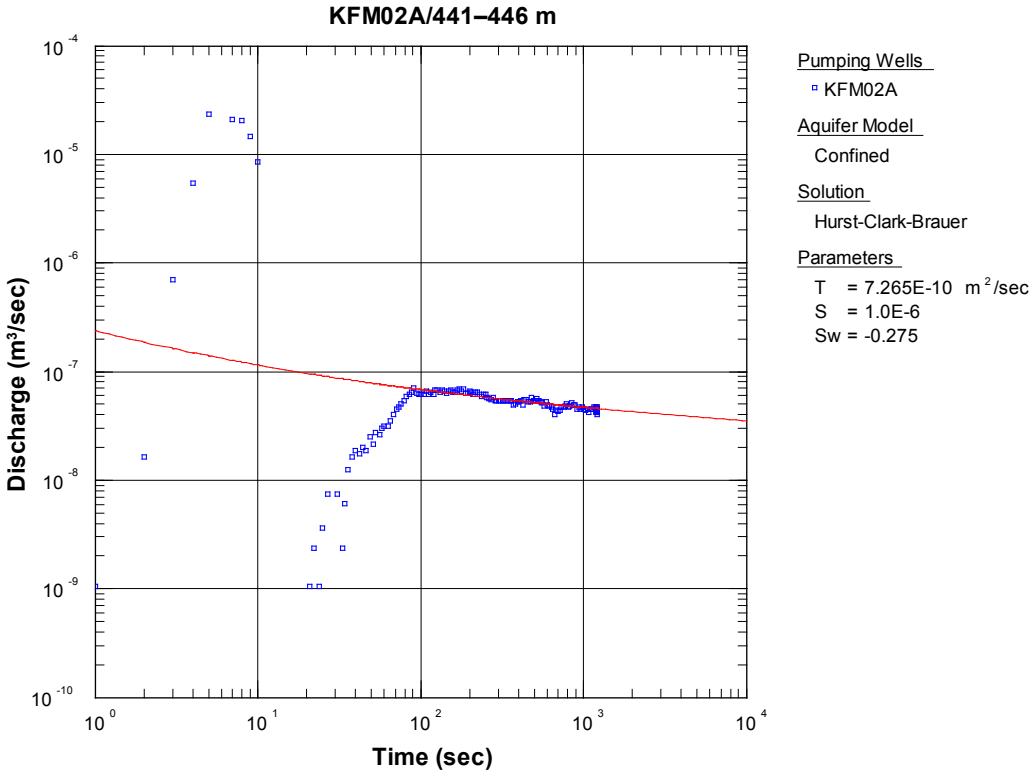

Figure A5:1-5. *Flow rate (blue) versus time during the flow period in section 441–446 m in KFM02A together with simulated flow rate (red) based on the evaluated hydraulic parameters from this period.*

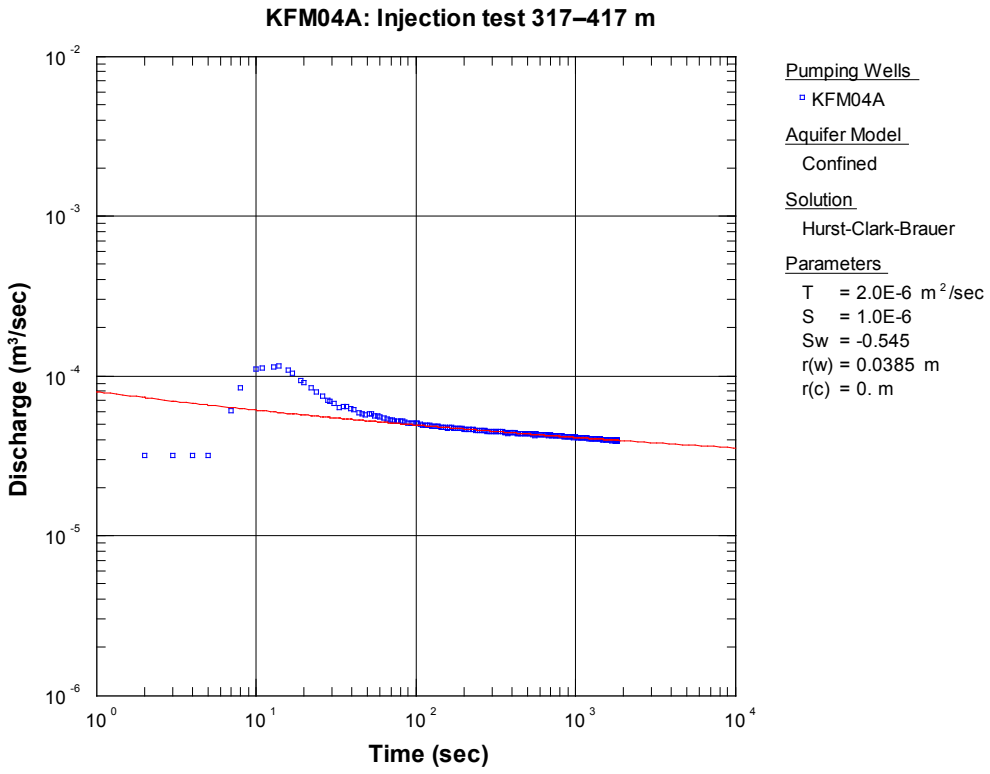

Figure A5:1-6. *Flow rate (blue) versus time during the flow period in section 317–417 m in KFM04A together with simulated flow rate (red) based on the evaluated hydraulic parameters from this period.*

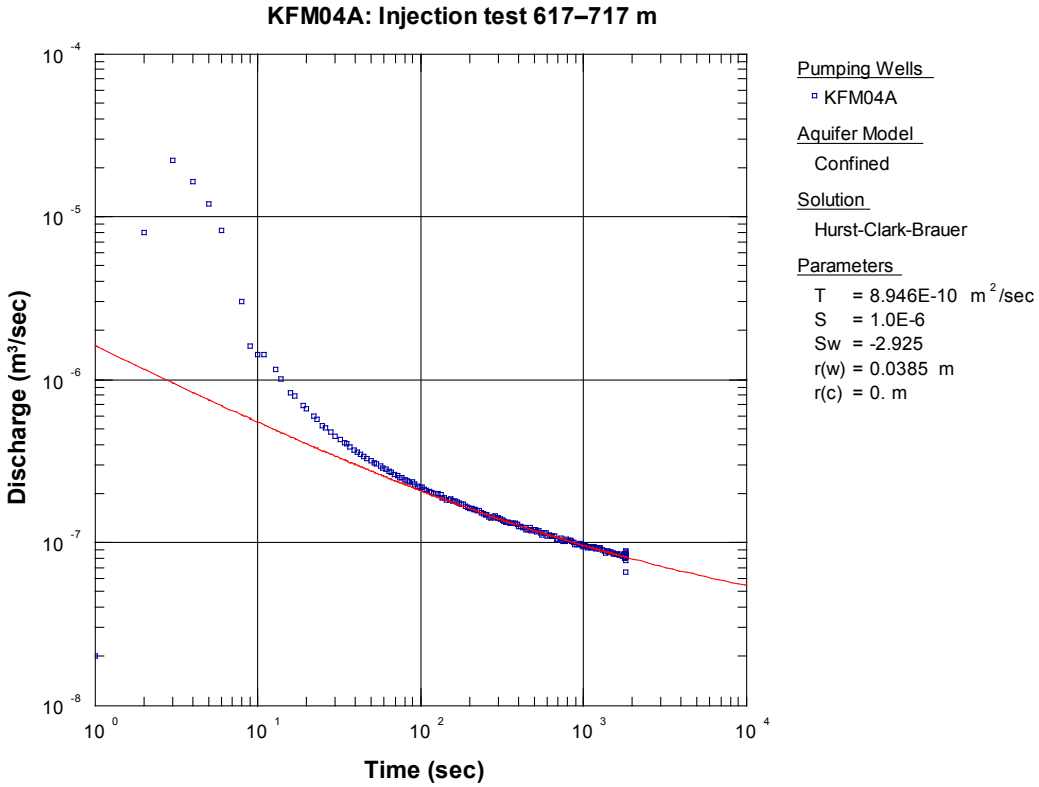

Figure A5:1-7. *Flow rate (blue) versus time during the flow period in section 617–717 m in KFM04A together with simulated flow rate (red) based on the evaluated hydraulic parameters from this period.*

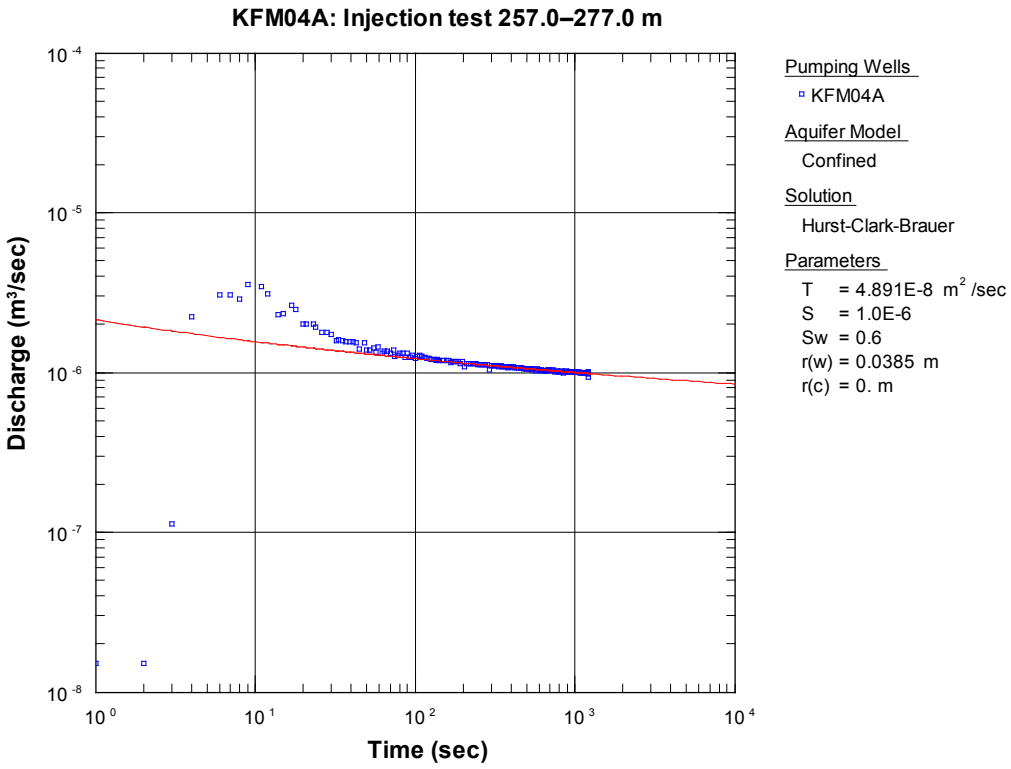

Figure A5:1-8. *Flow rate (blue) versus time during the flow period in section 257–277 m in KFM04A together with simulated flow rate (red) based on the evaluated hydraulic parameters from this period.*

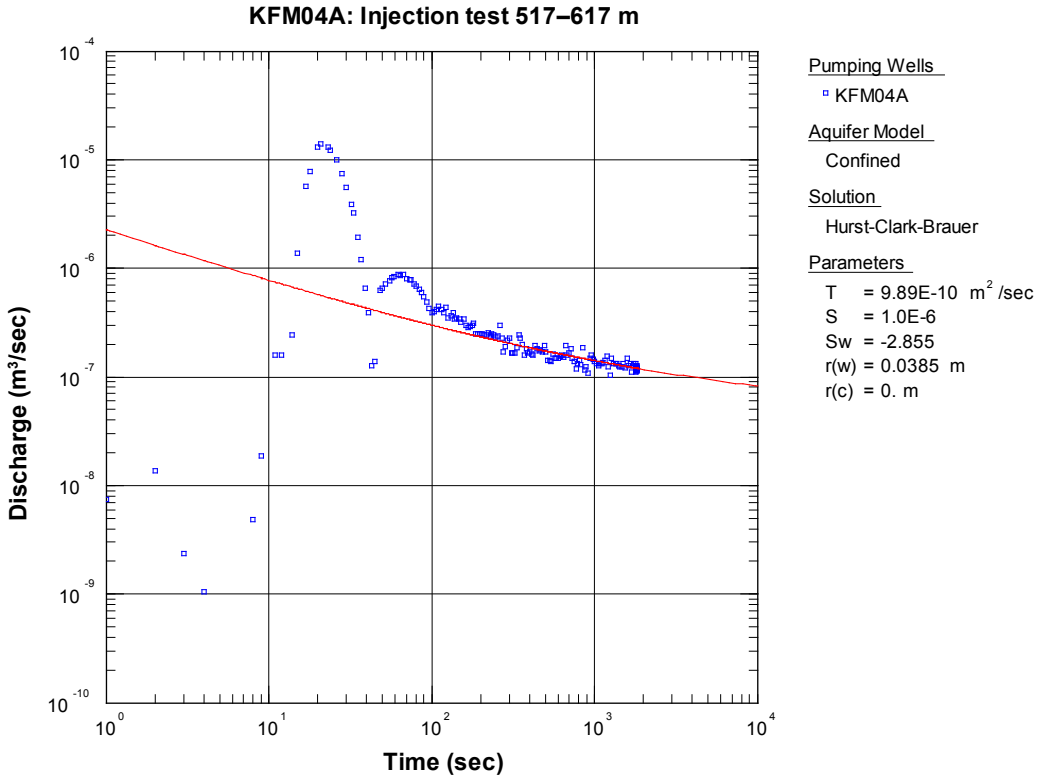

Figure A5:1-9. *Flow rate (blue) versus time during the flow period in section 517–617 m in KFM04A together with simulated flow rate (red) based on the evaluated hydraulic parameters from this period.*

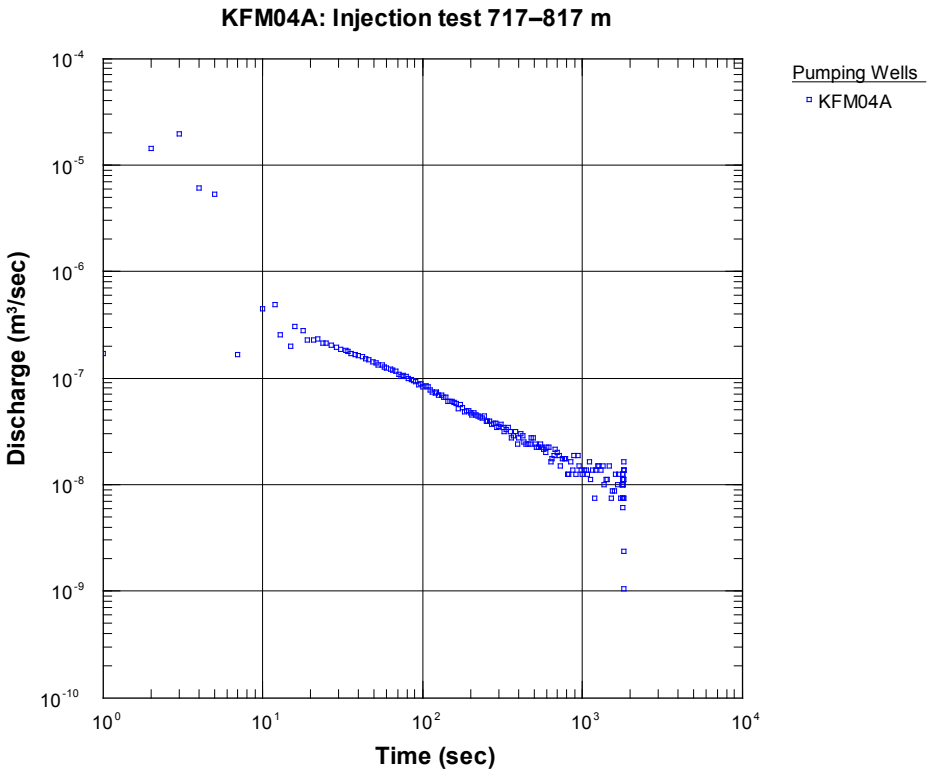

Figure A5:1-10. *Flow rate (blue) versus time during the flow period in section 717–817 m in KFM04A. No transient evaluation was made in this section.*

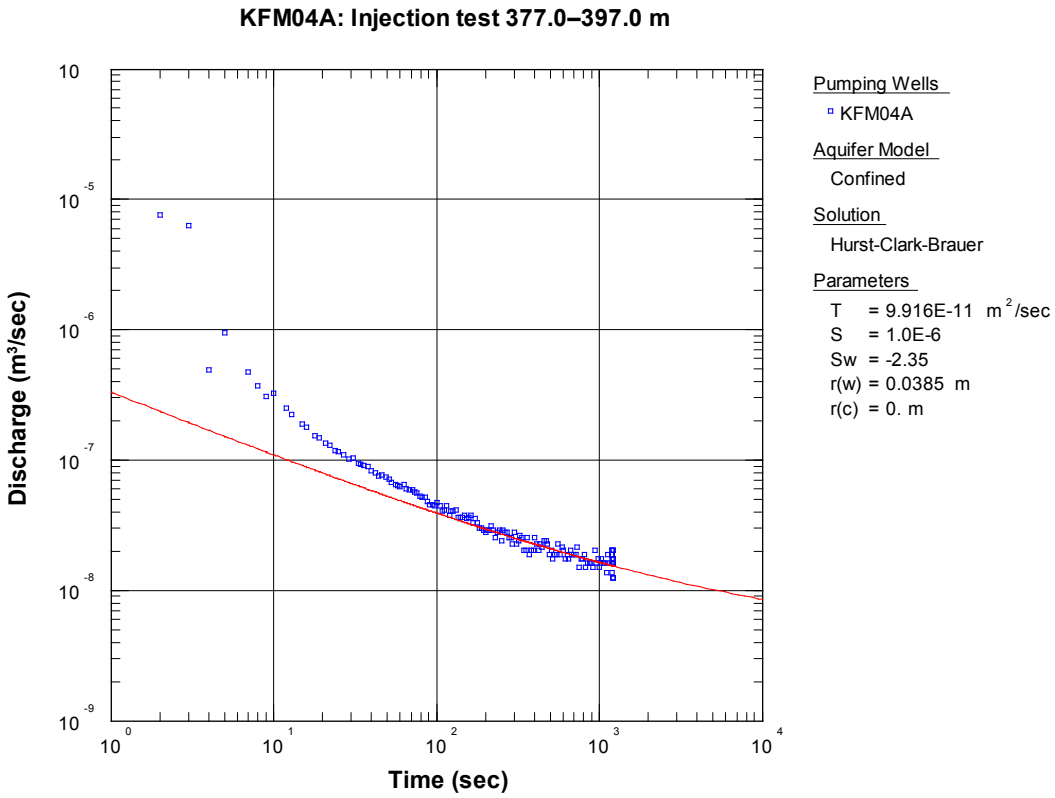

Figure A5:1-11. *Flow rate (blue) versus time during the flow period in section 377–397 m in KFM04A together with simulated flow rate (red) based on the evaluated hydraulic parameters from this period.*

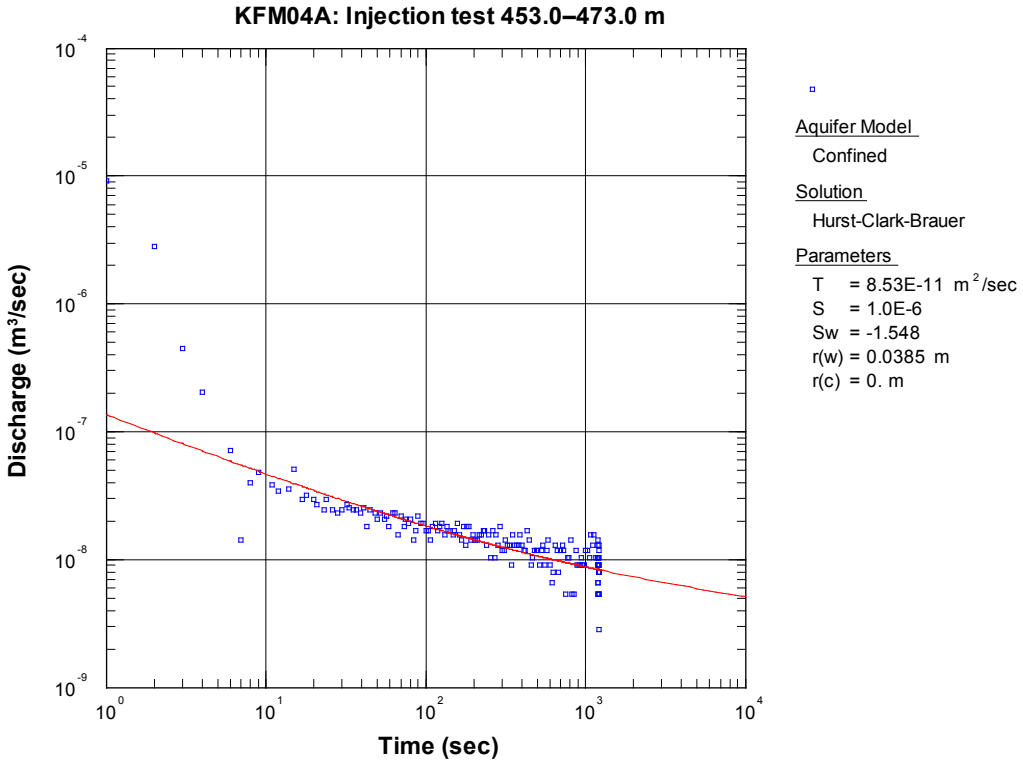

Figure A5:1-12. *Flow rate (blue) versus time during the flow period in section 453–473 m in KFM04A together with simulated flow rate (red) based on the evaluated hydraulic parameters from this period.*

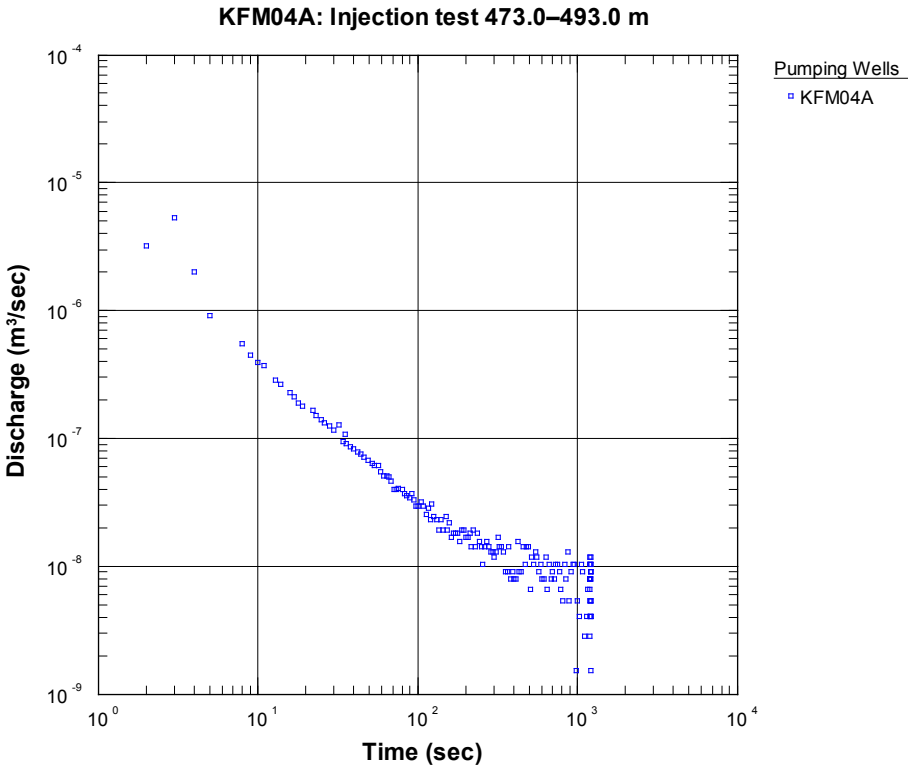

Figure A5:1-13. *Flow rate (blue) versus time during the flow period in section 473–493 m in KFM04A. No transient evaluation was made in this section.*

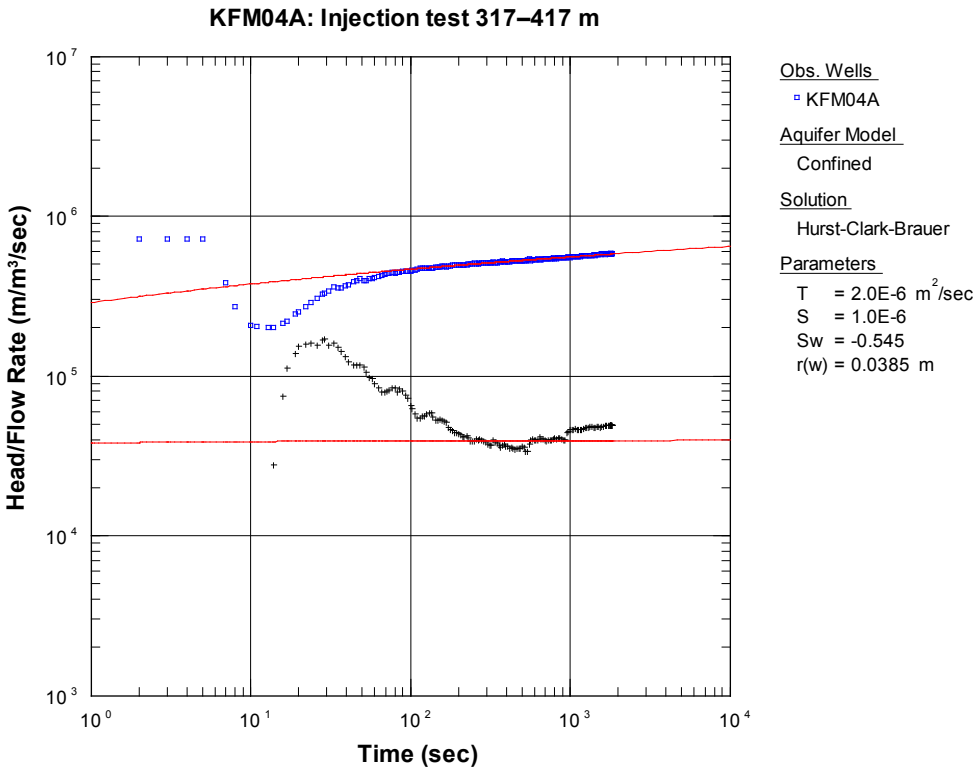

Figure A5:2-1. *Head/flow rate (blue) versus time and derivative (black) during the injection test in section 317–417 m in KFM04A together with the simulated responses (red) based on the evaluated hydraulic parameters from this period.*

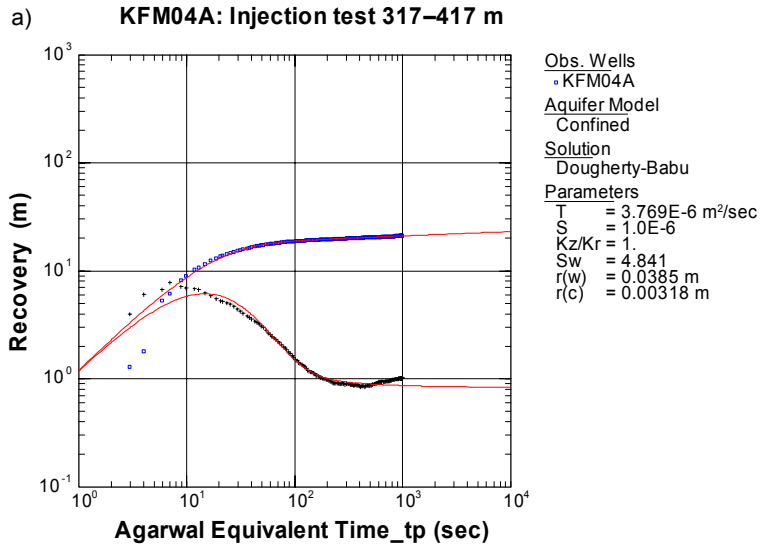

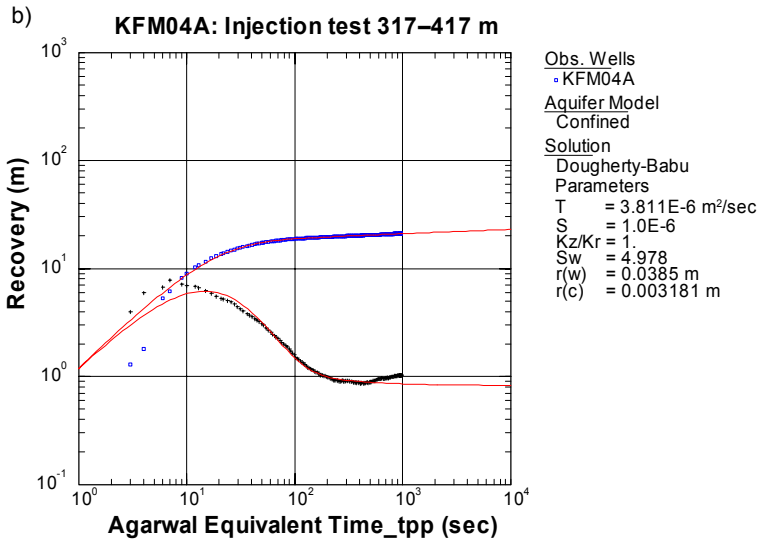

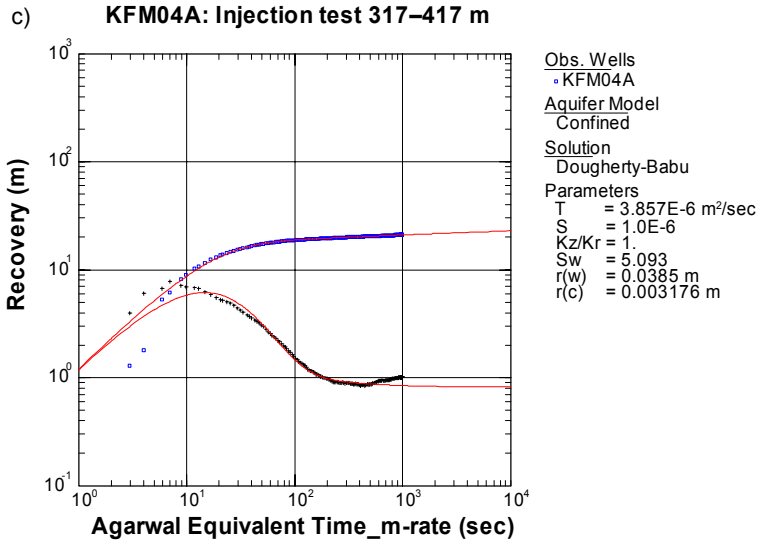

Figure A5:2-2a-c. *Recovery (blue) and -derivative (black) versus Agarwal equivalent time based on t_p, t_{pp} and multi-rate, respectively together with simulated responses (red) based on the evaluated hydraulic parameters in section 317–417 m in KFM04A.*

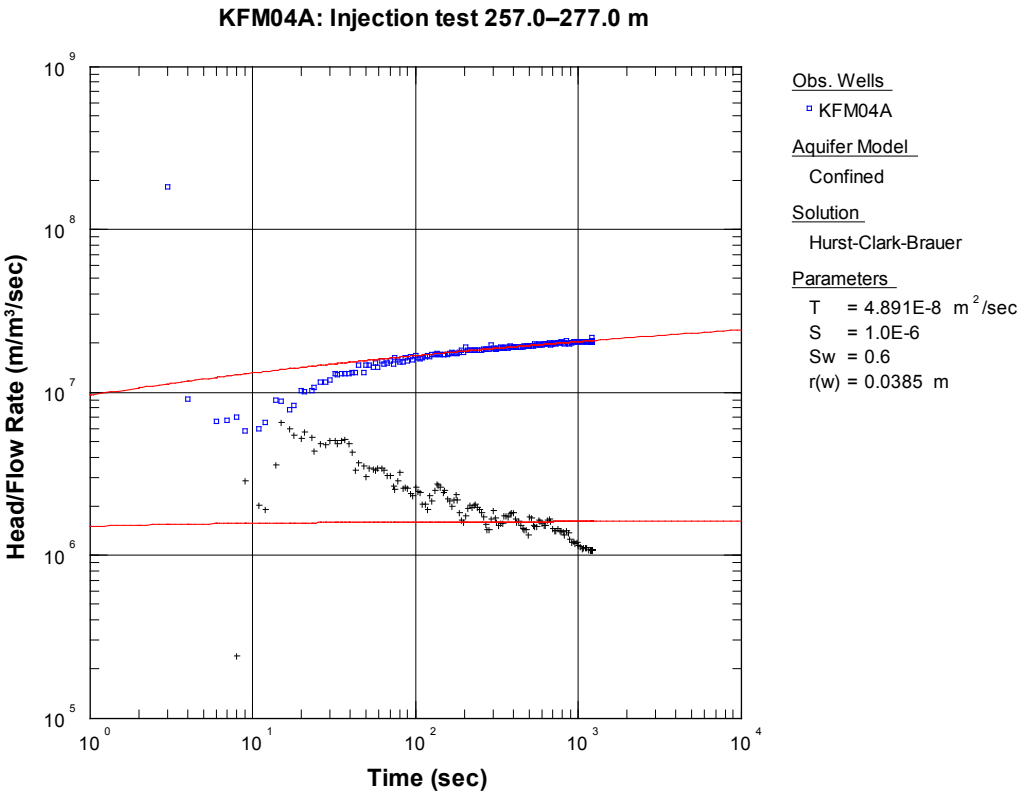

Figure A5:2-3. *Head/flow rate versus time (blue) and -derivative (black) together with the simulated responses (red) based on the evaluated hydraulic parameters from the injection test in section 257–277 m in KFM04A.*

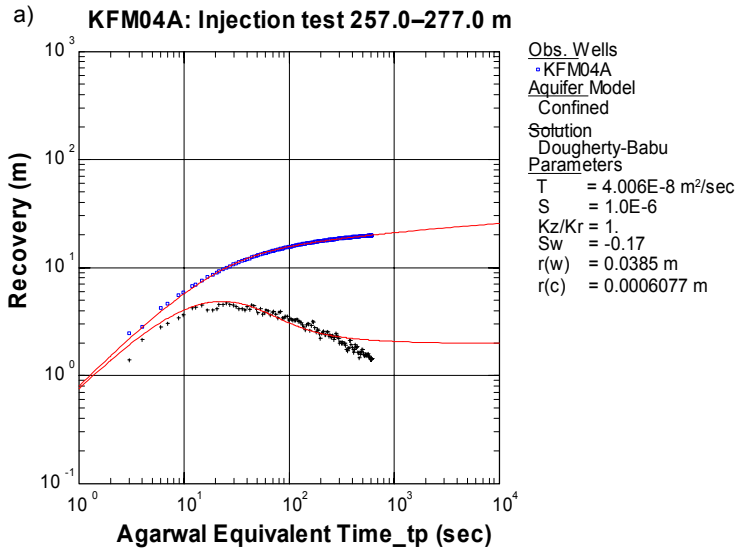

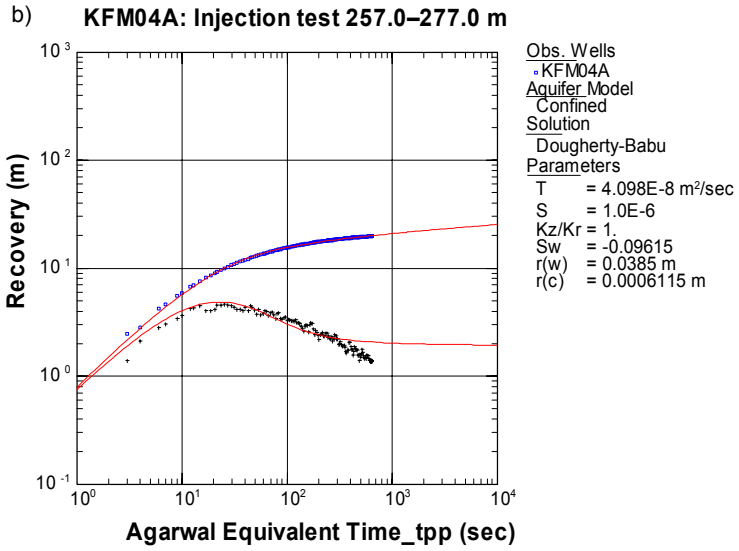

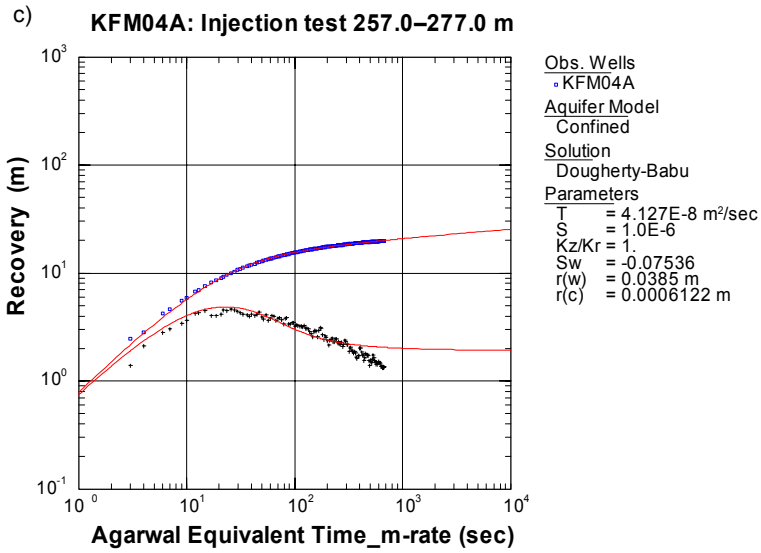

Figure A5:2-4a-c. *Recovery (blue) and -derivative (black) versus Agarwal equivalent time based on t_p, t_{pp} and multi-rate, respectively together with the simulated responses (red) based on the evaluated hydraulic parameters in section 257–277 m in KFM04A.*

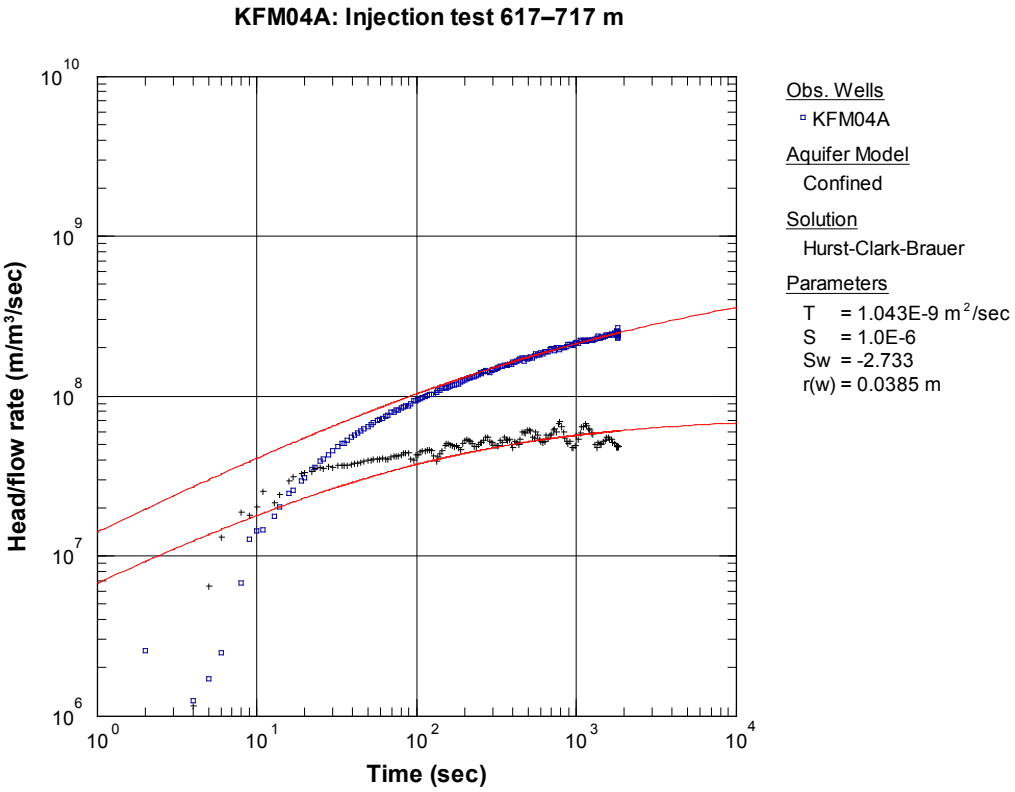

Figure A5:2-5. *Head/flow rate versus time (blue) and -derivative (black) together with the simulated responses (red) based on the evaluated hydraulic parameters from the injection test in section 617–717 m in KFM04A.*

a)

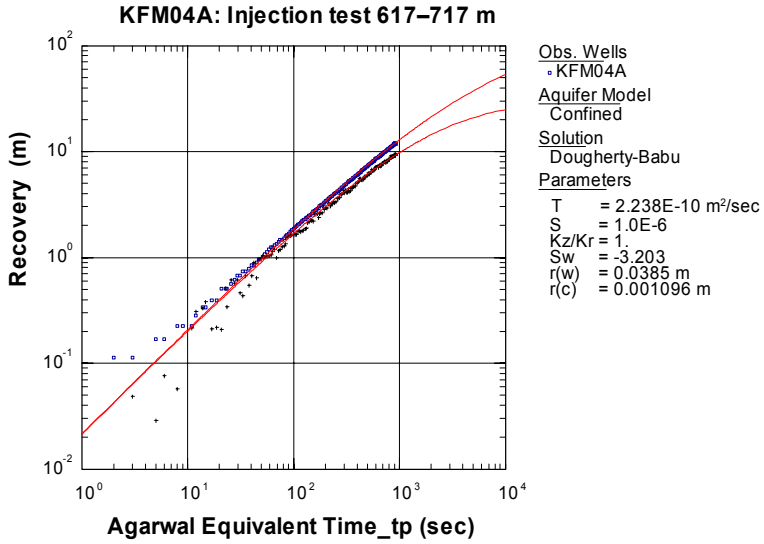

b)

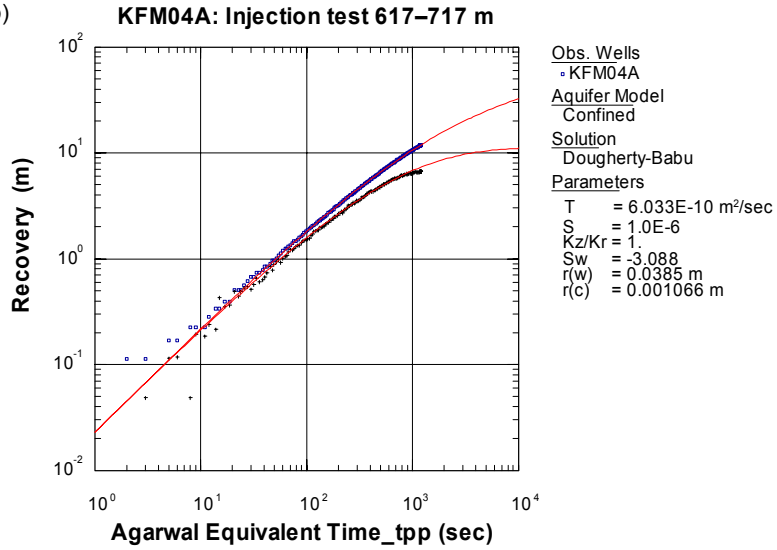

c)

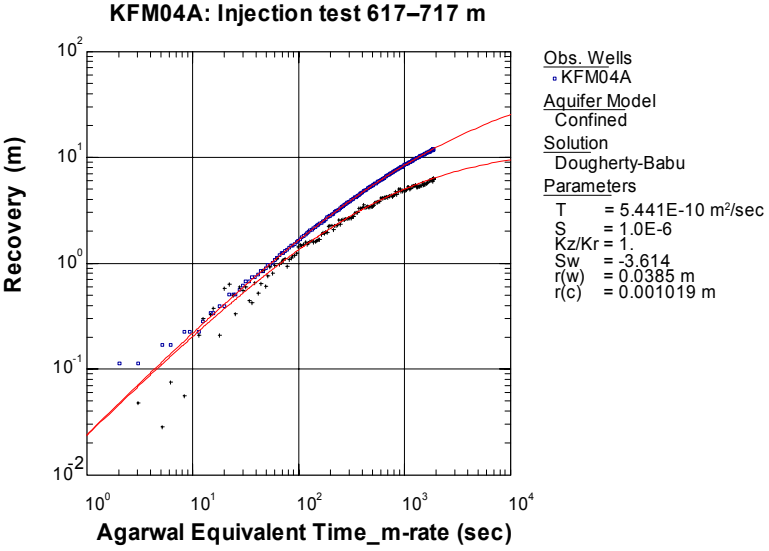

Figure A5:2-6a-c. *Recovery (blue) and -derivative (black) versus Agarwal equivalent time based on t_p, t_{pp} and multi-rate, respectively together with the simulated responses (red) based on the evaluated hydraulic parameters in section 617–717 m in KFM04A.*

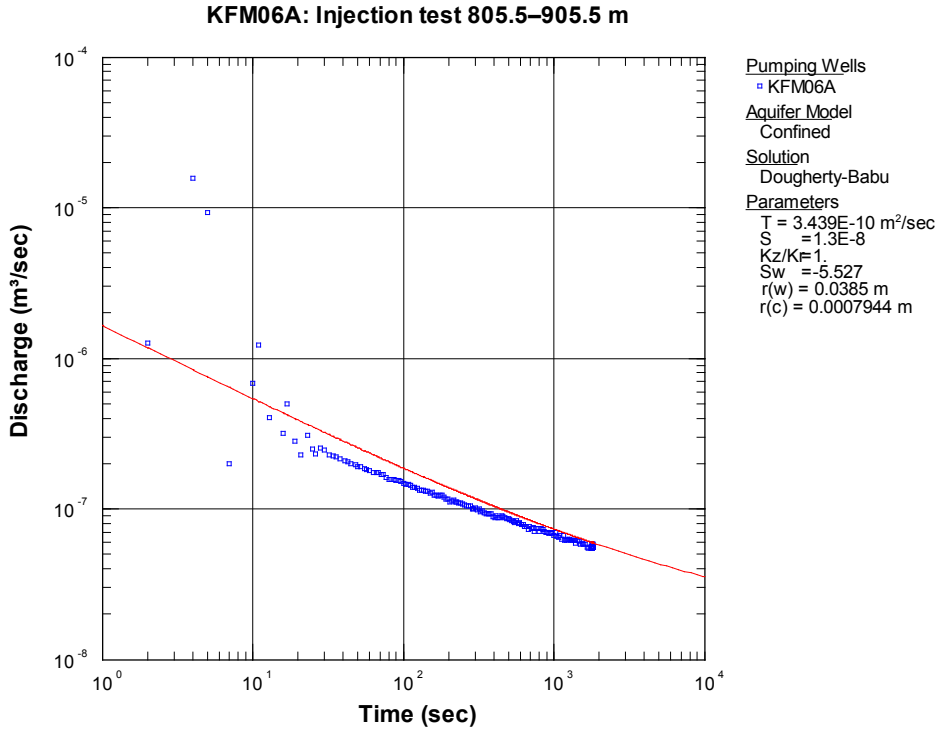

Figure A5:3-1. *Flow rate (blue) versus time together with the simulated flow rate (red) based on the evaluated hydraulic parameters from the recovery period of the injection test in section 805.5–905.5 m in KFM06A.*

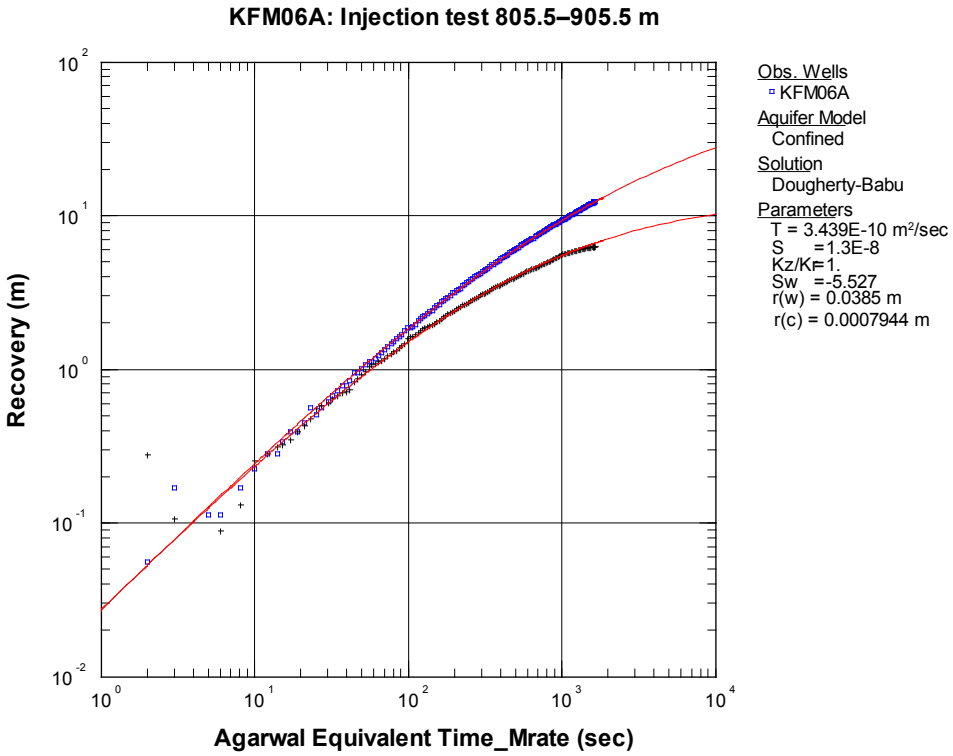

Figure A5:3-2. *Recovery (blue) and -derivative (black) versus Agarwal equivalent time based on multi-rate together with the simulated responses (red) based on the evaluated hydraulic parameters from the recovery period in section 805.5–905.5 m in KFM06A.*

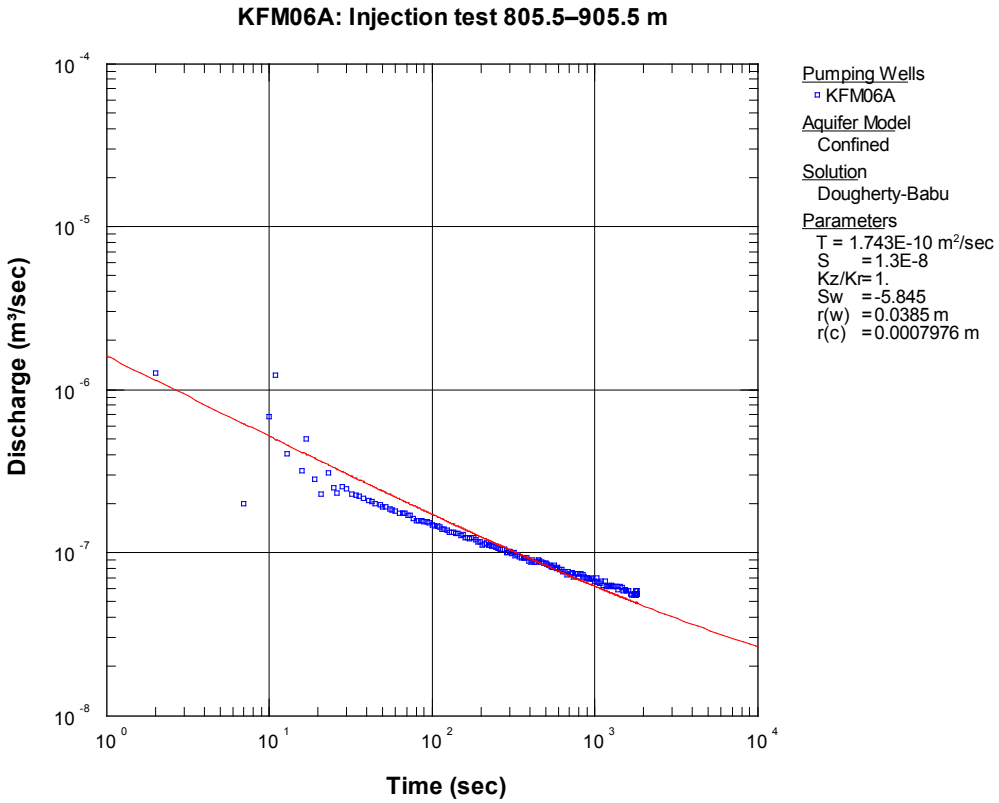

Figure A5:3-3. *Corrected flow rate (blue) versus time together with the simulated flow rate (red) based on the evaluated hydraulic parameters from the recovery period of the injection test in section 805.5–905.5 m in KFM06A.*

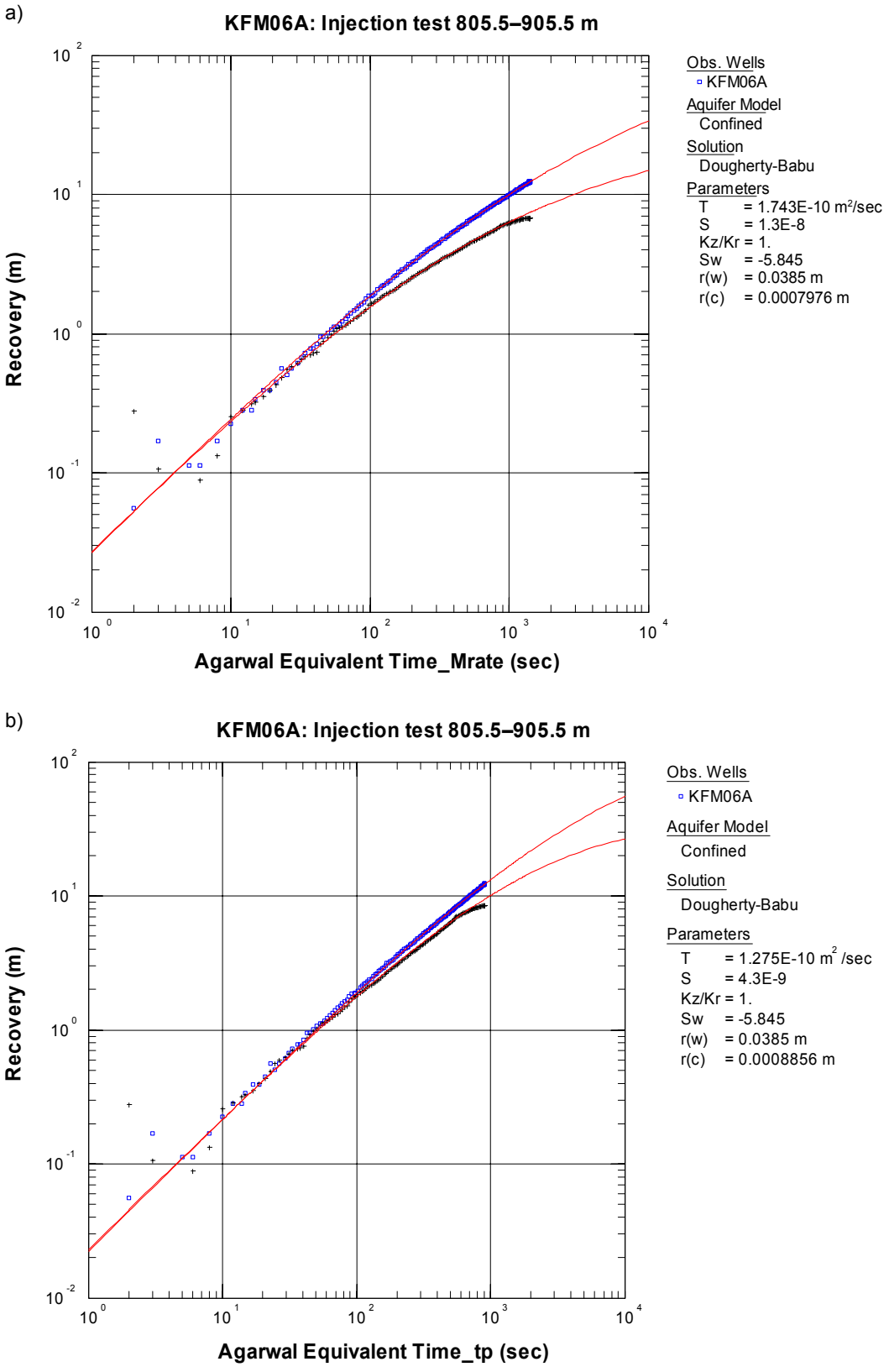

Figure A5:3-4a-b. *Corrected recovery (blue) and -derivative (black) versus Agarwal equivalent time based on a) multi-rate and b) t_p together with the simulated responses (red) based on the evaluated hydraulic parameters from the recovery period of the injection test in section 805.5–905.5 m in KFM06A.*

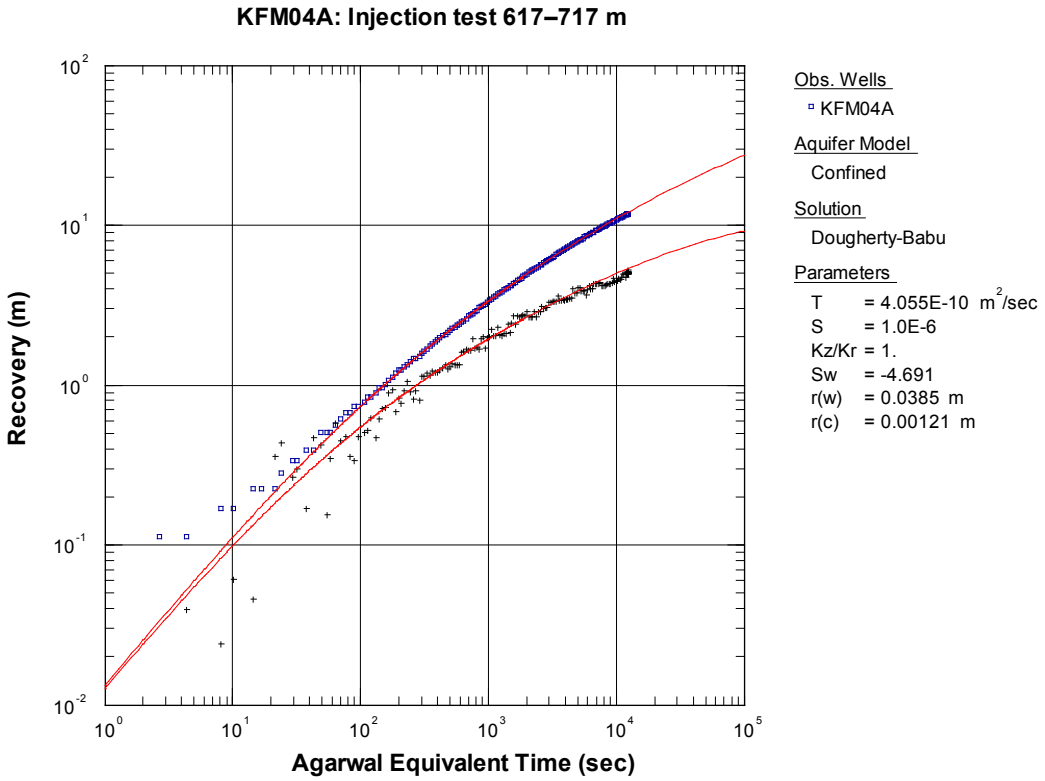

Figure A5:3-5. *Recovery (blue) and -derivative (black) versus Agarwal equivalent time based on multi-rate on the original flow rate data in Figure A5:1–7 in section 617–717 m in KFM04A together with the simulated responses (red) from the recovery period.*

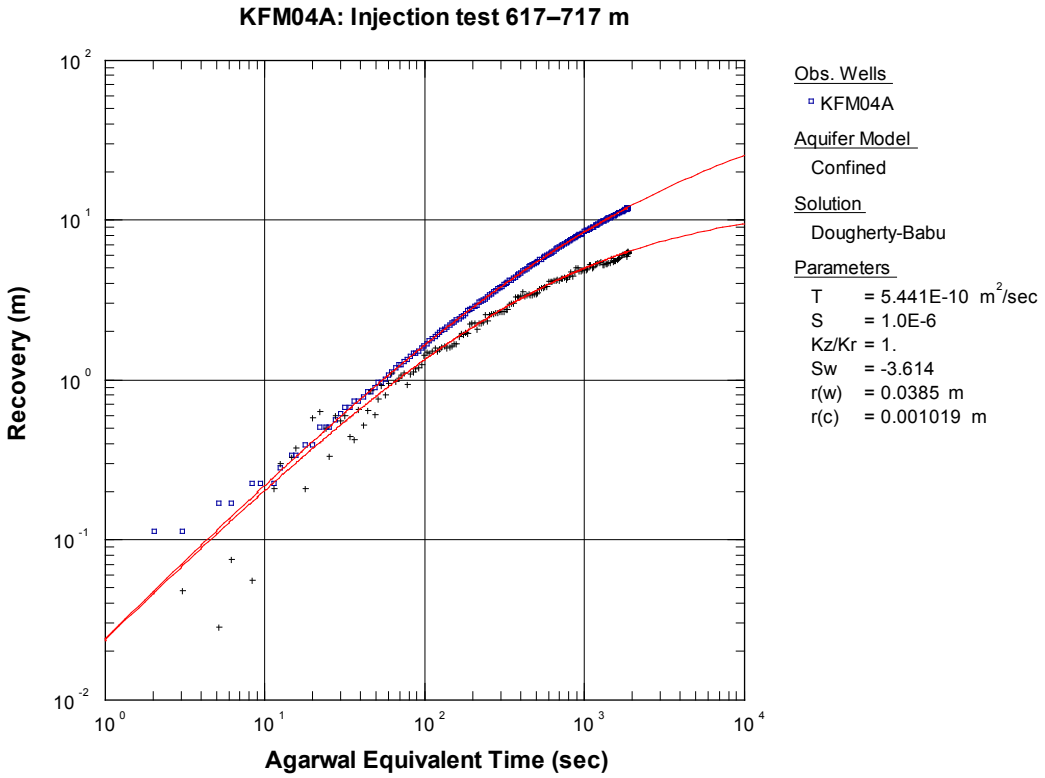

Figure A5:3-6. *Recovery (blue) and -derivative (black) versus Agarwal equivalent time based on multi-rate on corrected flow rate data in section 617–717 m in KFM04A together with the simulated responses (red) from the recovery period.*

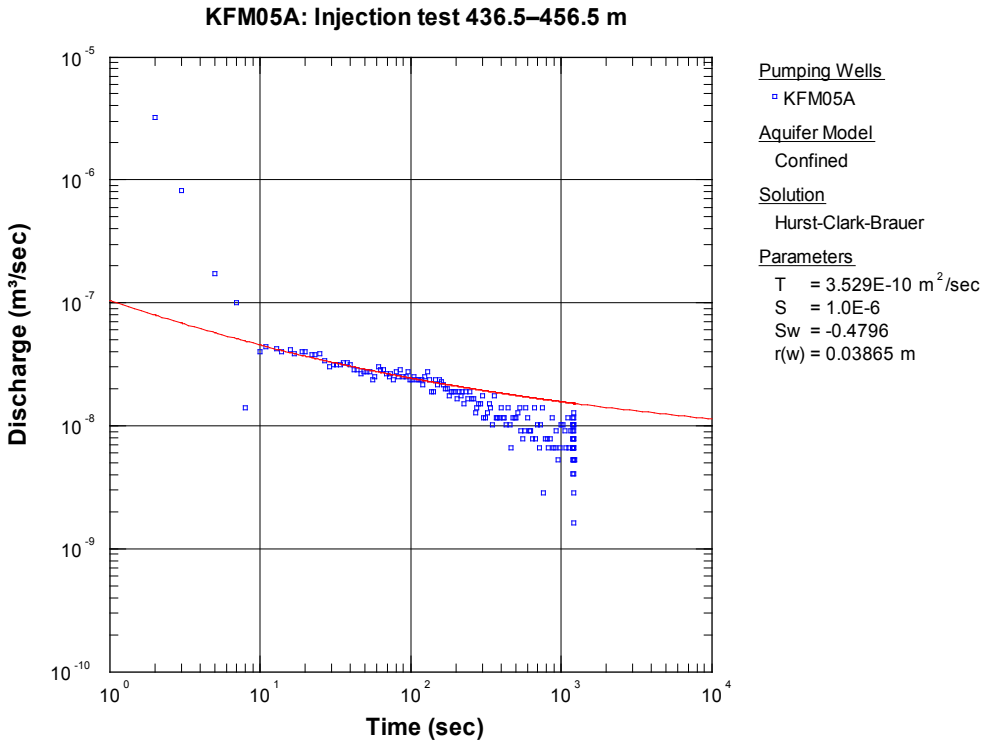

Figure A5:3-7. *Flow rate (blue) versus time during the flow period together with the simulated flow rate (red) based on the evaluated hydraulic parameters from the injection period in section 436.5–456.5m in KFM05A.*

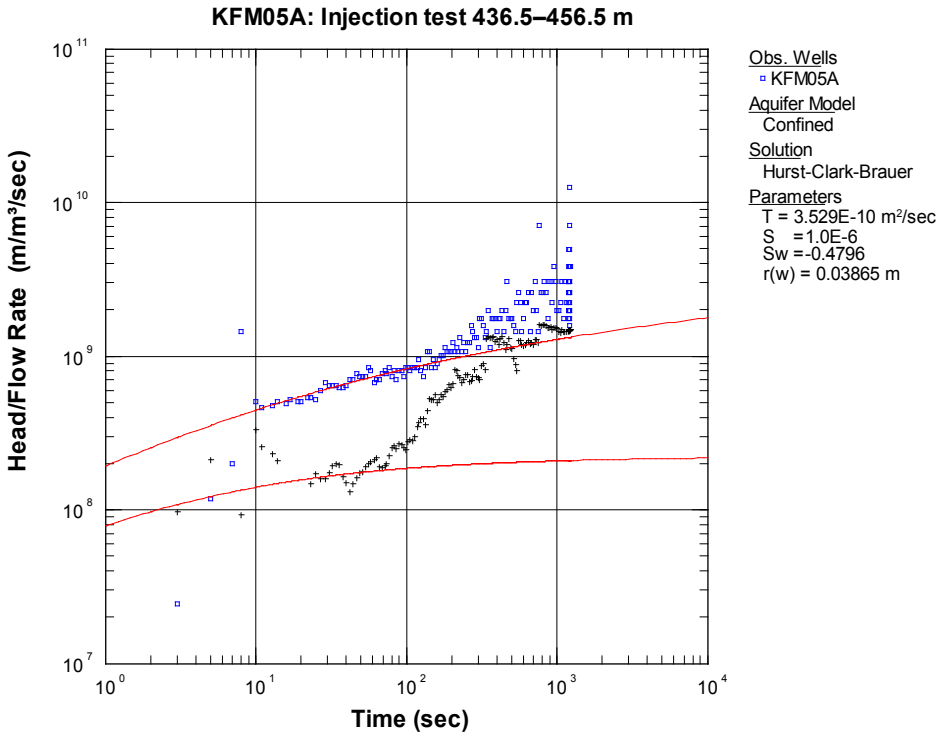

Figure A5:3-8. *Head/flow rate versus time (blue) and -derivative (black) together with the simulated responses (red) based on the evaluated hydraulic parameters from the injection period in section 436.5–456.5 m in KFM05A.*

a)

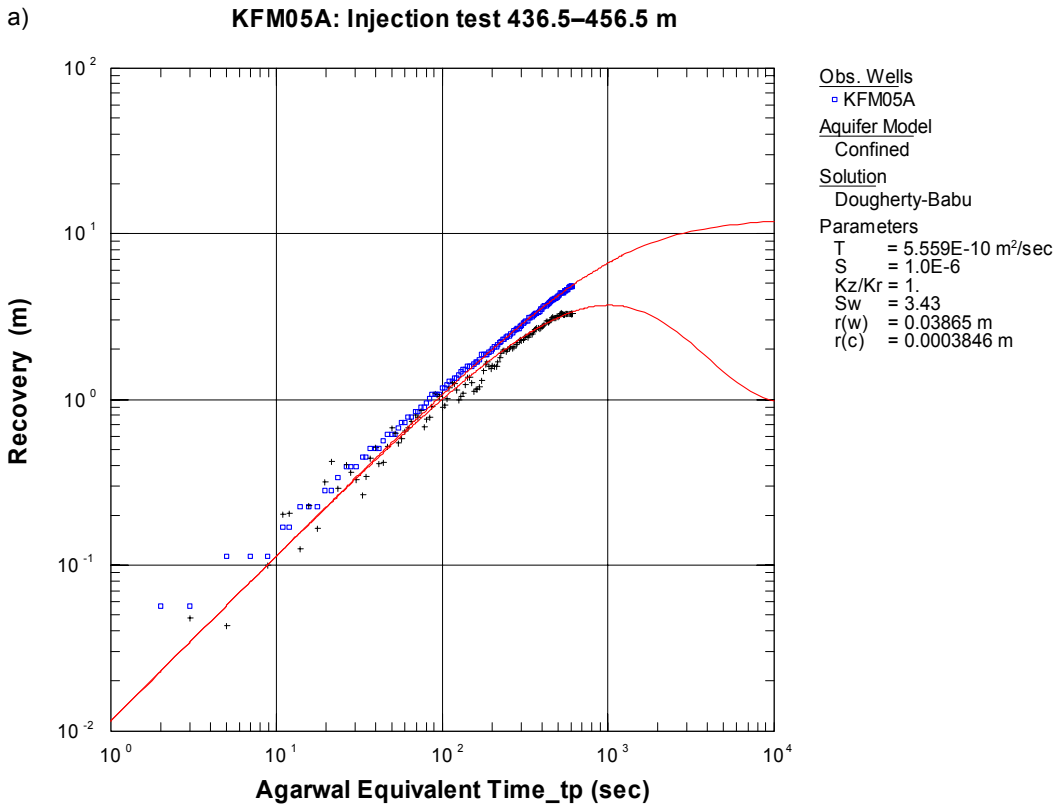

b)

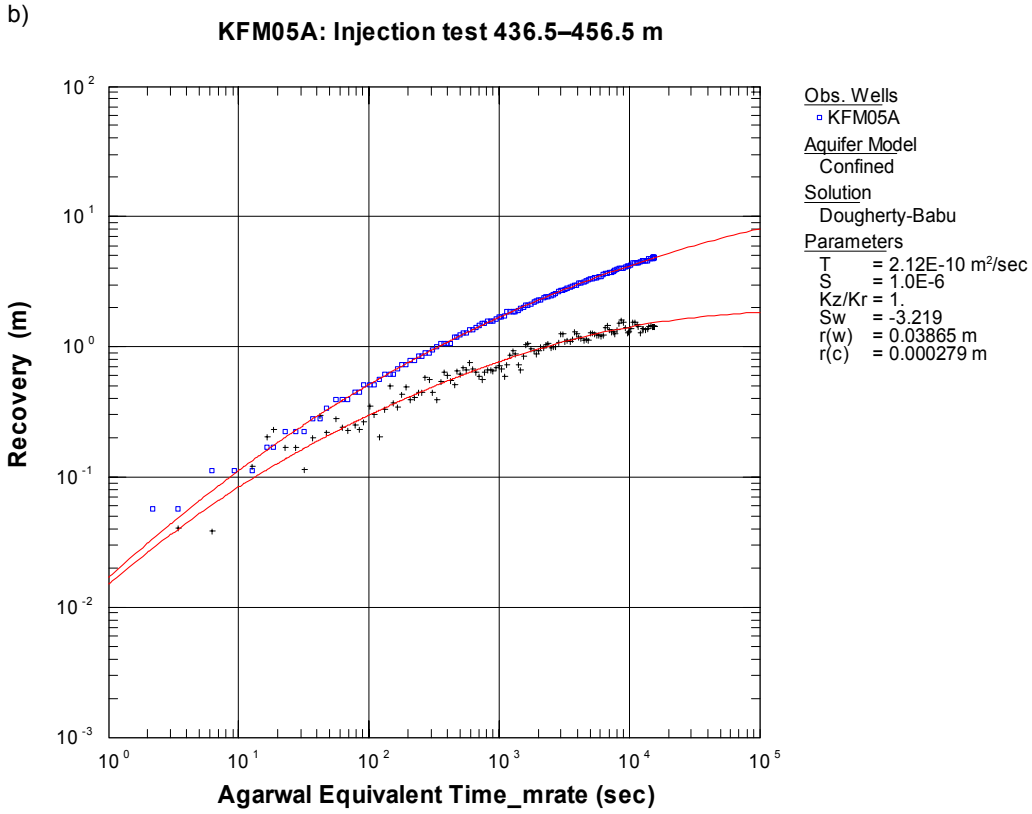

Figure A5:3-9a-b. *Recovery (blue) and -derivative (black) versus Agarwal equivalent time based on t_p and multi-rate, respectively together with the simulated responses (red) based on the evaluated hydraulic parameters in section 436.5–456.5 m in KFM05A.*

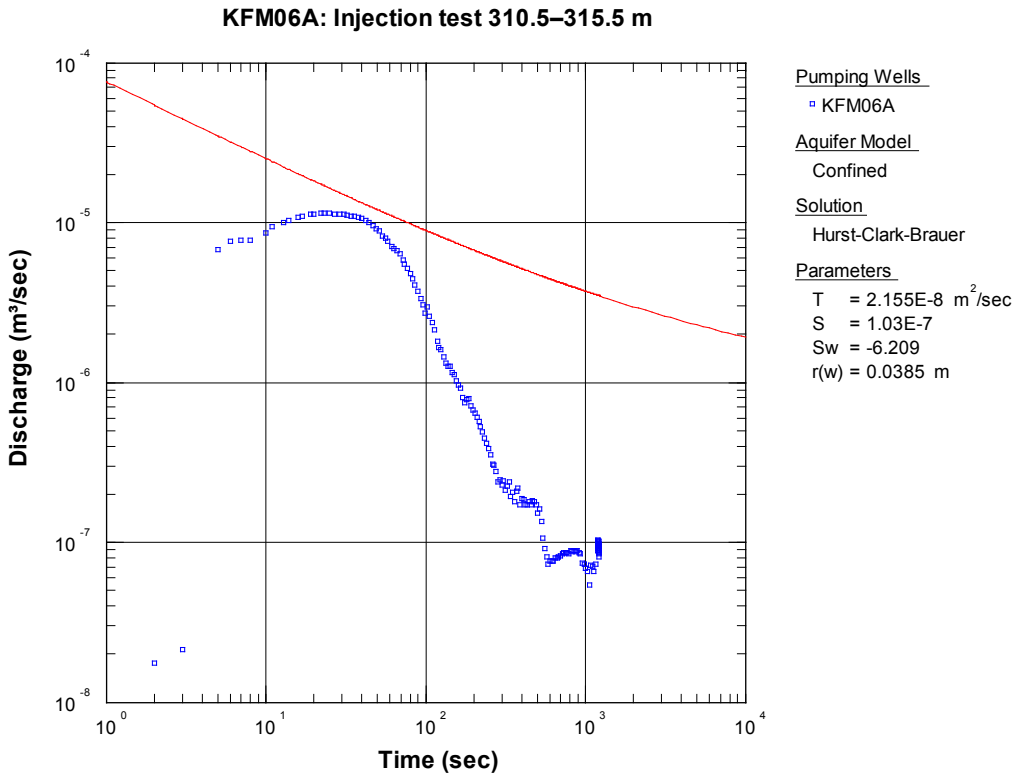

Figure A5:3-10. *Flow rate (blue) versus time during the flow period in section 310.5–315.5 m in KFM06A together with simulated flow rate (red) based on the evaluated hydraulic parameters from the recovery period.*

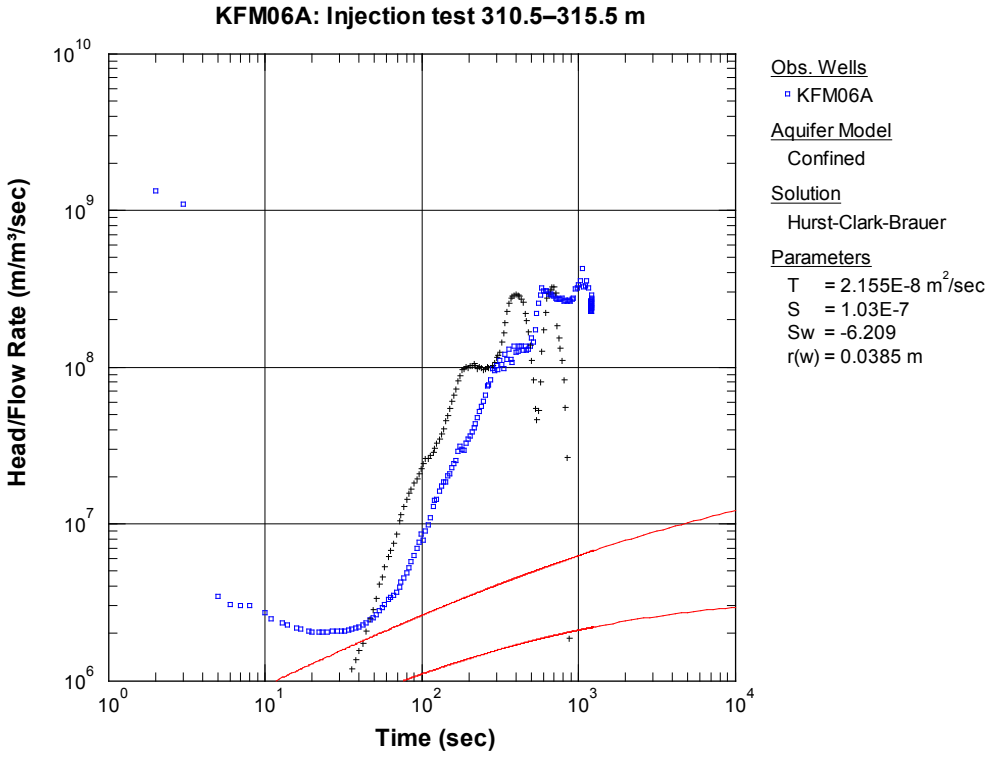

Figure A5:3-11. *Head/flow rate versus time (blue) and -derivative (black) during the flow period in section 310.5–315.5 m in KFM06A together with the simulated responses (red) based on the evaluated hydraulic parameters from the recovery period.*

a)

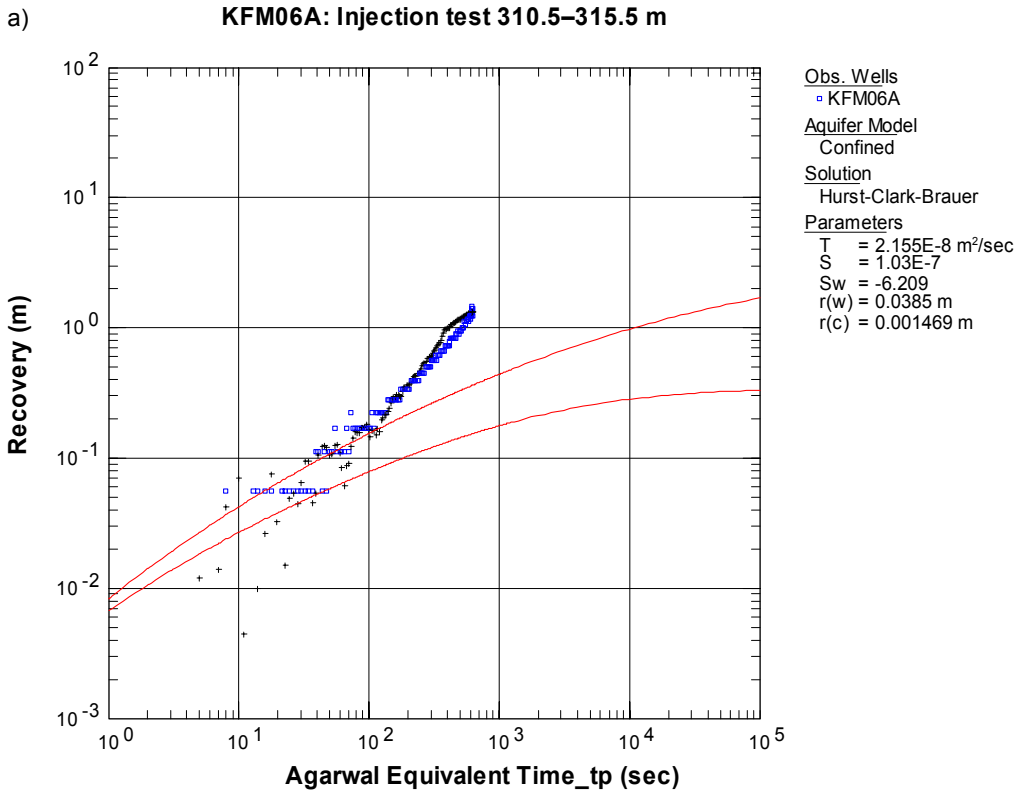

b)

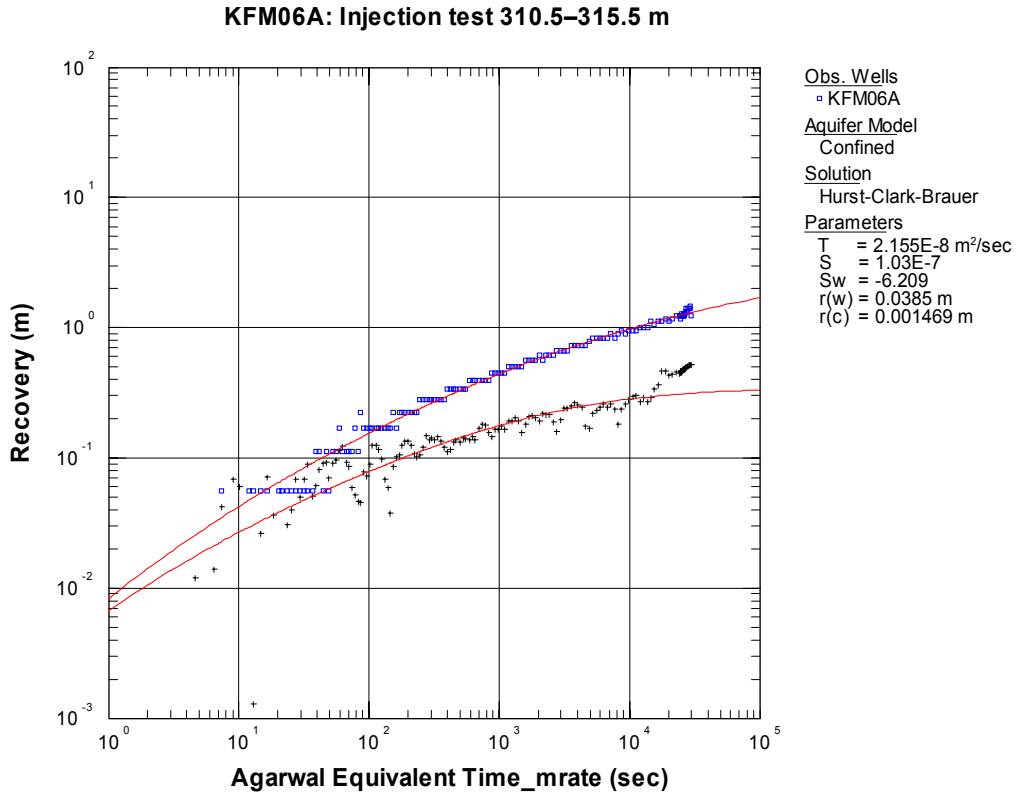

Figure A5:3-12a-b. *Recovery (blue) and -derivative (black) versus Agarwal equivalent time based on t_p and multi-rate, respectively together with the simulated responses (red) based on the evaluated hydraulic parameters in section 310.5–315.5 m in KFM06A.*